CLINICAL ASPECTS AND IN VITRO MODELLING OF GBA1 VARIANT-ASSOCIATED PARKINSON'S DISEASE

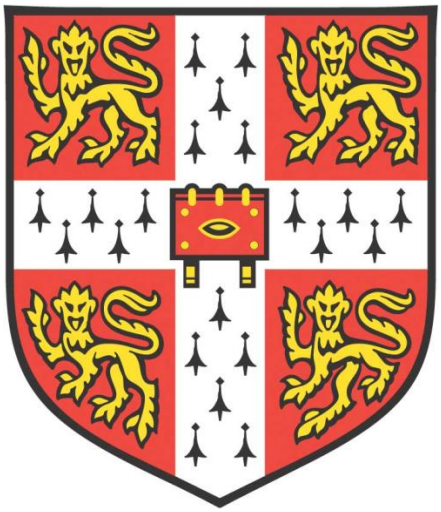

Thomas Benjamin Stoker

Robinson College

John van Geest Centre for Brain Repair

Department of Clinical Neurosciences

University of Cambridge

This dissertation is submitted for the degree of Doctor of Philosophy

September 2019

DECLARATION

This thesis is the result of my own work and includes nothing which is the outcome of work done in collaboration except as declared in the Preface and specified in the text. It is not substantially the same as any that I have submitted, or, is being concurrently submitted for a degree or diploma or other qualification at the University of Cambridge or any other University or similar institution except as declared in the Preface and specified in the text. I further state that no substantial part of my thesis has already been submitted, or, is being concurrently submitted for any such degree, diploma or other qualification at the University of Cambridge or any other University or similar institution except as declared in the Preface and specified in the text. It does not exceed the prescribed word limit for the relevant Degree Committee.

ABSTRACT

Parkinson's disease (PD) is the second most common neurodegenerative disease, characterised by a typical movement disorder, accompanied by a number of non-motor manifestations including cognitive impairment, neuropsychiatric symptoms, autonomic features and sleep disturbance. The aetiology of PD is incompletely understood, but there has been growing interest in the role of genetic risk factors contributing to the development of PD.

Mutations in the *GBA1* gene have been identified as numerically the most important in PD, being found in approximately 5 % to 10 % of patients, and increasing the risk of developing PD by up to 20- to 30-fold. However, there is correlation between the severity of the genetic variant and the degree to which PD risk is increased, with milder variants only increasing the risk by approximately two-fold. Furthermore, as well as being relatively common, *GBA1* mutations have also been reported to adversely affect prognosis, in terms of motor progression and risk of dementia, though questions remain about the incidence of these outcomes and the contribution of "non-pathogenic" variants in the *GBA1* gene. *GBA1* mutation-associated PD (*GBA1*-PD) therefore constitutes an important subgroup of the PD population, and one in which novel therapies could significantly reduce the burden of PD. The pathogenesis of *GBA1*-PD seems to be related to dysfunction of the lysosome-autophagy system, making this system a prime therapeutic target in this group.

This project consists of a combined epidemiological and *in vitro* study of *GBA1*-PD, with a focus on better characterisation of the clinical aspects of *GBA1*-PD, and establishing a novel disease model using directly reprogrammed induced neurons (iNs) in which to test putative disease-modifying treatments. Firstly, long-term data from two incident PD clinical cohorts is presented, which constitutes the longest follow-up study of *GBA1*-PD to date. Consistent with previous studies, *GBA1* abnormalities were found to increase the risk of dementia and motor progression, and also to increase the risk of death – an outcome which few studies have previously reported on. Additionally, it was found that carrying "non-pathogenic" *GBA1* variants also adversely affected disease course.

In order to set up a novel drug-screening model, iNs were generated from healthy controls, and PD patients with and without *GBA1* abnormalities. The use of iNs means that the age signature is preserved in the cells, such that they retain factors potentially important in pathogenesis, that are lost in similar *in vitro* models in which induced pluripotent stem cell-derived neurons are employed. The iNs were treated with pre-formed fibrils of pathogenic α-synuclein to induce formation of α-synuclein aggregates, which were formed in greater numbers in diseased cell lines compared to healthy controls. Additionally, PD iNs in particular developed a reduction in mitochondrial membrane potential following treatment with PFFs, suggesting that they were more susceptible to relevant downstream pathology. This system was then used to study the effects of two drugs previously suggested to enhance activity in the lysosome-autophagy system – trehalose and nortriptyline. Trehalose was found to alter autophagy activity in carriers and non-carriers of *GBA1* mutations, which resulted in a reduction in α-synuclein-induced pathology. In contrast, nortriptyline was ineffective in *GBA1*-PD patient-derived neurons, suggesting that it is not able to overcome the autophagy dysfunction seen in this subgroup, but was able to reduce pathology in PD patient cells without *GBA1* abnormalities.

In conclusion, this project describes the long-term clinical course in *GBA1*-PD, as well as a novel *in vitro* model for studying pathogenesis and drug-screening in this PD patient group. Two drugs tested were identified to reduce pathology in different PD subgroups, highlighting the power of this work to the future development of personalised therapies for PD.

For Caroline, Daniel and Conor

"It's a little embarrassing that after 45 years of research and study, the best advice I can give people is to be a little kinder to each other" – Aldous Huxley

ACKNOWLEDGEMENTS

Over the three years in which this work was undertaken, I have received a great deal of support from a number of people, that have provided guidance in performing this project, but that have also contributed to my learning and development as a researcher.

I would firstly like to thank the organisations that have provided funding for this work, which have included the Cure Parkinson's Trust and the National Institute for Health Research Biomedical Research Centre, Cambridge.

I would like to express my sincere gratitude to my supervisor Professor Roger Barker, who was instrumental in determining the aims and plan for my project. Professor Barker has been available to offer advice whenever I have needed it, and it has been a great pleasure to work in his group.

I started this PhD project with very little experience of laboratory work, and every procedure that I used was new to me. In learning these techniques, I received the help of several colleagues who I would like to thank. A large part of this project followed on from work done by Dr Lucy Collins, who acquired many of the cell lines that I worked with. Along with Lucy, Dr Nick Blair taught me the practicalities of cell culture and other laboratory techniques, and it was invaluable to learn from someone with the experience that Nick had. I also wish to thank Professor Malin Parmar, who welcomed me into her lab in Lund University for two weeks at the start of my PhD, where I learned to generate induced neurons. I am indebted to Dr Janelle Drouin-Ouellet who took me through the processes of direct conversion and virus production whilst in Lund, and was available to offer advice throughout my project. Janelle also kindly provided the initial stock of plasmids used to produce the reprogramming virus that I used in this project. I would also like to acknowledge the support of Dr Wei-Li Kuan, who provided the α-synuclein pre-formed fibrils which were central to my project, and who was always available to offer advice in experimental design. Other colleagues that helped with the laboratory part of my project included Veronika Romashova who supported me when learning to use the

Cellomics XTI microscope, and Dr Kelli Torsney who helped to perform some of the fibroblast experiments during her six months working in the group.

I am also grateful for the support offered by Dr Caroline Williams-Gray and Marta Camacho, which was crucial to the work discussed in the second chapter of this thesis. Caroline initially suggested performing the epidemiological study of the Parkinson's disease cohorts, and provided advice when undertaking this work. Marta ran database queries for me and provided the relevant data from the cohorts whenever I needed it, as well as offering advice about statistical analysis.

Having written tens of thousands of words for this PhD thesis, the following two paragraphs are the part that I have found the most difficult. As well as the professional help that I have received from so many colleagues, I would also like to make some personal acknowledgements. Over my three years working in the Barker group I have developed some great friendships, which have made it a thoroughly enjoyable place to work. In particular, I would like to thank my good friends Dr Shaline Fazal and Kate Harris. Shaline played a crucial role in large parts of my project by sharing her experience of cell culture and helping with Western blotting analysis. At various points over my three years in the group, Shaline and Kate both took on some induced neuron work, and shared with me the trials of working with this novel technique! There were times when work in the laboratory was hindered by a number of problems, but Kate and Shaline's friendship meant that even these challenging periods were great fun, and I am lucky to have worked with them. I would like to thank them both for everything they have done over these last few years.

Finally, I would like to extend enormous thanks to my family – Caroline, Daniel and Conor – who have offered great support through my PhD. It was a rare event that I entrusted even a medium change to a colleague, which meant that I had to attend the lab at least every two to three days – a pattern that frustrated any attempt at a family holiday! When work in the laboratory was challenging, Caroline and my boys lifted my spirits and made sure that my whole PhD was enjoyable, and I am truly lucky to have them in my life.

CONTENTS

List of Tables

LIST OF FIGURES

LIST OF ABBREVIATIONS AND ACRONYMS

3-MA:	3-methyladenine
γH2AX:	Serine 139-phosphorylated H2A histone family member X
ALK:	Activin receptor-like kinase receptor
AMPK:	Adenosine monophosphate-activated protein kinase
ApoE:	Apolipoprotein E
Ascl1:	Achaete-scute homolog-1
ATP:	Adenosine triphosphate
Baf:	Bafilomycin A1
BAF:	Brg1-like-associated factor
BAM:	Brn2, Ascl1, Myt1-L
BDI:	Beck depression inventory
BDNF:	Brain-derived neurotrophic factor
BMP:	Bone morphogenic protein
bHLH:	Basic helix-loop-helix
BSA:	Bovine serum albumin
CCCP:	Carbonyl cyanide 3-chlorophenylhydrazone
COMT:	Catechol-O-methyltransferase
cAMP:	Cyclic adenosine monophosphate
DAPI:	4′,6-diamidino-2-phenylindole
db-cAMP:	Dibutyryl cyclic adenosine monophosphate
DLB:	Dementia with Lewy bodies
DMEM:	Dulbecco's modified Eagle medium
DNA:	Deoxyribonucleic acid
DSM:	Diagnostic and Statistical Manual of Mental Disorders
EDTA:	Ethylenediaminetetraacetic acid

ER: Endoplasmic reticulum

ERAD: Endoplasmic reticulum-associated protein degradation

FACS: Fluorescence-activated cell sorting

FBS: Fetal bovine serum

FBXO7: F-box only protein 7

FCCP: Carbonyl cyanide-p-trifluoromethoxyphenylhydrazone

FoxA2: Forkhead box protein A2

FTDP-17: Fronto-temporal dementia with Parkinsonism linked to chromosome 17

GABA: Gamma-aminobutyric acid

***GBA1*-PD:** *GBA1* variant-associated Parkinson's disease

GCase: Glucocerebrosidase

GD: Gaucher disease

GD+PD: Gaucher disease with concomitant Parkinson's disease

GDNF: Glial cell line-derived neurotrophic factor

GFP: Green fluorescent protein

GHSR1α: Growth hormone secretagogue receptor 1α

Ghr: Ghrelin

GSK-3: Glycogen synthase kinase-3

HBSS: Hank's balanced salt solution

HCl: Hydrochloric acid

HEK293T: Human embryonic kidney 293T cells

HLA: Human leukocyte antigen

HP1: Heterochromatin protein-1

HRP: Horse radish peroxidase

iNs: Induced neurons

iPD: Idiopathic Parkinson's disease

iPSC:	Induced pluripotent stem cell
LAMP2A:	Lysosome associated membrane protein 2A
LAP2α:	Lamina-associated peptide-2α
LIMP-2:	Lysosomal membrane protein-2
LMX1a:	LIM homeobox transcription factor 1α
LB:	Lysogeny broth
MACS:	Magnetic-activated cell sorting
MAP2:	Microtubule associated protein 2
MAO-B:	Monoamine oxidase B
MDMA:	3,4-Methylenedioxy methamphetamine
Met:	Methionine
MET:	Metformin
MERRF:	Myoclonic epilepsy with ragged red fibres
MicroRNA:	Micro-ribonucleic acid
miR-9/9*:	MicroRNA-9/9*
miR-124:	MicroRNA-124
miR-137:	MicroRNA-137
MOCA:	Montreal Cognitive Assessment
MMSE:	Mini-Mental State Examination
MOI:	Multiplicity of infection
MPP^+:	1-methyl-4-phenylpyridinium
MPTP:	1-methyl-4-phenyl-1,2,3,6-tetrahydropyridine
mRNA:	Messenger ribonucleic acid
mTOR:	Mammalian target of rapamycin
mTORC1:	Mammalian target of rapamycin complex-1
NCAM:	Neural cell adhesion molecule
Nor:	Nortriptyline

NT3: Neurotrophin-3

Nurr1: Nuclear receptor related protein-1

PBS: Phosphate-buffered saline

PCR: Polymerase chain reaction

PD: Parkinson's disease

PFA: Paraformaldehyde

PFF: Pre-formed-fibrils

PFL: Poly-L-ornithine, fibronectin, laminin

pFTAA: Pentameric formyl theophene acetic acid

PGK: Phosphoglycerate kinase

PI3K: Phosphatidylinositol-3-kinase

PI3P: Phosphatidylinositol-3-phosphate

PI4K: Phosphatidylinositol-4-kinase

PINK-1: PTEN-induced putative kinase-1

PL: Poly-L-ornithine, laminin

PSF: Penicillin-streptomycin-fungomycin

qPCR: Quantitative polymerase chain reaction

RANBP17: RAN binding protein-17

RBD: REM sleep behaviour disorder

REM: Rapid eye movements

REST: RE1 silencing transcription factor complex

RNA: Ribonucleic acid

SA-β-galactosidase: Senescence-associated β-galactosidase

SD: Standard deviation

SDS: Sodium dodecyl sulphate

shRNA: Short-hairpin ribonucleic acid

siRNA: Short-interfering ribonucleic acid

SOC:	Super-optimal broth medium
SWI/SNF:	SWItch / sucrose non-fermentable
TBS-T:	Tris-burred saline with 0.1% Tween
TGFβ:	Tissue growth factor β
TH:	Tyrosine hydroxylase
TMRE:	Tetramethylrhodamine, ethyl ester
Tre:	Trehalose
Tris:	Tris(hydroxymethyl)aminomethane
TrkB:	Tropomyosin receptor kinase B
UPR:	Unfolded protein response
UPDRS:	Unified Parkinson's disease rating scale
Val:	Valine
WPRE:	Woodchuck hepatitis virus post-transcriptional regulator element
WT:	Wild-type

1 INTRODUCTION

1.1 Introduction to Parkinson's disease and project

Parkinson's disease (PD) is the second most common neurodegenerative disorder after Alzheimer's disease. It is characterised clinically by a motor syndrome consisting of bradykinesia, rest tremor, rigidity and as disease progresses, postural instability (Kalia and Lang 2015). In addition to the Parkinsonian movement disorder, non-motor features are common and include cognitive impairment and dementia, neuropsychiatric features such as depression, anxiety and hallucinations, anosmia, autonomic dysfunction and sleep-disturbance (Khoo et al. 2013). There are currently no disease-modifying treatments for PD, and the disorder generally follows a slowly progressive course with deterioration over years. However, clinical heterogeneity is seen, with some patients following a relatively benign course dominated by motor features, whilst in others non-motor features including cognitive impairment may predominate (Williams-Gray et al. 2013, Greenland, Williams-Gray and Barker 2019).

A number of novel and existing drugs have been purported as potential disease-modifying treatments in PD, based on their ability to act on the dysfunctional mechanisms that contribute to pathogenesis. There is increasing interest in the possibility of drug repurposing – the use of drugs that are already used for other conditions for a new indication – as this potentially offers an expedited route to clinic, given that safety data will already be available. Furthermore, as the pathogenic basis of clinical heterogeneity

is determined, different treatment approaches may be employed for different subgroups of patients – precision medicine. As such, there is therefore a rationale for studying the pathogenic mechanisms and treatment effects in specific populations of PD patients.

One important subpopulation of PD patients that has recently emerged are those carrying mutations in the *GBA1* gene (Migdalska-Richards and Schapira 2016). This group is characterised by distinct clinical features and specific pathological mechanisms, making it an interesting group to study the effects of putative disease-modifying treatments. The aim of this project has been to establish a novel *in vitro* model of PD pathology in which drugs can be screened for potential disease-modifying effects in this group of patients. This has involved the use of the novel technique of direct lineage conversion to generate adult patient-derived neurons, without passage through a stem cell stage and its associated problems. In this model four drugs have been screened for their ability to reverse pathology. A second aim of this project has been to detail the natural history of PD patients carrying *GBA1* mutations using long-term follow-up data from two cohorts of incident PD patients.

1.2 Aetiology of Parkinson's disease

The aetiology of PD remains poorly understood, and there are clearly genetic and environmental influences. The discovery that the toxin MPTP could cause selective death of dopaminergic neurons prompted interest in a potential environmental toxic cause of PD (Langston et al. 1983, Langston and Ballard 1983). One such putative toxin includes the herbicide paraquat, of which the molecular structure is similar to that of MPTP (McCormack et al. 2002). A meta-analysis of thirty potential risk factors found 11 to alter the risk of PD, with pesticide exposure bearing the strongest to be associated with the disease (Noyce et al. 2012). Other factors including cigarette smoking were reported to be protective, though it is possible that this observation is explained by the fact that PD patients more readily give up smoking than healthy controls – perhaps explained by a reduced reward mechanism due to dopamine depletion (Ritz et al. 2014). Similarly, caffeine consumption has been reported to reduce the risk of PD in several studies, though

the basis of this relationship is not known (Hernán et al. 2002). The environmental factors that contribute to PD remain poorly defined, and their significance remains unknown.

Mutations in several genes have been identified to cause rare forms of PD or Parkinsonian syndromes. These include syndromes inherited in autosomal dominant (e.g. mutations in *SNCA* and *LRRK2*) and autosomal recessive (e.g. mutations in *PRKN*, *PINK-1*, and *PARK7*) patterns, most of which are associated with early disease-onset (Klein and Westenberger 2012). Identification of these mutations has yielded useful insight into the pathogenic mechanisms of PD, but they account for only a very small proportion of PD patients, and most are characterised by distinct clinical syndromes, separating them from cases of sporadic PD.

It has more recently become increasingly clear that a number of genetic susceptibility factors contribute to the risk of developing PD, and indeed alter its clinical course. For example, individuals that carry the H2 haplotype of the *MAPT* gene have a reduced risk of PD (Goris et al. 2007). Additionally, the H2 allele is protective against development of dementia within PD patients (Evans et al. 2011). Genome-wide association studies have identified several genetic loci associated with an increased risk of PD, and it now seems likely that an individual's propensity for development of PD is determined by a polygenic risk profile, with or without superadded environmental exposures (Nalls et al. 2011, Nalls et al. 2014, Verstraeten et al. 2015). Mutations and low-frequency polymorphisms in the aforementioned *GBA1* gene have been identified as a particularly important genetic risk factor for PD (Sidransky et al. 2009), which will be discussed further below.

1.3 Pathogenesis of Parkinson's disease

The movement disorder of PD occurs in part due to the relatively selective loss of dopaminergic neurons of the substantia pars compacta, resulting in reduced delivery of dopamine to the striatum, though features such as tremor and gait disturbance have a largely non-dopaminergic basis. Non-motor features occur due to extra-nigral PD pathology with widespread neurodegeneration in the cortex and a number of brainstem

nuclei (Selikhova et al. 2009, Kalia and Lang 2015). Here, the mechanisms thought to contribute to neurodegeneration in PD are discussed.

1.3.1 The role of α-synuclein in Parkinson's disease

Whilst the pathogenesis of PD is not completely understood, it is clear that the neuronal protein α-synuclein plays a role. This association was first suggested after the description of a familial autosomal dominant form of PD occurring due to mutations in its gene, *SNCA* (Polymeropoulos et al. 1997). Since then, α-synuclein has been identified as the main constituent of the abnormal collections of protein (Lewy bodies and Lewy neurites) which represent the pathological hallmark of PD (Spillantini et al. 1997). Aggregates of α-synuclein are also found in other related neurodegenerative conditions (α-synucleinopathies) including Lewy body dementia and multiple system atrophy, and are thought also to play a role in the pathogenesis of these conditions (Spillantini et al. 1998a, Spillantini et al. 1998b). The native biological function of α-synuclein is poorly understood, but it has been suggested to play a role in the regulation of synaptic vesicles and release of neurotransmitters (Burré, Sharma and Südhof 2014).

Although some mutations in the *SNCA* gene result in the expression of aggregation-prone α-synuclein, these only account for rare familial forms of PD (Polymeropoulos et al. 1997), and the mechanisms by which accumulation and aggregation of α-synuclein occur in sporadic PD are not understood. It is known that the cell's major protein clearance pathways, the ubiquitin-proteasome system and lysosome-autophagy system are involved in the clearance of α-synuclein (Webb et al. 2003, Tofaris, Layfield and Spillantini 2001, Cuervo et al. 2004), and dysfunction of these systems have been implicated in PD development. This is supported by the fact that mutations in genes encoding some proteins involved in the proteasome pathway or the lysosome-autophagy system (e.g. *ATP13A2*, *VPS35*) cause familial forms of PD (Zimprich et al. 2011, Leroy et al. 1998, Ramirez et al. 2006, Gan-Or, Dion and Rouleau 2015). Additionally, the functional capacity of these pathways is known to decline with age, which could explain in part why PD incidence increases with age (Gray, Tsirigotis and Woulfe 2003). Of these two systems, the lysosome-autophagy pathway seems to be the most important for the

clearance of α-synuclein, as inhibition of this system (but not the ubiquitin-proteasome system) results in accumulation of α-synuclein (Vogiatzi et al. 2008). Mutations in the *GBA1* gene, which are discussed in detail below, result in dysfunction of the lysosome-autophagy system, which is thought to account for their association with development of PD (Fernandes et al. 2016, Schöndorf et al. 2014).

It is thought that α-synuclein accumulation and aggregation probably contributes to neuronal death in PD, though the mechanisms leading to neurodegeneration are not clear. In addition to the visible Lewy body aggregates, α-synuclein also accumulates in other forms such as oligomers, which are precursors for aggregate development, and are thought to be the more toxic form of α-synuclein (Kalia et al. 2013a). Neuronal pathology and clinical abnormalities occur in models in which α-synuclein aggregates are induced through the administration of pathogenic pre-formed fibrils (PFFs) of α-synuclein or expression of aggregate-prone forms of α-synuclein, suggesting that α-synuclein aggregation does indeed have potential neurotoxic effects (Luk et al. 2012a, Luk et al. 2012b, Giasson et al. 2002). However, Lewy bodies are absent in some forms of familial PD, including in some cases associated with mutations in the relatively common *LRRK2* gene (Kalia et al. 2015), and a degree of uncertainty remains regarding their significance in patients.

It has been postulated that the progression of PD occurs due to transmission of α-synuclein pathology, with intercellular transmission of toxic species of α-synuclein resulting in propagation of pathology in a prion-like fashion, following a predictable anatomical sequence (See Table 1.1) (Braak et al. 2003). In the early stages of disease, Lewy body pathology occurs in the dorsal motor nucleus of the glossopharyngeal and vagus nerves and the olfactory system, before being seen in other brainstem structures such as the locus coeruleus, caudal raphe nuclei, and gigantocellular reticular nucleus. Pathology then progresses to involve the substantia nigra, before the cortex is affected (Braak et al. 2003, Kalia and Lang 2015).

Pathological Stage	Brain Region	Structures Involved
Stage 1	Medulla oblongata	Dorsal IX/X motor nucleus
		Intermediate reticular zone
	Olfactory system	Olfactory bulb
		Anterior olfactory nucleus
	Peripheral nervous system	Autonomic neurons
Stage 2	Medulla oblongata	Caudal raphe nuclei
		Gigantocellular reticular nucleus
	Pons	Locus coeruleus
Stage 3	Pons	Pedunculopontinue nucleus
	Midbrain	Substantia nigra pars compacta
	Basal forebrain	Nucleus basalis of Meynert
Stage 4	Limbic system	Accessory cortical and basolateral nuclei of amygdala
		Ventral claustrum
		Interstitial nucleus of stria terminalis
	Thalamus	Intralaminar nuclei of thalamus
	Temporal mesocortex	Anteromedial temporal mesocortex
		CA2 region of hippocampus
Stage 5	Neocortex	High order sensory association areas
		Prefrontal cortex
Stage 6	Neocortex	First order sensory association areas
		Premotor areas

Table 1.1 – Braak staging of Parkinson's disease pathology.

The natural history of PD reflects this proposed spread of pathology. Motor symptoms are often preceded by a number of non-motor features including anosmia, rapid eye movement (REM) sleep behaviour disorder (RBD), and gastrointestinal dysfunction, whilst dementia develops later in the disease course. Further supportive evidence for this hypothesis first emerged when typical Lewy body pathology was found in fetal mesencephalic neurons grafted into the brains of some PD patients (Li et al. 2016, Kordower et al. 2008). Additionally, the administration of exogenous α-synuclein PFFs and Lewy body fractionate from brain homogenates of PD patients to animals results in α-synuclein accumulation and neurodegeneration (Recasens et al. 2014, Luk et al. 2012a, Luk et al. 2012b). However, it should be noted that many patients do not develop the aforementioned prodromal features, and in another α-synucleinopathy, dementia with Lewy bodies (DLB), cognitive impairment develops early, suggesting that the development of α-synuclein pathology does not always follow this sequential propagation.

The processes through which α-synuclein may spread between cells are poorly defined, but it has been suggested that exosomal release of α-synuclein oligomers may allow for transmission (Danzer et al. 2012). This process may be of particular relevance in cases of

PD associated with *GBA1* mutations, as lysosomal dysfunction has been shown to increase the release of α-synuclein via exocytosis (Alvarez-Erviti et al. 2011, Bae et al. 2014).

1.3.2 Mitochondrial dysfunction in Parkinson's disease

Mitochondrial dysfunction has frequently been implicated in PD, and is thought to be important in its pathogenesis. This was initially highlighted by the fact that inadvertent inoculation with 1-methyl-4-phenyl-1,2,3,6-tetrahydropyridine (MPTP), which is converted to the neurotoxin 1-methyl-4-phenylpyridinium (MPP^+), resulted in a Parkinsonian syndrome in a cohort of individuals (Langston et al. 1983, Langston and Ballard 1983). MPP^+ is an inhibitor of the mitochondrial complex I and also leads to the generation of free radicals (Chiueh et al. 1992, Ramsay et al. 1991). Similarly the pesticide rotenone (another complex I inhibitor) results in nigrostriatal degeneration, with some reports of Lewy body-like pathology in rodents treated with this toxin (Betarbet et al. 2000). Mitochondrial toxins such as MPTP and rotenone have formed the basis of *in vivo* and *in vitro* models which have been employed to study the pathogenesis of PD, and the potential effects of treatments (Testa, Sherer and Greenamyre 2005, Bayliss et al. 2016b). Additionally, mitochondrial complex I activity has been reported to be reduced in the substantia nigra from PD patients in comparison to healthy controls, with similar results subsequently seen in other cell types (Schapira et al. 1989, Parker, Boyson and Parks 1989).

Additionally, many of the familial forms of PD-like syndromes occur due to mutations in genes encoding proteins involved in mitochondrial homeostasis. Mutations in the *PRKN*, *PINK1* and *FBXO7* genes for example result in early-onset autosomal recessive Parkinsonian syndromes, albeit with distinct clinical features to sporadic PD (Kitada et al. 1998, Valente et al. 2004, Di Fonzo et al. 2009). The proteins encoded by these genes, Parkin, PTEN-induced putative kinase-1 (PINK-1) and F-box only protein 7 (Fbxo7) are involved in a common pathway which is important in the initiation of mitophagy – clearance of dysfunctional mitochondria through the lysosome-autophagy system (Chen and Dorn 2013). In mitophagy, Parkin (an E3 ubiquitin-ligase) is recruited to

mitochondria, in a process dependent on PINK-1 and Fbxo7 (Narendra et al. 2008, Narendra et al. 2010, Burchell et al 2014). The recruitment of Parkin to mitochondria results in ubiquitination of several targets including mitochondrial fusion proteins (Zivani et al. 2010, Gegg et al. 2010). Clearance of mitochondria via this pathway appears to be dependent on P62/SQSTM1, which co-localises to Parkin on depolarised mitochondria, with knockout of P62/SQSTM1 resulting in loss of mitochondrial clearance following treatment with carbonyl cyanide 3-chloroyphenylhydrazone (CCCP) (Geisler et al. 2010). There is therefore considerable interest in the role that dysfunction of the mitophagy system may play in sporadic PD (Ryan et al. 2015).Similarly, mutations in *PARK7* which encodes DJ-1 result in an autosomal recessive familial Parkinsonian syndrome (Bonifati et al. 2003). This protein is involved in sustaining mitophagy and mitochondrial function under conditions of oxidant stress, and is thought to act in parallel to PINK-1 (Thomas et al. 2011). Dysfunction in these pathways therefore leads to persistence of abnormal mitochondria, and accumulation of reactive oxygen species with subsequent oxidative stress (Joselin et al. 2012).

The relationship between α-synuclein aggregation and mitochondrial dysfunction is not clear, but it has been suggested that mitochondrial deficits can occur as a downstream consequence of α-synuclein pathology. α-synuclein has been reported to co-localise with mitochondria in cell and animal models of PD (Martin et al. 2006, Devi et al. 2008). Similarly, at post-mortem α-synuclein has been seen to accumulate in mitochondria in nigral neurons of PD patients, which is associated with a reduction in complex I activity, thought to be due to a direct interaction between α-synuclein and complex I (Devi et al. 2008). This association of α-synuclein with mitochondria appears to be dependent on a 32 amino-acid N-terminal targeting signal (Devi et al. 2008). Mitochondrial deoxyribonucleic acid (DNA) damage and degeneration occurs to a greater extent in the nervous system of mice expressing the aggregate-prone A53T and A30P α-synuclein, in comparison to wild-type controls (Martin et al. 2006). Overexpression of α-synuclein in neuronal cell models has also been seen to alter mitochondrial morphology, and lead to increases in free-radical levels and reduced mitochondrial activity (Hsu et al. 2000, Kamp et al. 2010, Parihar et al. 2009), suggesting that mitochondrial dysfunction occurs secondary to α-synuclein pathology. However, it has also been suggested that instead of occurring downstream of α-synuclein pathology, mitochondrial oxidant stress is an early step in a sequential pathogenic pathway, in which increased levels of oxidised dopamine

result in lysosomal dysfunction and accumulation of α-synuclein (Burbulla et al. 2017). So whilst both α-synuclein aggregation and mitochondrial dysfunction are important in PD pathogenesis, the way in which these cell autonomous pathogenic processes interrelate appears to be complex, and is not fully understood.

1.3.3 Neuroinflammation in Parkinson's disease

The pathological processes discussed so far involve dysfunction of intracellular pathways or altered protein homeostasis within the degenerative cells themselves. However, non-cell-autonomous processes are also thought to play a role in PD pathogenesis, including a neuroinflammatory response involving microglia and astrocytes (Tansey and Goldberg 2010, Hirsch and Hunot 2009). This is supported by the fact that a single nucleotide polymorphism in the human leukocyte antigen DQ1b (HLA-DQ1b) region has been identified as a risk factor for PD (Saiki et al. 2010, Nalls et al. 2014). Neurotoxin-based animal models used to study PD are often associated with a glial response, though in some cases, toxins (e.g. 6-hydroxydopamine) are introduced intracerebrally, with disruption of the blood-brain-barrier. This may in itself herald an inflammatory response, which should be taken into account when interpreting results of such studies (Akiyama and McGeer 1989, McGeer et al. 2003). Additionally, in the case of MPTP, though acute exposure is often associated with an inflammatory response this is not seen with chronic exposure (Furuya et al. 2004). However, activated microglia have been observed in the substantia nigra of PD patients at autopsy suggesting that a neuroinflammatory response does occur (McGeer et al. 1988, Imamura et al. 2003). Additionally, an increased density of astrocytes has been observed in the substantia nigra of PD patients, though it is not known whether these findings constitute a protective response, or whether they contribute to neurodegeneration (Damier et al. 1993). Nevertheless, the neuroinflammatory response is considered an interesting potential therapeutic target for treatment of PD.

1.4 Introduction to *GBA1* mutation-associated Parkinson's disease

It has recently become clear that variants in the *GBA1* gene are an important risk factor for the development of PD (Sidransky et al. 2009). As well as being relatively prevalent in the PD population, *GBA1* abnormalities are also associated with an accelerated clinical course, making these patients an important clinical group to study.

1.4.1 Glucocerebrosidase and the *GBA1* gene

The *GBA1* gene consists of 11 exons and 10 introns in a 7.6 kb sequence, situated on the long arm of chromosome one (Horowitz et al. 1989). Its product, glucocerebrosidase (GCase) is a lysosomal enzyme responsible for the hydrolysis of glucosylceramide (also referred to as glucocerebroside) glycosphingolipids to ceramide and glucose (Beutler 1992). Transcription of the *GBA1* gene yields at least two mRNA sequences, dependent on alternate polyadenylation sites. The amino acid peptide products are then processed to form the 496 amino acid mature protein (Sorge et al. 1987, Migdalska-Richards and Schapira 2016). Genetic sequencing of the *GBA1* gene is complicated by the presence of a 5.7 kb pseudogene, which has sometimes impeded the identification of novel mutations. This pseudogene is situated 17 kb downstream of the *GBA1* gene and shares high sequence homology with the gene (Horowitz et al. 1989).

The GCase protein consists of three domains, the third of which has a triose phosphate isomerase barrel structure, and contains the catalytic site (Dvir et al. 2003). It is synthesised in the rough endoplasmic reticulum (ER), before transit across the Golgi apparatus via a phosphatidylinositol-4-kinase (PI4K)-dependent pathway and delivery to the lysosome. In contrast to most other lysosomal enzymes, for which delivery to the lysosome is dependent on mannose-6-phosphate receptors, transit of GCase to the lysosome is mediated by a specific transporter – lysosomal membrane protein-2 (LIMP-2), encoded by the *SCARB2* gene (Jović et al. 2012, Reczek et al. 2007, Ludwig, Le Borgne and Hoflack 1995). GCase and LIMP-2 become associated in the ER, before traversing the Golgi apparatus as a complex. The low pH environment of the lysosome results in dissociation of GCase from LIMP-2 (Reczek et al. 2007) Figure 1.1). Saposin C, cleaved from prosaposin, acts as a substrate-presenting co-factor and is required for enzymatic activity (O'Brien and Kishimoto 1991).

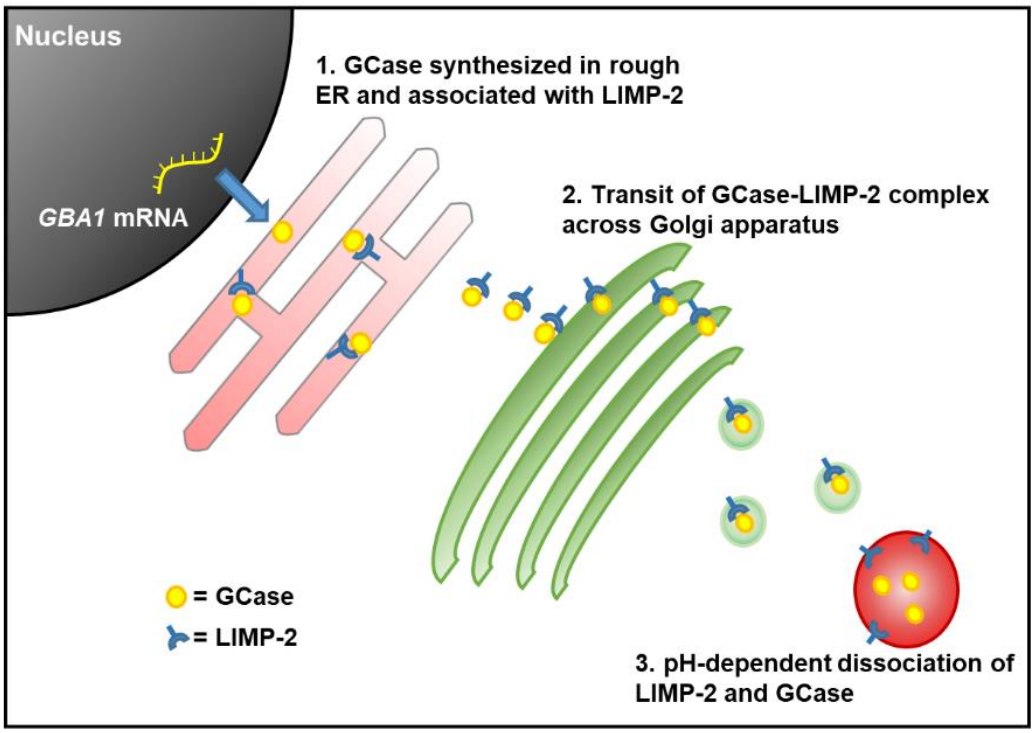

Figure 1.1 – Processing of GCase and LIMP-2. GCase is synthesised in the rough ER where it becomes associated with LIMP-2. The GCase-LIMP-2 complex is processed as it traverses the Golgi apparatus, before it reaches the lysosome. The acidic lysosomal environment causes dissociation of GCase from LIMP-2. Abbreviations: ER = endoplasmic reticulum; GCase = glucocerebrosidase; LIMP-2 = lysosomal membrane protein-2; mRNA = messenger ribonucleic acid. Adapted from (Stoker, Torsney and Barker 2018a).

1.4.2 Association between *GBA1* mutations and Parkinson's disease

Biallelic mutations in the *GBA1* gene result in the autosomal recessive storage disorder Gaucher disease (GD), in which there is negligible GCase enzymatic activity and accumulation of glucosylceramide in a number of cell types, particularly macrophages (Hruska et al. 2008). The classification of GD is determined by the presence or absence of neurodegenerative features, and the rate of progression (Grabowski 2008). Type one (non-neuronopathic) GD manifests with hepatosplenomegaly, bone lesions, thrombocytopaenia, and anaemia. Types two and three (neuronopathic) GD are characterised by progressive neurological decline in addition to peripheral features, with rapid progression in type three GD (Grabowski 2008). Over 300 mutations in the *GBA1*

gene have been reported, including point mutations, deletions and insertions, splice-site mutations and recombinations (Hruska et al. 2008, Lesage et al. 2011). There is a degree of genotype-phenotype correlation, with some mutations (e.g. L444P) being associated with neuronopathic disease and others (e.g. N370S) being associated with the more benign type one GD (Gan-Or et al. 2008).

At the end of the twentieth century, reports started to emerge linking PD to GD. It was initially noted that an adult-onset Parkinsonian syndrome developed in a proportion of type one GD patients (Neudorfer et al. 1996, Sidransky 2005, Tayebi et al. 2003). The subsequent observation that PD was prevalent in first-degree relatives of GD patients suggested that carrying a single *GBA1* mutation was a risk factor for the development of PD (Goker-Alpan et al. 2004, Halperin, Elstein and Zimran 2006). Approximately 10 % of type one GD patients develop PD by the age of 80 years, which is in comparison to about 3 to 4 % in the normal population (Rosenbloom et al. 2011). The prevalence of *GBA1* mutations in the PD population has been reported to be as high as 21 % (Lwin et al. 2004), though post-mortem studies, in which cohorts may be more likely to include early-onset or atypical forms of PD, have probably overestimated this figure, which is generally considered to be closer to 5 % (Winder-Rhodes et al. 2013, Kumar et al. 2013, Bras et al. 2009, Sidransky et al. 2009). This compares to a less than 1 % carrier rate in most healthy populations, though the prevalence varies in different ethnic groups (Sidransky et al. 2009). Mutations are particularly common in people of Ashkenazi Jewish origin, where there is carrier frequency of 15 to 20 % in the PD population, with the N370S mutation being by far the most common (Gan-Or et al. 2008, Sidransky et al. 2009). *GBA1* variants are overrepresented in early-onset PD, with about a 25 % carrier rate in those with disease onset under 50 years of age (Duran et al. 2013).

Mutations in the *GBA1* gene have also been associated with DLB, providing further support that there is a pathogenic link between this gene and α-synuclein pathology (Nalls et al. 2013, Goker-Alpan et al. 2006, Mata et al. 2008). Although an important genetic risk factor for PD, penetrance associated with *GBA1* mutations is low, with about 30% of carriers estimated to develop PD before age 80 years (Migdalska-Richards and Schapira 2016). Nevertheless, overall *GBA1* mutations increase the risk of PD by 20- to 30-fold, and taking into account their prevalence, they represent numerically the most significant

known genetic risk factor for PD (Lesage et al. 2011, Lesage and Brice 2009, Sidransky et al. 2009).

1.4.3 Pathogenesis and clinical features of *GBA1* mutation-associated Parkinson's disease

The clinical features and pathogenesis of *GBA1* mutation-associated PD are discussed in detail in chapters 2 and 4 respectively, but the general principals are introduced here.

The mechanisms through which *GBA1* variants predispose to PD are complex. Clinical manifestations of GD arise due to a reduction in GCase enzyme activity and accumulation of it substrates (Grabowski 2008). Similarly, GCase activity has been reported to be reduced in brains and blood spots of individuals with *GBA1* mutation-associated PD (hereafter referred to as *GBA1*-PD) (Rocha et al. 2015a, Alcalay et al. 2015). Additionally, chemical suppression of GCase activity results in accumulation of α-synuclein in cell and animal models, supporting the idea that a reduction in GCase activity can precipitate PD pathology (Rocha et al. 2015b, Manning-Boğ, Schüle and Langston 2009). Reduced GCase activity has also been noted in PD patients with "idiopathic" PD (with no *GBA1* mutations – hereafter referred to as iPD), and indeed in association with normal aging (Rocha et al. 2015a, Murphy et al. 2014) Furthermore, augmentation of GCase activity has been observed to reduce α-synuclein pathology in animal models and in induced pluripotent stem cell (iPSC)-derived neurons (Sardi et al. 2013, Osellame et al. 2013, Mazzulli et al. 2016). It is possible that reduced GCase activity allows for accumulation of sphingolipids (Schöndorf et al. 2014, Rocha et al. 2015a, Xu et al. 2011) which potentially stabilise the pathogenic forms of α-synuclein, facilitating its accumulation and aggregation (Mazzulli et al. 2011, Zunke et al. 2017). However, the role of sphingolipid accumulation in *GBA1*-PD is unclear. Higher glycosphingolipid levels have been correlated with reduced GCase enzyme activity in the brains of patients with iPD (Rocha et al. 2015a). However, in another post-mortem study there were no differences between the levels of glycosphingolipids in healthy controls, and patients with iPD or *GBA1*-PD (Gegg et al. 2015). Whilst reduced GCase enzyme activity may result in elevated glycosphingolipid levels, the importance of this in the pathogenesis of *GBA1*-PD is uncertain.

However, several observations are inconsistent with a primary loss-of-function mechanism in *GBA1*-PD. Firstly, PD only occurs in a minority of GD patients, where GCase activity is negligible (Rosenbloom et al. 2011). If the risk associated with heterozygous *GBA1* mutations could be attributed to loss of enzyme activity, a much higher incidence of PD within the GD population would be expected. Additionally, *GBA1* variants which are not associated with a significant reduction in enzyme activity (and are hence not associated with GD) are common in PD (Duran et al. 2013). The risk conveyed by *GBA1* mutations are therefore not completely explained by a reduction in GCase activity.

Alternatively, it has been argued that *GBA1* mutations may confer a deleterious gain-of-function effect. Most pathogenic *GBA1* mutations result in misfolding of GCase, such that it is retained in the ER, causing ER stress and subsequent activation of the unfolded protein response (Fernandes et al. 2016). Additionally, mutant GCase is more likely to be identified in Lewy bodies than wild-type GCase, suggesting that there is potentially a direct interaction between α-synuclein and toxic forms of GCase (Goker-Alpan et al. 2010). However, null mutations may be associated with increased risk of PD, and reduction in enzyme activity (through genetic knock-down or chemical inhibition) can recapitulate some aspects of PD pathology as discussed above (Mazzulli et al. 2011, Rocha et al. 2015b, Manning-Boğ et al. 2009, Cleeter et al. 2013). Hence, the pathogenesis of *GBA1*-PD cannot be fully accounted for by a toxic effect of mutant *GBA1*.

GBA1 mutations may therefore act through more than one mechanism to predispose to the development of PD. Dysfunction of the lysosome-autophagy system has been well established as a feature of *GBA1*-PD (Mazzulli et al. 2011, Li et al. 2018), and a smaller number of studies have identified mitochondrial dysfunction and ER stress (Fernandes et al. 2016, Cleeter et al. 2013, Osellame et al. 2013, Xu et al. 2014). The evidence for these pathogenic mechanisms are discussed in detail in chapter 4.

At an individual level, *GBA1*-PD is indistinguishable from iPD. However, at a population level, *GBA1* mutations confer an earlier age of onset by about five years, and a more

aggressive clinical course (Brockmann et al. 2015, Clark et al. 2007, Nichols et al. 2009, Jesús et al. 2016). Several epidemiological studies have identified an increased risk of cognitive impairment and PD dementia in the context of *GBA1* mutations (Setó-Salvia et al. 2012, Winder-Rhodes et al. 2013, Brockmann et al. 2015, Cilia et al. 2016, Lunde et al. 2018, Oeda et al. 2015). Additionally, motor progression seems to take a more rapid course in *GBA1*-PD (Winder-Rhodes et al. 2013, Davis et al. 2016b, Brockmann et al. 2015). A number of non-motor features including depression and rapid eye movement RBD are also said to be more common in *GBA1*-PD, potentially reflecting more widespread pathology (Neumann et al. 2009, Beavan et al. 2015, Goker-Alpan et al. 2008). Some of these features are also more prevalent in healthy carriers of *GBA1* mutations compared to non-carriers, potentially reflecting a prodromal stage of PD (Beavan et al. 2015). Clinical aspects of *GBA1*-PD are discussed further in chapter 2.

1.5 Current and emerging treatments for Parkinson's disease

There are no established disease-modifying treatments for PD, with current management being symptomatic. The mainstay of PD treatments are dopaminergic drugs, used to replenish striatal dopamine levels. Most patients ultimately require treatment with preparations containing the dopamine precursor, levodopa. Other commonly used drugs include dopamine receptor agonists and inhibitors of the enzymes responsible for dopamine metabolism (monoamine oxidase B (MAO-B) and catechol-O-methyltransferase (COMT)). These drugs can be effective in controlling the motor symptoms, but can be associated with significant adverse effects and they do not alter the course of disease (Jenner 2003). An alternative approach to the treatment of motor symptoms, particularly in patients that experience significant adverse effects from levodopa, is the use of deep brain stimulation, which again does not alter disease progression (Kalia, Sankar and Lozano 2013b). None of these approaches help with the, often disabling, non-motor aspects of PD which have a significant impact on quality of life.

A number of experimental treatment approaches are emerging, some of which are designed to control the motor symptoms in a more physiological manner than is achieved

by existing treatments, while others target the underlying pathogenic processes, with the aim of slowing disease progression. The former category includes cell-replacement therapies, such as embryonic stem cell- and iPSC-derived neural progenitors which are beginning to enter clinical trials (Barker et al. 2017). Gene therapies have also entered clinical trials, in which enzymes involved in the synthesis of dopamine are introduced into striatal cells, boosting striatal dopamine levels (Palfi et al. 2014). Theoretically, more physiological and targeted release of dopamine would allow for treatment of the motor aspects of PD with a reduced risk of the significant adverse effects associated with current treatments.

Putative disease-modifying approaches include the use of immunotherapies against α-synuclein, which aim to reduce α-synuclein levels and potentially propagation of pathology, and a number of these have entered clinical trials (Brundin, Dave and Kordower 2017, Stoker, Torsney and Barker 2018b). Other drugs targeting pathogenic mechanisms associated with PD (e.g. nilotinib a tyrosine kinase inhibitor which facilitates delivery of α-synuclein to lysosomes, and ambroxol hydrochloride which acts as a chaperone molecule facilitating the folding of GCase) have also entered clinical trials (Hebron, Lonskaya and Moussa 2013, Pagan et al. 2016, Silveira et al. 2019).

However, no agents so far have been able to translate promising pre-clinical results to clinical efficacy (Kieburtz and Ravina 2007). The detection of disease-modifying agents has been hindered by a lack of truly representative disease models of PD, which generally involve animals receiving acute treatment with nigral toxins such as MPTP or rotenone, introduction of aggregate-prone forms of α-synuclein which only occur in rare forms of familial PD, or overexpression of α-synuclein to supra-physiological levels (Beal 2001). These models are discussed further in chapter 5. The novel technique of direct reprogramming to generate induced neurons (iNs) potentially offers a more faithful disease model, and in this project iNs have been used to test drugs for potential disease-modifying effects.

1.6 Introduction to direct neuronal reprogramming

Given the limitations of the aforementioned experimental models used to study PD and other neurodegenerative diseases, a platform which better represents the pathological mechanisms and risk profiles that contribute to PD in patients is needed. It is desirable for such a model to involve adult human neurons from patients, which possess the (as yet poorly understood) polygenic risk factor profile that contributes to PD development. Additionally, given that PD is a disease of aged neurons, it would also be beneficial for such a model to retain the effects of age on cells, which may precipitate the development of, or increase vulnerability to PD pathology.

Direct conversion of patient-derived somatic cells into iNs is potentially a method of achieving these aims. Generation of iNs was first achieved in 2010 using mouse fibroblasts (Vierbuchen et al. 2010). Derivation of iNs from human cells proved more challenging, particularly from adult cells, but novel reprogramming protocols have allowed for the generation of aged, human iNs (Pang et al. 2011, Pfisterer et al. 2011b). However, the use of iNs for disease-modelling has been limited to only a small number of studies to date, which are discussed in chapter 3.

1.6.1 Transcription factor driven reprogramming

The first iN protocols involved the forced expression of proneural transcription factors in fibroblasts (Vierbuchen et al. 2010). In this study 19 candidate genes were initially investigated for their ability to drive conversion of fibroblasts into iNs, and a combination of three factors was found to achieve efficient conversion. These included achaete-scute homolog 1 (Ascl1 – a basic helix-loop-helix (bHLH) transcription factor expressed in neural progenitor cells (Lo et al. 1991)), Brn2 (a POU-homeodomain family transcription factor) and Myt1-L (a zinc finger superfamily transcription factor) – a combination termed the “BAM factors” (Vierbuchen et al. 2010). These factors were also capable of driving conversion of endodermal cells (e.g. hepatocytes) to iNs (Marro et al. 2011).

After the initial report of iN generation in murine fibroblasts, it was demonstrated that this technique could also be applied to human fetal fibroblasts (from gestational age 8 to 10 weeks), and to post-natal human fibroblasts (aged up to 11 years) (Pang et al. 2011).

However, whilst reprogramming using the BAM factors resulted in neuronal morphology and expression of the neuronal marker β3-tubulin, these cells were functionally immature. A further 20 factors were tested for their ability to improve the reprogramming, and it was found that the addition of NeuroD1 (another bHLH transcription factor) improved conversion efficiency by two to three-fold, as well as neuronal maturity (Pang et al. 2011). The BAM factors were also shown to drive the conversion of human adult lung fibroblasts (from donors aged up to 65 years) to functional iNs, at a conversion efficiency comparable to that achieved with human fetal and post-natal fibroblasts (Pfisterer et al. 2011b).

1.6.1.1 Direct conversion to neuronal subtypes

Early protocols for direct conversion generally yielded non-specific neuronal types, expressing a number of pan-neuronal markers such as microtubule-associated protein two (MAP2) and β3-tubulin (Pfisterer et al. 2011b, Pang et al. 2011, Vierbuchen et al. 2010). Given that many neurological diseases predominantly affect a specific type of neuron, it was therefore desirable to demonstrate that direct conversion could be used to generate populations of subtype-specific neurons. Caiazzo *et al* employed Ascl1 in combination with nuclear receptor-related-1 (Nurr1) and LIM homeobox transcription factor one α (Lmx1a – a transcription factors known to be expressed in nigral dopaminergic neurons) to generate dopaminergic neurons from murine and human fibroblasts (Caiazzo et al. 2011). In mouse embryonic fibroblasts, a relatively high purity of tyrosine hydroxylase-(TH-) positive, dopamine-releasing cells was generated (85 % of converted cells) (Caiazzo et al. 2011). In human fetal and adult fibroblasts, TH-positive cells could be produced, albeit at a much lower efficiency (6 % and 3 % of cells that were successfully transfected for fetal and adult fibroblasts respectively (Caiazzo et al. 2011)). It should be noted that the way in which conversion efficiency has been defined varies between studies, with some quoting the number of iNs as a proportion of the transfected cells, and others reporting the number of iNs as a proportion of the total number of cells in the starting population. Given that not all cells are successfully transfected with the viral vector, the absolute conversion efficiencies are therefore likely to be lower than the reported figures in some studies.

Around the same time, Pfisterer *et al* also attempted to generate subtype dopaminergic iNs from human embryonic fibroblasts (Pfisterer et al. 2011a). A pool of 10 genes involved in midbrain and dopaminergic neuron patterning were tested, which were used in combination with the BAM factors. The combination of all 10 factors resulted in the emergence of small numbers of TH-positive cells. The yield of TH-positive iNs was greatest when the transcription factor pool was limited to just two of these factors (Lmx1a and forkhead box protein A two (FoxA2)) in combination with the BAM factors. With this combination of transcription factors, approximately 5 to 10 % of the iNs were TH-positive (Pfisterer et al. 2011a).

Other studies have focused on the generation of striatal medium spiny neurons, which are particularly vulnerable in Huntington's disease (Walker 2007). The addition of the transcription factors CTIP2, DLX1, DLX2, and Myt1-L ("CDM" factors) to microRNA-mediated conversion protocols (discussed in section 1.6.2) has been shown to yield a high purity of medium spiny neurons (Huh et al. 2016, Victor et al. 2014), which when grafted into mice survive for long periods and integrate into functional circuits (Victor et al. 2014).

The addition of motor neuron specification factors (Lhx3, Hb9, Isl1 and Ngn2) to the BAM factors allowed for the generation of spinal motor neurons from mouse fibroblasts, which resembled embryonic motor neurons morphologically, electrophysiologically, and in terms of the transcriptome (Son et al. 2011). The addition of NeuroD1 to this combination of transcription factors allowed for the generation of cholinergic motor iNs from human fibroblasts. Sensory neurons have also been directly generated from fibroblasts, using the BAM factors, in combination with Isl1, Ngn1, and Klf7 (Wainger et al. 2015). Derivation of sensory neurons can also be achieved independently of Ascl1 expression, through the expression of Brn3a in combination with Ngn1 or Ngn2 (Blanchard et al. 2015).

1.6.1.2 Mechanisms of transcription factor driven direct reprogramming

BAM factor driven reprogramming has been shown to be dependent on a short period of transgene expression at the start of the conversion process. Withdrawal of inducible transgene expression at day three, does not significantly alter conversion efficiency (Pfisterer et al. 2011a). This observation suggests that, whilst it is important that defined factors are expressed early during a conversion, subsequent changes are mediated by endogenous downstream events. In the early stages of BAM-driven reprogramming, the majority of transcriptional changes represent upregulation of neuronal genes, with downregulation of the parent cell-type programme occurring later (Wapinski et al. 2013).

Several of the early iN studies showed that forced expression of Ascl1 alone is sufficient to induce conversion to iNs, albeit with less complex neuronal morphology and low efficiency when compared to reprogramming in combination with other factors (Pfisterer et al. 2011a, Pang et al. 2011, Vierbuchen et al. 2010, Liu et al. 2013). Chromatin immunoprecipitation and high-throughput sequencing analysis at 48 hours post-transduction with the BAM factors showed that Ascl1 had bound to a large number of sites across the genome, and it did so independent of Brn2 or Myt1-L expression (Wapinski et al. 2013). The Ascl1 binding sites in fibroblasts strongly overlapped with those in neural precursor cells, and were predominantly in regions deplete of open chromatin, suggesting that it acts as a pioneer factor (Wapinski et al. 2013).

There were fewer Brn2 binding sites in comparison to those for Ascl1, and these were predominantly in regions of accessible chromatin. About a quarter of the Brn2 sites were also bound by Ascl1, suggesting that Ascl1 recruits Brn2 to a proportion of its binding sites (Wapinski et al. 2013). Similarly, Myt1-L preferentially bound to open chromatin sites. In contrast to Ascl1 and Brn2 the function of Myt1-L in neuronal reprogramming is to down-regulate genes (Mall et al. 2017). Down-regulated genes include those important in differentiation programs of multiple non-neuronal systems (e.g. cartilage, heart and lung development) as well as negative-regulators of neuronal differentiation (such as those involved in the Notch and Wnt pathways) (Mall et al. 2017). This suggests that it is acting as a repressor of "all-but-one" cell fates, and its expression is important in suppressing the parent cell phenotype during direct reprogramming.

The mechanism of BAM factor-driven reprogramming therefore, appears to be dependent on two predominant processes. Firstly, Ascl1 accesses closed chromatin sites, causing upregulation of a number of transcription factors (including Zfp238, Lmo2, Rfx1, and Tcfl5), as well as recruiting Brn2 to its target sites, with subsequent expression of neuronal genes (Wapinski et al. 2013). Secondly, Myt1-L binds to a number of sites, which result in downregulation of non-neuronal programmes, and suppression of original parent cell properties (Figure 1.2) (Mall et al. 2017).

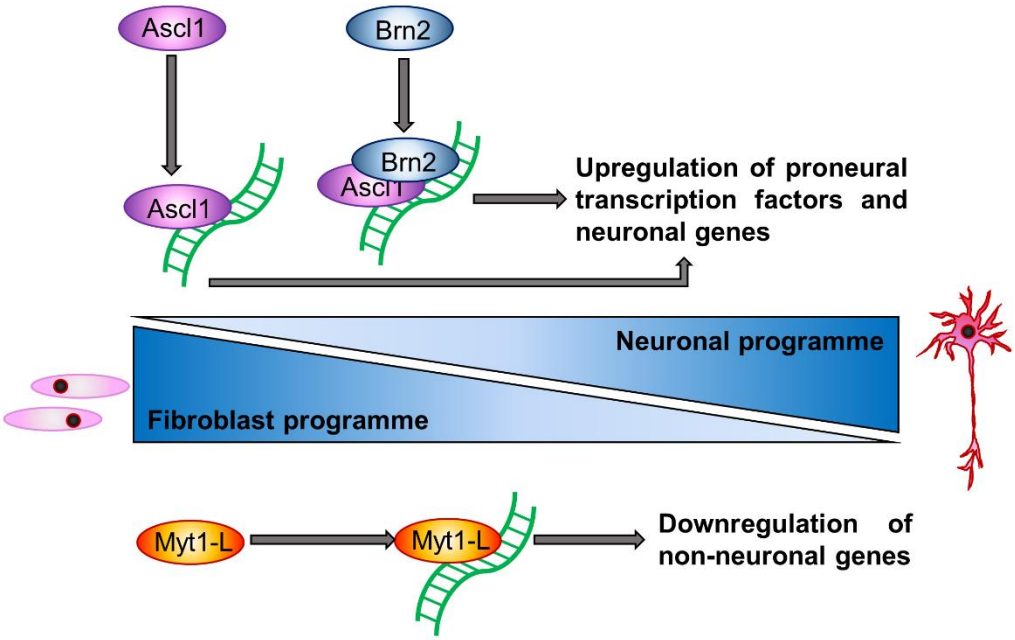

Figure 1.2 – Mechanisms of BAM factor-driven reprogramming. The proneural transcription factors Ascl1 and Brn2 bind to target sites on DNA resulting in upregulation of proneural transcription factors and neuronal genes. Ascl1 acts as a pioneer factor, binding to closed chromatin sites, and is involved in recruiting Brn2 to its target sites. Myt1-L acts through an alternative mechanism, resulting in the downregulation of non-neuronal transcripts.

1.6.2 The RE1-silencing transcription factor complex and microRNA-mediated reprogramming

Whilst it is possible to generate iNs from human cells through expression of proneural transcription factors, conversion efficiency is much lower than that seen when

reprogramming murine cells. However, the use of specific microRNA molecules in reprogramming protocols has been shown to enhance the direct reprogramming of human somatic cells into iNs (Huh et al. 2016, Victor et al. 2014, Yoo et al. 2011, Ambasudhan et al. 2011).

Neuronal differentiation is dependent on a conformational shift in Brg1-like-associated factor (BAF) chromatin remodelling complexes (the human analogues of SWItch/Sucrose Non-Fermentable- (SWI/SNF-) complexes). These are large multi-unit complexes in which different homologues and splice variants confer functional specificity (Zheng et al. 2012, Wu, Lessard and Crabtree 2009). For example neuronal cells contain the components BAF53B and BAF45B, while their progenitors contain BAF53A and BAF45A (Olave et al. 2002, Lessard et al. 2007). The microRNA molecules, microRNA-9/9* (miR-9/9*) and microRNA-124 (miR-124) have been shown to be particularly important in driving this switch (Yoo et al. 2009). Additionally, miR-124 has been shown to reduce non-neuronal transcripts, suggesting that it has a permissive function for neuronal differentiation (Conaco et al. 2006, Lim et al. 2005). Expression of these microRNA molecules alone is sufficient for fibroblasts to be reprogrammed into iNs, but neuronal purity improves when combined with the bHLH transcription factor, neuroD2 as well as Ascl1 and Myt1-L (Yoo et al. 2011).

The RE1-silencing transcription factor (REST) complex is known to prevent expression of these neuron-specific microRNAs, as well as neuronal genes containing the 23 bp repressor element RE-1 (Conaco et al. 2006, Johnson et al. 2007). As such, REST prevents expression of the neuronal programme in early neural progenitors, and in non-neuronal cells, in which it is highly expressed (Chong et al. 1995). As a cell transitions from an immature progenitor to a post-mitotic neuron, REST is downregulated, permitting expression of neuronal genes and microRNAs (Ballas et al. 2005). REST levels are higher in adult fibroblasts compared to fetal fibroblasts, posing a specific barrier to the reprogramming of human adult cells (Drouin-Ouellet et al. 2017). An alternative approach to improving the efficiency of direct conversion in adult human cells therefore, is to suppress the REST complex, which in turn allows for the expression of miR-9/9*, miR-124 and other neuronal genes (Drouin-Ouellet et al. 2017, Villanueva-Paz et al. 2019, Xue et al. 2013, Masserdotti et al. 2015). Additionally, miR-9/9* and miR-124 have

been shown to impair the pathway leading to the REST complex accessing DNA, so that they prevent its neurorepressive effect (Lee et al. 2018).

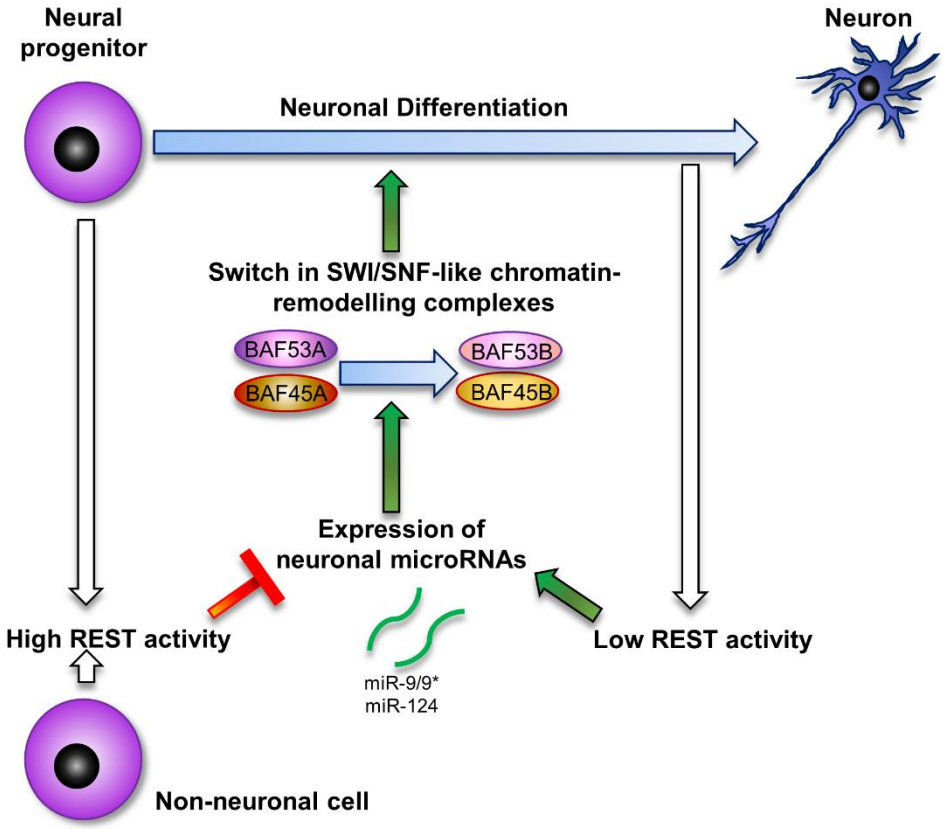

Figure 1.3 – MicroRNAs and the REST complex in neuronal differentiation. Neuron-specific microRNAs (miR-9/9* and miR-124) cause a switch in SWI/SNF-like chromatin remodelling complexes, allowing for neuronal differentiation to occur. In non-neuronal cells, the REST complex prevents expression of these microRNAs, preventing neuronal differentiation. Downregulation of, or suppression of REST, allows for the expression of these microRNAs, and differentiation to a neuronal phenotype. Abbreviations: miR-9/9* = microRNA-9/9*; miR-124 = microRNA-124; REST = RE1-silencing transcription factor complex.

1.6.3 Small molecules used in direct neuronal reprogramming

The use of specific small molecules and growth factors can significantly enhance the efficiency of direct reprograming protocols. The use of SMAD inhibition (using

SB431542 and noggin), in combination with the glycogen synthase kinase three β (GSK-3β) inhibitor CHIR99021 for up to two weeks significantly enhances transcription factor-driven direct reprograming of human cells (Ladewig et al. 2012). Prolongation of exposure to these factors beyond two weeks, does not enhance conversion any further, but impairs the acquisition of neuronal morphology, which is thought to be due to the effect of GSK-3β inhibition on neurite development (Ladewig et al. 2012).

It has also been shown to be possible to generate iNs using a set of small molecules, without introducing proneural transcription factors or microRNAs (Hu et al. 2015). This required induction using a cocktail of seven factors (valproic acid, CHIR99021, repsox, forsokolin, SP600125, GO6983, Y-27632), before switching to a maturation medium containing CHIR99021, forsokolin and doromorphin, along with the neurotrophic growth factors glial cell line-derived neurotrophic factor (GDNF), brain-derived neurotrophic factor (BDNF) and neurotrophin three (NT3), after eight days. Other small molecule targets including cyclic adenosine monophosphate- (cAMP) and bone morphogenic protein (BMP) signalling have also been shown to enhance reprogramming (Liu et al. 2013). Combinations of these factors are therefore now routinely incorporated into direct conversion protocols.

Study	Reprogramming Methods	Parent Cell Type	Neuronal Subtype	Efficiency and Purity
Vierbuchen et al. 2010	Ascl1, Brn2, Myt1-L	Mouse embryonic fibroblasts Mouse tail-tip fibroblasts	Glutamatergic and GABAergic	Conversion efficiency 3.6-23.1 % Neuronal purity ~45 %
Pang et al. 2011	Ascl1, Brn2, Myt1-L, neuroD1	Human fetal fibroblasts	Glutamatergic (53.7 %), TH (9 %); forebrain (17%), peripheral neuron (21%)	Conversion efficiency 2-4 %
		Human post-natal fibroblasts (up to age 11)	Glutamatergic (72.5 %), forebrain (81 %), peripheral neuron (15 %)	
Pfisterer et al. 2011b	Ascl1, Brn2, Myt1-L	Adult human lung fibroblasts (age 23 to 65 years)	Not reported	Conversion efficiency ~1-4 %
Ambasudhan et al. 2011	miR-124, Brn2, Myt1-L	Human post-natal fibroblasts	Glutamatergic and GABAergic	Conversion efficiency 4-8 %
		Human adult fibroblasts	Glutamatergic	Conversion efficiency ~6 %
Son et al. 2011	Ascl1, Brn2, Myt1-L, Lhx3, Hb9, Isl1, Ngn2	Mouse embryonic fibroblasts Mouse tail-tip fibroblasts	Spinal motor neurons	Conversion efficiency 5-10 % for spinal motor neurons
	Ascl1, Brn2, Myt1-L, Lhx3, Hb9, Isl1, Ngn2, NeuroD1	Human embryonic fibroblasts	Cholinergic motor neurons	10-15 % of infected cells converted to spinal motor neurons
Caiazzo et al. 2011	Ascl1, Nurr1, Lmx1a	Mouse embryonic fibroblasts	Dopaminergic (85 % of iNs)	18 % neuronal purity
		Human fetal fibroblasts	Dopaminergic	10 % of infected cells converted to iNs 6 % of infected cells converted to TH-positive iNs
		Human adult fibroblasts	Dopaminergic	5 % of infected cells converted to iNs 3 % of infected cells converted to TH-positive iNs
Pfisterer et al. 2011a	Ascl1, Brn2, Myt1-L	Human embryonic fibroblasts (5.5 to 7 week gestation)	Not reported	Conversion efficiency 16 % at day 24
		Human post-natal fibroblasts	Glutamatergic and GABAergic	Conversion efficiency 4.3 % at day 12
	Ascl1, Brn2, Myt1-L, Lmx1a2, FoxA2	Human embryonic fibroblasts (5.5 to 7 week gestation)	Dopaminergic	~5-10 % of iNs positive for TH
Yoo et al. 2011	miR-9/9*, miR-124, NeuroD2, Ascl1, Myt1-L	Human post-natal fibroblasts	Glutamatergic and GABAergic	Neuronal purity ~ 80% at day 30 Conversion efficiency ~ 5% at day 30
		Human adult fibroblasts	Not reported	Not reported

Ladewig et al. 2012	*Ascl1*, *Ngn2*, SB431542, noggin, LDN-193189, CHIR99021	Human post-natal fibroblasts	Glutamatergic, GABAergic, serotoninergic	Neuronal purity 75 % Conversion efficiency 168.5 %
Liu et al. 2013	NGN2, forskolin, dorsomorphin	Human fetal lung fibroblasts	Glutamatergic Cholinergic	95 % of transduced cells MAP2 positive
		Human post-natal and adult fibroblasts	Cholinergic	95 % of transduced cells β3-tubulin-positive
Victor et al. 2014	miR-9/9*, miR-124, CTIP2, DLX1, DLX2, Myt1-L, Bcl-xL	Human post-natal fibroblasts	Striatal medium spiny neurons	Neuronal purity ~90 % at five weeks (70 % purity for DARPP-32-positive GABAergic neurons)
		Human adult fibroblasts		Not reported
Hu et al. 2015	Small molecules and growth factors (see above)	Human adult fibroblasts	Glutamatergic	Conversion efficiency ~15 % Neuronal purity ~20-25 %
Huh et al. 2016	miR-9/9*, miR-124, CTIP2, DLX1, DLX2, Myt1-L, Bcl-xL		Striatal medium spiny neurons	Neuronal purity ~70-80 % at day 30
Drouin-Ouellet et al. 2017	Ascl1, Brn2, REST suppression	Human adult fibroblasts		Conversion efficiency ~ 35 % to 45 % Neuronal purity ~60 %
Villanueva-paz 2019	Ascl1, Brn2, REST suppression	Human adult fibroblasts		Conversion efficiency and neuronal purity ~50 % in healthy controls and ~70 % in MERRF patients

Table 1.2 – Summary of published iN conversion protocols. Abbreviations: GABA = gamma-aminobutyric acid; MERRF = myoclonic epilepsy with ragged red fibres; REST = RE1-silencing transcription factor complex; TH = tyrosine hydroxylase

1.7 Overview of project

The following chapters detail the studies that have been performed as part of my thesis. Broadly, these can be divided into a clinical study of the natural history of *GBA1*-PD, and an *in vitro* study in which patient-derived fibroblasts and iNs have been used to investigate pathology and as a screening tool for drugs in *GBA1*-PD.

In chapter 2, the results of a clinical study are described in which two locally acquired community-based cohorts of incident PD patients have been analysed, with a view to better characterisation of the natural history of *GBA1*-PD, in contrast to iPD. This study was perhaps better positioned to do this than most previous epidemiological studies of *GBA1*-PD given that all patients were incident, with most being followed up from the time of diagnosis to the onset of adverse outcomes including development of dementia, development of postural instability, and death. Additionally, the long duration of follow-up meant that most patients reached these outcomes.

Chapters 3 to 5 focus on the generation of iNs from patients with *GBA1*-PD, as well as those with iPD and healthy controls. iNs, and the parent fibroblasts have been used to establish baseline pathology of *GBA1*-PD. Treatment with PFFs of α-synuclein were used to induce PD-relevant pathology in this system, which was greatest in the *GBA1*-PD group. This model was then used as the basis for initial drug-screening studies for four putative disease-modifying treatments targeting the lysosome-autophagy system and mitochondrial function.

2 CLINICAL ASPECTS OF *GBA1* VARIANT-ASSOCIATED PARKINSON'S DISEASE

2.1 Abstract

GBA1 mutations are considered an important risk factor for PD, being found in approximately 5 % to 10 % of patients with so called sporadic disease. Furthermore, they have previously been reported to adversely affect clinical course, with increased risk of dementia, and potentially increased rate of motor progression. Previous observational studies have been limited by relatively short follow-up periods, and in some cases, small sample sizes. The impact of *GBA1* mutations on mortality in PD has not been established. Additionally, a number of polymorphisms in the *GBA1* gene have been associated with PD, though their role in terms of altering disease course is disputed. In this study, two cohorts of incident PD patients have been investigated to determine the effect of *GBA1* mutations and polymorphisms on key disease milestones, including development of dementia, progression to postural instability, and time to death. Additionally, the effect of concomitant genetic risk factors in *GBA1*-PD has also been studied. *GBA1* mutations and polymorphisms were found to significantly adversely alter the natural history of PD, which included a shorter time to death in both groups of patients.

2.2 Introduction to chapter

Several epidemiological studies have been performed, aiming to characterise the natural history of *GBA1*-PD in patient cohorts. Whilst it has become clear that *GBA1* mutations adversely affect the clinical course of PD, there remain questions about the degree to which *GBA1*-PD differs clinically from iPD, and about the importance of some "non-

pathogenic" *GBA1* variants. The epidemiological study of *GBA1*-PD has been limited by the fact that most studies have been performed in prevalent cohorts of PD patients, with a relatively short follow up period, often meaning that only a small proportion of patients reach outcome measures. In order to get a clearer picture of the natural history of PD, it would be preferable to follow up incident PD patients longitudinally, from diagnosis to the development of relevant disease milestones such as dementia or death.

Prospective follow up of incident PD patients has been limited to only a small number of studies to date (Winder-Rhodes et al. 2013, Lunde et al. 2018). This chapter discusses the analysis of the long-term follow up from two incident PD cohorts, including the CamPaIGN cohort which now has a longer follow up time than any previously published epidemiological study of *GBA1*-PD. *GBA1* variants seen in PD include mutations known to cause GD (e.g. N370S, L444P) and polymorphisms that have not been associated with GD (e.g. E326K and T369M), with most studies either focussing on one or other of these groups, or analysing them separately. In this study, data is presented for carriers of pathogenic mutations, "non-pathogenic" polymorphisms, as well as all variant carriers (combining the first two groups).

2.2.1 Cognitive decline and dementia in *GBA1* variant-associated Parkinson's disease

The most consistent finding in clinical studies of *GBA1*-PD has been an increased risk of cognitive impairment and dementia, which has been demonstrated in a number of studies in European (Setó-Salvia et al. 2012, Winder-Rhodes et al. 2013, Brockmann et al. 2015, Cilia et al. 2016, Lunde et al. 2018) and Japanese (Oeda et al. 2015) cohorts. Carriers of pathogenic *GBA1* mutations have been shown to have an approximately three- to eight-fold increased risk of development of dementia, in comparison to non-carriers in longitudinal studies (Winder-Rhodes et al. 2013, Lunde et al. 2018, Oeda et al. 2015, Cilia et al. 2016). Additionally, pathogenic mutations have also been associated with accelerated decline in cognitive function as defined by Montreal Cognitive Assessment (MOCA) (Brockmann et al. 2015) and Mini-Mental State Examination (MMSE) scores (Cilia et al. 2016).

The impact of *GBA1* polymorphisms, such as E326K and T369M is less clear, but in most studies in which carriers of such variants have been included, these have been associated with a trend towards an increased risk of dementia. In incident cohorts from the United Kingdom (Winder-Rhodes et al. 2013) and Northern Europe (Lunde et al. 2018), carriers of these *GBA1* polymorphisms had an increased risk of dementia in comparison to patients with no *GBA1* abnormality, with hazard ratios of 3.3 and 2.0 respectively. However, a Japanese study (in which 29 PD patients carrying *GBA1* abnormalities not known to cause GD were followed up) found that these polymorphism carriers had no increase in dementia risk in comparison to non-carriers (Oeda et al. 2015). It should be noted that in this study, the polymorphisms identified did not include the common E326K or T369M variants, so the authors could not comment on the significance of these (Oeda et al. 2015). In a longitudinal multi-centre study of 32 E326K carriers in the USA, this polymorphism was found to confer an approximately three-fold greater risk of progression to mild cognitive impairment and dementia in comparison to non-carriers, with almost 50 % of E326K carriers reaching these outcomes within the three year follow up (Davis et al. 2016b). It should be noted that in this study there was no increase in risk of mild cognitive impairment or dementia in the carriers of pathogenic mutations, even despite a particularly high frequency of the aggressive L444P mutation (Davis et al. 2016b). These longitudinal studies have been performed in small cohorts, with relatively short follow-up times, which probably accounts for the inter-study variability.

As well as conveying an increased risk of dementia in PD patients, one study of healthy carriers of *GBA1* mutations with no symptoms of PD found an accelerated rate of decline in cognitive scores (MMSE and MOCA) in comparison to non-carriers, after a two year follow up period (Beavan et al. 2015). The authors postulated that this decline may represent an increased frequency of mild cognitive impairment as a prodromal feature of PD in carriers of *GBA1* mutation, though it is not known how many of these patients subsequently went on to develop PD.

A large meta-analysis of seven longitudinal cohorts, investigated the clinical heterogeneity seen in patients with different *GBA1*-variants, grouping patients into those with no *GBA1* abnormality, those with polymorphisms not known to cause GD, those

with the common non-neuronopathic N370S GD mutation, and those with aggressive neuronopathic GD-causing mutations. In the latter group, there was a significant increase in the risk of global cognitive impairment compared to non-carriers, with non-significant trends towards increased cognitive impairment in N370S carriers, and carriers of polymorphisms not causative of GD (Liu et al. 2016a). Taking this and the prior literature into account, it seems that the clinical impact of *GBA1* abnormalities lies on a genotype-dependent spectrum, with carriers of severe GD-causing mutations (such as L444P) having a more aggressive course than those with less severe GD-causing mutations (such as N370S) and polymorphisms.

2.2.2 Motor progression in *GBA1* variant-associated Parkinson's disease

Most epidemiological studies of *GBA1*-PD have found that *GBA1* variants are associated with an increased rate of motor progression, compared to that in non-carriers, though the association is less clear than that with cognitive decline. Longitudinal follow-up in an incident cohort found that median time to the development of postural instability (Hoehn and Yahr stage three) was approximately halved in carriers of pathogenic *GBA1* mutations in comparison to patients with wild-type *GBA1* (23.5 months versus 49.0 months respectively). Median time to development of postural instability in polymorphism carriers was intermediate between these groups (32.0 months), which was statistically significant when controlled for age. Relative risk of progression to Hoehn and Yahr stage three was 3.2 in polymorphism carriers and 4.2 in pathogenic mutation carriers, in comparison to non-carriers (Winder-Rhodes et al. 2013). The same pattern was seen in an American cohort, which found pathogenic mutation carriers and carriers of the common E326K polymorphism to have a significantly higher rate of progression in the Unified Parkinson's Disease Rating Scale (UPDRS) part III score, compared to non-carriers (Davis et al. 2016b). This supports the fact that the clinical severity of *GBA1*-PD lies on a spectrum in which polymorphisms have an adverse effect, but to a lesser extent than pathological mutations. Increased rate of motor progression has also been observed in other longitudinal cohort studies (Brockmann et al. 2015, Davis et al. 2016a).

However, other longitudinal studies have found there to be no differences in motor progression in association with *GBA1* abnormalities (Setó-Salvia et al. 2012, Lunde et al. 2018). In one of these studies females (who have been reported to have reduced motor progression (Lyons et al. 1998)) were overrepresented in the *GBA1* mutation group (72.7 %), which may account for this finding (Setó-Salvia et al. 2012). Additionally, a large meta-analysis involving seven cohorts also found that neither pathogenic mutation carriers nor polymorphism carriers had an increased rate of motor progression, though it should be noted that the maximum follow-up time was relatively short in most of these cohorts (Liu et al. 2016a). The natural history of motor features in *GBA1*-PD remains somewhat unclear.

Dyskinesias and motor fluctuations are reported to occur more commonly in *GBA1*-PD (Jesús et al. 2016). This is possibly explained by the fact that patients with *GBA1*-PD require higher levodopa doses due to more severe symptoms, rather than an underlying increased susceptibility to these complications. Nevertheless, their increased incidence contributes to the overall picture of more severe disease in *GBA1*-variant carriers compared to non-carriers.

2.2.3 Other non-motor features of *GBA1* variant-associated Parkinson's disease

Non-motor features may also be more common in *GBA1*-PD when compared to iPD. RBD has been reported to be more common in *GBA1*-PD, and also in healthy carriers of *GBA1* mutations – perhaps reflecting a prodromal phase of PD (Jesús et al. 2016, Beavan et al. 2015). Depression scores have also been found to deteriorate more quickly in healthy carriers of *GBA1* mutations, and *GBA1*-PD has been associated with an increased risk of depression in some studies (Beavan et al. 2015, Swan et al. 2016). Other neuropsychiatric features such as hallucinations and psychosis have also been reported to occur at increased frequencies in *GBA1* variant-carriers (Cilia et al. 2016, Jesús et al. 2016). These findings are likely to reflect more widespread and rapid neurodegeneration in *GBA1*-PD in comparison to iPD, and add to the overall increased severity of disease.

2.2.4 Mortality in *GBA1* variant-associated Parkinson's disease

Few studies have commented on the risk of mortality in *GBA1*-PD in comparison to iPD, possibly due to the relatively short follow-up time in most studies. Brockmann *et al* reported an increased risk of mortality in carriers of *GBA1* mutations in comparison to non-carriers over three years (Brockmann et al. 2015). However, this study only screened for the pathogenic mutations N370S and L444P, so was unable to comment on the risk associated with the more common polymorphisms. Additionally, an Italian study in which patients were followed up for a mean period of 7.2 years reported an increased risk of mortality in carriers of pathogenic *GBA1* mutations in comparison to iPD patients, which was independent of the development of dementia (Cilia et al. 2016). This study excluded any carriers of polymorphisms, and almost all of the *GBA1*-PD group carried N370S or L444P mutations, similar to the Brockmann study.

The risk of mortality in *GBA1*-PD has not been reported on in an incident cohort, and the significance of *GBA1* polymorphisms in terms of mortality risk remains unknown.

2.2.5 The role of non-pathogenic *GBA1* variants

GBA1 variants not known to cause GD are frequently identified in PD cohorts, and the clinical significance of these is often undetermined, as has been discussed above. The most commonly encountered of these polymorphisms is the E326K variant, though in a large multi-centre study of *GBA1* mutations this was not found to be associated with PD (Sidransky et al. 2009) – a finding supported by some other studies (Jesús et al. 2016). However, most studies have indicated that the E326K variant is found at a significantly higher frequency in PD patients (2.4 % to 5 %) compared to healthy controls (0.9 % to 2.8 %), with an odds ratio for the diagnosis of PD 1.7 to 2.4 (Lesage et al. 2011, Park et al. 2002, Mata et al. 2016, Berge-Seidl et al. 2017). In a cohort of PD patients with onset below age 50, the frequency of E326K was 7.6 %, in comparison to 2.5 % of age-matched controls (Duran et al. 2013). The E326K variant has only been identified in GD patients that have concomitant biallelic pathogenic mutations, and it is not thought to be sufficient for the development of GD. Though the E326K variant appears to be more common in

PD patients compared to healthy individuals, questions remain over the impact that it has on clinical course.

Here the natural history of *GBA1*-PD has been detailed in two community-based incident cohorts to test the hypothesis that carrying a *GBA1* variant conveys a worse prognosis in PD. The time to three important clinical milestones – dementia, postural instability and death – has been determined for carriers of any *GBA1* variant, as well as for those specifically carrying a pathogenic variant or a variant considered to be non-pathogenic.

2.3 Materials and Methods

2.3.1 Patients

Clinical data for incident PD patients from the Cambridgeshire Incidence of Parkinson's disease from General Practice to Neurologist (CamPaIGN) and Parkinsonism: Incidence, Cognition and Non-motor heterogeneity in Cambridgeshire (PICNICS) cohorts was obtained (Table 2.2). The diagnosis of PD was based on the UK Parkinson's Disease Society Brain Bank Criteria. Patients were followed up at 18 month intervals, with clinical, cognitive and neuropsychiatric assessments, including UPDRS, MMSE, Beck depression inventory, and dyskinesia rating assessments. *GBA1* mutation status was determined by sequencing in 250 patients, as described previously (Winder-Rhodes et al. 2013). Briefly, separate PCRs were performed to amplify DNA in three fragments as described in Stone et al. 2000. PCR products were visualised on 0.8% agarose gel for confirmation of amplification. The PCR product was then cleaned-up using ExoSAP-IT® (Affymetrix Inc.) prior to exon-by-exon sequencing (Winder-Rhodes et al. 2013). For a further 127 patients *GBA1* status was determined using Illumina NeuroX chip array (MEGA chip array (Bien et al. 2016)) screening for specific *GBA1* mutations (performed by Clemens Scherzer's group, Harvard) (Table 2.1).

	PICNICS (n)	CamPaIGN (n)	Total (n)
Sequencing	136	114	250
MEGA Chip Array	111	16	127
Total	247	130	377

Table 2.1 - Genetic analysis in the incident PD cohorts.

2.3.2 Genetic analysis of secondary genetic risk factors

Genetic analysis of the *MAPT, SNCA, COMT* and *APOE* genes had been performed historically on the CamPaIGN and PICNICS cohorts by previous group members. Genotyping for the *MAPT* and *SNCA* gene is described in Goris et al. 2007. Briefly single nucleotide polymorphism genotyping was performed with Taqman Assays-on-Demand and Assays-by-Design on a 7900HT Sequence Detection System (Applied Biosystems). Microsatellites were genotyped by amplification with primers from Stefansson et al. 2005, with separation of fluorescently labelled fragments on a 3700 capillary sequencer (Applied Biosystems) (Goris et al. 2007). *COMT* codon 158 genotyping was performed on extracted DNA using a 5′ exonuclease allelic discrimination Taqman assay as described in Foltynie et al. 2004. APOE allelic status was determined by typing two non-synonomous single nucleotide polymorphisms (rs429358 and rs7412) which allows for differentiation of ε2, ε3 and ε4 alleles. These polymorphisms were analysed using Taqman Assays (Applied Biosystems Assay-On-Demand part numbers C__3084793_20 and C__904973_10) on a 7900HT Sequence Detection System (Applied Biosystems) (Williams-Gray et al. 2009).

2.3.3 Survival analyses

For survival analyses, patients were grouped into those with wild-type *GBA1* (iPD) and those with any *GBA1* variant (*GBA1*-PD), with the latter group also being stratified into those with pathogenic mutations, and polymorphisms not known to cause GD as indicated below. All 250 patients that had undergone full sequencing were included in survival analyses, as well as 12 patients that had been found to have a *GBA1* abnormality on MEGA chip array. Patients that had undergone MEGA chip screening only with no

detected *GBA1* abnormality were excluded, given the possibility that they carried a *GBA1* mutation that had not been screened for, such as the common severe L444P mutation.

Subgroup analysis was also performed in which the *GBA1*-PD group was divided into those with non-pathogenic *GBA1* variants (genetic variants not known to cause GD), and those with pathogenic *GBA1* mutations (those known to cause GD). All patients that had had full sequencing were included, as well as six patients that that had pathogenic mutations detected in the MEGA chip array. Subjects in which only the MEGA chip array was performed with no pathogenic mutation identified were excluded from analysis, to ensure that no patients with missed pathogenic mutations were included in the non-carrier or polymorphism carrier groups. Mean follow-up times for the cohort are shown in Table 2.3.

	Wild-type	**All *GBA1* variants**	**P-value**	***GBA1* polymorphism carriers**	**Pathogenic *GBA1* mutation carriers**	**P-value**
Number	223	39	-	16	17	-
Gender M:F	134:89	25:14	0.636	11:5	10:7	0.782
Age at diagnosis (SD)	69.28 (9.84)	67.42 (8.12)	0.265	64.65 (9.14)	67.54 (6.33)	0.150
Years in education (SD)	11.94 (3.11)	11.05 (2.31)	0.094	10.40 (1.18)	11.47 (2.67)	0.143
Total UPDRS at baseline (SD)	43.90 (18.61)	44.63 (12.54)	0.816	43.75 (14.24)	44.38 (10.46)	0.994
Motor UPDRS at baseline (SD)	28.43 (12.09)	29.82 (9.38)	0.495	28.81 (9.85)	30.25 (9.21)	0.808
Hoehn & Yahr at baseline (SD)	1.75 (0.69)	2.0 (0.79)	0.067	1.94 (0.63)	2.0 (0.83)	0.224
MMSE at baseline (SD)	28.43 (1.47)	28.38 (1.66)	0.861	28.43 (1.47)	28.59 (1.37)	0.915
BDI at baseline (SD)	7.34 (5.45)	6.38 (4.03)	0.305	8.81 (3.88)	4.94 (2.86)	0.103
Baseline levodopa equivalent dose (SD)	183.98 mg (239.68)	219.74 mg (234.14)	0.389	169.38 mg (181.93)	274.12 mg (277.0)	0.309

Table 2.2 – Patient demographics. Demographics shown for all patients included in survival analyses. For subgroup analysis, subjects were excluded if they had only had MEGA chip genetic screening and were found to have a *GBA1* polymorphism, to ensure that no patients with missed pathogenic mutations were included in the other groups. P-values comparing non-carriers to all *GBA1* variant carriers determined by independent samples t-tests, and for gender, chi-squared test. P-values for subgroup analysis determined by one-way ANOVA. Abbreviations: BDI = Beck depression inventory; F = female; M = male; MMSE = Mini-Mental State Examination; SD = standard deviation; UPDRS = Unified Parkinson's Disease Rating Scale.

Comparison of time to death, postural instability and dementia were performed with Kaplan-Meier curves, and a Cox Regression model controlling for age at diagnosis and sex. Cox regression analysis was also used to investigate the effect of other genetic susceptibility factors (*MAPT*, *COMT*, *SNCA*, *APOE*) on time to the aforementioned

outcome measures, controlling for *GBA1* mutation status, in addition to age at diagnosis and sex. Postural instability was defined as the progression to Hoehn & Yahr stage three, whilst dementia was defined as fulfilling Diagnostic and Statistical Manual of Mental Disorders (DSM)-IV criteria (functional impairment with cognitive deficits in at least two domains) with an MMSE score of 24 or less. In the PICNICS cohort in which follow up time was shorter, onset of dementia was defined differently, so only patients from the CamPaIGN cohort were included in the analysis for time to dementia.

	CamPaIGN	**PICNICS**	**Combined**
Number	115	147	262
Mean follow-up time from diagnosis (SD)	7.95 years (4.44)	5.79 years (3.47)	6.74 years (4.06)
Range in follow-up time from diagnosis	0 to 18.0 years	0 to 11.42 years	0 to 18.0 years

Table 2.3 – Follow-up time for survival analysis cohorts. Abbreviations: SD = standard deviation.

2.3.4 Statistical analysis

Hazard ratios for each of the outcome measures were determined using a Cox regression model. Statistically significant differences in survival times to outcomes were determined with log-rank tests. Independent samples T-tests and chi-squared tests were used for comparison of patient demographics. One-way ANOVA was used for comparison of multiple groups. All statistical tests were performed using IBM SPSS software.

2.4 Results

2.4.1 Incidence and spectrum of *GBA1* abnormalities in Parkinson's disease

Of the 377 patients that had had genetic testing of the *GBA1* gene, 39 (10.3 %) carried abnormalities in the coding regions of the gene. A further eight patients harboured

variants in the non-coding regions of the gene, which were included in the wild-type group, given that these were felt unlikely to have had any pathological effect.

In total, 17 patients (4.5 %) carried mutations that are known GD-causing mutations (hereafter referred to as "pathogenic mutations"). These included N370S (n=7), L444P (n=3), R4643C (n=2), G10S (n=2), R257Q (n=1), R48W (n=1) and N426K (n=1). Additionally, 22 patients (5.8 %) carried abnormalities in the *GBA1* gene which occur at low frequencies, but have not been associated with GD (hereafter referred to as "polymorphisms"). These included the polymorphisms E326K (n=10; one patient carried a concomitant R48W mutation so was considered a pathogenic mutation carrier for survival analyses), T369M (n=10), E388K (n=2), and L119L (n=1) (Table 2.4).

It should be noted that 127 patients only had targeted screening for *GBA1* mutations through the MEGA chip array, rather than full sequencing (Table 2.1). Whilst this screened for a number of common mutations, it did not screen for all known *GBA1* mutations, meaning that some *GBA1* mutation-carriers may have been missed. The incidence of *GBA1* abnormality in these cohorts is therefore likely to be slightly higher than the 10.3 % reported above. Of these 127 patients, 115 were not found to carry a *GBA1* variant. The most notable omission from the MEGA chip array was the L444P mutation. Based on the observed frequency of L444P in the patients that underwent sequencing of the *GBA1* gene (1.2 %), it would be expected that an additional one to two patients in the study population carried an L444P mutation.

Pathogenic Mutations	**Non-Pathogenic Variants**
N370S (n=7)	E326K (n=10)
L444P (n=3)	T369M (n=10)
R463C (n=2)	E388K (n=2)
G10S (n=2)	L119 (n=1)
R257Q (n=1)	
R48W (n=1)	
N462K (n=1)	

Table 2.4 – Spectrum of *GBA1* abnormalities in CamPaIGN and PICNICS cohorts. Pathogenic mutations were identified in 17 patients, and polymorphisms identified in 23 patients. One patient carried the E326K in addition to the pathogenic R48W mutation, so was analysed as part of the pathogenic mutation group.

2.4.2 Natural history of *GBA1* variant-associated Parkinson's disease

2.4.2.1 Cognitive decline and risk of dementia

There were no differences in MMSE score at baseline between *GBA1* variant-carriers and non-carriers (Table 2.2). Carrying any *GBA1* variant led to a trend towards increased risk of progression to dementia compared to PD patients with wild-type *GBA1*, which was short of statistical significance (p=0.074). However, when controlling for age at diagnosis and sex, carriers of any *GBA1* variant were significantly more likely to develop dementia, with a hazard ratio of 3.9 (95 % confidence interval 1.7 to 8.7, p=0.001). Five, ten and fifteen year dementia-free survival are shown in Table 2.5. At 10 years, only 25 % of carriers of *GBA1* abnormalities remained dementia-free, in comparison to 55.5 % of those without *GBA1* abnormalities. At 15 years, approximately half of wild-type patients remained dementia-free, whilst no *GBA1*-PD patients survived to this time-point. For *GBA1*-PD the estimated median time to dementia was 7.1 years (95 % confidence interval 5.2 to 9.0), compared to 12.0 years (95 % confidence interval 10.5 to 13.5) for the iPD group (Figure 2.1).

	Non-carriers	All *GBA1* variants	Non-pathogenic variants	Pathogenic mutations
Number	97	18	11	6
Estimated mean time to dementia (years)	12.0 (10.5-13.5)	7.1 (5.2-9.0)	7.1 (5.7-8.5)	6.1 (2.8-9.3)
Estimated median time to dementia (years)	13.75	6.5 (5.9-7.1)	6.6 (5.6-7.6)	4.1 (0-8.2)
5 year survival without dementia (%)	81.1 (SE 4.2)	75.0 (SE 10.8)	90.0 (SE 9.5)	50 (SE 20.4)
10 year survival without dementia (%)	55.5 (SE 6.2)	25.0 (SE 14)	22.5 (SE 18.5)	23 (SE 20.4)
15 year survival without dementia (%)	49.1 (SE 7)	Nil surviving	Nil surviving	Nil surviving
Log-rank p-value	-	0.074	0.346	**0.049**
Hazard ratio	-	**3.9 (1.7-8.7; p=0.001)**	**3.1 (1.2-8.5; p=0.024)**	**5.6 (1.8-17.1; p=0.002)**

Table 2.5 – Long-term follow-up data for progression to dementia in patients with iPD, carriers of any *GBA1* mutation, carriers of non-pathogenic polymorphisms, and carriers of pathogenic mutations. Hazard ratios determined by Cox regression analysis controlling for age at diagnosis and sex. 95 % confidence intervals for hazard ratio and estimated mean and median shown in brackets. Log-rank p-values shown for comparison between the *GBA1* groups and the non-carrier group. Abbreviations: SE = standard error of the mean.

When sub-classifying the *GBA1* abnormalities into carriers of non-pathogenic polymorphisms and pathogenic mutations, the increase in dementia risk was only statistically significantly in the pathogenic mutation group (p=0.049). There was no significant difference between the pathogenic mutation and polymorphism group (Figure 2.1). However, when controlling for age at diagnosis and sex, both groups had significantly increased risk of progression to dementia, with hazard ratios of 3.1 (95 % confidence interval 1.2 to 8.5, p=0.024) and 5.6 (95 % confidence interval 1.8 to 17.1, p=0.002) for the polymorphism and pathogenic mutation groups respectively.

2.4.2.2 Motor progression

There were no differences in UPDRS motor score, Hoehn and Yahr stage, or levodopa equivalent dose between the groups at baseline (Table 2.2). There was an increased risk

of progression to postural instability (Hoehn and Yahr stage three), in the *GBA1*-PD group in comparison to the iPD group (p=0.048). At five years from diagnosis, 68 % of *GBA1*-PD patients had progressed to Hoehn and Yahr stage three, compared to 44 % of iPD patients (Table 2.6). All *GBA1*-PD patients were censored prior to 10 years, so 10 and 15 year rates of progression to Hoehn and Yahr stage three could not be calculated. When controlling for age at diagnosis and sex, both carriers of non-pathogenic polymorphisms and pathogenic mutations had a significantly increased risk of progression to postural instability, with hazard ratios of 2.5 (95 % confidence interval 1.3 to 4.8, p=0.005) and 2.1 (95 % confidence interval 1.2 to 3.8, p=0.013) respectively (Figure 2.1). The increased risk of progression to Hoehn and Yahr stage three was independent of the development of dementia (hazard ratio 2.2 (95% confidence interval 1.2 to 4.1, p=0.009)).

	Non-carriers	**All *GBA1* variants**	**Non-pathogenic variants**	**Pathogenic mutations**
Number	222	39	16	17
Estimated mean time to HY3 (years)	6.7 (5.8-7.5)	4.7 (3.3-6.0)	4.8 (2.8-6.8)	4.4 (3.0-5.9)
Estimated median time to HY3 (years)	5.8 (4.7-7.0)	3.2 (2.7-3.6)	3.0 (2.7-3.3)	4.4 (2.6-6.2)
5 year survival without postural instability (%)	56.0 (SE 3.5)	32.0 (SE 8.2)	30.8 (SE 12.8)	32.4 (SE 11.8)
10 year survival without postural instability (%)	27.3 (SE 4)	8.1 (SE 7.1)	10.3 (SE 9.4)	0
15 year survival without postural instability (%)	7.4 (SE 4)	Nil surviving	Nil surviving	Nil surviving
Log-rank p-value	-	**0.048**	0.314	0.12
Hazard ratio	-	**2.1 (1.4-3.3; p=0.001)**	**2.5 (1.3-4.8; p=0.005)**	**2.11 (1.2-3.8; p=0.013)**

Table 2.6 – Long-term follow-up data for progression to Hoehn and Yahr stage three in patients with iPD, carriers of any *GBA1* mutation, carriers of non-pathogenic polymorphisms, and carriers of pathogenic mutations. Hazard ratios determined by Cox regression analysis controlling for age at diagnosis and sex. 95 % confidence intervals for hazard ratio and estimated mean and median shown in brackets. Log-rank p-values shown for comparison between the *GBA1* groups and the non-carrier group. Abbreviations: HY3 = Hoehn and Yahr stage three; SE = standard error of the mean.

2.4.2.3 Mortality

In addition, carrying any *GBA1* abnormality was associated with a significantly increased risk of death over the follow-up period in comparison to non-carriers (p=0.042). Five, ten and fifteen year survival rates are shown in Table 2.7. At 10 years from diagnosis, 66.1 % of carriers of *GBA1* abnormalities had died, in comparison to 50 % of those with iPD. At 15 years, 79.8 % of iPD patients had died, whilst all *GBA1*-PD patients had died. For *GBA1*-PD the estimated median time to death was 8.8 years (95 % confidence interval 8.2 to 9.4), compared to 10.7 years (95 % confidence interval 10.0 to 11.3) for the iPD group. When controlling for age and sex, the hazard ratio for mortality in carriers of any *GBA1* abnormality was 2.2 (95 % confidence interval 1.4 to 3.5, p=0.001). Both carriers of non-pathogenic variants and pathogenic mutations had significantly increased risk of mortality, with hazard ratios of 2.0 (95 % confidence interval 1.1 to 3.7, p=0.034) and 2.1 (95 % confidence interval 1.1 to 4.3, p=0.035) respectively (Figure 2.1).

To explore whether the increase in mortality associated with *GBA1* variants was attributable to the increased risk of dementia, the dementia outcome was incorporated into the Cox regression model, along with age and sex. When controlling for dementia status, the increased risk of mortality associated with carrying any *GBA1* variant persisted (hazard ratio 2.6 (95 % confidence interval 1.5 to 4.6, p=0.001)), suggesting that it is independent of the development of dementia.

	Non-carriers	**All *GBA1* variants**	**Non-pathogenic variants**	**Pathogenic mutations**
Number	223	39	16	17
Estimated mean time to death (years)	10.7 (10.0-11.3)	9.1 (8.1-10.1)	9.6 (8.5-10.7)	9.5 (7.8-11.3)
Estimated median time to death (years)	10.1 (9.5-10.7)	8.8 (8.2-9.4)	9.6 (8.7-10.5)	8.5 (7.7-9.3)
5 year survival (%)	89.2 (SE 2.1)	94.3 (SE 3.9	100	100
10 year survival (%)	50.0 (SE 3.8)	33.9 (SE 9.5)	42.2 (SE 14.7)	29.8 (SE 14.1)
15 year survival (%)	20.2 (SE 3.8)	0	0	0
Log-rank p-value	-	**0.042**	0.263	0.261
Hazard ratio	-	**2.2 (1.4-3.5; p=0.001)**	**2.0 (1.1-3.7; p=0.034)**	**2.1 (1.1-4.3; p=0.035)**

Table 2.7 – Long-term follow-up mortality data for patients with iPD, carriers of any *GBA1* mutation, carriers of non-pathogenic polymorphisms, and carriers of pathogenic mutations. Hazard ratios determined by Cox regression analysis controlling for age at diagnosis and sex. 95 % confidence intervals for hazard ratio and estimated mean and median shown in brackets. Log-rank p-values shown for comparison between the *GBA1* groups and the non-carrier group. Abbreviations: SE = standard error of the mean.

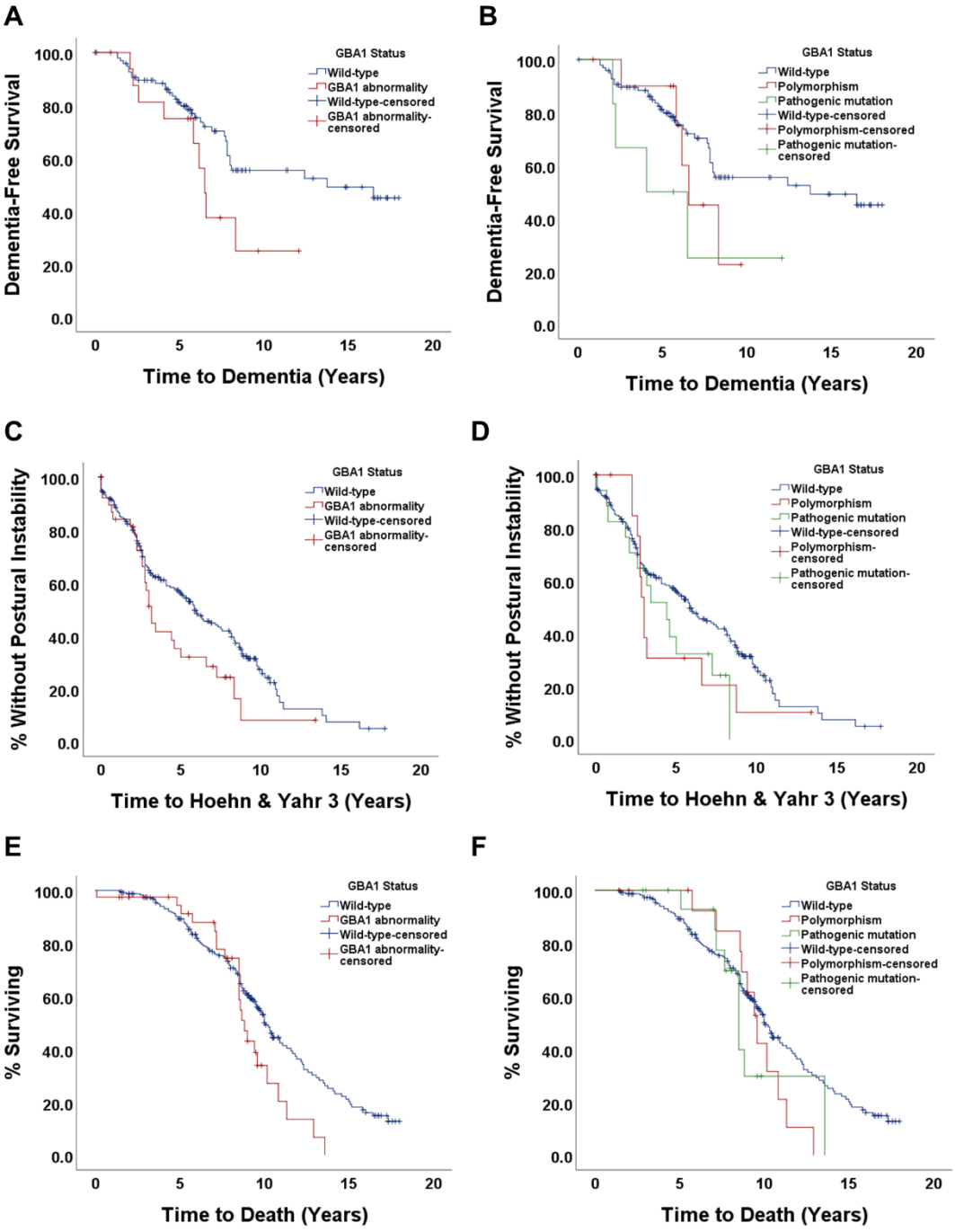

Figure 2.1 – Survival analyses for time to dementia, time to Hoehn and Yahr stage three, and time to death based on *GBA1* status. A), C) and E) show Kaplan-Meier curves comparing all *GBA1*-variant carriers to non-carriers. B), D) and F) show Kaplan-Meier curves comparing pathogenic mutation carriers, polymorphism carriers and non-carriers.

2.4.3 Interaction between *GBA1* abnormalities and other genetic susceptibility factors

A number of common genetic variants have been previously associated with PD and its clinical expression and progression. It is not known whether the clinical effect of *GBA1* abnormalities in PD are altered by these other genetic risk factors. The natural history of *GBA1*-PD was therefore studied, in the presence or absence of other genetic risk factors for which information was available in the CamPaIGN and PICNICS cohorts. These included the *MAPT* haplotype, the *SNCA* rs356219 polymorphism, the *COMT* codon 158 polymorphism, and the apolipoprotein E (*APOE*) ε4 polymorphism (Table 2.8).

The *MAPT* gene encodes the neuronal protein tau, which may be hyperphosphorylated or form abnormal fibrillary tangles in PD as well as other neurodegenerative diseases (Spillantini and Goedert 2013). The *MAPT* gene can exist in two forms – H1 and H2 (Baker et al. 1999). Carrying the H2 form in the heterozygous or homozygous state has previously been associated with a reduced risk of PD, and reduced risk of cognitive decline in PD patients. A meta-analysis demonstrated that the odds ratio for developing PD in individuals with the *MAPT* H1/H1 genotype was 1.4 when compared to H2 carriers (Goris et al. 2007). Additionally, the H1/H1 genotype is associated with a greater risk of an early dementia (Evans et al. 2011, Goris et al. 2007). This study also demonstrated that G/G homozygotes for the *SNCA* rs356219 polymorphism had a greater susceptibility to PD in comparison to those with the G/A or A/A genotypes. Furthermore, the presence of both of these risk factors was found to have a synergistic effect with regards to increasing the risk of PD.

The role of the *COMT* codon 158 polymorphism and *APOE* status in PD are less clear. Codon 158 of the *COMT* gene encodes for the presence of methionine or valine. Methionine homozygosity (met/met) reduces the activity of COMT (an enzyme involved in dopamine metabolism) by three to four times, in comparison to valine homozygotes (val/val). COMT activity in heterozygotes (val/met) is thought to be midway between the homozygous states (Lachman et al. 1996). The met/met genotype has been associated with specific cognitive abnormalities in PD, including planning and attentional control (Foltynie et al. 2004, Williams-Gray et al. 2008). Carrying the *APOE* ε4 allele is known

to significantly increase the risk of Alzheimer's disease, and has been suggested to increase the risk of dementia in PD (Farrer et al. 1997). Though studies have yielded variable results, a recent meta-analysis has suggested that the ε4 allele is associated with an increased risk of developing dementia in PD (Sun et al. 2019).

Gene	"High-Risk" Variants	"Low-Risk" Variants
MAPT	H1/H1	H2/H1 or H2/H2
***SNCA* rs356219**	G/G	A/A or G/A
***COMT* codon 158**	met/met or met/val	val/val
APOE	Heterozygous or homozygous for ε4 allele	No ε4 alleles

Table 2.8 – Genetic susceptibility factors for PD. *GBA1*-PD patients in the CamPaIGN and PICNICS cohorts were stratified based on the presence or absence of high- or low-risk variants in secondary genetic risk factors as indicated. Abbreviations: met = methionine; val = valine.

In order to assess the clinical impact of these risk factors in the context of *GBA1* mutation, patients with *GBA1*-PD were grouped based on the presence or absence of "high-" or "low-" risk variants of the relevant susceptibility gene, as shown in Table 2.8 and survival analyses performed for time to death, time to dementia, and time to Hoehn and Yahr stage three. It should be acknowledged that the effect of the COMT variants in particular are thought to differ as a function of disease stage, so their designation as "high-" or "low-" risk is somewhat artificial (Williams-Gray et al. 2008). Carriers of any *GBA1* variant in whom the status of the secondary genetic risk factor was known were included.

Firstly, survival analyses were performed for each of the secondary genetic risk factors alone, comparing time to death, development of postural instability and dementia in those with "low –risk" genotypes to those with "high-risk" genotypes. None of the four genetic risk factors assessed were found to significantly alter mortality, progression to postural instability, or dementia. However, when controlling for age, sex and *GBA1* status, the *MAPT* H1/H1 haplotype did convey a slight increase in the risk of death (hazard ratio 1.6 (95 % confidence interval 1.1 to 2.1, p=0.005)) and to a greater extent, the risk of dementia (hazard ratio 2.3 (95 % confidence interval 1.2 to 4.4, p=0.016) compared to carriers of an H2 allele. There was no increase in the risk of progression to Hoehn and Yahr stage 3. Interestingly, when controlling for these confounders, the "high-risk" group

for *COMT* codon 158 were found to have a reduced risk of dementia, with hazard ratio of 0.4 (95 % confidence interval 0.2 to 0.8, p=0.012). There was no effect on risk of death or progression to Hoehn and Yahr stage three. For *APOE* and the *SNCA* rs356219 polymorphism there were no differences in any of the three outcome measures when controlling for age, sex and *GBA1* mutation status (Figure 2.2 and Table 2.9 to Table 2.12).

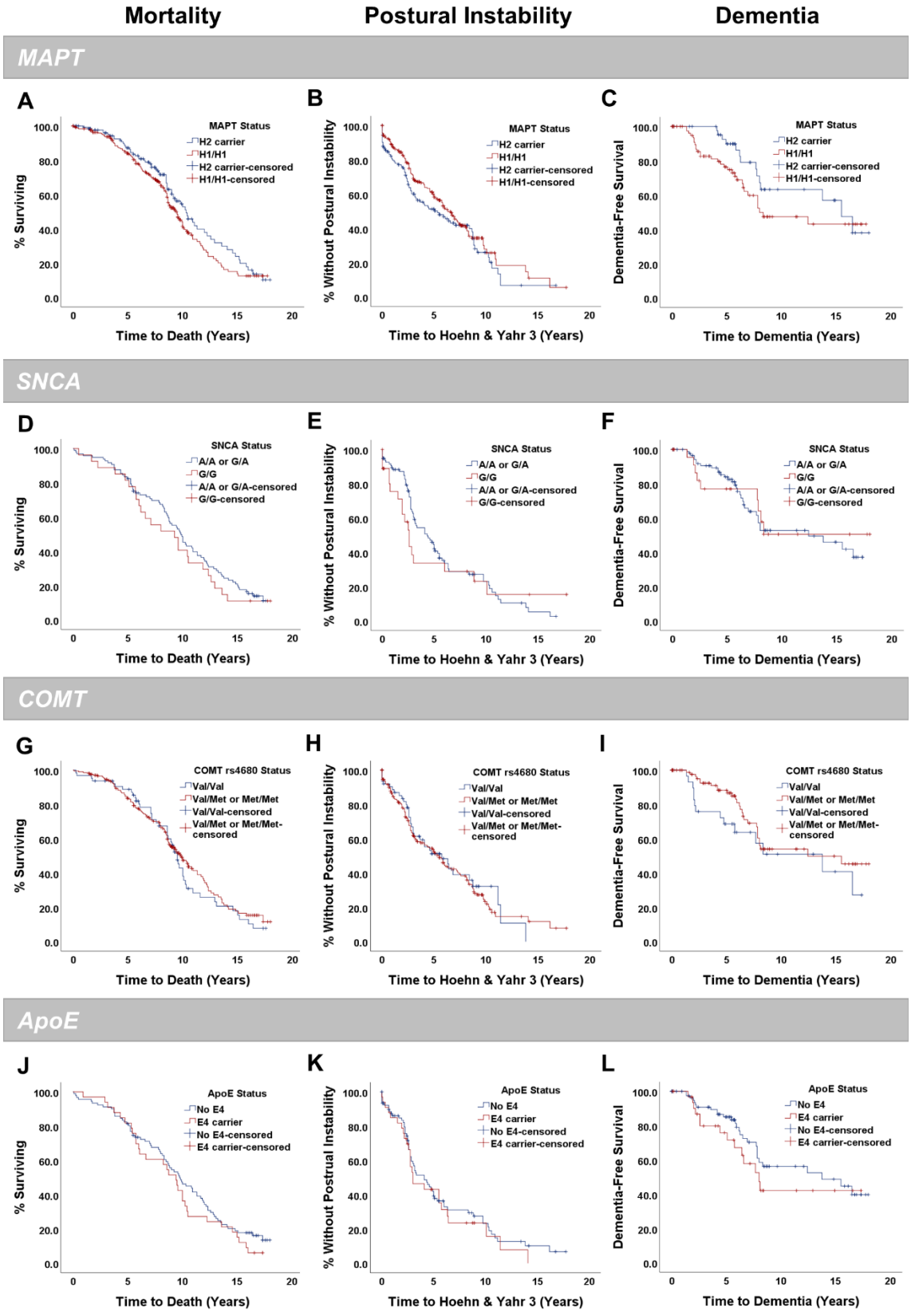

Figure 2.2 – Survival analyses for time to dementia, time to Hoehn and Yahr stage three, and time to death based on genetic susceptibility factors. Patients from the CamPaIGN and PICNICS cohorts were stratified based on the presence of high- or low-

risk variants in *MAPT* (A-C), *SNCA* (D-F), *COMT* (G-I) and *APOE* (J-K). Kaplan-Meier curves for the three disease milestones are shown.

	Mortality		**HY3**		**Dementia**	
	H2 carriers	H1/H1	H2 carriers	H1/H1	H2 carriers	H1/H1
Number	134	252	133	251	49	89
Estimated mean time to outcome (years)	10.7 (9.8-11.7)	9.7 (9.0-10.4)	6.0 (5.0-7.0)	7.2 (6.2-8.1)	13.1 (11.1-15.1)	10.8 (9.1-12.5)
Estimated median time to outcome (years)	10.3 (9.0-11.7)	9.4 (8.6-10.2)	5.3 (3.0-7.7)	5.3 (3.0-7.7)	15.5 (12.1-18.9)	8.0 (3.4-12.6)
5 year survival (%)	87.2 (SE 3.1)	84.1 (SE 2.4)	51.3 (SE 4.7)	58.2 (SE 3.5)	89.8 (SE 4.8)	76.4 (SE 5)
10 year survival (%)	52.9 (SE 5.4)	41.4 (SE 3.9)	26.0 (SE 5.4)	27.9 (SE 4.7)	63.2 (SE 9.1)	47.3 (SE 7.2)
15 year survival (%)	23.9 (SE 5.6)	13.8 (SE 3.6)	6.7 (SE 4.3)	11.0 (SE 5.2)	56.9 (SE 10.2)	43.0 (SE 7.7)
Log-rank p-value	-	0.141	-	0.147	-	0.138
Hazard ratio	-	1.6 (1.1-2.1; p=0.005)	-	1.0 (0.7-1.3; p=0.777)	-	**2.3 (1.2-4.4; p=0.016)**

Table 2.9 – Time to death, progression to Hoehn and Yahr stage three, and dementia in PD patients with low-risk (H2 carriers) versus high risk (H1/H1) *MAPT* haplotype. Hazard ratios determined by Cox regression analysis controlling for age at diagnosis, sex and *GBA1* mutation status. 95 % confidence intervals for hazard ratio and estimated mean and median shown in brackets. Log-rank p-values shown for comparison between the high- and low-risk *MAPT* carriers. Abbreviations: HY3 = Hoehn and Yahr three; SE = standard error of the mean.

	Mortality		**HY3**		**Dementia**	
	Val/Val	Val/Met or Met/Met	Val/Val	Val/Met or Met/Met	Val/Val	Val/Met or Met/Met
Number	64	206	64	204	33	95
Estimated mean time to outcome (years)	9.7 (9.4-10.9)	10.2 (9.4-10.9)	6.4 (5.1-7.8)	6.5 (5.6-7.4)	10.4 (7.8-13.0)	12.1 (10.5-13.7)
Estimated median time to outcome (years)	9.5 (8.8-10.2)	9.8 (8.8-10.8)	5.8 (3.3-8.2)	5.5 (4.4-6.6)	13.8 (4.6-22.9)	12.4
5 year survival (%)	88.8 (SE 4)	83.6 (SE 2.7)	51.2 (SE 7)	52.4 (SE 4)	68.6 (SE 9)	88.3 (4)
10 year survival (%)	38.1 (SE 7)	47.4 (SE 3.9)	32.2 (SE 8)	23.4 (SE 4)	51.0 (SE 11)	54.0 (7)
15 year survival (%)	15.5 (SE 5.6)	17.8 (3.9)	0	11.7 (SE 4)	40.8 (SE 13)	49.8 (SE 8)
Log-rank p-value	-	0.525	-	0.727	-	0.164
Hazard ratio	-	1.0 (0.7-1.4; p=0.856)	-	1.0 (0.7-1.5; p=0.835)	-	**0.4 (0.2-0.8; p=0.012)**

Table 2.10 – Time to death, progression to Hoehn and Yahr stage three, and dementia in PD patients with low-risk (val/val) versus high-risk (met/met or met/val) *COMT* codon 158 genotype. Hazard ratios determined by Cox regression analysis controlling for age at diagnosis, sex and *GBA1* mutation status. 95 % confidence intervals for hazard ratio and estimated mean and median shown in brackets. Log-rank p-values shown for comparison between the high- and low-risk *COMT* groups. Abbreviations: HY3 = Hoehn and Yahr three; Met = methionine; SE = standard error of the mean; val = valine.

	Mortality		HY3		Dementia	
	G/A or A/A	G/G	G/A or A/A	G/G	G/A or A/A	G/G
Number	27	97	27	96	27	97
Estimated mean time to outcome (years)	10.0 (9.0-11.0)	9.0 (7.2-10.8)	5.8 (4.8-6.8)	5.4 (2.8-8.0)	11.3 (9.9-12.8)	11.7 (8.6-14.8)
Estimated median time to outcome (years)	9.8 (8.7-11.0)	9.3 (6.1-12.4)	4.3 (2.7-6.0)	2.6 (2.0-3.2)	12.4 (5.5-19.4)	N/A#
5 year survival (%)	82.5 (SE 4)	81.5 (SE 8)	42.1 (SE 5)	33.7 (SE 10)	84.0 (SE 4)	77.0 (SE 9)
10 year survival (%)	45.3 (SE 5)	40.7 (SE 9.5)	23.0 (SE 5)	23.1 (SE 9)	52.8 (SE 7)	50.5 (SE 12.3)
15 year survival (%)	19.9 (SE 4)	11.1 (SE 6)	5.2 (SE 3)	1.5 (SE 9)	46.0 (SE 8)	50.5 (SE 12.3)
Log-rank p-value	-	0.422	-	0.533	-	0.921
Hazard ratio	-	1.0 (0.6-1.7; p=0.933)	-	1.0 (0.6-1.7; p=0.996)	-	0.8 (0.4-1.8; p=0.633)

Table 2.11 – Time to death, progression to Hoehn and Yahr stage three, and dementia in PD patients with low-risk (G/A or A/A) versus high-risk (G/G) *SNCA* rs356219 genotype. Hazard ratios determined by Cox regression analysis controlling for age at diagnosis, sex and *GBA1* mutation status. 95 % confidence intervals for hazard ratio and estimated mean and median shown in brackets. Log-rank p-values shown for comparison between the high- and low-risk *SNCA* rs356219 carriers. Abbreviations: HY3 = Hoehn and Yahr three; SE = standard error of the mean.

	Mortality		HY3		Dementia	
	No ApoE4 alleles	ApoE4 Carrier	No ApoE4 alleles	ApoE4 Carrier	No ApoE4 alleles	ApoE4 Carrier
Number	91	33	90	33	91	33
Estimated mean time to outcome (years)	10.0 (8.9-11.1)	9.2 (7.7-10.7)	5.9 (4.7-7.1)	5.1 (3.5-6.7)	12.0 (10.4-13.7)	10.2 (7.7-12.8)
Estimated median time to outcome (years)	9.8 (8.0-11.5)	9.4 (7.9-10.9)	4.1 (2.7-5.5)	3.0 (1.2-4.8)	13.8 (4.2-23.4)	8.0 (6.0-10.0)
5 year survival (%)	81.3 (SE 4)	81.8 (SE 7)	39.2 (SE 6)	43.1 (SE 9)	85.1 (SE 4)	75.8 (SE 8)
10 year survival (%)	46.2 (SE 5)	36.4 (SE 8)	23.2 (SE 5)	23.5 (SE 8)	56.2 (SE 7)	42.1 (SE 11)
15 year survival (%)	19.0 (SE 4)	15.2 (SE 6)	10.1 (SE 4)	0	48.7 (SE 8)	42.1 (SE 11)
Log-rank p-value	-	0.303	-	0.54	-	0.292
Hazard ratio	-	1.3 (0.8-2.1; p=0.251)	-	0.9 (0.6-1.5; p=0.679)	-	1.4 (0.7-2.7; p=0.348)

Table 2.12 – Time to death, progression to Hoehn and Yahr stage three, and dementia in PD patients with low-risk (No ε4 alleles) versus high-risk (ε4 carriers) *APOE* haplotype. Hazard ratios determined by Cox regression analysis controlling for age at diagnosis, sex and *GBA1* mutation status. 95 % confidence intervals for hazard ratio and estimated mean and median shown in brackets. Log-rank p-values shown for comparison between the high- and low-risk *APOE* carriers. Abbreviations: ApoE = apolipoprotein E; SE = standard error of the mean.

In order to study whether the presence of the high-risk variants in the secondary genetic risk factors alters the course of *GBA1*-PD, carriers of all *GBA1* abnormalities were subdivided into those with the low-risk and high-risk state for the secondary genetic factor, and survival analyses for time to death, dementia and Hoehn and Yahr stage three were performed (Figure 2.3). None of the secondary factors increased the risk of dementia or mortality in *GBA1*-PD. However, there was a trend towards an increased risk of death, which fell slightly short of statistical significance (hazard ratio 2.6 (95 % confidence interval 1.0-7.1, p=0.058) in *GBA1*-PD patients with the H1/H1 *MAPT* haplotype in comparison to H2 carriers, when controlling for age at diagnosis and sex. It may be that the small groups resulting from such stratification meant that these analyses were insufficiently powered to detect significant differences. The 10 year survival for the H1/H1 group was 28.6 % compared to 43.0 % in H2 carriers. There were only two carriers

of the *APOE* ε4 allele within the *GBA1*-PD cohort precluding any comment on the significance of this variant, but both patients had particularly aggressive disease courses, with both developing dementia within seven years of diagnosis, and both dying within nine years of diagnosis. Projected mean times to these outcomes are shown in Table 2.13.

GBA1-PD patients with the high-risk variant in the *SNCA* rs356219 locus had an increased risk of progression to Hoehn and Yahr stage three when controlling for age at diagnosis and sex (hazard ratio 5.3 (95 % confidence interval 1.1-26.2, p=0.041)), with all patients reaching Hoehn and Yahr stage three within three years. None of the other genetic risk factors tested increased the risk of progression to Hoehn and Yahr stage three.

	Number	**Estimated Mean Time to Dementia (Years)**	**Estimated Mean Time to Postural Instability (Years)**	**Estimated Mean Time to Death (Years)**
Low-risk *MAPT*	20	8.3 (5.5-11.2)	5.1 (2.9-7.3)	9.9 (8.3-11.5)
High-risk *MAPT*	18	5.7 (3.9-7.6)	4.2 (2.8-5.6)	8.3 (7.0-9.5)
Low-risk *COMT*	5	6.7 (3.0-10.4)	4.0 (1.4-6.6)	9.6 (7.0-12.2)
High-risk *COMT*	21	6.5 (4.5-8.6)	4.7 (3.0-6.3)	9.0 (7.5-10.5)
Low-risk *SNCA*	11	6.5 (5.8-7.2)	3.2 (2.5-3.8)	8.8 (8.5-9.2)
High-risk *SNCA*	5	5.0 (2.1-7.9)	2.6 (0-6.5)	7.1 (4.2-10.9)
Low-risk *APOE*	14	7.4 (5.2-9.7)	4.3 (2.0-6.5)	8.7 (6.9-10.6)
High-risk *APOE*	2	4.6 (0.7-8.5)	2.8 (2.4-3.2)	7.2 (4.4-9.9)

Table 2.13 –Time to death, dementia and Hoehn and Yahr stage three based on presence of secondary genetic susceptibility factors in *GBA1*-PD. Patients from the CamPaIGN and PICNICS cohorts with *GBA1*-PD were stratified based on the presence of high- or low-risk variants in *MAPT*, *COMT*, *SNCA* or *APOE*. Estimated mean time to death, Hoehn and Yahr stage three, and dementia are shown in the table, with 95 % confidence intervals shown in brackets.

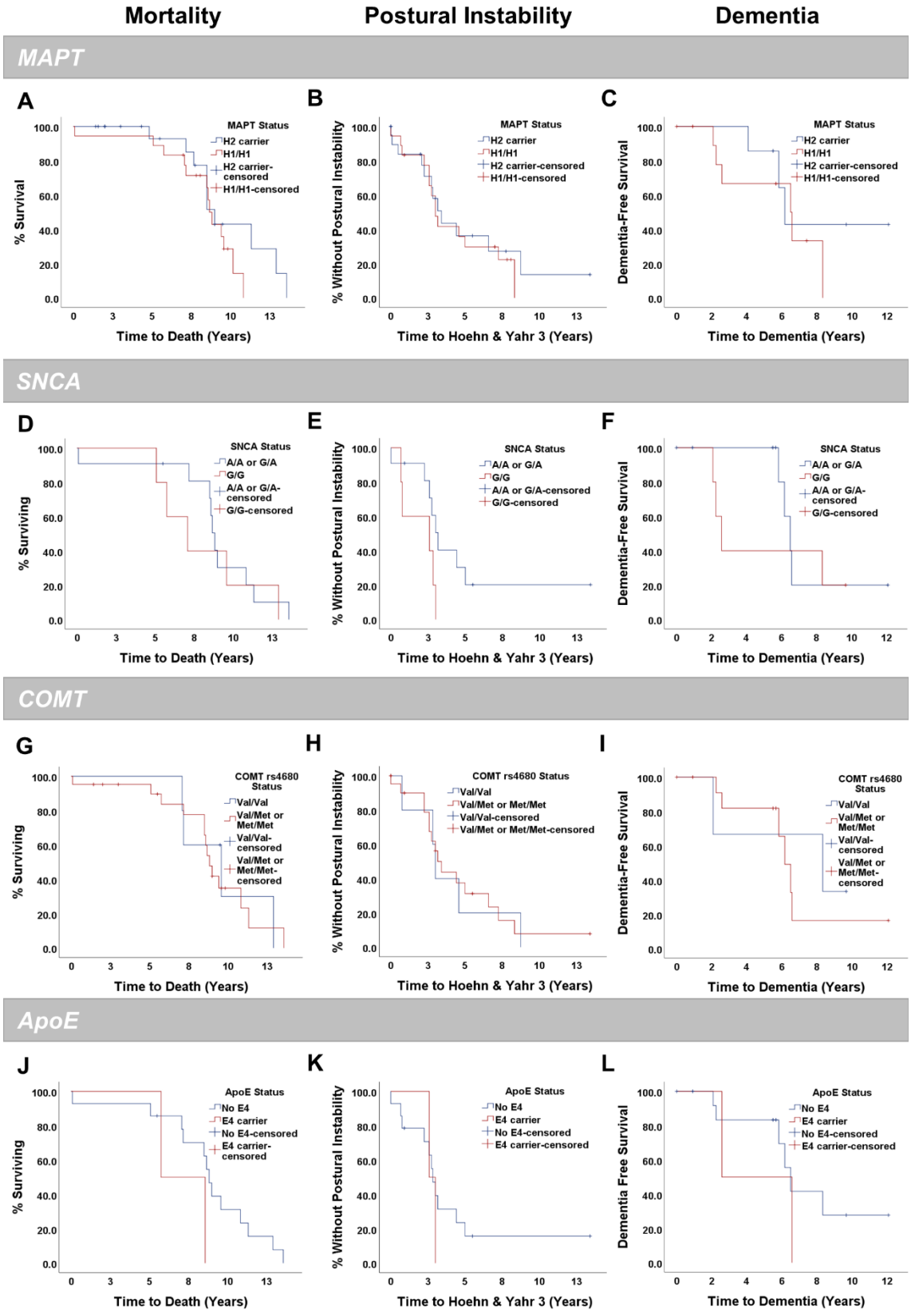

Figure 2.3. Survival analyses for time to death, postural instability and dementia in patients with *GBA1*-PD with and without secondary genetic risk factors. Patients from the CamPaIGN and PICNICS cohorts with *GBA1*-PD were stratified based on the

presence of high- or low-risk variants in *MAPT* (A-C), *SNCA* (D-F) *COMT* (G-I) or *APOE* (J-L) and survival analyses performed.

2.5 Discussion

This study represents the longest follow-up in incident PD patients with *GBA1*-PD, and the inclusion of two community-based cohorts allowed for this to be done in a relatively large study population. In contrast, most previous longitudinal studies of *GBA1*-PD have employed prevalent cohorts in which variation in disease duration for example may confound the results. Consistent with most previous studies, *GBA1* variants were found to significantly influence the course of PD in terms of motor and cognitive decline. Additionally, the long follow-up time allowed for the study of mortality in *GBA1*-PD – something that has only been commented on in a very limited number of studies – which was found to be significantly elevated in variant-carriers. *GBA1* polymorphisms, in addition to pathogenic mutations, were significantly associated with worse outcomes when controlling for confounders. Time to death, diagnosis of dementia, and development of postural instability were chosen as outcome measures, given that these represent important milestones in the natural history of PD.

2.5.1 Incidence and clinical significance of *GBA1* variants in Parkinson's disease

In these cohorts, *GBA1*-variants were found in approximately 10 % of PD patients, with about half of those carrying GD-causing pathogenic mutations. However, there were 115 patients who were not found to carry a *GBA1* variant, but had only targeted screening for a limited number of *GBA1* abnormalities, meaning that it is likely that some of these carried a mutation that was not screened for. The observed frequency of *GBA1* mutations is therefore likely to be slightly higher in these cohorts. These patients were excluded from survival analyses to ensure that there were no potential *GBA1*-variant carriers in the iPD group.

GBA1 mutations have previously been associated with an earlier age of onset in PD (Brockmann et al. 2015, Clark et al. 2007, Nichols et al. 2009). Here, there were no significant differences in the age of onset based on *GBA1* status. In both the pathogenic mutation group and polymorphism group, the mean age of onset was approximately two years earlier than in the iPD group, and it may be that the sample size meant that this study was underpowered to detect a difference in the age at onset.

GBA1-PD was found to result in a generally more aggressive disease course. The most consistent clinical feature associated with *GBA1*-PD in comparison to iPD, is an increased risk of cognitive decline and dementia. In this study, in carriers of any *GBA1* mutation the projected mean time to dementia was 7.1 years – approximately five years earlier than in the iPD group – which was statistically significant when controlling for confounding factors. This was true for pathogenic mutations, of which carriers had a 5.6-fold greater risk of dementia than in iPD ($p=0.002$), and also, to a lesser extent, in carriers of non-pathological polymorphisms in which the risk of dementia was increased 3.1-fold ($p=0.024$).

The conclusions on motor progression in *GBA1*-PD have been more variable in previous studies, with some studies finding that *GBA1* mutations are associated with an adverse clinical course (Davis et al. 2016b, Davis et al. 2016a, Winder-Rhodes et al. 2013, Brockmann et al. 2015), and others finding no effect (Liu et al. 2016a, Setó-Salvia et al. 2012, Lunde et al. 2018). Here, carrying any form of *GBA1*-variant led to an increase in motor progression, as judged by the onset of postural instability. Only approximately one third of patients carrying any *GBA1* variant remained free of postural instability at the five year time point, which compared to more than half of the iPD patients. As for the risk of dementia, both non-pathogenic and pathogenic *GBA1* variants increased the risk of progression to postural instability, both by approximately two-fold.

Few studies have commented on mortality in *GBA1*-PD, but the long duration of observation in this study allowed for the effect of *GBA1* mutation abnormality on mortality in PD to be investigated. Both non-pathogenic polymorphism and pathogenic mutation carriers had an approximately two-fold greater risk of death than that in non-carriers. All carriers of any *GBA1* variant had died within 15 years of diagnosis,

supporting the fact that carrying a *GBA1* abnormality of any kind results in a significantly worse prognosis, when compared to patients with wild-type *GBA1*. The increased risk of death associated with *GBA1*-PD was independent of the development of dementia, suggesting that other mechanisms may contribute to the increased risk of death in this group. For example, the increased risk of motor progression may result in an earlier risk of falls and immobility in *GBA1*-PD which may contribute to death. Other factors that have not been investigated in this study, including the incidence of autonomic features for example, may also contribute to the increased risk of mortality in *GBA1*-PD. Similarly, the development of postural instability was also independent of dementia status, suggesting that *GBA1* variants have widespread detrimental effects, accelerating degeneration in motor and cognitive pathways.

2.5.2 Effect of concomitant genetic susceptibility factors in *GBA1* variant-associated Parkinson's disease

A growing number of genetic susceptibility loci have now been reported in PD, and it is thought that an individual's risk of developing PD may be in part due to a polygenic risk profile (Nalls et al. 2011, Nalls et al. 2014, Polito, Greco and Seripa 2016). As such, it was hypothesised that the clinical course of *GBA1*-PD would be adversely affected by the presence of concomitant genetic risk factors. For the CamPaIGN cohort, data on *MAPT* haplotype, *COMT* codon 158 status, *SNCA* rs356219 polymorphism and *APOE* haplotype were available, with the former two also being available for patients in the PICNICS cohort.

Carrying a *MAPT* H2 allele led to a slight but statistically significantly better prognosis, with a reduced risk of mortality and dementia, in comparison to those with the H1/H1 haplotype, independent of *GBA1* status. None of the other genetic risk factors (*COMT*, *SNCA*, *APOE*) alone were found to adversely affect clinical course, which may be attributed to the small sample size and a relatively small biological effect in comparison to carrying a *GBA1* abnormality. In fact, methionine-carriers at *COMT* codon 158 actually had a significantly reduced risk of dementia in these cohorts. The previous literature regarding the impact of *COMT* codon 158 in PD is limited, and the clinical significance of this result is questionable in this small sample.

When investigating the effect of carrying a secondary genetic risk factor within the *GBA1*-PD population, none of the four genetic risk factors significantly altered the risk of dementia or mortality. Though not significant, there was a trend that carrying the H1/H1 *MAPT* haplotype in addition to a *GBA1* variant led to a reduced time to mortality, with mean time to death being more than a year earlier in *GBA1*-PD patients carrying the H1/H1 *MAPT* haplotype in comparison to those carrying an H2 allele. The small sample size meant though that our study was probably under-powered to detect a significant difference. In addition, because of the small sample size, patients with all *GBA1* abnormalities were included in this analysis including those with non-pathogenic polymorphisms, which are probably associated with a more benign clinical picture than those with pathogenic mutations. In a larger cohort, it would be useful to stratify patients based on whether they carry pathogenic or non-pathogenic *GBA1* variants, in addition to the high-risk *MAPT* haplotype. Nevertheless, this observation lends some support to the hypothesis that carrying both a *GBA1* mutation and the high-risk *MAPT* haplotype leads to a particularly aggressive clinical course, and it would be useful to investigate this with a larger clinical cohort.

The presence of the *SNCA* rs356219 high risk genotype in *GBA1*-PD led to a significantly increased risk of progressing to Hoehn and Yahr stage three, with all patients reaching this outcome within three years, when controlling for age at onset and sex. There was no effect on mortality or development of dementia, suggesting that any synergistic interaction between these two genetic risk factors has a predominant effect on pathology contributing to motor features. However, it should be acknowledged that only five patients across the cohorts carried both a *GBA1* abnormality and the high-risk *SNCA* genotype, making it difficult to ascertain the true clinical significance of this observation. Previous studies have suggested that GCase directly interacts with α-synuclein, though the significance of this *in vivo* remains unknown (Yap et al. 2011, Yap et al. 2013). Additionally, GCase has been identified in Lewy bodies, with mutant forms more likely to be found in these structures (Goker-Alpan et al. 2010). The clinical observation of accelerated motor course raises the interesting possibility that, just as *GBA1* mutations alter the propensity of GCase to interact with α-synuclein, polymorphisms in α-synuclein may also alter the dynamics between the two proteins, with clinical consequences.

The stratification of risk of adverse outcomes in PD is potentially important when determining inclusion criteria for future clinical trials, particularly as regenerative and more targeted disease modifying therapies begin to enter the clinic. For example, it would be preferable to trial treatments targeting the motor aspects of PD in patients with predominantly motor symptoms and low risk of dementia, in whom the potential benefits are greatest. A greater understanding of how the genetic risk factors for PD interact will potentially allow us to categorise patients more accurately into those with low- and high-risk for development of dementia and/or early death, based on the presence of only a small number of genetic susceptibility factors. This latter group may be ideal for the trial of putative disease modifying therapies.

2.5.3 Clinical significance of non-pathogenic *GBA1* polymorphisms

As has been discussed, as well as the GD-causative pathogenic *GBA1* mutations, a number of *GBA1* variant polymorphisms have been found at increased frequency in PD. These include the E326K, T369M and E388K polymorphisms for example, all of which were represented in this study. Of these, the E326K variant has been most extensively reported on, with the majority of studies finding that there is an increased risk of PD, as well as a more severe clinical course than in non-carriers. The role of the other common variant, T369M, is less clearly defined (Davis et al. 2016b, Mallett et al. 2016).

In this study, the E326K and T369M polymorphisms were each found in 10 of the 377 patients (2.7 %) in which they were screened for, making them the most commonly identified variants. This frequency is consistent with what has been reported in previous studies. The large meta-analysis of *GBA1* mutations and variants in PD by Sidransky *et al*. did not identify the E326K variant to be associated with PD (Sidransky et al. 2009). This may be due to the fact that the study population was enriched for individuals from Jewish, Portuguese, and Asian populations, in which the E326K allele is absent or relatively infrequent (Bras et al. 2009, Ruskey et al. 2019).

Here, carrying a non-pathogenic *GBA1* polymorphism significantly increased the risk of dementia and motor progression, indicating that they should be considered significant adverse genetic factors in PD. Additionally, this is the first study to have found that these polymorphisms are associated with a significantly increased risk of mortality in comparison to non-carriers. The long follow-up period in this study meant that all patients carrying *GBA1* abnormalities, including those with non-pathogenic polymorphisms, died during the follow-up period. This association may not have been seen in previous studies due to shorter follow-up time.

2.5.4 Limitations

The major limitations of this epidemiological study are related to sample size. Combination of two incident cohorts allowed for an initial relatively large study population. However, for survival analyses, 115 patients were excluded from the analysis due to the fact that they had only had limited genetic analysis of the *GBA1* gene, such that they could potentially have carried unidentified *GBA1* mutations. Additionally, for dementia outcome, only the CamPaIGN patients were included, because of differences in the definition of dementia onset between the two cohorts.

The limited sample size was a particular problem when investigating potential synergistic effects of *GBA1* variants and concomitant secondary genetic risk factors. Though some interesting results were observed, such as the trend towards increased risk of mortality in *GBA1*-PD patients carrying the H1 *MAPT* haplotype, and the significantly increased rate of motor progression in those carrying the high-risk *SNCA* allele, the small groups meant that the significance of these findings is uncertain. Nevertheless, these observations are worth exploring further in larger cohorts.

2.5.5 Concluding remarks

Consistent with most previous studies, analysis of the CamPaIGN and PICNICS cohorts suggested that *GBA1* mutations adversely affect clinical course. The effect of non-

pathogenic polymorphisms on clinical course in prior studies has been less clear. The E326K and T369M polymorphisms in particular are common in PD, though studies have yielded conflicting results in terms of their impact on prognosis. Here, carriers of these variants did indeed have a significantly worse prognosis, and the presence of these therefore seems likely to be of clinical significance. Additionally, no other studies have reported on the effect of concomitant genetic susceptibility factors in *GBA1*-PD, and although it is difficult to draw robust conclusions here due to the limited sample size, there are interesting observations that indicate that the presence of certain genetic variants may further worsen prognosis when associated with *GBA1* mutations. This is hypothesis would be interesting to address in larger cohorts.

Despite the disadvantages relating to small group sizes, this study also had some advantages over some previous reports. Most notably, the follow-up time in these cohorts of up to 18 years from diagnosis is longer than has previously been published, offering a fuller picture of the natural history of *GBA1*-PD. The two cohorts included patients with incident PD only, meaning that patients were observed from diagnosis to death (or loss to follow-up) so there was a high incidence of patients meeting the clinical outcomes studied. Furthermore, in contrast to previous epidemiological studies of *GBA1*-PD which have often involved hospital-based cohorts, which may over-represent those with atypical or more aggressive disease, this study included patients recruited from the community. The findings in relation to the frequency of *GBA1* abnormalities and in relation to their impact on clinical course, are therefore probably more representative of the overall PD population than some previous studies have been.

3 GENERATION OF INDUCED NEURONS

3.1 Abstract

Generation of iNs offers a source of aged adult neurons which can be used for the study of age-related neurodegenerative diseases. Direct conversion of somatic cells may be driven through the expression of proneural transcription factors, the expression of neuronal microRNAs or inhibition of the REST complex. The major potential advantage of iNs over similar iPSC-derived neurons, is that they maintain the age signature of the host, potentially retaining important aspects that determine the propensity for pathology to develop. In this study, iNs have been generated from healthy controls and PD patients through the expression of Ascl1 and Brn2, combined with REST suppression. The iNs produced expressed neuronal markers including α-synuclein, and neuronal purities and conversion efficiencies of up to around 35 % and 50 % respectively were achieved. iNs took on a typical simple neuronal morphology, with the extension of neurites. Limitations of the iN system included an impure population of cells that are relatively immature.

3.2 Introduction to chapter

Identification of disease-modifying drugs for neurodegenerative conditions such as PD is hindered by the limitations of existing disease models. The propensity for development of PD pathology clearly has cell-type specific properties, as evidenced by the fact that neurodegeneration occurs in well-defined anatomical structures, such as the substantia nigra pars compacta (Dickson 2012, Kalia and Lang 2015, Braak et al. 2003). Additionally, other than in rare genetic forms of the disease, PD is a disease of aged cells, with incidence of disease rising with age (Pringsheim et al. 2014). Furthermore, it is thought that an individual's risk of PD is, at least in part, dependent on a profile of poorly

defined genetic susceptibility factors (Ferreira and Massano 2017, Lill et al. 2012). As such, it is desirable for a disease model to retain the following aspects in order to faithfully represent the propensity for intracellular PD pathology to develop:

i) A relevant cell type (i.e. human neurons)

ii) Cellular properties related to age

iii) The genetic profile associated with PD risk

These factors will not only determine the pathology that is observed in a disease model, but will also potentially influence the behaviour of an experimental drug in the system, so the more closely that they reflect patient neurons, the more reliably the model would be expected to predict the ability of a drug to have a beneficial effect. In addition to these factors, there are also practical aspects important in a disease model, such as being derived from accessible tissue, reproducibility, and ability to scale up.

Many systems have been used to study the pathogenesis of PD, and to screen drugs for the condition. These include standard cell lines, such as neuroblastoma cells, in which an insult is applied such as α-synuclein overexpression, introduction of a pathogenic mutation or application of a toxin, but these fail to capture any of the three factors mentioned above (Wang et al. 2012, El-Agnaf et al. 1998). Additionally, introducing these experimental insults greatly exaggerates properties such as the propensity for α-synuclein aggregation (e.g. through supra-physiological levels of the protein, or introduction of aggregate-prone mutant forms of the protein), such that they are a further step removed from what happens in patients. Similarly, animal (rodent, primate and drosophila) models rely on the introduction of significant insults (such as the use of dopaminergic neuron toxins or transgene expression) for any relevant pathology to be seen (Masliah et al. 2000, Giasson et al. 2002, Kikuchi et al. 2017), as these animals do not develop PD spontaneously. Findings in these systems therefore will also not fully represent those occurring in patients. It is possible to generate patient neurons from patient-derived iPSCs, fulfilling the first and third criteria listed above. Highly pure populations of subtype-specific (e.g. dopaminergic) neurons can be generated (Kikuchi et al. 2017), meaning that it is possible to study disease mechanisms in relevant cell-types

(Fernandes et al. 2016, Sánchez-Danés et al. 2012). However, these cells fail to recapitulate age meaning that they may miss out on important aspects of pathogenesis (Lapasset et al. 2011, Horvath 2013, Victor et al. 2018). Furthermore, the way in which a drug behaves in these cells may be fundamentally different to the way it acts in an aged intracellular environment. Another potential disadvantage of iPSCs for disease-modelling, is the clonal nature of the derived differentiated cells. They therefore fail to represent genetic variations between individual cells which may contribute to the cell's susceptibility to pathology (Grskovic et al. 2011). Furthermore, it is known that long-term culture of stem cells results in the acquisition of genetic aberrations, with those that confer a growth advantage coming to dominate the cell population, potentially altering disease phenotypes (Hussein et al. 2011, Gore et al. 2011).

Direct lineage conversion of fibroblasts to iNs offers a source of aged adult neurons, which retain relevant host genetic risk factors. The retention of the aged cellular phenotype potentially means that iNs can provide a more faithful disease model than similar iPSC-derived neurons, in which DNA methylation patterns, transcriptomes and extent of DNA damage for example, revert to those of young cells (Mertens et al. 2015, Huh et al. 2016). In this project therefore, iNs were generated to form the basis of a novel drug-screening tool for PD.

Generation of iNs through direct reprogramming is a relatively novel technique, first reported in 2010. The application of iNs has been limited to date, largely due to inefficient conversion protocols. However, an understanding of microRNA-mediated differentiation pathways has allowed for the development of reprogramming protocols in which these microRNAs are utilised or bypassed, leading to a dramatic improvement in direct lineage conversion efficiencies.

In this project, iNs were generated through constitutive expression of two proneural transcription factors (Ascl1 and Brn2), as well as two short-hairpin ribonucleic acid (shRNA) sequences which suppress the REST complex – a neuronal inhibitory target of miRNA-9/9* and miRNA-124. In this chapter the reprogramming methods and iN product are described.

3.2.1 Rationale for use of induced neurons

As is discussed above, accurate representation of PD pathology in experimental models is challenging. Given that the clinically relevant pathology that occurs in PD is largely confined to neurons, and that the disease does not occur spontaneously in animals, it is preferable for an *in vitro* disease model to be based on human neurons. Furthermore, neurodegenerative diseases such as PD, Alzheimer's disease, motor neuron disease, and Huntington's disease for example, are strongly associated with aging, thus it is also desirable to retain elements of age in models of these conditions. Of course, aged human neurons are not easily accessible, and post-mortem tissue does not allow for the study of dynamic events involved in PD pathogenesis, or the study of drug effects. The conversion of adult somatic cells to iPSCs through forced expression of defined pluripotency factors, with subsequent differentiation to neurons has offered a new avenue for studying pathogenesis and for *in vitro* therapeutic screening in PD. However, the use of iPSC-derived neurons fails to capture an important aspect of PD – age.

It has been shown that iPSC-reprogramming essentially results in rejuvenation of the cell to an embryonic state, in terms of the epigenetic landscape, telomere length, and gene expression profile as well as a number of other parameters (Huh et al. 2016, Mertens et al. 2015, Horvath 2013, Maherali et al. 2007). Additionally, observation of pathology in iPSC-derived neurons employed for disease-modelling often requires the use of significant insults such as oxidative stressors, autophagy inhibition, prolonged culture time or chemically-mediated proteasome inhibition, making the system less reflective of the processes that lead to disease in patients (Jeon et al. 2012, Nekrasov et al. 2016, HD_iPSC_Consortium 2012). Direct lineage conversion to generate iNs in contrast, has been shown to lead to retention of age-dependent signatures in a number of domains, suggesting that these cells better retain an important aspect of PD pathogenesis. This has been demonstrated in a number of studies through direct comparison of age-related phenotypes in iNs and iPSC-derived neurons from the same individuals, and iNs may therefore offer a more faithful disease model (Mertens et al. 2015, Yang et al. 2015, Tang et al. 2017, Kim et al. 2018, Huh et al. 2016). iNs are a relatively novel technology, with only a small number of studies utilising them for disease-modelling to date, but it is

beginning to emerge that they are able to capture elements of pathology that are not seen in iPSC-derived neurons (Victor et al. 2018).

3.2.2 Markers of cellular aging

Aging is associated with a number of changes in a variety of intracellular structures and processes (Table 3.1). These changes reflect the age of the individual from which they were derived, rather than simply the age of the individual cell. Whilst these age-related changes may not be directly related to the pathogenesis of diseases such as PD, they suggest that the intracellular environment of an aged cell is different to that of a young cell, which may have implications for the development of disease and response to treatments.

Perhaps the best characterised of these age-related changes, are in the epigenetic landscape of the cell (Fraga and Esteller 2007, Rodríguez-Rodero et al. 2010). The methylation status at CpG dinucleotide sites in the DNA has been clearly shown to change with age, with a number of genomic regions becoming either hyper- or hypomethylated (Horvath et al. 2012, Christensen et al. 2009, Bollati et al. 2009, Bell et al. 2012). Determination of the pattern of DNA methylation in a cell allows for prediction of the chronological age of the host organism, with high accuracy – an observation that is preserved across a wide range of tissue and cell types, including neurons (Horvath 2013). The pattern of methylation at 353 CpG sites has been termed the "epigenetic clock," and it has been suggested that the hyper- or hypomethylation at these sites reflects the cumulative work performed by a cell's epigenetic maintenance system, and thus reflects age. Assessment of the DNA methylation status in different types of blood cells, some of which have very short lifespans (e.g. CD14-positive monocytes) while others have prolonged lifespans (e.g. CD4-positive T lymphocytes), revealed similar methylation age (Horvath 2013). Importantly therefore, the epigenetic clock appears to reflect the chronological age of an organism, rather than of the individual cell.

Additionally, age-dependent differences exist in terms of the gene expression profile in a number of cell types (Lu et al. 2004, Berchtold et al. 2008, Mertens et al. 2015, Fraser et

al. 2005, Glass et al. 2013). In dermal fibroblasts from young individuals, 78 genes were differentially expressed in comparison to in dermal fibroblasts from individuals over 40 years old (Mertens et al. 2015). In the human frontal cortex, age is associated with down-regulation of genes involved in mitochondrial function, synaptic plasticity and vesicular transport (Lu et al. 2004). In contrast, stress response and DNA repair genes were upregulated with aging. Those genes that were downregulated were under the control of promoters that were particularly susceptible to DNA damage associated with aging, which may account for some of the age-related transcriptomic changes that are seen (Lu et al. 2004). The profile of gene expression in aging has been shown to differ between different anatomical regions within the brain, suggesting that there are inherent differences in how certain brain regions are affected by age, which may potentially underlie the vulnerability of specific anatomical regions in certain neurodegenerative diseases (Berchtold et al. 2008, Fraser et al. 2005).

A number of other biochemical properties are also altered with aging, which also supports the concept that the intracellular environment in an aged cell is inherently different to that in cells from young individuals. For example, nuclear membrane integrity is disrupted with ageing, as evidenced by loss of nuclear-cytoplasmic compartmentalisation, reduced expression of the nuclear pore-associated transport receptor RAN binding protein 17 (RANBP17), and abnormalities in nuclear morphology (Mertens et al. 2015, Miller et al. 2013, Tang et al. 2017). Accumulation of double-stranded DNA breaks also occurs with age, as demonstrated by the increased presence of serine 139-phosphorylated H2A histone family member X (γH2AX) foci in fibroblasts from older individuals (Tang et al. 2017, Miller et al. 2013). Mitochondrial aberrations also appear to accumulate in cells from aged individuals. For example, increased levels of reactive oxygen species (Yang et al. 2015, Miller et al. 2013), oxidised proteins (Kim et al. 2018) and oxidative DNA damage (Prigione et al. 2011, Lu et al. 2004), and reduced mitochondrial membrane potential and adenosine triphosphate (ATP) synthesis (Kim et al. 2018) are all observed in cells from aged individuals.

Epigenetic	- Methylation status at defined CpG sites - Loss of trimethylated H3K9m23 - Loss of HP1γ
Transcriptome	- Altered gene expression profiles with aging
Nuclear membrane integrity	- Reduced RANBP17 - Loss of nucleocytoplasmic compartmentalisation - Nuclear blebbing - Loss of LAP2α
Senescence	- Increased SA-β-galactosidase activity - Reduced telomere length
Mitochondrial	- Fragmentation - Oxidative damage - Reduced membrane potential - Reduced ATP synthesis
DNA / Chromosome integrity	- Double-stranded DNA breaks - Oxidative DNA damage

Table 3.1 – Age-related intracellular changes. Ageing is associated with a number of alterations to epigenetic parameters, gene expression, DNA integrity and mitochondrial function for example. Abbreviations: ATP = adenosine triphosphate; DNA = deoxyribonucleic acid; HP1γ = heterochromatin protein one γ; LAP2α = lamina-associated peptide two α; RANBP17 = RAN binding protein 17; SA-β-galactosidase = senescence-associated-β-galactosidase.

3.2.3 Rejuvenation of induced pluripotent stem cells

Reprogramming to iPSCs using pluripotency factors results in loss of the cellular markers of aging discussed in the previous section. This is perhaps desirable when aiming to develop iPSC-based regenerative therapies, but limits the utility of iPSC-derived cells for disease-modelling, particularly with regard to neurodegenerative diseases which are strongly associated with aging. Telomere length and telomerase activity is increased in iPSCs (Lapasset et al. 2011, Marion et al. 2009, Agarwal et al. 2010, Prigione et al. 2011, Suhr et al. 2010), whilst senescence-associated markers such as $P16^{INK4A}$ and $P21^{CIP1}$ expression, and senescence-associated-β-galactosidase (SA-β-galactosidase) activity are reduced in comparison to their parent cells (Lapasset et al. 2011). iPSC reprogramming also results in epigenetic changes, such that the DNA methylation age is reset to that of an embryonic stem cell (Horvath 2013, Marion et al. 2009, Maherali et al. 2007). Additionally, iPSCs resemble human ESCs in terms of gene expression profile (Lapasset et al. 2011, Patterson et al. 2012, Prigione et al. 2011) and mitochondrial health (Lapasset et al. 2011, Prigione et al. 2011). Mitochondria in iPSCs from both young and old

individuals take on a morphology that resembles those of embryonic stem cells, switching from a tubular shape with dense cristae to a rounded shape with poorly developed cristae. Additionally, iPSC-reprogramming results in reduced reactive oxygen species production, and increased mitochondrial membrane potential, with levels of oxidative DNA damage also being reset to the minimal levels seen in embryonic stem cells (Prigione et al. 2011). Differentiated progeny derived from iPSCs also resemble their embryonic stem cell-derived counterparts in terms of proliferative potential and transcriptome (Lapasset et al. 2011, Patterson et al. 2012). It has also been suggested that neural precursor cells derived from human iPSCs resembled fetal neural cells from a very early developmental stage (Patterson et al. 2012).

Comparison of iPSCs derived from young and old individuals showed that these are indistinguishable in terms of markers of aging including expression of RANBP17, lamin A, lamina-associated protein two α (LAP2α), heterochromatin protein one γ (HP1γ), and trimethylated H3K9me (Miller et al. 2013, Mertens et al. 2015). Additionally, double-stranded DNA damage and accumulation of mitochondrial reactive oxygen species was also eradicated during iPSC-reprogramming (Miller et al. 2013). The gene expression signature in iPSCs derived from young and old individuals is also similar, which contrasts with the age-dependent changes that are observed in differentiated cells (Prigione et al. 2011, Mertens et al. 2015). Furthermore, the loss of age-associated signature persists on differentiation of iPSCs into fibroblasts or dopaminergic neurons, with iPSC-derived products from old individuals closely resembling those from young individuals (Miller et al. 2013, Mertens et al. 2015).

However, age-related phenotypes have been restored in iPSC-derived fibroblasts through the expression of progerin – an abnormal protein which results in the premature aging syndrome Hutchinson-Gilford Progeria syndrome (Hennekam 2006). The expression of progerin induced several of the aforementioned markers of cellular aging, including nuclear morphology abnormalities, reduced LAP2α expression, accumulation of double strand DNA breaks, increased mitochondrial reactive oxygen species, shortened telomere length and increased SA-β-galactosidase levels (Miller et al. 2013). The age profile of progerin-expressing iPSC-derived fibroblasts resembled that of primary fibroblasts from aged individuals. However, induction of age in iPSC-derived dopaminergic neurons was

less effective. Whilst age-related changes in nuclear morphology, DNA damage and reactive oxygen species levels were observed in iPSC-derived neurons, there were no changes in LAP2α or SA-β-galactosidase levels for example (Miller et al 2013). Further studies are necessary to characterise the effect of progerin-expression in iPSC-derived neurons, but this potentially represents an avenue to iPSC-based models that capture elements of the aging profile.

3.2.4 Retention of age in direct conversion

Whilst iPSCs lose these age-related effects, iNs have been shown to retain the changes associated with the age of the individual from which they are generated. iNs derived from human adult fibroblasts display age-dependent differences in the transcriptome (Mertens et al. 2015, Huh et al. 2016). Interestingly, whilst the transcriptome is different when comparing young and old fibroblasts and iNs, only a small number of the differentially expressed genes are shared by both of these cell types (Mertens et al. 2015). This suggests that there may be transcriptomic aging profiles that are different in different cell types, and that this is reflected during direct reprogramming. Similarly, the microRNA profile in iNs derived from young and old individuals differs (Huh et al. 2016).

iNs have also been shown to retain age-related changes in mitochondrial function. An analysis of the expression of 1118 mitochondrial genes in iNs, found that 70% of the analysed genes were downregulated in cells derived from individuals over 40 years old, compared to in those derived from individuals under 40 years old (Kim et al. 2018). Within the downregulated genes, 93% of the genes related to electron transport chain complexes I to IV were downregulated, along with genes involved in the tricarboxylic acid cycle and pentose phosphate pathway (Kim et al. 2018). iNs derived from older individuals also had a reduced density of axonal mitochondria, with increased mitochondrial fragmentation in comparison to those from younger individuals (Kim et al. 2018). iNs have also been shown to demonstrate age-dependent reductions in mitochondrial membrane potential and ATP synthesis, and accumulation of reactive oxygen species and oxidative protein damage (Kim et al. 2018, Huh et al. 2016). Interestingly, whilst these changes are observed in fibroblasts from aged individuals, they

are not as pronounced as in iNs (Kim et al. 2018). This observation could be a result of the direct conversion process itself, but alternatively may be a demonstration that iNs recapitulate neuron-specific aging profiles.

Other age-related changes that have been shown to be preserved in iNs include disruption of nuclear membrane permeability (Mertens et al. 2015), methylation age (Huh et al. 2016), DNA damage (Huh et al. 2016, Tang et al. 2017) and telomere shortening (Huh et al. 2016).

3.2.5 The use of induced neurons in disease-modelling studies

The number of published studies involving iNs has grown considerably over the past few years. However, only a small number of studies have employed iNs for disease-modelling or *in vitro* treatment testing.

Jovicic *et al* generated iNs from two adult humans with, and three without mutations in *c9orf72*, through lentiviral expression of Ascl1 and Ngn2, and culture with small molecules and neurotrophic factors for three weeks. These iNs were then co-cultured with mouse astrocytes for a further week (Jovičić et al. 2015). Characterisation of the neuronal product was limited in this study to determining expression of β3-tubulin. The morphology of the iNs generated was not discussed, but they appeared to have multiple short neurite processes emerging from the cell body. The iNs were utilised to assess the integrity of nuclear-cytoplasmic transport, with differences observed in the localisation of regulator of chromosome condensation one (RCC1 – a Ran guanine nucleoside exchange factor), in iNs derived from healthy controls compared to those derived from mutation carriers.

A recent study in which medium spiny neurons were generated from Huntington's disease patients and healthy controls via direct conversion identified relevant pathological changes in the Huntington's disease iNs in comparison to the control iNs (Victor et al. 2018). These included the presence of mutant huntingtin aggregates in about 10 % of the

iNs (reflecting human post-mortem findings), oxidative DNA damage and double-stranded DNA breaks, and reduced viability. Mitochondrial dysfunction was also evident in the Huntington's disease iNs, as evidenced by increased mitochondrial superoxide production and a reduction in mitochondrial membrane potential. These changes were not observed in unconverted fibroblasts, demonstrating the importance of using a relevant cell type. Additionally, this group compared the pathology seen in these iNs, to that seen in iNs derived from embryonic fibroblasts that had been generated from iPSCs from the same patient lines. This allowed for comparison of the same neuronal product, with the only differences being related to passage through the stem cell stage and the associated cellular rejuvenation. Interestingly, no huntingtin aggregates were observed in the iPSC-derived, "embryonic" iNs, demonstrating the importance of retention of age, and the potential for iPSC-derived reprogramming to miss important aspects of pathology (Victor et al. 2018).

iNs have also been used for drug screening in a study of motor neuron disease (Liu, Zang and Zhang 2016b). In this study, cholinergic motor neurons were generated from three patients with *FUS* mutations. The localisation of FUS was found to be cytoplasmic (in contrast to the usual nuclear localisation) in mutation-carrying iNs, and this mislocalisation was not seen in fibroblasts from the same individuals, adding further support to the idea that using a relevant cell type is necessary for the modelling of neurodegenerative disease *in vitro*. The iNs from FUS-mutation carriers also had altered morphology, abnormal electrophysiological activity, and reduced viability, in comparison to iNs derived from healthy donors. They used this pathology as a platform for screening potential therapeutic agents, and found that one drug, the cyclin-dependent kinase inhibitor kenpaullone, improved neuronal morphology and viability in the mutation-carrying iNs.

Son *et al* have also generated a protocol for developing spinal motor neurons from mouse and human fibroblasts (Son et al. 2011). When co-cultured with glial cells containing the G93A mutations in the *SOD1* gene (the basis for a mouse model of amyotrophic lateral sclerosis), there was a reduction in the number of surviving iNs compared to when co-cultured with wild-type glial cells. Introduction of the G93A *SOD1* mutation into iNs also resulted in reduced neuronal viability (Son et al. 2011). Induced motor neurons have also

been generated directly from spinal muscular atrophy patients, which had a reduced neurite growth rate, and accelerated neurite degeneration in comparison to controls (Zhang et al. 2017).

iNs have also been used in a study of the pre-synaptic effects of polymorphisms in the microRNA, miR137 – a gene that has been linked to the risk of schizophrenia (Siegert et al. 2015). This group generated iNs through expression of Ascl1, Brn2, and Myt1-L. After four weeks they transduced the iNs with a virus containing a construct to induce mCherry expression under the control of the glutamatergic neuron-specific CAMK2A promotor, to allow for isolation of neurons from the fibroblast population. They identified elevated levels of miR-137 in iNs derived from individuals carrying polymorphisms in the minor alleles of miR-137. Importantly, these changes were not seen in fibroblasts from the same individuals.

iNs have also been employed in preliminary studies of familial Alzheimer's disease. iNs were generated from controls, as well as patients with mutations in the *APP* (which encodes amyloid precursor protein) and *PSEN1* (which encodes presenilin one) genes using a combination of chemical factors. Increased levels of Aβ40 and Aβ42 were observed in comparison to controls, along with increased levels of tau and phosphorylated tau (Hu et al. 2015).

Recently, iNs have been used to characterise cellular aspects in patients with the mitochondrial disease, myoclonic epilepsy with ragged red fibres (MERRF), in comparison to iNs derived from healthy controls (Villanueva-Paz et al. 2019). iNs derived from the two MERFF patients in this study had reduced complexity of neuronal morphology, abnormal mitochondrial morphology, reduced mitochondrial membrane potential, higher reactive oxygen species levels, reduced ATP production, and evidence of a block in the autophagy pathway.

In this chapter the details of the direct generation of iNs from patient-derived fibroblasts are discussed, including the acquisition of neuronal markers and morphology. In addition,

technical approaches aiming to optimise the direct conversion process for disease-modelling are considered.

3.3 Materials and methods

3.3.1 Derivation and expansion of primary fibroblast cultures

Skin biopsies were obtained from the medial forearm of patients with PD and healthy controls, in the John van Geest Centre for Brain Repair PD research clinic, with approval from the Cambridge Central Research Ethics Committee (REC09/H0311/88). PD patients and healthy controls were recruited through the PD research clinic. GD patients and their relatives had previously been recruited by Dr Lucy Collins, through the Cambridge University Hospitals NHS Foundation Trust lysosomal storage disorder clinic, with the support of Professor Tim Cox. Genetic analysis of the *GBA1* gene had been previously carried out on these individuals by Dr Sophie Winder-Rhodes as described in Winder-Rhodes et al. 2013.

The biopsy site was cleaned with ChloraPrep applicators, and 1 to 2 ml of 1 % lidocaine was instilled subcutaneously. A 4 mm punch biopsy was performed, and the skin sample was dissected from the subcutaneous tissue with a blade, and placed immediately into 25 ml of pre-warmed fibroblast medium (Dulbecco's Modified Eagle Medium (DMEM) + glutamax (Gibco) + 10% fetal bovine serum (FBS – Biosera) + 1 % penicillin / streptomycin / fungomycin (PSF – Sigma)).

Skin samples were washed twice in fresh medium and sectioned into six to eight pieces. These were added to a six-well plate coated in 0.1 % gelatin (Sigma), and cultured in fibroblast medium at $37^{O}C$ with 5 % carbon dioxide. The medium was topped up on days two and four, and then full medium changes were performed every two to three days thereafter until fibroblasts had reached full confluency. They were then passaged as described below. Biopsy specimens were transferred to a new six-well plate and the

process repeated to obtain more fibroblasts. This was repeated until the biopsy specimen stopped yielding fibroblasts.

3.3.2 Fibroblast and HEK-293T cell culture

Cells were cultured in fibroblast medium at 37^{O}C in 5 % carbon dioxide. The medium was changed every two to three days, and cells were passaged once they were at 80 to 90 % confluency. Fibroblasts were dissociated in 0.05 % trypsin for five minutes, and remaining cells flushed with medium. They were centrifuged at 400 x G for five minutes at room temperature and the supernatant discarded. The cell pellet was re-suspended and re-plated in T75 flasks (Thermo Scientific Nunc) for ongoing culture or frozen in 45 % DMEM + glutamax, 45 % FBS and 10 % dimethyl sulfoxide (DMSO – Sigma).

HEK-293T cells (Clontech) were dissociated in 0.05% trypsin for five minutes and remaining cells were flushed with medium. The cell solution was inverted three times to distribute cells evenly, and cells were re-plated in T175 flasks or frozen as above.

Cells were thawed by placing the cryovial in a 37^{O}C water bath until only a small amount remained frozen, and then added to 5 ml of pre-warmed fibroblast medium. The cell solution was then centrifuged at 400 x G for five minutes at room temperature (for fibroblasts) or 100 x G for five minutes at room temperature (for HEK-293T cells). The supernatant was aspirated and discarded and the cell pellet re-suspended in medium.

3.3.3 Plasmid amplification and purification

Vector plasmids were kindly provided by Janelle Drouin-Ouellet (University of Montreal). These included the third generation lentivirus packaging vectors pRSV-REV, pMD2.G, and pMDL, and the transfer vector 3410 (containing open reading frames for *ASCL1*, *BRN2* and the shRNA sequences targeting the REST complex, under control of non-regulated phosphoglycerate kinase (pGK) and U6 promotors and the Woodchuck

hepatitis virus post-transcriptional regulator element (WPRE)) (Drouin-Ouellet et al. 2017).

Plasmids were amplified using chemically competent One Shot™ Top 10 *Escherichia coli* (Invitrogen), and purified using the Nucleobond® Xtra endotoxin-free Midiprep or Maxiprep kits (Machery-Nagel). Bacterial transformation was performed by adding 2 to 5 µl of plasmid solution to a vial of *E. coli* which was then kept on ice for 30 minutes. The *E. coli* were then heat-shocked at 42^{O}C for 30 seconds before 250 µl of super optimal broth (SOC) medium was added. The vial was then incubated for one hour at 37^{O}C with shaking at 225 rpm before being spread onto Lysogeny broth (LB) agar (Sigma) plates containing 100 µg/ml ampicillin (Sigma) and incubated at 37^{O}C overnight. A single colony was picked and added to 3 ml of LB broth (Sigma) containing ampicillin 50 µg/ml as a starter culture. This was incubated for eight hours at 37^{O}C with shaking at 225 rpm. LB broth from the starter culture was then diluted 1:1000 in 100 ml (Midiprep) or 300ml (Maxiprep) of fresh LB broth, which was then incubated overnight at 37^{O}C with continuous shaking at 225 rpm. The plasmids were then extracted and purified as per the instructions from the Nucleobond® Xtra Midiprep or Maxiprep kit. Verification of plasmid amplification was performed with agarose gel electrophoresis after fragmentation using restriction endonucleases (Supplementary Table 7.1).

3.3.4 Lentivirus production and titration

HEK-293T cells were seeded at a density of 12.5 million cells per T175 flask (Thermo Scientific Nunc), with two flasks per batch of virus. Packaging and transfer vector plasmids were mixed for each batch of virus in the following proportions: pMDL 7.5 µg, pMD2.G 5.5 µg, pRSV-Rev 3.9 µg, and 3410 25 µg, with 3.5 ml of DMEM + 1 % PSF (with no serum). Polyethylenimine (Polysciences) 1 mg/ml (126 µl) was then added and the mixture vortexed for 10 seconds and kept at room temperature for 15 minutes. The medium in the T175 flasks was changed, and 1.8 ml of the transfection mix was added to each flask. These were then incubated for 45 hours at 37^{O}C. The medium from the T175 flasks was harvested and centrifuged at 800 x G for 10 minutes at 4^{O}C. The resulting supernatant was filtered through a 0.45 µm sterile filter, and then centrifuged at 25000

rpm for 90 minutes at 4^{O}C. The supernatant was discarded and the pellet covered in 100 µl of phosphate-buffered saline (PBS) and kept at 4^{O}C for two hours, before it was resuspended by vortexing for five seconds, and then frozen. Alternatively, 12 ml Lenti-X^{TM} concentrator (Clontech) was added to 36 ml of the filtered supernatant, before incubation at 4^{O}C for two to four hours. The Lenti-X^{TM} supernatant solution was then centrifuged at 1500 x G at 4^{O}C for 45 minutes. The supernatant was discarded and the cell pellet was gently resuspended in PBS before being snap frozen and stored at -80^{O}C.

Lentivirus titre was calculated by a comparative quantitative PCR (qPCR) performed on the 3410 virus and a reference virus containing a green fluorescent protein (GFP)-transfer vector that had previously been quantified through fluorescence-activated cell sorting (FACS). HEK-293T cells were transfected with 0.1 µl, 1 µl or 3 µl of the test virus or the reference virus, and the DNA was extracted using the DNeasy Blood and Tissue Kit (Qiagen) as per the manufacturer instructions. The albumin gene was used as an endogenous control, with WPRE as the reporter gene. The qPCR reaction consisted of 1 µl DNA sample, 5 µl primer/probe mastermix (Eurofins Genomics), and 4 µl Taqman^{TM} mastermix (Applied Biosystems), and qPCR was performed in technical triplicate. The primer/probe mastermix consisted of 0.95 M forward and reverse primers, and 0.7 M probe for the relevant gene Supplementary Table 7.2. Viral titre was calculated using the delta delta Ct method (Rao et al. 2013).

3.3.5 Direct neural reprogramming

Culture vessels were coated with 0.1 % gelatin and incubated at 37^{O}C for 30 minutes to one hour. Other culture matrices used included poly-L-ornithine, fibronectin and laminin (PFL), poly-L-ornithine alone, poly-L-ornithine combined with laminin (PL), and Geltrex^{TM}. For PFL- and PL-coated plates, poly-L-ornithine (Sigma) 15 µg/ml in PBS with Ca^{2+} and Mg^{2+} was added, before incubation at 37^{O}C overnight. The poly-L-ornithine was removed, and laminin (Thermo Fisher) 5 µg/ml in PBS with Ca^{2+} and Mg^{2+} was added to the wells which were incubated for two hours 45 minutes. After three washes with PBS, for the PFL-coated plates fibronectin (Thermo Fisher) 5 µg/µl was then added and the plates incubated overnight at 37^{O}C. PBS was then added to PL- or PFL-

coated plates, which were then kept at 4^{O}C. To prepare Geltrex™ plates, Geltrex™ was diluted 1:100 in DMEM/F12 medium and added to wells. The plate was then incubated at 37^{O}C for 30 minutes to one hour. All plates were pre-warmed in the incubator prior to use.

Fibroblasts in culture were passaged as described in section 3.3.2. and the desired number of cells were plated in fibroblast medium, at densities of 13393 cells/cm^2 to 27777 cell/cm^2 as detailed below. Conversions were performed in 96-, 24- or 6-well plates (Thermo Scientific Nunc), 48-well plates (Greiner CELLSTAR®), or Ibidi 96-well square plates. Viral transduction was performed the following day at a multiplicity of infection (MOI) of 20 (day zero). A full change of fibroblast medium was performed the following day. On day three the medium was changed to neural conversion medium (Ndiff227 – Clontech) with added small molecules and growth factors as per Table 3.2. Half medium changes were performed every two to three days throughout the conversion process. At day 17 post-transduction, the medium was changed to late conversion medium (Ndiff 227 containing only growth factors, without small molecules), with ongoing half-medium changes every two to three days until the day of analysis.

Factor	Manufacturer	Concentration	Mechanism
Small molecules			
CHIR99021	Axon	2 μM	Activation of canonical Wnt signalling pathway through inhibition of GSK3
SB431542	R & D Systems	10 μM	Inhibition of TGFβ superfamily SMAD signalling via ALKs 5,4 and 7
Valproic acid	Merck Millipore	1 μM	Remodelling of chromatin via inhibition of histone deacetylase, facilitating binding of ectopic transcription factors
Noggin	R & D Systems	50 ng/ml	Binds BMPs (members of TGFβ superfamily) preventing activation of their receptors
LDN-193189	Axon	0.5 μM	Inhibition of TGFβ superfamily SMAD signalling via ALKs 2 and 3
Growth factors and signalling molecules			
GDNF	R & D Systems	2 ng/ml	Neurotrophic factor
NT-3	R & D Systems	10 ng/μl	Neurotrophic factor
LM-22A4	R & D Systems	2 μM	Synthetic partial agonist of trkB receptor (BDNF receptor)
Db-cAMP	Sigma	0.5 mM	Activation of cAMP signalling transduction cascade and neurotrophic factor-mediated neuronal survival

Table 3.2. Small molecules and growth factors used during neural reprogramming. Abbreviations: ALK = activin receptor-like kinase receptor; BDNF = brain-derived neurotrophic factor; BMP = bone morphogenic protein; Db-cAMP = dibutyryl cyclic adenosine monophosphate; GDNF = glial cell line-derived neurotrophic factor; GSK3 = glycogen synthase kinase 3; NT-3 = neurotrophin-3; TGFβ = transforming growth factor β; trkB = tropomyosin receptor kinase B.

3.3.6 Immunocytochemistry

Cells were fixed in 4 % paraformaldehyde at room temperature for 20 minutes, or in ice cold methanol for 10 minutes. After fixation with paraformaldehyde, cells were permeabilised in 0.1 % triton-X-100 for 10 minutes at room temperature (there was no additional permeabilisation after fixing with methanol). Blocking was performed for 60

minutes at room temperature with 5 % serum in PBS. Primary antibody diluted in 5 % serum was then added to the cells and they were kept at 4^{O}C overnight. They were washed twice with PBS before Alexa Fluor fluorophore-conjugated secondary antibodies (Thermo Fisher) diluted to 1:500 in 5 % serum were applied, and they were kept at room temperature for two hours. They were then washed in PBS before nuclear counterstaining with 4′,6-diamidino-2-phenylindole (DAPI) 1 µg/ml or Hoescht 333412 2 µg/ml for 10 minutes at room temperature was performed. Cells were washed in PBS before analysis. The antibodies used are listed in Supplementary Table 7.3.

3.3.7 Calculation of conversion efficiency and neuronal purity

Imaging was performed using the Cellomics^{TM} Array Scan XTI (Thermo Fisher). The average fluorescence intensity for each cell, and the number of cells in the well was quantified using a "target activation" program at 10x or 20x magnification. Conversion efficiency was defined as the number of cells expressing neuronal markers over the total number of fibroblasts originally plated, and neuronal purity was defined as the number of neuronal marker-expressing cells over the total number of cells within the well, as shown below:

$$\boldsymbol{Conversion\ efficiency} = \frac{Number\ of\ cells\ expressing\ neuronal\ markers}{Number\ of\ fibroblasts\ plated\ at\ start\ of\ conversion} \times 100$$

$$\boldsymbol{Neuronal\ purity} = \frac{Number\ of\ tau\ or\ MAP2\ positive\ cells}{Total\ number\ of\ cells\ in\ well} \times 100$$

3.3.8 Magnetic cell sorting

Fibroblasts were initially plated in six-well plates coated with Geltrex™, at a density of 200000 cells per well, and converted to iNs as described above. Prior to sorting, the converting cells were dissociated with trypsin 0.05 % and centrifuged for five minutes at 400 x G. The cell pellet was resuspended in NDiff227 medium before a cell count was performed to determine the total number of cells prior to sorting. The cells were centrifuged again for five minutes at 300 x G and the pellet resuspended in 80 µl magnetic-activated cell sorting (MACS) running buffer (pH 7.2 PBS with 0.5 % bovine serum albumin (BSA) and 2 mM ethylenediaminetetraacetic acid (EDTA)). Human neural cell adhesion molecule (NCAM) CD56 microbeads (20 µl – Miltenyi) were added and the solutions incubated for 30 minutes at room temperature. One ml of MACS buffer was then added and the solutions centrifuged at 300 x G for 10 minutes. Cell pellets were resuspended in 500 µl MACS buffer and solutions were passed through pre-soaked LS columns (Miltenyi).

NCAM-negative cells were collected in a tube and centrifuged at 400 x G for five minutes, before the cell pellet was resuspended in neuronal medium and counted. NCAM-positive cells were flushed from the MACS cylinder with 5 ml MACS buffer, before being centrifuged for five minutes at 400 x G. The cell pellet was resuspended in neuronal medium. The NCAM-positive cell count was estimated by subtracting the NCAM-negative cell count from the total count prior to sorting. Cells were plated at a density of 7500 cells per well in a 96-well plate (Ibidi), coated with Geltrex™. NCAM-positive cells were plated in neuronal medium. NCAM-negative cells were plated in fibroblast medium, and then either kept in fibroblast medium or switched to neuronal medium the following day. Cells were fixed at day 24 post-transduction for analysis. Magnetic cell sorting was performed with the assistance of Dr Shaline Fazal.

3.3.9 Details of adult dermal fibroblast cell lines

A total of 15 cell lines were used in this study, as shown in Table 3.3. These included a number that had been previously acquired as described above, as well as those from some newly recruited patients. The cell lines included four healthy control individuals, though only two of these were confirmed not to carry *GBA1* mutations. Six iPD lines, three

GBA1-PD lines, and two lines with concomitant GD and PD (GD+PD) were used. Experiments were carried out using two to five cell lines per phenotype, as detailed in the relevant sections.

The mean age was 58.5 years (standard deviation 4.7) for the healthy control group, 65.5 years (standard deviation 4.4) for the iPD group, 63.3 years (standard deviation 6.0) for the *GBA1*-PD group, and 54.7 years (standard deviation 1.4) for the GD+PD group. There were no statistically significant age differences between any of the groups, as determined by one-way ANOVA with post-hoc Tukey analysis (p=0.093).

Cell Line	Sex	Age at Biopsy	Phenotype	GBA1 Genotype
C1	F	54	Healthy control	WT/WT
C2	M	57	Healthy control	WT/WT
CT1	F	65	Healthy control	Unknown
CTS2	F	58	Healthy control	Unknown
PD5	F	68	iPD	WT/WT
PD6	F	66	iPD	WT/WT
PD7	M	65	iPD	WT/WT
PDTS262	M	69	iPD	WT/WT
PDTS41	F	68	iPD	WT/WT
PDTS1192	M	57	iPD	WT/WT
PD2	F	64	*GBA1*-PD	N370S/WT
PD4	M	57	*GBA1*-PD	E326K/WT
PD3	M	69	*GBA1*-PD	E326K/WT
GD5	M	56	GD+PD	L444P/R463C
PD1	F	58	GD+PD	R463C/R463C

Table 3.3. – Details of primary adult fibroblast cell lines. Abbreviations: F = female; *GBA1*-PD = *GBA1*-mutation-associated PD; GD = Gaucher disease; GD+PD = concomitant GD and PD; iPD = idiopathic PD; M = male; WT = wild-type.

3.3.10 Statistical analysis

All statistical tests were performed using IBM SPSS software. For comparison between two independent groups Levene's test of equal variance was performed to determine if equal variance could be assumed, and p-values were determined with independent samples T tests. Multiple group comparisons were performed with one-way ANOVA with post-hoc Tukey analysis. Statistical significance is indicated by asterixes as follows: * = $p \leq 0.05$; ** = $p \leq 0.01$; *** = $p \leq 0.001$.

3.4 Results

3.4.1 Conversion efficiency and neuronal purity

iNs were initially generated from fibroblasts derived from healthy control (n=2), iPD (n=2), *GBA1*-PD (n=3) and GD+PD (n=2) individuals, as described in section 3.3.5, and cultured to day 17 post-transduction. Immunocytochemistry for β3-tubulin was performed, and high-throughput microscopy was used to measure the mean fluorescence intensity for each cell. Each cell line was analysed in technical triplicate, with the mean of these replicates taken to provide a single value for neuronal purity and conversion efficiency for each individual line.

Conversion efficiency for the nine cell lines ranged from 4.6 % to 19.8 %, with an overall mean conversion efficiency of 11.5 % (95 % confidence interval 7.6 % to 15.3 %). The conversion efficiency of the *GBA1*-PD group was lower than in the healthy control group ($p=0.027$), with no other significant differences between the groups. Neuronal purity ranged from 6.7 % to 18.4 % with an overall mean neuronal purity of 12.6 % (95 % confidence interval 9.2 % to 16.0 %). There were no significant differences in neuronal purity between any of the groups (see Figure 3.1).

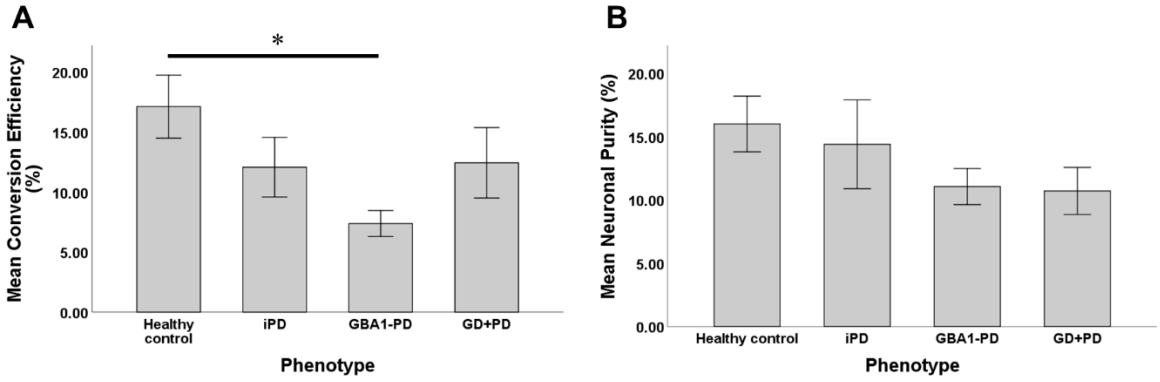

Figure 3.1 – Conversion efficiency and neuronal purity. iNs were generated from healthy control (n=2), iPD (n=2), *GBA1*-PD (n=3) and GD+PD (n=2) fibroblast cell lines. At day 17, immunocytochemistry was performed for the neuronal marker β3-tubulin. Each cell line was analysed in triplicate, with 12 fields (20x) per well imaged. The total number of cells analysed for each cell line ranged from 3059 to 11653. Error bars represent the standard error of the mean. Statistical significance based on one-way ANOVA with post-hoc Tukey analysis indicated by asterixes.

It was noted that with subsequent conversions, conversion efficiencies and neuronal purities were generally higher than in these initial experiments, and a retrospective analysis of 56 conversions taken to different time points ranging between day 10 and day 29 post-transduction, involving 13 cell lines was performed (Figure 3.2) . No statistically significant differences in neuronal purity or conversion efficiency were found between the different phenotypic groups at day 17, 20, or 29 (statistical significance could not be calculated at the other time points when only single values were available for some of the groups). Overall, neuronal purities were generally in the region of 15 % to 35 %, with conversion efficiencies of approximately 15 % to 50 %. The overall mean values for neuronal purity and conversion efficiency in each group are shown in Table 3.4. Overall, the highest mean neuronal purities and conversion efficiencies were noted in the *GBA1*-PD cell lines at day 24 and day 27. However, this is most likely to be due to the fact that these were the cell lines most used, and were over-represented in experiments performed at a later date when technical experience was higher, rather than any biological phenomenon.

	Number of conversions	Mean neuronal purity (%)	Mean conversion efficiency (%)
Healthy control	10	23.3 % (11.2 % to 35.5 %)	28.6 % (15.0 % to 42.3 %)
iPD	12	19.0 % (11.1 % to 26.9 %)	23.5% (10.7 % to 36.3 %)
***GBA1*-PD**	28	26.2% (21.4 % to 31.1 %)	44.5% (32.2 % to 56.9 %)
GD+PD	6	16.4% (9.2 % to 23.5 %)	14.8% (5.5 % to 24.2 %)

Table 3.4 – Retrospective analysis of conversion efficiency and neuronal purity data. A total of 56 conversions were retrospectively analysed with the mean values for neuronal purity and conversion efficiency determined for each patient group (95% confidence intervals shown in brackets).

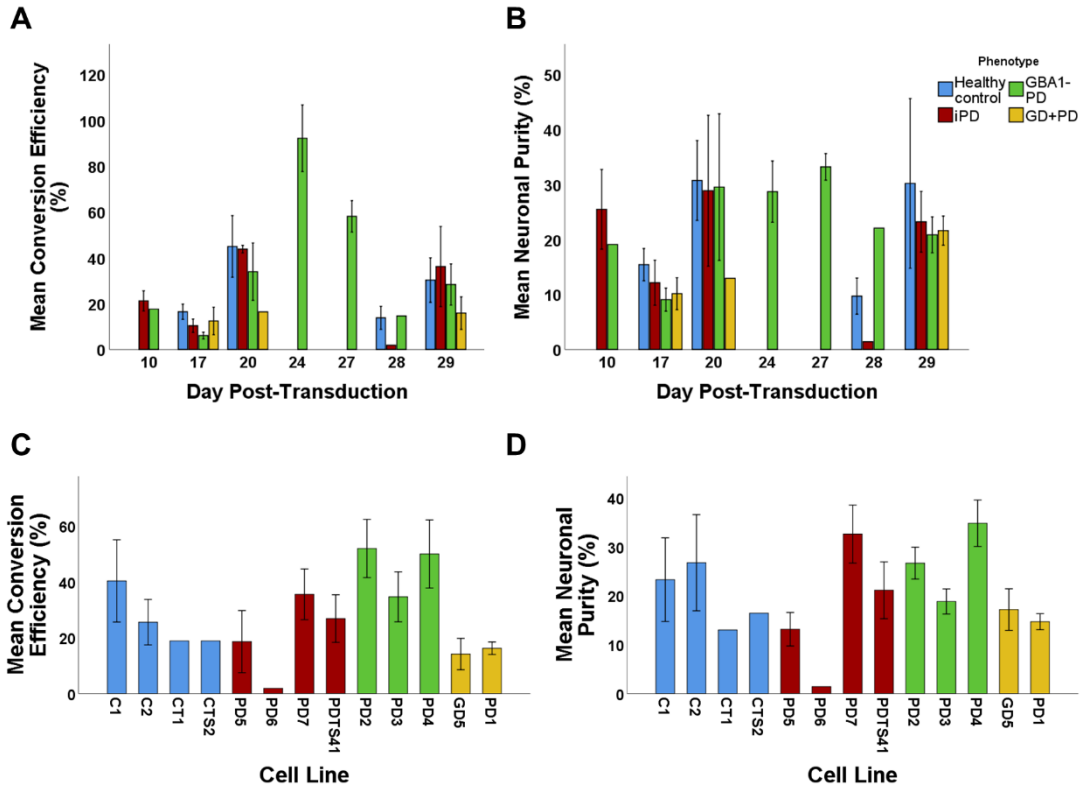

Figure 3.2 – Cumulative conversion efficiency and neuronal purity data. Mean conversion efficiency (A and C) and neuronal purity (B and D) was determined retrospectively for healthy controls (n=4), iPD (n=4), *GBA1*-PD (n=3), and GD+PD (n=2) cell lines, across 56 conversions. The numbers of cells counted in each conversion ranged from 485 to 31236 for individual cell lines. There were no significant differences between the phenotypes at any of the time points assessed, or between the cell lines. Statistics performed with one-way ANOVA for multiple comparisons, and independent sample T-tests for time points in which there were only two groups represented.

3.4.2 Acquisition of neuronal markers and morphology

In order to characterise neuronal marker acquisition over the conversion period, iNs were generated from three PD lines, including one that carried a *GBA1* mutation. These were fixed in ice-cold methanol at day zero (i.e. unconverted fibroblasts), day 10 post-transduction, and day 17 post-transduction, before immunocytochemistry for neuronal markers (see Figure 3.4 and Figure 3.5). Expression of β3-tubulin, tau, MAP2 and α-synuclein was induced over the course of the conversion. β3-tubulin and tau expression was seen by day ten, with further increases in the proportion of cells expressing these markers at day 17, when 23.4% were positive for β3-tubulin, and 38.6% were positive for tau. MAP2 and α-synuclein were not expressed at day ten, but there were significant increases in the expression of these markers at day 17, suggesting that these are induced later than β3-tubulin and tau. Demonstration of α-synuclein expression was then performed in seven cell lines (two healthy control, three *GBA1*-PD and two GD+PD) at day 17 post-transduction, with significant increases in mean α-synuclein intensity in iNs when compared to fibroblasts, in all cell lines (Figure 3.3).

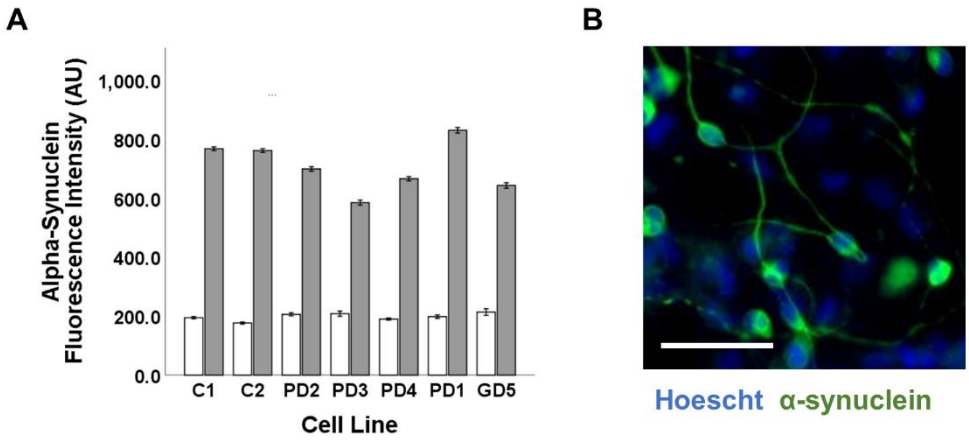

Figure 3.3 – Induction of α-synuclein expression in patient-derived iNs. A) Mean α-synuclein intensity increased significantly in all iN lines tested when compared to the unconverted parent fibroblasts. B) Representative image demonstrating α-synuclein expression in iNs at day 17 post-transduction. Scale bar represents 50μm.

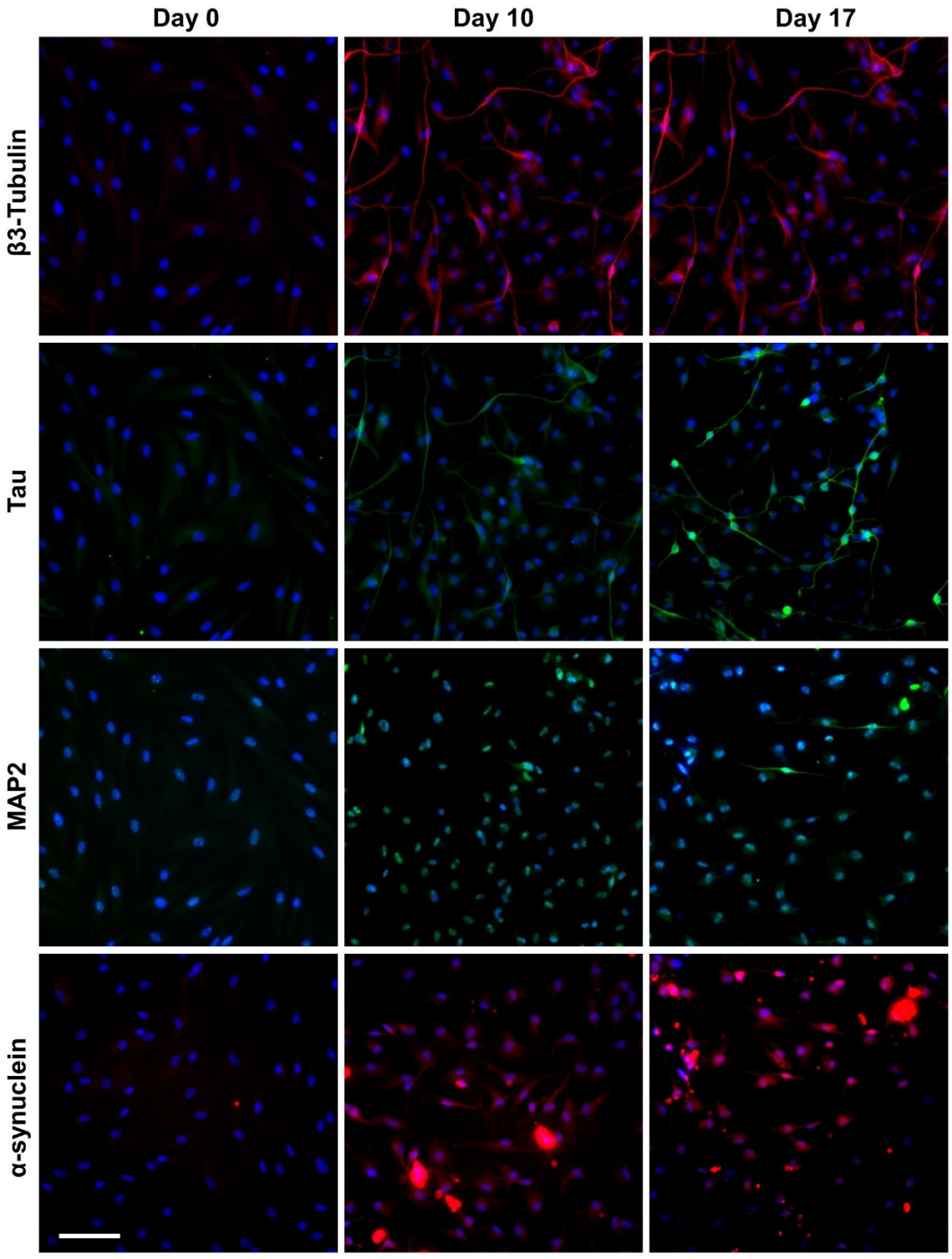

Figure 3.4 – Neuronal marker acquisition during conversion process. Images taken at 20x magnification showing expression of β3-tubulin, tau, MAPT and α-synuclein in untransduced fibroblasts, and at day 10 and 17 post-transduction. Scale bar represents 100µm.

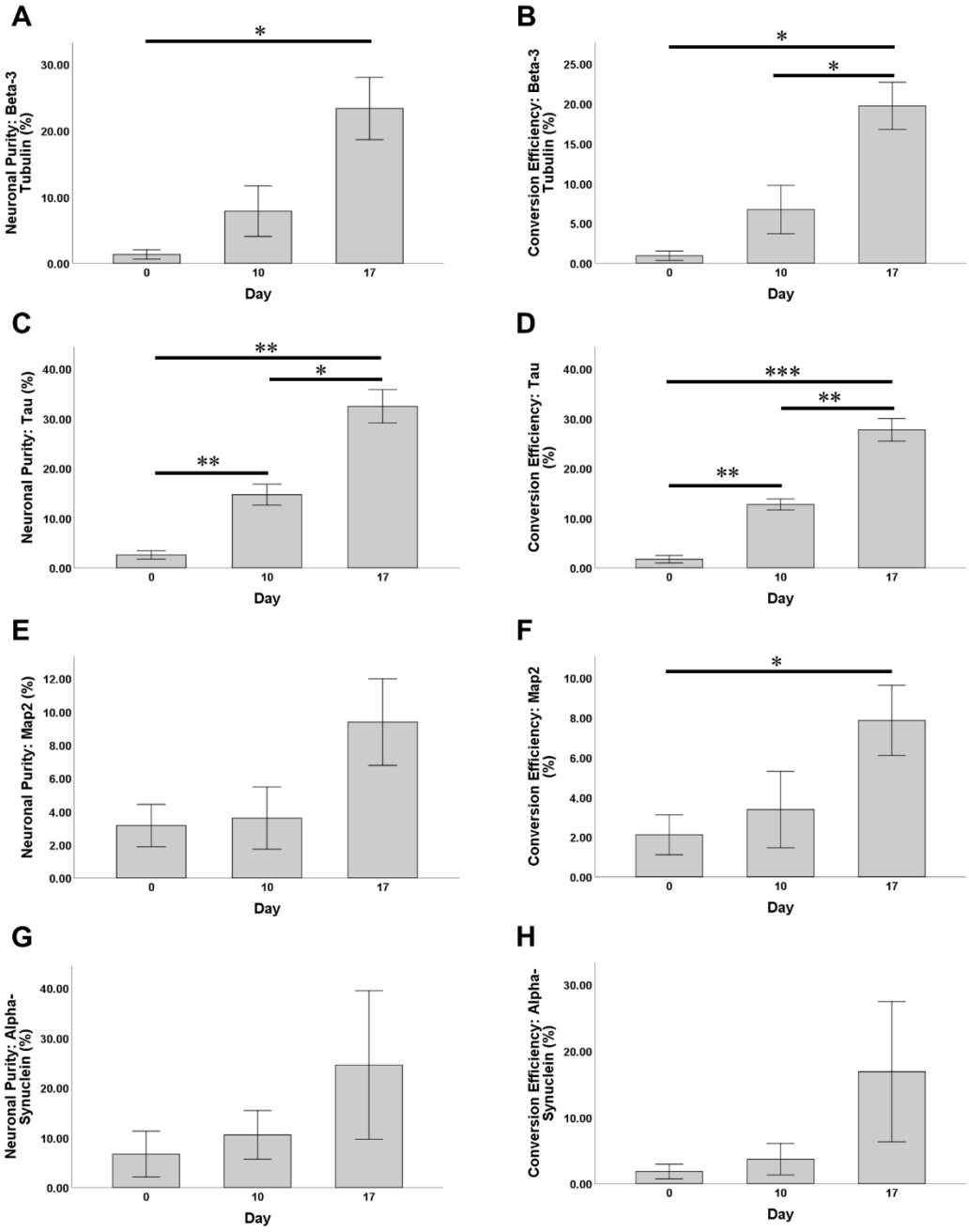

Figure 3.5 – Time-course analysis of neuronal purity and conversion efficiency. Fibroblasts from three PD patients were converted to iNs and fixed at day 0, 10 or 17 post-transduction and stained for neuronal markers (β3-tubulin (A, B), tau (C, D), MAP2 (E, F), α-synuclein (G, H). Cells were considered to express each neuronal marker when the mean intensity was greater than two standard deviations above the mean value for the unconverted fibroblasts. Statistical significance based on independent samples t-tests indicated by asterixes.

The conversion process results in the acquisition of neuronal morphology, with converted cells extending neurite outgrowths. At day 17, 9.8 % of cells had neurites greater than 120 µm in length, with 15.0 % of cells having neurites between 60 µm and 120 µm in length. It should be noted that even in the unconverted fibroblasts 7.9 % of cells were adjudged to have neurites between 60 µm and 120 µm, which was due to a limitation in the neurite analysis protocol, which could not completely discriminate between elongated cell processes seen in fibroblasts, and authentic neurites. Cells judged to have no, or very short (less than 60µm in length) neurites, made up 91.7 % of cells in the unconverted fibroblasts, dropping to 75.2 % of the cells at day 17 post-transduction (see Figure 3.6).

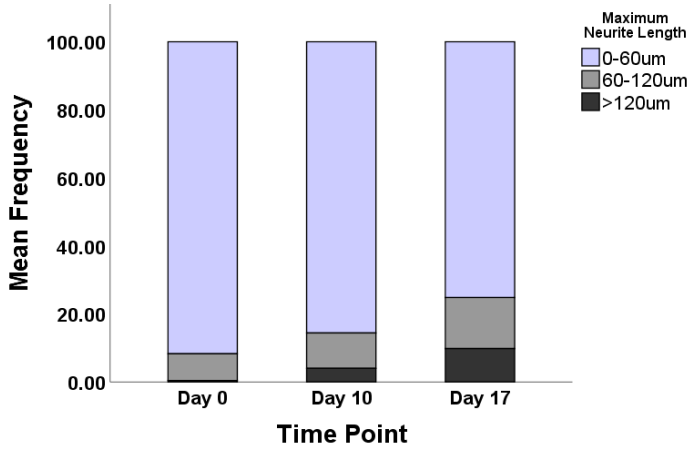

Figure 3.6 – Neurite Length Analysis. iNs from two iPD and a *GBA1*-PD line were generated and fixed prior to transduction (day zero), and at day 10 and day 17 post-transduction. Maximum neurite length was calculated using a Cellomics^{TM} XTI neuronal profiling assay. Bars represent the mean values of all three cell lines. The proportion of cells with short neurites (0 to 60 µm) decreased through the conversion, whilst the proportions with medium (60 to 120 µm) and long (greater than 120 µm) neurites increased.

3.4.3 Impact of Culture Matrix

At the start of the conversion process, fibroblasts were plated onto wells coated with 0.1 % gelatin. This is a substrate to which fibroblasts adhere strongly, and therefore may result in reduced neuronal purities, due to the persistence of unconverted fibroblasts in the culture vessel. Furthermore, it is known that neuronal culture and neurite growth can be enhanced by the use of charged culture matrices with substrates such as poly-L-

ornithine (Richner et al. 2015, Ge et al. 2015). When cultured on gelatin, iNs frequently degenerated beyond day 35, and it was considered that culture on an alternative matrix would be necessary for long-term studies.

Generation of iNs on a number of different culture matrices and surfaces was performed to investigate whether one allowed for prolonged culture and increased purity. First, fibroblasts from a healthy control and an iPD line were plated onto a 0.1% gelatin matrix before being converted to iNs. At day 12 post-transduction, cells were dissociated with accutase and re-plated in new wells coated with PFL. This resulted in an increase in neuronal purity, which was statistically significant in the iPD line based on the mean values of the technical replicates (p=0.002, Figure 3.7). However, though this approach resulted in higher purities than culture on gelatin alone, further conversion attempts in which the cells were passaged at day 12 yielded highly variable outcomes, resulting from detachment of the cells after a few days following re-plating, limiting the utility of this approach.

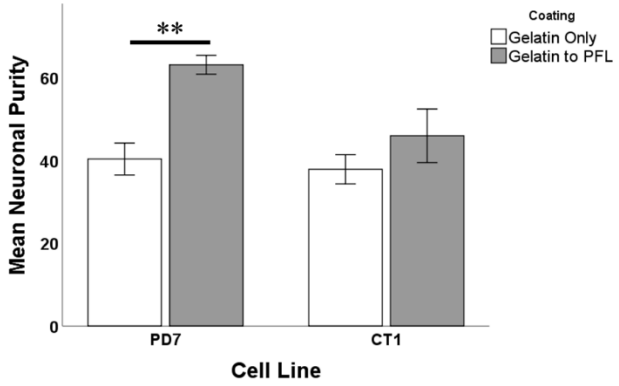

Figure 3.7 –Neuronal purity after passaging iNs and plating onto PFL matrix. Fibroblasts from an iPD and a healthy control cell line were passaged at day 12 post-transduction and re-plated onto wells coated with PFL. These were compared to cells cultured on gelatin throughout. Statistical significance, indicated by asterixes, was determined with independent samples T tests based on the mean values of the technical replicates for gelatin- and PFL-coated wells, for each cell line.

Because of the variability seen with the day 12 passaging approach, combined with the technical difficulty of scaling this up to the high numbers of wells that would be required

for disease-modelling and drug-screening, other culture conditions were trialled. These included the use of the PFL matrix, poly-L-ornithine alone, PL, and Geltrex™ from the start of conversion. This was performed directly on plastic, and also on glass cover slips, given that it had previously been reported that neuronal extensions developed better on glass (Richner et al. 2015). Whilst cells took on typical neuronal morphologies on all of these surfaces none allowed for the preservation of neuronal morphology for prolonged culture times. Culture on the PFL matrix, and its constituents often resulted in cells peeling away from the surface after approximately one to two weeks post-transduction (Figure 3.8). Geltrex™ allowed for the development of neuronal morphology, but when prolonged culture was attempted the cells degenerated as with the gelatin condition. Given the problems with reliability and lack of efficacy in the use of these matrices with regards to increasing the longevity of the cultures, subsequent experiments were performed using 0.1% gelatin as the culture matrix, which yielded consistent results with acceptable neuronal purities for analysis at day 20 to day 30.

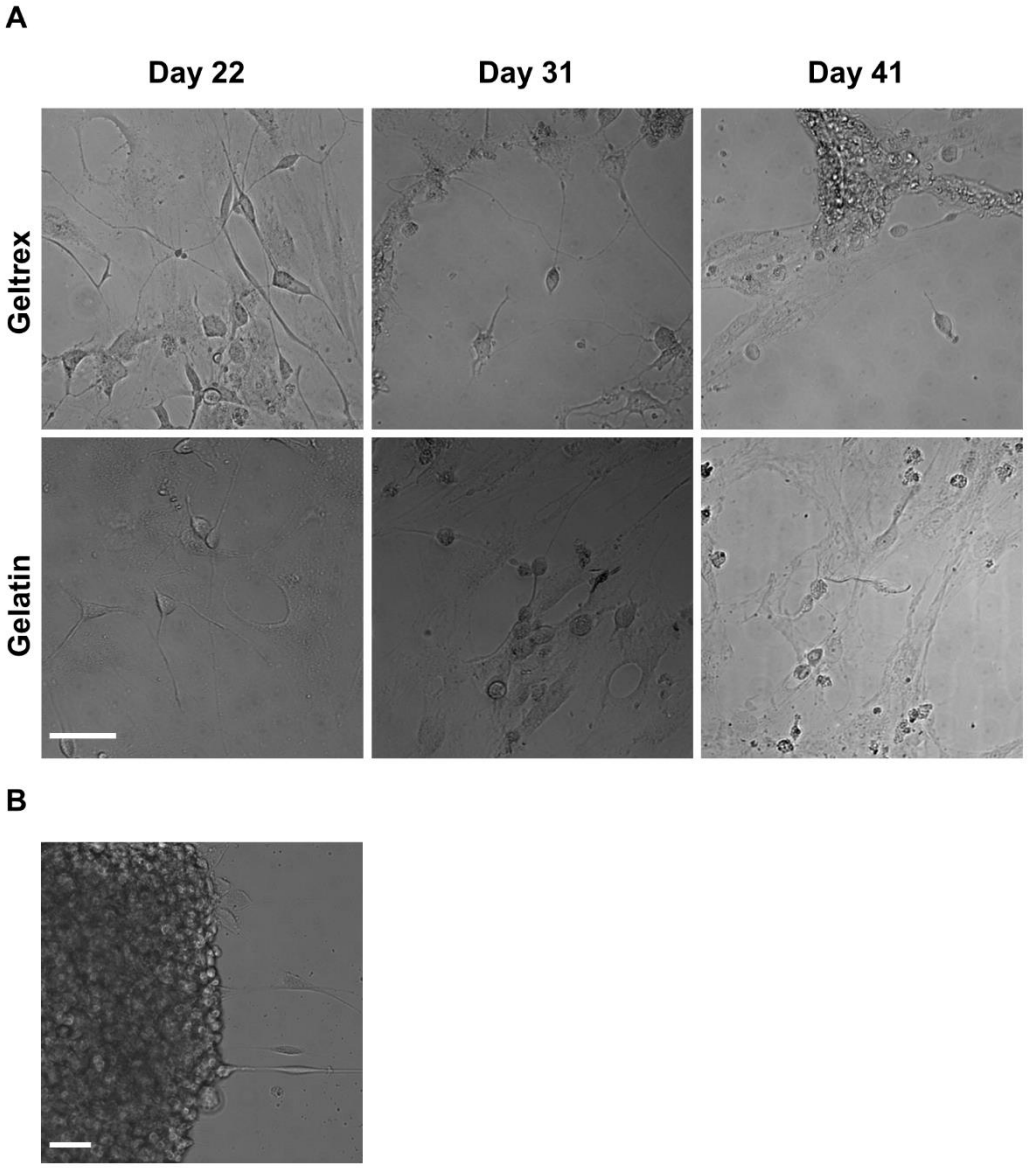

Figure 3.8 – Impact of culture matrix on neuronal morphology. A) iNs cultured to days 22, 31 and 41 on gelatin or Geltrex™ matrices. B) iNs cultured on PFL matrix. Image shows cells peeling from surface at day ten. Scale bars represent 200 µm.

3.4.4 Magnetic-activated cell sorting

One of the main limitations of the iN approach, is that the resulting cell population is not pure. In addition to iNs, there remain some unconverted fibroblasts, and probably a population of cells which have taken on some neuronal characteristics whilst retaining some fibroblast characteristics. Given that the efficacy of reprogramming varies between different cell lines, the neuronal population of one cell line will be contaminated by these

other cell types to a greater or lesser extent when compared to other cell lines, posing limitations on analyses.

The use of MACS was investigated as a potential means of increasing neuronal purity. NCAM, a neuronal cell surface adhesion molecule, expression was induced during the neuronal reprogramming process, and was not present on unconverted fibroblasts. Cells from a healthy control, a PD and a Huntington's disease line were converted to iNs, with magnetic sorting at day 3, 10 and 17. In addition, untransduced fibroblasts from the cell lines were also sorted to determine whether a significant number of false positives occurred.

Untransduced fibroblasts did not express NCAM. Even so, a mean of 10.5 % of sorted cells were retained in the "NCAM-positive" fraction. However, in this "NCAM-positive" fraction, β3-tubulin and NCAM fluorescence intensity was negligible, suggesting that there were some false-positives and that sorting on NCAM is not completely specific (Figure 3.9).

Sorting at day 3, 10 or 17 post-transduction led to relatively high neuronal purities of approximately 50 % as judged by the proportion of cells expressing β3-tubulin. Mean fluorescence intensity for β3-tubulin and NCAM were significantly higher in the NCAM-positive population of transduced cells, when compared to NCAM-negative cells at all time points after day minus one (Figure 3.9).

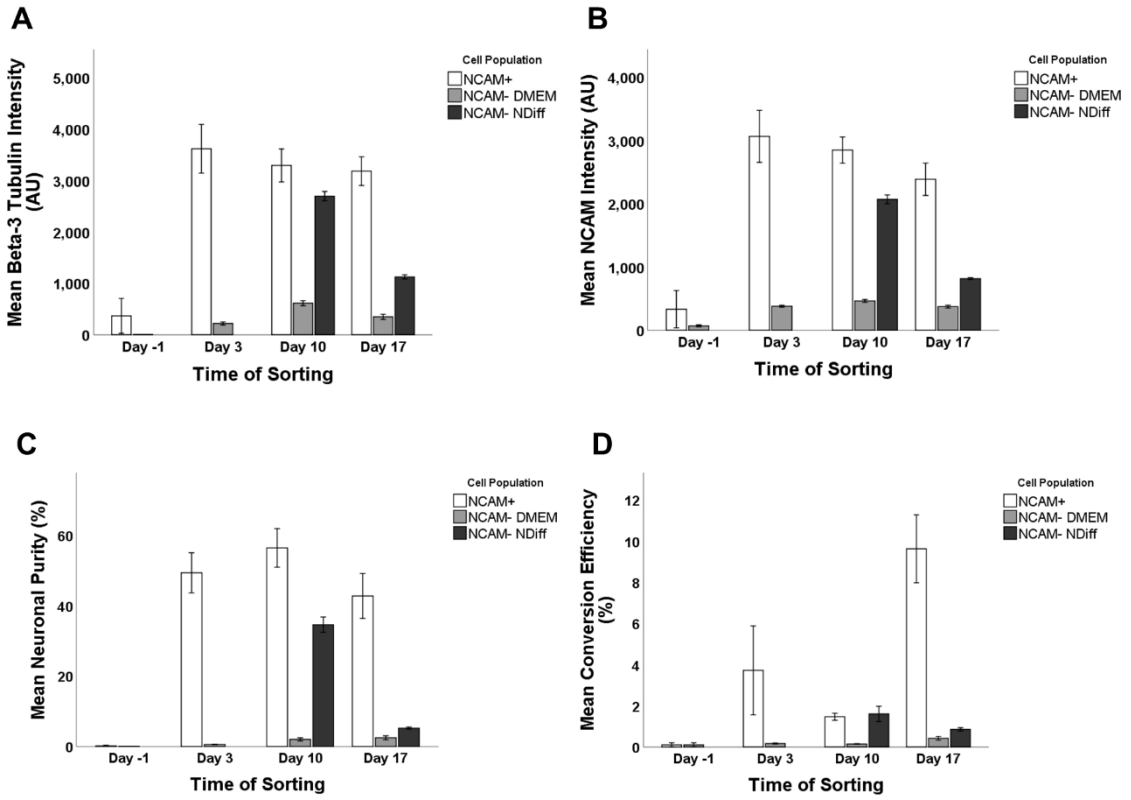

Figure 3.9 – MACS sorting for NCAM expression of iNs at multiple time points. White bars at all time points represent the NCAM-positive portion of cells. Light grey bars at all time points indicate the NCAM-negative portion of cells, cultured in fibroblast medium. Dark grey bars for the day 10 and day 17 time point indicate an additional population of NCAM-negative cells that were subsequently cultured in neuronal medium. When compared to the NCAM-negative portion cultured in fibroblast medium, the mean β3-tubulin intensity (A) and NCAM intensity (B) was significantly higher in the NCAM-positive portion at all time points post-transduction, but not in untransduced fibroblasts. Similarly, neuronal purity (C) was increased in the NCAM-positive portion. Conversion efficiency (D) was greatest in the day 17 sorted cells. Error bars represent standard error of the mean.

In contrast, conversion efficiencies were low, particularly when sorted at early time points. The highest mean conversion efficiency was achieved at day 17, which was 9.6 %. It is likely that loss of cells during the multiple centrifugation steps and sorting process, as well as some cell death during the sorting process limited conversion efficiency. So whilst sorting allowed for the generation of higher purity yields than had previously been

achieved, it is a resource expensive process, requiring large numbers of starting cells. As a result, this approach was not taken further in this work.

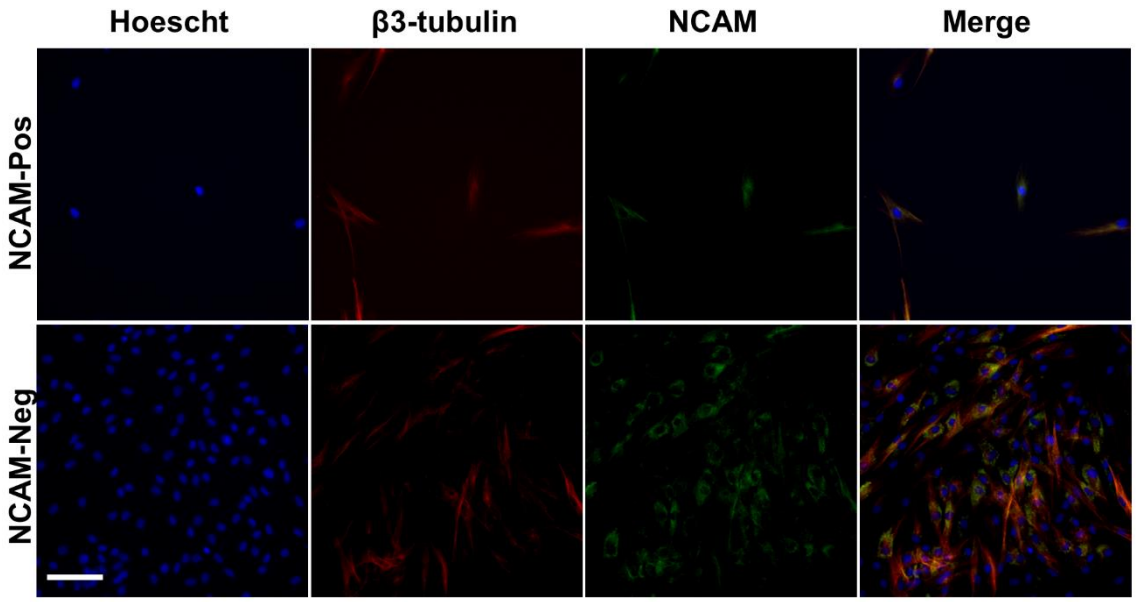

Figure 3.10 – β3-tubulin and NCAM expression in untransduced fibroblasts from a PD cell line sorted with MACS. Scale bar represents 100 µm.

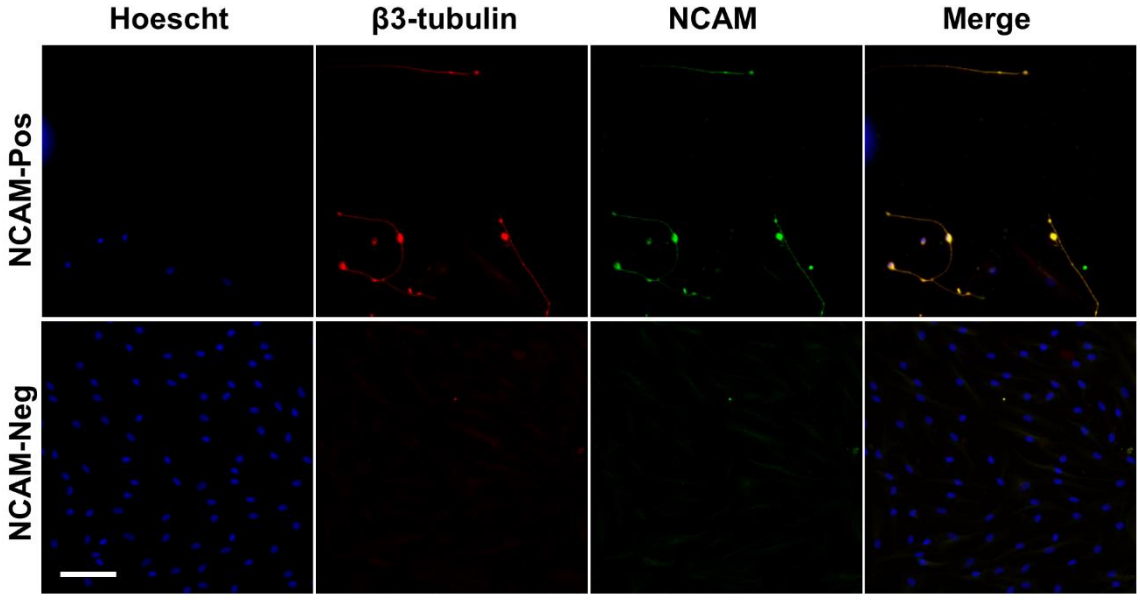

Figure 3.11 – β3-tubulin and NCAM expression in PD cells sorted with MACS at day three post-transduction. Scale bar represents 100 µm.

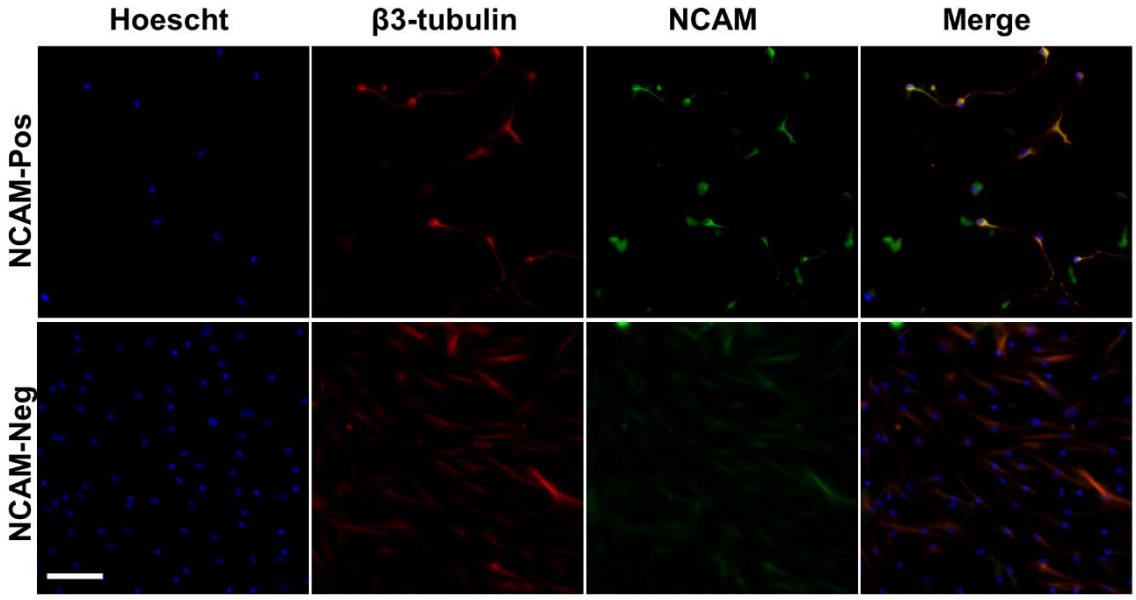

Figure 3.12 – β3-tubulin and NCAM expression in PD cells sorted with MACS at day 10 post-transduction. Scale bar represents 100 µm.

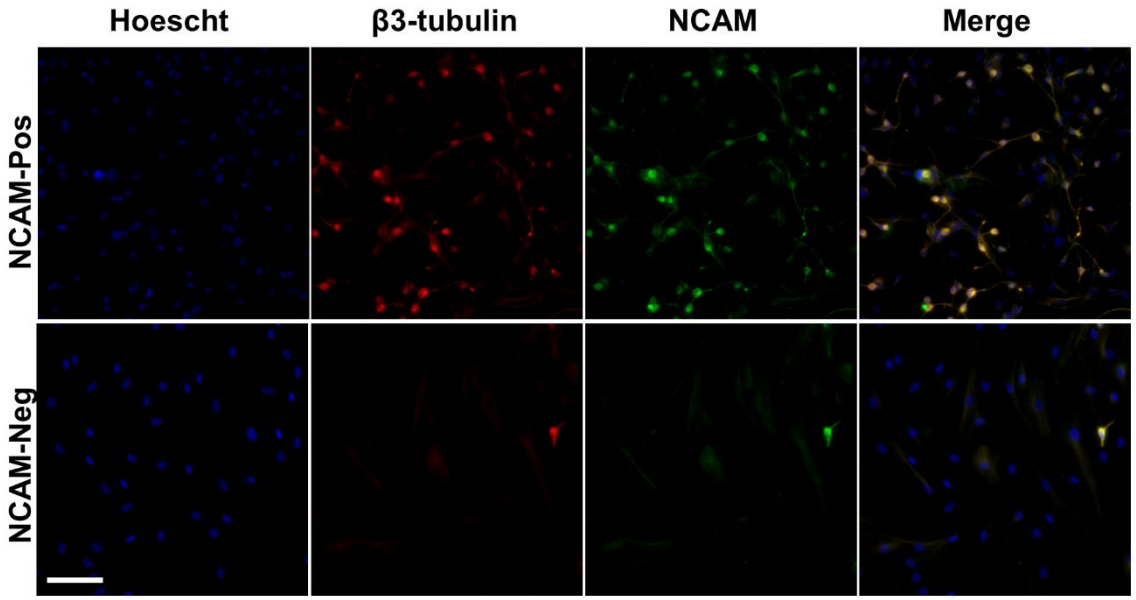

Figure 3.13 – β3-tubulin and NCAM expression in PD cells sorted with MACS at day 17 post-transduction. Scale bar represents 100 µm.

NCAM-negative cells were cultured in fibroblast medium till day 24. At all time points neuronal purity remained under 3 % in this portion. In addition, for the day 10 and 17 sorted cells, NCAM-negative cells were also cultured in neuronal medium until day 24, to see if any of they still had the potential to convert post-sorting. Indeed, at day 10 further culture of the NCAM negative cells in neuronal medium allowed for neuronal purity of 34.6 %, suggesting that there were a population of cells that were capable of converting to iNs, but had not done so by day ten. At day 17, there was also some further conversion of the NCAM-negative cells when cultured in neuronal medium. However, this was much lower than in the day 10 sorted cells, with a neuronal purity of only 5.2 % (Figure 3.9). This suggests that if a cell has not successfully converted to an iN by day 17, then it is unlikely to do so.

These results suggest that the population of cells in a conversion can broadly be divided into three subgroups:

i. Cells that convert to iNs efficiently and quickly – These cells had started expressing NCAM prior to sorting.
ii. Cells that convert slowly, but have the potential to convert to iNs over time – These cells had not acquired neuronal identity at the time of sorting, but acquired it thereafter.
iii. A population of cells that fail to convert – This may include cells that were not successfully transduced with the virus, cells in which the transfer vector failed to integrate, and cells with an inherent resistance to conversion.

Although sorting led to an increase in neuronal purity, it required very high numbers of cells, due to cell loss during the process. As such it was not felt practical for disease-modelling studies, which were carried out on unsorted cells. For immunocytochemistry-based studies this was not a limitation, as iNs could be isolated from unconverted cells through visualisation of neuronal markers, but for other assays this constituted a limitation of this model.

3.5 Discussion

Since the first description of iNs in 2010, several other protocols have been published (Vierbuchen et al. 2010, Pang et al. 2011, Ambasudhan et al. 2011, Caiazzo et al. 2011, Son et al. 2011, Drouin-Ouellet et al. 2017, Yoo et al. 2011, Ladewig et al. 2012). Despite the growing number of reports documenting iN protocols, their application in terms of disease-modelling, and particularly drug screening has been limited to only a small number of studies, discussed in section 3.2.5. In this project, a combination of the two main reprogramming approaches (forced expression of proneural transcription factors, and of specific microRNAs) has been used to generate iNs, with a view to their application as a drug-screening tool.

The conversion efficiencies (approximately 20 % to 50 %) and neuronal purities (approximately 15 % to 35 %) achieved here, far exceed that seen in the early iN protocols, and is similar to other groups that have used this method (Drouin-Ouellet et al. 2017).

3.5.1 Limitations and challenges of iN reprogramming

The use of iNs means that it is possible to generate patient-derived adult human neurons, relatively quickly. As has been discussed, the major theoretical advantage of iNs over iPSC-derived neurons is that they have consistently been shown to retain the effects of aging (Mertens et al. 2015, Kim et al. 2018, Huh et al. 2016), which has been demonstrated to be important in recapitulating pathology in neurodegenerative diseases (Victor et al. 2018). Of course, as with all disease models, there are limitations to this approach, which will now be discussed.

Firstly, while relatively consistent conversion efficiencies were achieved, there was variability between different cell lines, with some cell lines reprogramming well consistently, and others failing to reprogram effectively. There was also a degree of variability in the efficacy of reprogramming within the same cell line, across different

conversions. In this study, the main determinant of this factor was probably related to technical experience, with conversions performed at later dates proving more effective compared to the first conversions attempted. However, it is also possible that there are biological determinants, such as epigenetic and transcriptomic factors that determine the reprogramming capacity of a cell line (Biddy et al. 2018, Rais et al. 2013, Guo et al. 2014). In initial conversions, the conversion efficiency in the *GBA1*-PD group was lower than in healthy controls, with neuronal purities being similar across all groups. This may be explained by differences in the growth rate between cell lines, as an increased growth rate in the first 24 hours of the conversion would result in a lower MOI at the time of transfection. It would therefore be important to determine the growth rate of each cell line in future studies. Additionally, factors relating to cell line storage and maintenance, such as the duration and method of freezing, number of passages, and the skin biopsy processing may also contribute to the variability seen between conversions. It is therefore important that these elements are controlled for as far as is possible. The effect of these factors has not been studied in great depth (though it has been reported that passage number does not dramatically alter conversion efficiency (Drouin-Ouellet et al. 2017)), and optimisation of these factors for iN reprogramming is important for this technique to generate truly reproducible disease models, using similar approaches to those being performed with stem cell products being generated for clinical trials.

Secondly, although neuronal purities were relatively high in this study (in comparison to many previous studies), a high number of unconverted cells remained in the culture, which poses some limitations on the applicability of the iN system. The population of unconverted cells has not been characterised, and it probably consists of a mixture of fibroblasts which failed to convert, cells which began to switch fate and reverted to the fibroblast state, cells that possess traits of both fibroblasts and iNs, and cells that are converting but are doing so at a slower rate than other cells in the well. The impure population means that assays may be restricted to fluorescence-based assays in which the absence of neuronal markers can be used to exclude unconverted cells from the analysis. Assays that require cell lysis will be affected by contaminating unconverted fibroblasts, limiting the utility of this system. For example, protein detection via Western blot on a mixed population of unconverted fibroblasts, partly converted cells, and iNs will yield results that are a product of these different cell types, making their interpretation challenging. The variability in conversion efficiency for any particular cell line between

different conversions further compounds this, as individual experiments will be influenced to differing degrees by impure populations, increasing variance between experimental replicates. In contrast, iPSC-based models allow for the generation of neuronal purities approaching 100 %, which constitutes a significant advantage over current iN protocols (Kikuchi et al. 2017). However, if consistent neuronal purities can be achieved across all cell lines, this problem is somewhat circumvented, as all lines would be affected similarly. Additionally, for assays focussing on neuron-specific pathology (for example that induced by α-synuclein PFFs which is discussed at depth in the next chapter), the presence of unconverted cells should not dramatically alter the read-out. Optimising neuronal purity was attempted here through the use of alternative culture matrices, with no benefit found, and through magnetic cell sorting. The latter was attempted as a relatively atraumatic means of sorting (in contrast to FACS) after which cells could be re-plated, and though this did boost neuronal purity, it was still only at 50 %, with significant cell loss leading to low efficiencies. One potential use of the MACS technique would be to interrogate the biological factors that prevent reprogramming. If the NCAM-negative portion were to be harvested and cultured, they would represent a population of cells that is enriched with cells that were resistant to conversion. It would be interesting to compare the epigenetic and transcriptomic profiles of these cells, to an unsorted fibroblast population, as this may provide insight into why some cells are resistant to reprogramming.

Another potential limitation is that the iNs generated through this approach are not of any specific subtype, though they express some cortical neuron markers such as TBR and consist of predominantly glutamatergic and GABAergic neurons (Drouin-Ouellet – unpublished results and Drouin-Ouellet et al. 2017). Though there are iN protocols that have yielded specific neuronal types (Son et al. 2011, Victor et al. 2014), the generation of dopaminergic neurons, which would be useful for the modelling of PD, has been difficult to achieve (Caiazzo et al. 2011, Pfisterer et al. 2011a). In contrast, differentiation of iPSCs offers the potential for the derivation of dopaminergic neurons expressing midbrain dopaminergic neuron (e.g. En1 and nurr1) and floor-plate (e.g. FoxA2) markers (Hartfield et al. 2014, Kikuchi et al. 2017), allowing for the study of disease mechanisms on a population of cells that appear to be specifically susceptible to PD pathology. Having said this, the most consistent factor that differentiates *GBA1*-PD from iPD clinically, is the increased incidence of dementia, reflecting more widespread cortical disease.

Therefore, cortical neurons are perhaps the best neuronal type to interrogate the specific pathogenic mechanisms associated with *GBA1* mutations in PD. Though the iN system employed here does not generate authentic cortical neurons, the presence of cortical markers and the neurotransmitter expression resembling that in most cortical neurons, means that this system yields a population of cells that could provide insight into the pathogenic mechanisms of *GBA1*-PD.

Perhaps the most important limitation of the iN system described is the inability to cultivate the cells in large numbers for longer than a month. Though it is an advantage of iN reprogramming that neurons can be generated from adult somatic cells in a short space of time, the limited culture longevity brings about some significant drawbacks. First, it is known that the iNs generated from this and other protocols are functionally immature at about a month post-transduction, in that they do not generate spontaneous action potentials at this stage (Liu et al. 2013). It has been possible for iNs derived using this protocol to be cultured on glass coverslips for several months, and they have been demonstrated to be electrophysiologically active after 60 to 90 days (Drouin-Ouellet et al. 2017). However, only a small proportion of cells survive to these time points, such that the numbers of cells required for disease-modelling and drug-screening cannot be taken to this late stage. So, although the iNs retain the age profile of the cell with regard to genetic, epigenetic, mitochondrial, and protein-clearance system parameters for example, they are functionally young cells. So while iNs offer a useful platform for investigating intracellular pathogenic processes, or the behaviour of drugs, in aged cells, they are not practical for studying the effects of these things on functionality of the cell, with current protocols at least.

Another problem associated with the restricted time in cell culture is that there is only a limited time in which pathology can develop. Ideally, when studying neurodegenerative conditions such as PD *in vitro,* one would see the characteristic intracellular protein aggregates which are central to the pathogenic process. Of course, such pathology takes time to develop *in vitro*, and in this iN system, little in the way of intracellular protein aggregation was seen (this is discussed in detail in chapter 4). Some previous studies involving other model systems have applied other insults to the cells to induce the formation of α-synuclein aggregates or accumulation of α-synuclein, including

expression of aggregate-prone forms of α-synuclein, overexpression of α-synuclein to supraphysiological levels, or inhibition of the proteasome (Rideout et al. 2001, Hasegawa et al. 2004, Xu et al. 2002). However, the use of these insults takes the model further away from the processes that occur in patients, meaning that they may be less able to predict whether a drug will effectively attenuate pathology in patients.

3.5.2 Future Work

It is now possible for iNs to be generated relatively reliably using a variety of techniques, and the iN field has now reached the point at which questions should primarily focus on the applicability of these cells for disease-modelling and drug testing. As cell-based treatments for PD move towards the clinic, there will continue to be interest in the potential of iNs to form the basis of a regenerative therapy, but due to the limitations discussed above, it is unlikely that they will offer a superior cell product to stem cell-derived neural progenitors, and it is likely that the retention of the age signature would have a detrimental effect on survival times of iNs grafted into patients. The role of iNs is therefore likely to be in answering questions about disease mechanisms and drug effects in patient cells.

To facilitate the progression of iN reprogramming techniques to a widely used *in vitro* tool, there are some general areas that future work should focus on. As has been mentioned, there is variability in the efficacy of reprogramming between different cell lines, and also between different conversions in the same cell line. This may be in part due to inherent properties of the cell lines, such as the epigenetic landscape which will determine the propensity for proneural transcription factors to bind to target sites, but there may also be variability introduced by the way cell lines have been handled. A systematic investigation of the optimal culture methods for the parent fibroblasts (including cell density, cryopreservation process, thawing process) would therefore potentially be useful in reducing the variability seen.

Next, the inability to generate completely pure populations of neurons also hinders the use of iNs as is discussed above. This is particularly important when studying autonomous

intracellular pathways such as autophagy, in which there may be cell type-specific differences in activity. If there are differing proportions of unconverted fibroblasts in different cell lines at the time of analysis, it is difficult to draw firm conclusions when comparing between them. It is desirable, but not necessary, for neuronal purities of 100% to be achieved, with the most important thing being consistency of neuronal purity between cell lines. This could theoretically be achieved through several approaches. Firstly, improving conversion efficiency should drive up neuronal purity. This may be possible with improved vectors, but there is a probably a biological limit as to what can be achieved here, as there are likely to be some cells that are incapable of converting effectively for reasons that remain unknown. Some studies have co-transfected cells with vectors encoding anti-apoptotic genes (such as *Bcl-xL*) which has boosted conversion efficiency (Victor et al. 2018). However, apoptosis is the mechanism of neuronal death in PD and other neurodegenerative diseases, so interfering with this process will distance the model from the processes occurring in patients. Another possibility would be selectively killing unconverted cells. This however, is difficult to achieve given that the cell population is not dichotomous, and the majority of cells in the culture are probably in an intermediate state, with some fibroblast and some neuronal properties. This means that it is therefore a significant challenge to identify a property that will reliably and efficiently segregate unconverted from converted cells.

A number of toxins can be used *in vitro* to kill replicating cells. However, if there were residual dividing cells within the culture, the well would become overcrowded during the reprogramming process, which does not happen. It therefore seems unlikely that these toxins will be able to selectively kill the unconverted or partly converted cells. Some groups have used sorting methods, using the neuronal surface marker NCAM-1 to segregate unconverted cells from iNs (Mertens et al. 2015), though in this project it was not possible to generate great improvements in neuronal purity with this approach. Furthermore, the sorting process (either FACS or MACS) is traumatic for the cells, and may reduce cell survival. Nevertheless, if a marker which is suitably specific for successfully converted iNs can be identified, then this will be a useful tool.

An alternative method would be to incorporate a gene for an autofluorescent protein into the transfer vector, which would then allow for transduced cells to be accurately detected

with FACS. However incorporating the required genetic material for this, in addition to all reprogramming factors, may result in genetic cargos that exceed the capacity of lentivirus vectors. Additionally, the presence of the fluorescent marker would identify cells that had successfully been transfected, but these would not necessarily all have reprogrammed to iNs.

A third important target for future iN work is maximisation of culture longevity and neuronal maturity. As has been discussed, in most reported iN papers prolonged culture is required for iNs to become electrophysiological active, and as such, experiments are often carried out on cells that retain the age-signature of the individual, but that do not function as a mature neuron. In this study, it was not possible to culture cells to the time points at which they would be expected to be electrophysiologically active, and it would therefore be desirable to undertake a systematic assessment of the optimal culture conditions for prolonged culture, and also to investigate the potential of other reprogramming factors to speed up the maturation of iNs (Ruetz et al. 2017). In the protocol employed in this project, five small molecules, and four growth factors are employed. It is known that exposure to some of these small molecules for prolonged periods is detrimental to neuronal growth (Ladewig et al. 2012) (hence they are withdrawn from day 17), and it may be that as iNs mature further the optimal culture conditions change.

3.5.3 Concluding remarks

Here, iNs have been generated from healthy control individuals, as well as PD patients with no *GBA1* abnormalities, or heterozygous or homozygous *GBA1* variants. Whilst there are a number of limitations to the use of iNs, and there are several areas for future work, conversion efficiencies in this study were approximately 15 % to 50 % and neuronal purities were approximately 15 % to 35 %. In contrast to early iN protocols, the efficacy of conversion was therefore sufficient to allow for disease-modelling studies to be performed, and this platform was taken forward to serve as the basis for the drug-screening model discussed in the next chapter.

4 INTRACELLULAR PATHOLOGY OF *GBA1* VARIANT-ASSOCIATED PARKINSON'S DISEASE

4.1 Abstract

The mechanisms by which heterozygous *GBA1* mutations predispose to PD are not known. Some studies have suggested that the pathogenesis is predominantly dependent on loss of enzyme activity, whilst other observations suggest that a gain of toxic function is more likely. Dysfunction of the lysosome-autophagy system has been strongly linked to *GBA1*-PD, with a smaller number of studies identifying mitochondrial dysfunction in models of *GBA1* mutation-associated disease. In this study, differences were identified in the lysosome-autophagy system of *GBA1*-PD patients in comparison to healthy controls and patients with iPD, though there was no evidence of mitochondrial dysfunction under baseline conditions. iNs were treated with α-synuclein PFFs, to induce the formation of α-synuclein aggregates and subsequent pathology, which occurred to a greater extent in *GBA1*-PD iNs compared to the other groups. This iN model of PFF-induced pathology yielded a number of reproducible outcome measures to be taken forward for drug-screening studies.

4.2 Introduction to chapter

GBA1 mutation-associated disease has been studied in a number of model systems, including those in which GCase enzyme activity is suppressed chemically (e.g. through the inhibitor, conduritol-β-epoxide) or through genetic knock-down, transgenic cell lines

and animals carrying *GBA1* mutations, as well as cell lines and post-mortem tissue from patients. Of course, each model has its own limitations and may miss out on certain aspects of disease. For example, enzyme-suppression models may provide insight into any pathogenic loss-of-function mechanisms, but cannot tell us about the effects of the misfolded protein itself. Knock-in of pathogenic mutations in cell lines results in high non-physiological levels of mutant protein expression, such that they exceed the levels occurring in patients, which may lead to pathological effects that do not occur *in vivo*. Neurons derived from iPSCs from patients fail to capture any contribution of age to the pathogenic process as is discussed in the previous chapter.

The first section of the chapter focuses on studies involving patient-derived dermal fibroblasts, in which basic pathogenic pathways (the lysosome-autophagy system and mitochondrial function) have been studied, which has provided the basis for the initial drug selection, for testing in this novel model. The second half of the chapter focuses on the use of iNs to establish a drug-screening model. iNs were chosen for this study for several reasons that have been discussed. Importantly, iNs allow for the study of α-synuclein pathology without artificially overexpressing the protein, which cannot be performed in the native fibroblasts which do not express α-synuclein. As has been discussed in detail in chapter 3, iNs also retain cellular age, so that they potentially capture age-related elements of pathogenesis, and so can be used to more accurately predict the behaviour of a drug in patients, in comparison to similar iPSC-derived neurons. Because α-synuclein aggregates were not observed spontaneously in iNs, aggregate-formation was induced by treating the cells with PFFs of α-synuclein. The induction of aggregates in iNs and associated pathology offers a number of outcome measures that could be taken forward to drug-screening studies.

The mechanisms by which *GBA1* mutations predispose to PD are incompletely understood, but a number of intracellular pathways have consistently been implicated. These pathways would therefore be reasonable initial targets for putative disease-modifying treatments. The current understanding of these mechanisms are discussed in the following sections.

4.2.1 The lysosome-autophagy system

Dysfunction of the lysosome-autophagy system appears to be central to *GBA1*-PD, with abnormalities in these pathways being identified in a growing number of studies. However, the exact mechanism of dysfunction in this system is not clear. Autophagy refers to a number of processes through which a cell is able to clear protein and dysfunctional organelles, allowing the products of degradation to be recycled. The major autophagy pathways involved in clearance of α-synuclein are chaperone-mediated autophagy and macroautophagy (Figure 4.1) (Cuervo et al. 2004, Webb et al. 2003).

4.2.1.1 Overview of autophagy pathways

In chaperone-mediated autophagy, chaperone molecules allow for soluble proteins to be targeted to lysosomes and broken down by lysosomal enzymes (Cuervo and Dice 1998, Dunn 1994). Proteins carrying the KFERQ peptide motif are targeted to lysosome-associated membrane protein two A (LAMP2A), situated in the lysosomal wall (Cuervo and Wong 2014, Chiang et al. 1989). In contrast, macroautophagy involves the formation of double membrane-bound vacuolar organelles (autophagosomes) through the elongation of cytosolic phagophore membrane fragments. This process involves a number of autophagy-related (ATG) proteins, with phagophore expansion dependent on a complex consisting of ATG5, ATG12 and ATG16L1. These autophagosomes engulf proteins and organelles targeted for degradation, before they fuse with lysosomes to form autolysosomes. The contents are then degraded through lysosomal hydrolysis (Rubinsztein, Bento and Deretic 2015).

Initiation of macroautophagy may occur due to a variety of stimuli, including starvation and nutrient depletion (Chen et al. 2014), ATP depletion (Hardie, Ross and Hawley 2012), and pharmacological agents such as rapamycin (Noda and Ohsumi 1998). The most well-known pathway by which macroautophagy is initiated is mediated by the mammalian target of rapamycin complex one (mTORC1) – a pathway that is highly conserved across species. This protein complex prevents the initiation of macroautophagy through phosphorylation of a number of ATG proteins, restricting autophagosome formation

(Hosokawa et al. 2009). Other, mTORC1-independent, regulatory pathways for the initiation of macroautophagy also exist. Adenosine monophosphate-activated protein kinase (AMPK) inhibits the activity of mTORC1 but is also able to increase the formation of autophagosomes independently. AMPK is activated by reduced ATP levels, so is important in initiation of macroautophagy in the context of energy depletion (Cárdenas et al. 2010). In a third pathway, stimulation of phosphatidylinositol 3-kinase (PI3K or VPS34), for example by beclin-1, results in recruitment of ATG16L to sites of autophagosome formation, through increased levels of phosphatidylinositol 3-phosphate (PI3P) (Dooley et al. 2014, Furuya et al. 2005).

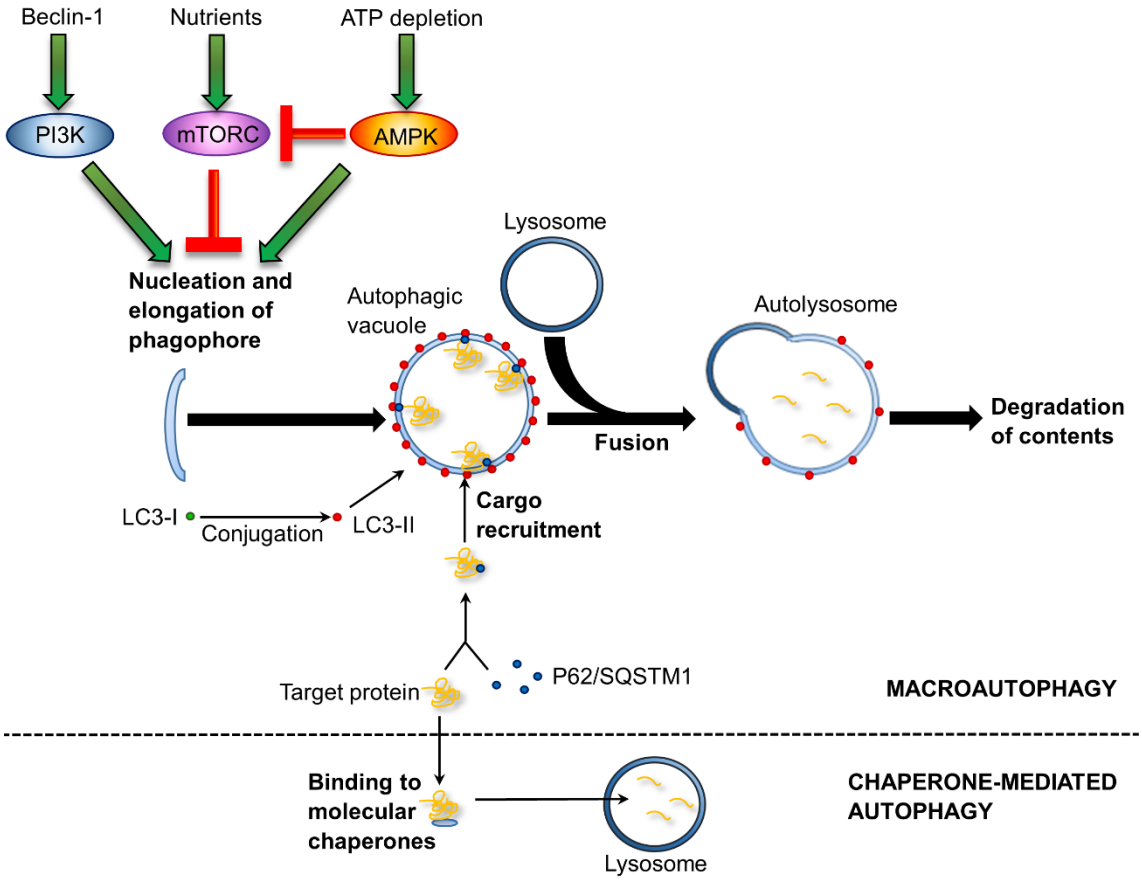

Figure 4.1 – Major mammalian autophagy pathways. In macroautophagy, phagophore membrane forms in response to multiple triggers, heralding the formation of autophagosomes. Targets of degradation are taken into autophagosomes, facilitated by proteins such as P62/SQSTM1. The contents are degraded after fusion of autophagosomes with lysosomes. In chaperone-mediated autophagy, proteins are targeted directly to lysosomes, mediated by chaperone-molecules. Abbreviations: AMPK = Adenosine monophosphate activated protein kinase; ATP = adenosine triphosphate; mTORC = Mammalian target of rapamycin complex; PI3K = Phosphatidylinositol 3-kinase.

4.2.1.2 Measurement of autophagy

During the formation of autophagosomes, LC3b (ATG8) is cleaved by ATG4 to form LC3b-I. LC3b-I is then conjugated with phosphatidylethanolamine to form LC3b-II, which is associated with the autophagosome membrane (Figure 4.1). This process can be exploited in analysing the initiation of autophagy, as an increase in LC3b-II levels relative

to LC3b-I or total protein levels indicates an increased number of autophagosomes. Additionally, identification of fluorescent LC3b puncta can allow for the visualisation of, and quantification of autophagosomes. It is important to note that a rise in autophagosome numbers may occur due to increased activation of autophagy, but may also arise due to an impairment in the later stages of autophagy (preventing clearance of autophagosomes). It is therefore necessary to interpret changes in LC3b-II levels or puncta in context, and to utilise modulators of various steps in the macroautophagy pathway (for example, inhibitors of lysosome-autophagosome fusion (e.g. bafilomycin A1) or inducers of autophagosome formation (e.g. starvation conditions, rapamycin)), to understand their meaning (Klionsky et al. 2016).

P62/SQSTM1 is another widely used marker of activity of the macroautophagy pathway. This protein has been identified in Lewy bodies, as well as neurofibrillary tangles of Alzheimer's disease, and the huntingtin aggregates seen in Huntington's disease, and it has been suggested that P62/SQSTM1 binds to ubiquitinated protein aggregates, potentially being involved in the targeting of them for degradation (Pankiv et al. 2007). It is also involved as an autophagy receptor in the process of mitochondrial priming, when dysfunctional mitochondria are removed through the autophagy pathway (mitophagy) (Geisler et al. 2010). P62/SQSTM1 facilitates the uptake of degradation targets into autophagosomes, and is itself degraded during the macroautophagy process following the formation of the autolysosome (Pankiv et al. 2007, Klionsky et al. 2016). Therefore, there is generally accepted to be an inverse correlation between levels of P62/SQSTM1 and macroautophagy activity – as macroautophagy activity increases, so does the rate of P62/SQSTM1 degradation, resulting in lower levels (Klionsky et al. 2016). However, there are some circumstances in which P62/SQSTM1 levels increase in association with increased autophagy, as its expression may be upregulated, meaning that, as with LC3b-II, interpretation of changes in the P62/SQSTM1 level must be taken in context (Colosetti et al. 2009, Toepfer et al. 2011). For example, increased transcription of P62/SQSTM1 may occur in response to oxygen radical stress (Ishii et al. 1997), inhibition of proteasome activity (Kuusisto, Suuronen and Salminen 2001), or expression of mutant huntingtin (Nagaoka et al. 2004).

As well as determining P62/SQSTM1 levels, it is also possible to quantify fluorescent P62/SQSTM1-positive cytoplasmic puncta. Whilst some of these puncta mark non-membrane bound aggregates representing targets for autophagic degradation (sequestosomes, or P62/SQSTM1 bodies) (Pankiv et al. 2007), the majority have been shown to represent autophagosomes or autolysosomes (Bjørkøy et al. 2005). Again, this poses challenges to interpretation of data, as an increase in puncta may represent an increase in the number of autophagosomes, but may also represent an increase in the number of sequestosomes implying a defect in autophagic protein clearance. Establishing the size of the puncta may allow for differentiation of these, with autophagosomes being 0.1 µm to 0.2 µm in diameter, and sequestosomes being 0.5 µm to 1 µm in diameter (Bjørkøy et al. 2005).

4.2.1.3 Autophagy dysfunction in *GBA1* mutation associated-Parkinson's disease

Several studies have demonstrated perturbations in the lysosome-autophagy system in *GBA1*-PD, but the exact nature of this is yet to be elicited. Dysfunction of this system could occur at any of the steps involved in this pathway, including:

i. Biosynthesis of autophagosomes and lysosomes
ii. Uptake of targets of degradation into autophagosomes
iii. Formation of autolysosomes through fusion of lysosomes and autophagosomes
iv. Enzymatic degradation of cargo by lysosomal enzymes (Stoker et al. 2018a).

Knock-down of *GBA1* in mouse cortical neurons using an shRNA results in reduced levels of lysosomal proteolysis (Mazzulli et al. 2011). Increased numbers of autophagosomes and lysosomes have been identified in neuroblastoma cells and in iPSC-derived dopaminergic neurons carrying *GBA1* mutations (Fernandes et al. 2016, Schöndorf et al. 2014, Bae et al. 2015). Similar observations have been made in mouse cortical neurons, in the setting of inhibition of GCase activity using conduritol-β-epoxide (Rocha et al. 2015b) and shRNA-mediated *GBA1* knockdown (Mazzulli et al. 2011), suggesting that a reduction in enzyme activity is sufficient to induce these changes. These findings suggest that the synthesis of these structures is not the underlying problem in

GBA1-PD, but that instead any problem is due to the later stages in the pathway, which may result in accumulation of lysosomes and autophagosomes.

Reduced co-localisation of autophagosomes and lysosomes has been noted in iPSC-derived neurons derived from carriers of *GBA1* mutations, in comparison to isogenic controls, which may imply that the mutation is associated with a reduction in formation of autolysosomes (Schöndorf et al. 2014). There is also evidence that lysosomal function is abnormal in the context of *GBA1* mutation or reduced GCase activity. For example, iPSC-derived neurons derived from *GBA1* mutation carriers have enlarged lysosomes, containing increased amounts of electron dense material, in comparison to those from isogenic controls (Fernandes et al. 2016). Knock-down of *GBA1* in primary mouse cortical neurons also results in enlargement of lysosomes (Mazzulli et al. 2011).

The results discussed here are consistent with there being a defect in the lysosome-autophagosome fusion stage of autophagy. However, it is important to note that most of these observations have been made in models of GCase enzyme activity suppression, meaning that any effects of the mutant protein are not captured. In a study involving hippocampal neurons and hippocampal allocortex from transgenic mice carrying a single *GBA1* allele with the L444P mutation (L444P/wt), deficits in both lysosome-autophagosome fusion and also in the initiation of autophagy were observed (Li et al. 2018). To further interrogate this, LC3b levels were assessed in SH-SY5Y cells with *GBA1* knocked-out (-/-), and in those expressing L444P in addition to normal *GBA1* (L444P-wt/wt), with preserved enzyme activity. *GBA1* knock-out resulted in increased LC3b-II levels compared to wild-type cells consistent with a block in the late-stages of autophagy, whilst expression of L444P resulted in reduced autophagosome numbers. Autophagic flux was assessed through the use of leupeptin and pepstatin to inhibit the fusion stage, which was found to be reduced in knock-out cells, but preserved in L444P-wt/wt cells. Together this data suggests that there may be dual mechanisms involved, with loss of enzyme activity resulting in an impairment in lysosome-autophagosome fusion, and the presence of mutant enzyme having a gain-of-function effect resulting in an impairment in autophagosome formation (Li et al. 2018).

Lysosomal dysfunction and inhibition of GCase activity are known to increase the amount of α-synuclein released by the cell through exocytosis (Bae et al. 2014, Alvarez-Erviti et al. 2011, Papadopoulos et al. 2018). It may therefore be, that rather than simply increasing the propensity of an individual cell to develop α-synuclein pathology, *GBA1*-mediated dysfunction of the lysosome-autophagy system facilitates the propagation of pathology, as extracellular α-synuclein may be taken up by adjacent neurons. This could theoretically explain the more widespread pathology and more aggressive clinical course seen in *GBA1*-PD than those in iPD.

4.2.2 Mitochondrial dysfunction in *GBA1* mutation-associated-Parkinson's disease

Whilst the role of mitochondrial dysfunction in PD is incompletely understood, it is clear that it contributes, at least in some cases. It's importance is illustrated by the observation that mitochondrial toxins such as MPTP and rotenone induce death of nigral dopaminergic neurons (Langston et al. 1983, Testa et al. 2005, Schapira 2008), and the fact that some familial forms of PD arise due to mutations of genes involved in mitochondrial function and health (e.g. *PARK7* and *PINK1*) (Kalia and Lang 2015). The importance of mitochondrial dysfunction in *GBA1*-PD is not clear, and only a small number of studies have commented on mitochondrial dysfunction in this setting (Cleeter et al. 2013, Osellame et al. 2013, Xu et al. 2014, de la Mata et al. 2015, Li et al. 2018). Importantly with regard to *GBA1*-PD, dysfunctional mitochondria may be cleared by the lysosome-autophagy system through mitophagy, and problems with this system as occur in *GBA1*-PD may therefore exaggerate any mitochondrial-mediated pathogenic mechanisms.

Most of the studies of mitochondrial dysfunction in *GBA1*-PD have been performed in enzyme suppression models (which fail to represent any potential effects from mutant GCase protein), or in models involving biallelic *GBA1* abnormalities, more closely reflecting GD rather than *GBA1*-PD. Suppression of GCase activity through treatment with conduritol-β-epoxide in neuroblastoma cells (Cleeter et al. 2013) and wild-type neurons (Xu et al. 2014) reduces oxygen consumption and ATP production suggesting that a loss-of-function effect can precipitate mitochondrial dysfunction. Additionally, a

progressive decline in mitochondrial membrane potential *in vitro* has also been reported with prolonged GCase suppression in SH-SY5Y cells, lending further support to this idea (Cleeter et al. 2013). Mitochondrial morphology and function is also disrupted in *GBA1* knockout mice, with abnormalities being of greater significance in those in which both alleles were knocked-out compared to those with one preserved allele (Osellame et al. 2013).

Transgenic mice carrying heterozygous *GBA1* mutations (L444P/wt), as occurs in *GBA1*-PD, have also been found to have abnormal mitochondrial morphology, reduced mitochondrial membrane potential, and increased superoxide production, with similar findings in fibroblasts from patients with *GBA1*-PD (Li et al. 2018, McNeill et al. 2014). Increased levels of the antioxidant NQ01 have also been seen in patient fibroblasts (McNeill et al. 2014). All of these findings support a potential role for mitochondrial dysfunction in *GBA1*-PD.

Mitophagy, a specific form of macroautophagy, is important in the clearance of dysfunctional mitochondria. In transgenic mice with the L444P/wt *GBA1* genotype also expressing mt-Keima (a protein targeted to mitochondria, with bimodal fluorescence properties, such that under neutral conditions it fluoresces green and under acidic (i.e. lysosomal) conditions it fluoresces red), reduced delivery of mitochondria to the lysosomes has been detected (Li et al. 2018). Treatment with CCCP or antimycin, which normally induce mitophagy, failed to increase mitochondrial co-localisation to lysosomes, suggesting that induction of mitophagy is impaired in the context of *GBA1* mutation. Mitochondrial priming is the process through which dysfunctional mitochondria are targeted for degradation through mitophagy, which involves the recruitment of autophagy receptors to the mitochondria (Geisler et al. 2010). Levels of these autophagy receptors were reduced in mitochondrial fractions from L444P/wt mice hippocampi, suggesting that there is a failure in mitochondrial priming, leading to a reduction in mitophagy (Li et al. 2018).

The discussion so far suggests that perturbations in mitochondrial function arise downstream of *GBA1*-mediated autophagy dysfunction. However, it has recently been suggested that oxidative stress is an earlier component of the pathogenic process in PD

(Burbulla et al. 2017). Mitochondrial oxidant stress is associated with *PARK7* (DJ-1) knockout or dysfunction in dopaminergic neurons generated from patient-derived iPSCs, and after prolonged culture, this is accompanied by a reduction in GCase enzyme activity and impaired lysosomal proteolysis (Burbulla et al. 2017). While this process occurs in cells from patients with sporadic PD, it was accelerated in neurons derived from patients with homozygous *PARK7* mutations, supporting the idea that mitochondrial dysfunction is an important aspect of PD pathogenesis, and that it potentially induces lysosomal dysfunction. Furthermore, mitochondrial antioxidants reduce the levels of soluble α-synuclein, suggesting that oxidant stress contributes to α-synuclein accumulation (Burbulla et al. 2017). This study suggests that a sequential pathogenic pathway exists in PD, with mitochondrial oxidant stress leading to a reduction in GCase enzyme activity and lysosomal function, with consequent α-synuclein accumulation (Stoker et al. 2018a). *GBA1* mutation may feed into this by lowering the threshold for, or altogether bypassing the need for, mitochondrial oxidant stress.

4.2.3 Endoplasmic reticulum stress in *GBA1* mutation associated-Parkinson's disease

As has been mentioned, loss of GCase enzyme activity does not fully explain the pathogenic basis of *GBA1*-PD, and there is therefore probably a contribution from the gain of a toxic function of the misfolded protein. Normal processing of GCase involves folding within the ER, prior to delivery to the lysosomes via the Golgi apparatus (Jović et al. 2012, Reczek et al. 2007). Mutations that result in misfolding of GCase potentially lead to retention of the protein in the ER, where ER-chaperone molecules attempt refolding to restore the correct protein structure (Brodsky and McCracken 1999, Sitia and Braakman 2003). Failure to correctly re-fold the protein results in its removal through ER-associated protein-degradation (ERAD) and the ubiquitin-proteasome system (Brodsky and McCracken 1999, Sitia and Braakman 2003, Yoshida 2007, Kopito 1997). Once the capacity of this mechanism is surpassed, and there is failure to clear the misfolded protein, the unfolded protein response (UPR) is activated (Høyer-Hansen and Jäättelä 2007). If ER stress is prolonged, the UPR may fail to restore normal homeostasis, and the cell may be directed to an apoptotic fate.

Endoglycosidase-H can be used to determine the transit of GCase to lysosomes, as the lysosomal form of the enzyme is resistant to endoglycosidase-H-mediated degradation, whilst the pre-Golgi form is not (Ron and Horowitz 2005, Bendikov-Bar et al. 2013). The proportion of endoglycosidase-H-resistant GCase is significantly lower in association with *GBA1* mutations when compared to the wild-type protein, indicating that there is failure of the proper processing of mutant GCase. Additionally, mutant GCase is seen to co-localise with calnexin (an ER marker), suggesting that it is retained in the ER, and the propensity for ER retention seems to contribute to the severity of GD (Ron and Horowitz 2005). The levels of ER-resident chaperones Bip/GRP78 and calreticulin have been shown to be increased in iPSC-derived neurons derived from *GBA1*-PD patients carrying N370S mutations, with mediators of the UPR also being upregulated (Fernandes et al. 2016). UPR-mediators are also increased in post-mortem brain tissue from patients with *GBA1*-PD in comparison to those with iPD (Gegg et al. 2012). Markers of ER stress are also increased in transgenic drosophila expressing mutant human *GBA1* compared to those expressing wild-type human *GBA1* (Suzuki et al. 2013, Sanchez-Martinez et al. 2016). The use of molecular chaperones (ambroxol and isofagamine) which facilitate the correct folding of GCase reduce ER stress markers in human fibroblasts and in drosophila overexpressing mutant *GBA1*. Indeed, such chaperones are considered a potential therapeutic approach in *GBA1*-PD, having entered clinical trials (Sanchez-Martinez et al. 2016, Bendikov-Bar et al. 2013).

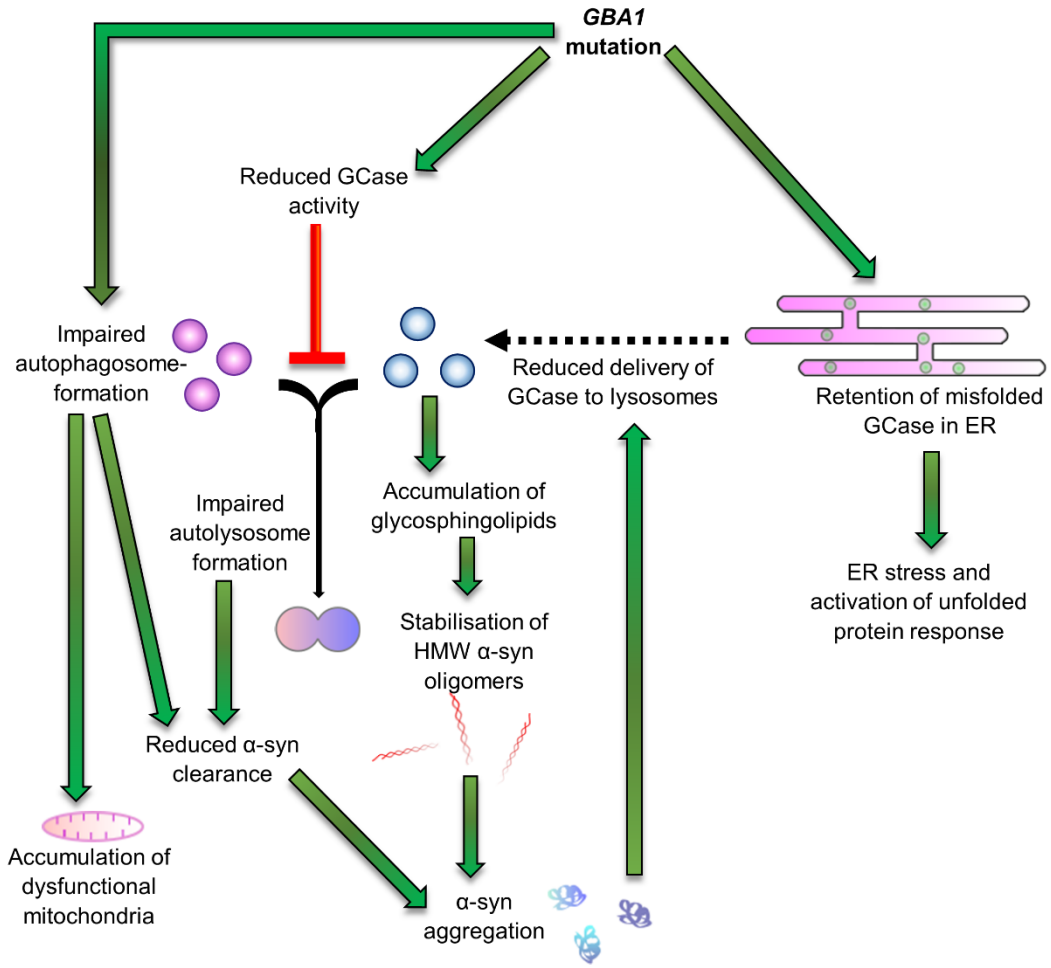

Figure 4.2 – Pathogenic mechanisms of *GBA1*-PD. Reduced GCase enzyme activity results in a block in the autophagy pathway and accumulation of glycosphingolipid substrates which stabilise pathogenic oligomeric species of α-synuclein. The mutant protein also impairs autophagosome formation. Autophagy dysfunction results in accumulation of α-synuclein and impaired clearance of dysfunctional mitochondria. A bi-directional loop occurs in which α-synuclein further impairs normal processing of GCase, and reduces its delivery to lysosomes. Additionally, the misfolded enzyme is retained in the ER, resulting in activation of the unfolded protein response. Abbreviations: α-syn = α-synuclein; ER = Endoplasmic reticulum; GCase = Glucocerebrosidase; HMW = High-molecular weight.

4.2.4 α-synuclein accumulation and aggregation in *GBA1* mutation-associated Parkinson's disease

Abnormalities of *GBA1* and GCase have been shown to increase α-synuclein levels in a number of *in vitro* and in *vivo* studies (Table 4.1). Most of these studies have correlated the accumulation of α-synuclein to reduced GCase activity, though others have suggested that it is more likely to occur due to the presence of misfolded enzyme. For example, conduritol-β-epoxide treatment in mice (Rocha et al. 2015b, Manning-Boğ et al. 2009) and in neuroblastoma cells (Manning-Boğ et al. 2009, Cleeter et al. 2013) was associated with increased levels of α-synuclein. The aforementioned study in which *GBA1* expression was suppressed with an shRNA molecule also identified increased levels of high-molecular weight α-synuclein in association with reduced lysosomal proteolysis, supporting the idea that reduced GCase activity may lead to accumulation of α-synuclein (Mazzulli et al. 2011). Introduction of *GBA1* mutations that result in loss of enzyme function in neuroblastoma cells also has been shown to lead to accumulation of oligomeric α-synuclein levels – an effect that was not seen when *GBA1* mutations that did not affect GCase activity were introduced (Bae et al. 2015).

However, although increased levels of α-synuclein were seen in MES23.5 and PC12 cells with knock-in pathogenic *GBA1* mutations, this did not correlate with a reduction in GCase enzyme activity, and could not be recapitulated through chemical GCase inhibition, raising the possibility that the elevated levels of α-synuclein were mediated by an alternative, gain-of-function mechanism (Cullen et al. 2011). Knocking in a single *GBA1* L444P mutation in mouse cortical neurons also impaired clearance of α-synuclein, and resulted in increased steady-state levels (Fishbein et al. 2014). The inconsistent results regarding the importance of enzyme activity further suggests that the mechanisms of risk conveyed by *GBA1* mutations are complex, and that there may be more than one mode of pathology (Li et al. 2018).

Age-associated α-synuclein accumulation has been seen *in vivo*, in mouse models incorporating *GBA1* mutations. In the first of these studies, α-synuclein levels increased over time, in mice homozygous for D409V mutations in the *GBA1* gene (Cullen et al. 2011). Aggregates of α-synuclein also accumulate in mice with homozygous *GBA1* mutations combined with a hypomorphic prosaposin transgene (Xu et al. 2011, Xu et al. 2014). These studies suggest that a reduction in GCase enzyme activity and/or the presence of mutant GCase protein could facilitate the development of α-synuclein

aggregates *in vivo*, but it should be noted that the biallelic insults in these systems mimic the pathogenic state of GD, and the relevance to *GBA1*-PD is unclear.

Reduction in GCase enzyme activity leads to the accumulation of sphingolipid substrates in lysosomes. This process is known to be important in the pathogenesis of GD, but the role of substrate accumulation in *GBA1*-PD is not clear. It has been shown that the GCase substrate glucosylceramide leads to stabilisation of pathogenic high molecular weight recombinant α-synuclein oligomers *in vitro*, which is followed by an increased propensity for aggregates to form, and it may be that sphingolipids contribute to the increased risk of PD associated with *GBA1* mutations (Mazzulli et al. 2011, Zunke et al. 2017).

Study	Model	Result
***In vitro* studies**		
Mazzulli et al. 2011	shRNA-mediated knockdown of *GBA1* in primary mouse cortical neurons	Increased soluble monomeric and oligomeric α-synuclein levels, and increased insoluble high molecular weight α-synuclein assemblies
Manning-Boğ et al. 2009 **Cleeter et al. 2013**	Chemical suppression (CβE) of GCase in neuroblastoma cells	Increased levels of monomeric α-synuclein
Cullen et al. 2011	Overexpression of mutated GCase (L444P, D409V or N370S) in MES23.5 and PC12 cells expressing wild-type or A53T α-synuclein	Increased levels of α-synuclein (reversible with induction of autophagy)
Fishbein et al. 2014	Primary cortical neuron cultures from mice carrying heterozygous L444P *GBA1* mutations	Reduced clearance of α-synuclein Increased steady-state levels of α-synuclein
Bae et al. 2015	Neuroblastoma cells with *GBA1* mutations that reduce enzyme activity, or *GBA1* mutations with no effect on enzyme activity	Increased oligomeric α-synuclein levels and exosomal release of α-synuclein aggregates, associated with mutations that reduce enzyme activity (not those where enzyme activity is preserved)
***In vivo* studies**		
Rocha et al. 2015b	Chemical suppression (CβE) of GCase in wild-type mice	Accumulation of insoluble α-synuclein aggregates
Manning-Boğ et al. 2009	Chemical suppression (CβE) of GCase in wild-type mice	Increased levels of monomeric α-synuclein
Xu et al. 2011 **Xu et al. 2014**	Transgenic mice with homozygous D409V or V394L *GBA1* mutations combined with hypomorphic prosaposin transgene	Age-dependent accumulation of α-synuclein aggregates
Cullen et al. 2011	Mice with homozygous D409V *GBA1* mutations	Age-dependent increase in α-synuclein levels

Table 4.1 – Studies demonstrating accumulation of α-synuclein in the context of *GBA1* mutation or GCase activity suppression. Abbreviations: CβE = conduritol-β-epoxide; GCase = glucocerebrosidase; shRNA = short-hairpin ribonucleic acid.

It is clear that the relationship between α-synuclein, the GCase protein and GCase enzyme activity is complex (Figure 4.2). Several studies associate reduced enzyme activity with increased α-synuclein levels or aggregates, as discussed above. A bidirectional loop has been proposed in which reduced GCase activity, perturbed lysosomal function and accumulation of glycosphingolipid substrates leads to the accumulation of α-synuclein, including pathogenic oligomeric species. The loop is completed by the fact that α-synuclein impedes transit and normal processing of the GCase protein across the Golgi apparatus, resulting in reduced delivery of GCase to the lysosomal compartment, and a further reduction in lysosomal activity. Overexpression of α-synuclein results in an

increase in the ER-associated form of GCase, with a reduction of the glycosylated, post-ER form (Mazzulli et al. 2011). GCase activity has been reported to be reduced in PD patients without *GBA1* mutations, which may be in part explained by this process (Alcalay et al. 2015, Gegg et al. 2012). Further support for this idea comes from the fact that knocking out α-synuclein in mice results in an increase in GCase enzyme activity (Fishbein et al. 2014).

The favoured explanation for accumulation of α-synuclein in the context of *GBA1*-PD is the reduced protein-clearance associated with dysfunction of the lysosome-autophagy system. It has also been shown *in vitro* that recombinant GCase and α-synuclein directly interact with one another, with α-synuclein reducing GCase enzyme activity (Yap et al. 2011, Yap et al. 2013). This interaction may account for the reduction in GCase enzyme activity that has been observed in patients without *GBA1* mutations (Alcalay et al. 2015, Gegg et al. 2012). GCase is known to occur in Lewy bodies, and this is seen to a greater extent in carriers of *GBA1* mutations, leading some to postulate that the mutant enzyme serves as a platform for aggregate formation (Goker-Alpan et al. 2010). However, α-synuclein has a lower propensity to interact with N370S GCase than with wild-type GCase, suggesting that this interaction does not account for the increased tendency for α-synuclein aggregation in *GBA1*-PD (Yap et al. 2011). It is possible instead, that this interaction constitutes an element of the bidirectional feedback loop, whereby increased levels of α-synuclein exacerbate the pre-existing defect in GCase enzyme activity in *GBA1*-PD.

Here, it was hypothesised that *GBA1* variants in patient-derived fibroblasts and iNs would harbour aberrations in the lysosome-autophagy system and of mitochondrial function. The following sections detail the characterisation of these deficits in patient cells. Additionally, iNs were treated with PFFs of α-synuclein in order to induce PD relevant α-synuclein pathology, with a view to taking this forward to drug testing trials.

4.3 Materials and methods

4.3.1 Immunocytochemistry for autophagy markers

Fibroblasts were cultured to 80 to 90 % confluency before being passaged and plated on 96-well plates (Thermo Scientific Nunc) at a density of 5000 cells per well. The cells were incubated at 37^{O}C for 24 hours. Medium was removed, and the cells washed once in PBS, before HBSS with Ca^{2+} and Mg^{2+} (starvation conditions), bafilomycin 100 nM in fibroblast medium, wortmannin 100 nM in fibroblast medium, or DMSO vehicle control were then added to the cells, each in technical triplicate. The cells were then incubated for four hours at 37^{O}C. The treatments were then removed, and the cells were washed in PBS before being fixed in ice cold methanol for 10 minutes.

For immunocytochemistry, blocking was performed by incubating the cells in 5 % goat serum in PBS, for one hour at room temperature. Primary antibodies against P62/SQSTM1 (Genetex GTX629890) and LC3b (sigma L7543) diluted to 1:500 in 5 % goat serum was added to the cells, which were then incubated overnight at 4^{O}C. The cells were washed twice in PBS before secondary antibodies (Thermo Fisher Scientific Alexa Fluor) 1:500 in 5 % goat serum were added for two hours at room temperature. The cells were washed once in PBS without electrolytes and then nuclear counterstaining was performed with DAPI 1 µg/ml in PBS for 20 minutes at room temperature. High-throughput analyses using Cellomics^{TM} XTI spot count and cell health profiling protocols were performed to quantify the number of fluorescent puncta and mean intensity.

Reagents were prepared as follows: Bafilomycin A1 (Sigma SML1661 or Sigma B1793) and wortmannin (Tocris 1232) were dissolved in DMSO to give a stock concentration of 10 µM and 200 µM respectively. Stock solutions were diluted in fibroblast medium to give working concentrations of 100 nM. Vehicle control consisted of fibroblast medium with 1:100 DMSO.

4.3.2 Lysotracker^{TM} red DND-99 assay

Fibroblasts from two healthy controls, two patients with iPD and three patients with *GBA1*-PD were passaged and plated on a 24-well plate (Thermo Scientific Nunc) at a density of 5000 cells per well, in technical triplicate. The cells were incubated at 37^{O}C for five days, with a medium change being performed on day three.

The medium was removed from the wells, and Lysotracker^{TM} DND-99 (Thermo Fisher Scientific) diluted to 50 nM in HBSS with Ca^{2+} and Mg^{2+} was added to each well, and the plate was incubated at 37^{O}C for 30 minutes. The cells were then washed in HBSS and fixed in 4 % paraformaldehyde (PFA) for 20 minutes. Nuclear counter-staining with DAPI 1 µg/ml was then performed for 20 minutes at room temperature.

High-throughput imaging analysis were performed using Cellomics^{TM} XTI. A total of 20 fields per well were imaged at 20 times magnification. Spot count and spot area per well were calculated using the spot detector protocol, and the mean values for all cells in each cell line was used to give a single value for each individual cell line which was used for statistical analysis.

4.3.3 MitoSOX^{TM} red assay

Fibroblasts from healthy controls (n=2), and patients with iPD (n=1) and *GBA1*-PD (n=2) were passaged and plated at a density of 20000 cells per well in a 96-well plate (Ibidi), in technical triplicate. They were incubated for 48 hours at 37ºC before the medium was removed and the cells were washed in HBSS. MitoSOX^{TM} 5 µM and DAPI 1 µg/ml in HBSS with Ca^{2+} and Mg^{2+} without phenol red was then added, and the plate incubated at 37^{O}C, protected from light, for 30 minutes. The plate was transferred to the plate reader and fluorescence intensity was read at 544 nm / 590 nm for MitoSOX^{TM} red and at 355 nm / 460 nm for DAPI. The MitoSOX^{TM} fluorescence intensity for each well was corrected based on the corresponding value for DAPI fluorescence intensity, to ensure that differences seen were not due to variations in the number of cells. A mean value of the technical replicates was obtained to provide a single value for each cell line which was used for analysis.

4.3.4 TMRE assay for mitochondrial membrane potential and MitoTracker™ green assay for mitochondrial content

Fibroblasts from healthy controls (n=2), or patients with iPD (n=2) and *GBA1*-PD (n=3) were passaged and plated at a density of 12000 cells per well in a 96-well plate (Ibidi) in technical triplicate. This plate was then incubated at 37^{O}C for 72 hours. The medium was removed and replaced with 1 µM tetramethylrhodamine, ethyl ester (TMRE) in HBSS with Ca^{2+} and Mg^{2+}, and the plate was then incubated for 30 minutes at 37^{O}C, protected from light. The TMRE was then removed and the cells were washed twice in 0.2 % BSA in PBS, before being transferred to the cell plate reader for fluorescence intensity measurement at excitation / emission frequencies 544 nm / 590 nm. The mean value for the technical replicates was used to generate a single value for each cell line which was used for analysis.

When analysis was performed in iNs, medium was removed and the cells were washed once with PBS, before TMRE 200 nM or MitoTracker™ Green 200 nM in Ndiff227 was added. The plate was incubated for 20 minutes at 37ºC before the TMRE or MitoTracker™ solution was removed and replaced with Hoescht 33342 2 µg/ml in HBSS with Ca^{2+} and Mg^{2+} with further incubation at 37ºC for 10 minutes. The cells were washed twice in PBS before fluorescence intensity was measured at excitation / emission 355 nm / 460 nm (Hoescht) and 544 nm / 584 nm (TMRE) or 485 nm / 520 nm (MitoTracker™ Green) using the cell plate reader.

4.3.5 Adenosine triphosphate production assay

Fibroblasts from healthy controls (n=3), and patients with iPD (n=2) and *GBA1*-PD (n=3) were passaged and plated at a density of 10000 cells per well in a 96-well plate (Ibidi), with four wells per line. After 48 hours incubation, carbonyl cyanide 4-(trifluoromethoxy) phenylhydrazone (FCCP) was added to one well for each line, to give a final concentration of 10 µM, and the cells were incubated for a further 12 hours. The ATP

luminescence assay (Abcam) was then performed as per the manufacturer's instructions. Medium was replaced with HBSS with Ca^{2+} and Mg^{2+}, before 50 µl detergent was added, followed by a five minute incubation at room temperature, shaking at 300 rpm. Substrate (50 µl) was added to each well before a further five minutes of shaking. The plate was then incubated, at room temperature protected from light, for 10 minutes, before luminescence was read on the microplate reader.

4.3.6 Transfection of fibroblasts and treatment with α-synuclein pre-formed fibrils

Fibroblasts were plated at a density of 5000 cells per well in a 24-well plate (Thermo Scientific Nunc) coated with 0.1 % gelatin. After three days of culture, 50 ng of plasmid DNA encoding eGFP-tagged wild-type α-synuclein was added to each well, kindly supplied by Professor David Rubinsztein (University of Cambridge). Lipofectamine 3000 (Thermo Fisher Scientific) was diluted in Opti-MEM medium, and combined with P3000 reagent and plasmid mixture as per the manufacturer's protocol. The mixture was incubated for 15 minutes at room temperature before being added drop-wise into the cell medium.

α-synuclein PFFs or PBS vehicle control were added to the cells the following day, and the cells were incubated for a further three days before being fixed. Immunocytochemistry for GFP and α-synuclein was performed. Images were acquired on the Cellomics™ XTI microscope, and spot detector analysis was performed to determine total spot count and total spot area per cell for both GFP and α-synuclein. For each condition, 20 microscopy fields were acquired at 20 times magnification, and the mean value from the 20 fields was used for statistical analysis.

4.3.7 Treatment with α-Synuclein pre-formed fibrils

PFFs were generated by Dr Wei-Li Kuan by dissolving recombinant wild-type human α-synuclein monomers in pH 7.6 10 mM Tris-HCl and 50 mM sodium chloride at a

concentration of 5 mg/mL. This solution underwent shaking at 1000 rpm for seven days at 37^{O}C. The resultant PFF product was then verified using transmission electron microscopy, an ultracentrifigation-sedimentation assay, and through seeding onto primary human fetal neurons. PFFs were stored at a concentration of 5 µg/µl. Prior to use stock PFF was diluted 1:52 in Ndiff227 medium. This working solution of PFFs was then sonicated for 60 minutes in a sonicator water bath, before the desired volume was added to wells. A half medium change was performed three days later, with further half medium changes every two to three days until the time of analysis. Final concentrations of PFFs were 0.3 to 2.7 ng/µl as detailed below.

To assess the effect of PFFs in fibroblasts, 50000 fibroblasts were plated in a six well plate coated with 0.1 % gelatin in 2 ml medium. The following day 40 µl of sonicated PFFs were added. Half medium changes were performed every two to three days and the cells were fixed in methanol after 10 days of PFF exposure. Immunocytochemistry for α-synuclein was performed prior to imaging using the confocal microscope.

4.3.8 Caspase activity assay

Fibroblasts from iPD lines (n=4) and *GBA1*-PD lines (n=2) were converted to iNs. At day 17 post-transduction, they were treated with a single dose of sonicated α-synuclein PFFs at a dose of 0.4 µg/ml or 1.5 µg/ml, or vehicle control, in technical triplicate. They were then cultured for a further 10 days, with medium changes every two to three days.

On day 27 post-transduction, a total caspase activity assay was performed (Thermo Fisher Scientific I35104). The polycaspase reagent FAM-VAD-FMK was diluted as per manufacturer's instructions, in Ndiff227, before being added to the cells which were then incubated for one hour at 37^{O}C. The medium was then removed and replaced with Hoescht 33342 2 µg/ml diluted in HBSS with Ca^{2+} and Mg^{2+}, with incubation for five minutes at 37^{O}C. The cells were then washed twice in wash buffer, before being fixed in apoptosis fixative solution for 20 minutes at room temperature. Fluorescence intensity was measured using a cell plate reader at 355 nm / 460 nm for Hoescht and at 480 nm /

520 nm for the polycaspase reagent. The polycaspase signal was divided by the Hoescht signal to correct for differences in cell numbers.

4.3.9 Western blot analysis

Fibroblasts were plated at 100000 cells per well in six-well plates and converted to iNs. iNs were dissociated with trypsin 0.05 % and flushed from the well with Ndiff227 medium, and centrifuged at 400 x G for five minutes. Cell pellets were resuspended in 40 µl lysis buffer (5 M urea, 2.5 % sodium dodecyl sulphate (SDS), 50 mM Tris pH 6.8 and 30 mM sodium chloride) and incubated on ice for five minutes. Lysates were centrifuged at 10000 rpm for 2 minutes at 4^{o}C and the supernatants transferred to new tubes. Protein was quantified using a BCA assay kit (Thermo Scientific), and 20 µg protein was loaded onto acrylamide gels and run alongside standard molecular weight markers. Gels were transferred onto polyvinylidene difluoride membranes (30 V for ninety minutes at 4^{o}C), followed by blocking in 5 % fat-free milk powder in Tris-buffered saline with 0.1 % Tween (TBS-T) for one hour, and incubation overnight at 4°C in 5 % milk with the LC3b primary antibody (Sigma L7543) 1:500. Horseradish peroxidase (HRP)-conjugated secondary antibodies were then added and membranes were developed with ECL^{TM} detection reagent (GE Healthcare). Membranes were stripped with two 15 minute washes in pH 2.2 stripping buffer containing 15 g glycine, 1 g SDS, and 10 ml Tween 20 in 1 l ultrapure water, before being washed three times in TBS-T. Protein detection using P62/SQSTM1 antibody (abcam 91526) 1:500 was then performed as described above. Densitometric quantification of Western blots was performed using ImageJ analysis software. The measurements were normalized to β-Actin as the loading control. Western blotting was performed with the assistance of Dr Shaline Fazal.

4.3.10 Statistical analysis

All statistical tests were performed using IBM SPSS software. When comparing two independent groups, p-values were determined with independent samples T tests, after determining the equality of variance with Levene's test for equal variance. Multiple group

comparison was performed with one-way ANOVA and post-hoc Tukey analysis. Statistical significance is indicated by asterixes as follows: * = $p \leq 0.05$; ** = $p \leq 0.01$; *** = $p \leq 0.001$.

4.4 Results

4.4.1 Lysosome-autophagy dysfunction

GCase protein levels and activity had previously been assessed in the fibroblasts from the cell lines used in this study, with *GBA1*-PD lines showing a non-significant reduction in GCase protein levels, and a significant reduction in GCase enzyme activity to 36.5% of the mean activity of that in healthy controls (Collins et al. 2017).

To first investigate whether *GBA1* mutation was associated with differences in activity of the lysosome-autophagy system, immunocytochemistry for the macroautophagy markers P62/SQSTM1 and LC3b was performed in patient derived fibroblasts from healthy controls (n=3), and patients with iPD (n=4) and *GBA1*-PD (n=3) (Figure 4.3). Fibroblasts were cultured under starvation conditions for four hours to induce macroautophagy. Mean P62/SQSTM1 intensity was significantly higher in the *GBA1*-PD group than the healthy control (p=0.003) and iPD (p=0.007) groups, suggesting that *GBA1*-PD is associated with reduced ability to induce macroautophagy. There were no differences between any of the other groups. LC3b intensity was also greater in the *GBA1*-PD group in comparison to healthy controls and iPD patients but this did not reach significance (p=0.068 and p=0.08 respectively). It was not possible to obtain images of sufficient resolution to quantify LC3b-positive puncta to determine the number of autophagosomes.

P62/SQSTM1 levels were then quantified following treatment with bafilomycin A1 (an inhibitor of autophagosome-lysosome fusion) or wortmannin (an inhibitor of PI3K), which is important in autophagosome formation. Bafilomycin treatment led to a significant increase in P62/SQSTM1 levels in healthy controls (p=0.003), signalling reduced autophagic flux, as expected. There was a similar rise in the iPD group though

this did not reach statistical significance. The rise in P62/SQSTM1 intensity with bafilomycin in the *GBA1*-PD group was lower than in the other groups.. All groups did however have a statistically significant increase in the P62/SQSTM1 spot count following bafilomycin A1 treatment (Figure 4.3 and Figure 4.4). The difference between the P62/SQSTM1 spot count after bafilomycin A1 treatment and the spot count in baseline conditions was used as an estimate of autophagic flux. There was no difference in autophagic flux between any of the groups (p=0.77).

Wortmannin treatment did not alter P62/SQSTM1 levels in the healthy control or iPD groups, suggesting that they had sufficient reserve in their capacity to initiate autophagy through PI3K-mediated or alternative pathways. In contrast, there was a non-significant increase in P62/SQSTM1 levels in the *GBA1*-PD group, with a significant increase in the number of P62/SQSTM1 positive puncta (p=0.002). These structures were large in size, suggesting that they represented sequestosomes (rather than autophagosomes), indicating that wortmannin significantly impaired autophagic degradative capacity in the *GBA1*-PD group (Figure 4.3 and Figure 4.4).

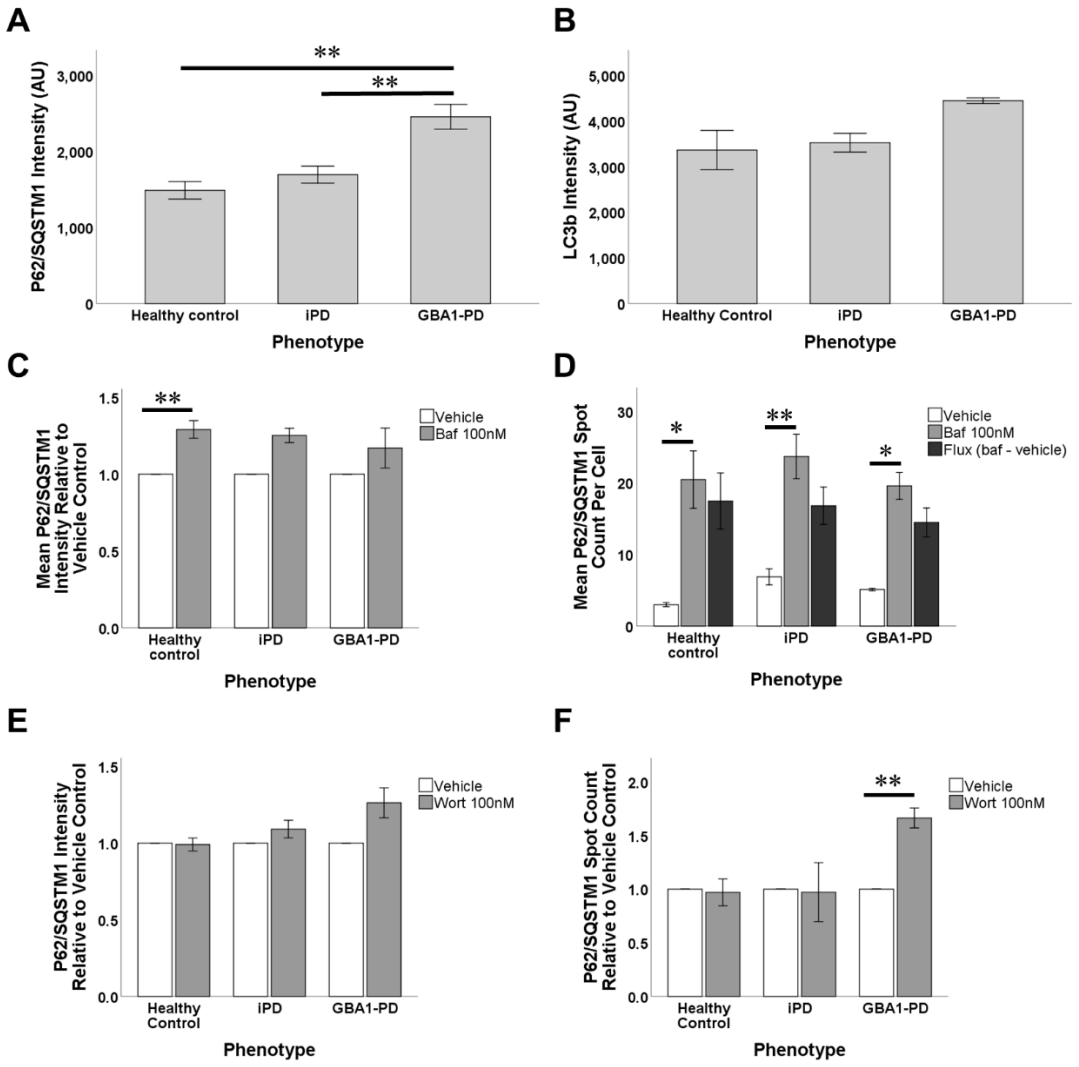

Figure 4.3 – Autophagy markers in patient-derived fibroblasts. P62/SQSTM1 (A) and LC3b (B) intensity were increased in *GBA1*-PD fibroblasts after starvation in comparison to other groups. C) P62/SQSTM1 intensity increased following bafilomycin A1 treatment in healthy control fibroblasts. D) The number of P62/SQSTM1 puncta increased following bafilomycin A1 100nM treatment in fibroblasts. There were no differences in autophagic flux (the difference in P62/SQSTM1 spot count after bafilomycin A1 treatment and under baseline conditions) between groups. Wortmannin increased P62/SQSTM1 intensity (E) and spot count (F) only in *GBA1*-PD fibroblasts. For comparison between the three phenotypic groups, statistical significance was determined with one-way ANOVA and post-hoc Tukey analysis. Independent samples T tests were used to compare baseline to treatment conditions within each group. Statistical significance indicated by asterixes.

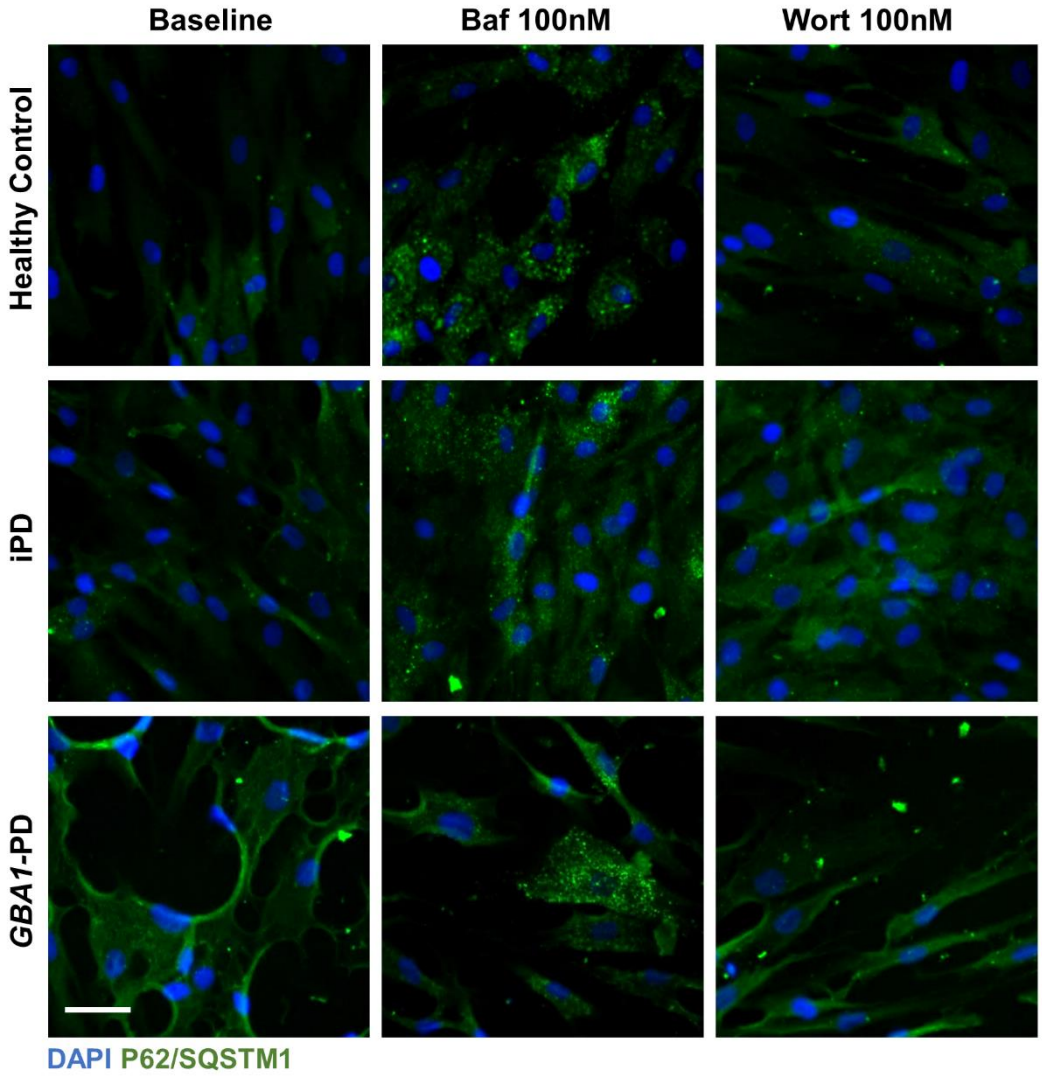

Figure 4.4 – P62/SQSTM1 immunocytochemistry in patient fibroblasts with bafilomycin A1 and wortmannin treatment. Bafilomycin A1 increased the number of small P62/SQSTM1-positive puncta in healthy control, iPD, and *GBA1*-PD fibroblasts. Wortmannin did not significantly alter P62/SQSTM1 immunocytochemistry in healthy controls or iPD cells, but led to accumulation of large P62/SQSTM1-positive puncta in *GBA1*-PD fibroblasts. Scale bar represents 50 µm.

Lysosomal mass in the fibroblasts was quantified using Lysotracker^{TM} red DND-99 (Figure 4.5). The lysosome count (p=0.035) and total lysosome area (p-0.031) were statistically higher in the *GBA1*-PD group when compared to healthy controls – a finding consistent with previous reports (Bae et al. 2015). There were no significant differences between the iPD group and the control or *GBA1*-PD groups.

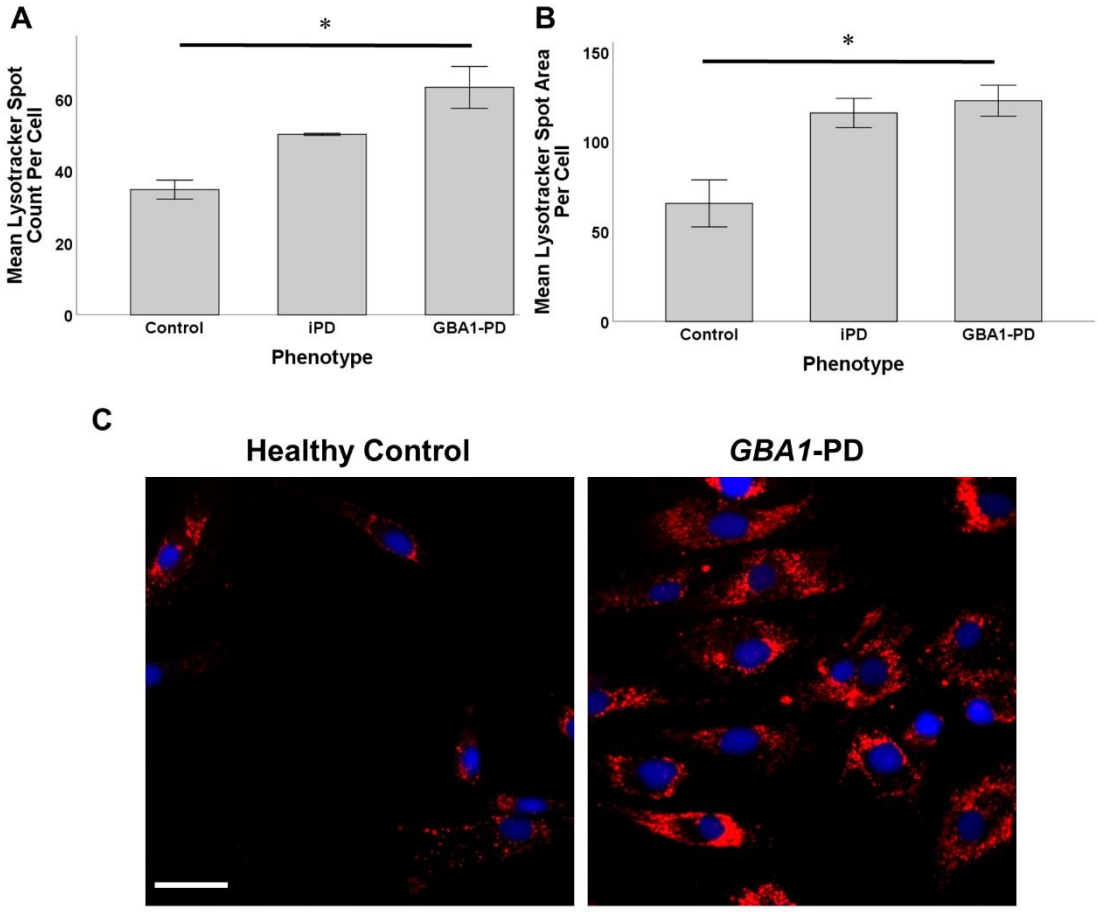

Figure 4.5 – Lysosomal mass in patient fibroblasts. Lysotracker™ red DND-99 was used to quantify lysosomal mass. Lysosomal count (A) and area (B) were higher in *GBA1* variant-carrying fibroblasts, compared to healthy controls. C) Representative images of Lysotracker™ DND-99 staining. Cell lines were analysed in triplicate. Independent samples T tests were used to compare mean values between groups. Statistical significance indicated by asterixes. Scale bar represents 50 µm.

P62/SQSTM1 intensity was also assessed at baseline in iNs, where no difference was observed between the groups (Supplementary Figure 7.1). This may be explained by the fact that only baseline staining was performed in iNs, without the use of starvation to induce autophagy, or chemical inhibitors of the various stages of autophagy. LC3b-II levels were determined in iNs from healthy controls (n=2), and patients with iPD (n=4) and *GBA1*-PD (n=3) with Western blot analysis (Supplementary Figure 7.3). Under starvation conditions, LC3b-II levels were non-significantly reduced in the *GBA1*-PD group compared to healthy controls, by approximately 50% (p=0.074) (Figure 4.6). There

were no significant differences between any of the groups under non-starvation conditions.

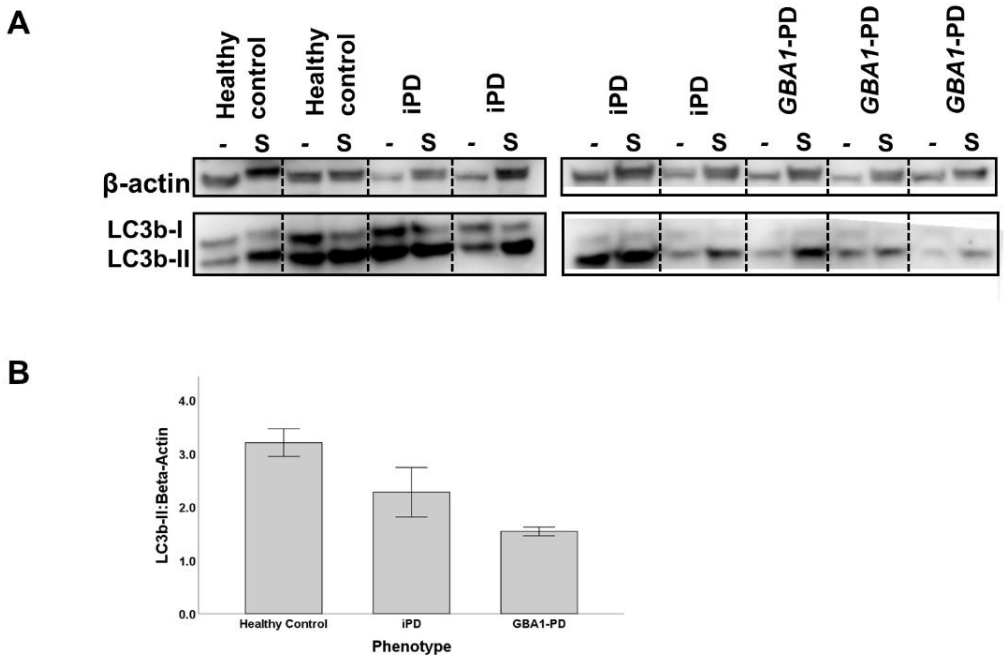

Figure 4.6 – LC3b quantification in iNs. iNs were generated from healthy controls (n=2), and patients with iPD (n=4) and *GBA1*-PD (n=3). At day 22 post-transduction iNs were kept in neuronal medium or starved in HBSS with calcium and magnesium for six hours, before protein was harvested in 5 M urea lysis buffer. A) Western blot for LC3b in iN cell lysates. B) Autophagosome numbers after starvation were reduced in iNs from *GBA1*-PD patients compared to those from healthy controls and iPD patients, as judged by LC3b-II levels. Abbreviations: S=starvation.

4.4.2 Mitochondrial dysfunction

Because autophagy is important for the clearance of dysfunctional mitochondria, and because mitochondrial abnormalities have been reported in a small number of studies of *GBA1*-PD, mitochondrial superoxide production, and mitochondrial membrane potential were determined in fibroblasts using MitoSOX^{TM} red and TMRE-based assays respectively. There were no significant differences in mitochondrial superoxide production (p=0.053) or mitochondrial membrane potential (p=0.362) between any of the

groups. There was a trend towards lower mitochondrial membrane potential in the *GBA1* mutation-carrying cell lines, and it may be that the small sample size prevented detecting a true difference in mitochondrial membrane potential (Figure 4.7 and Figure 4.8).

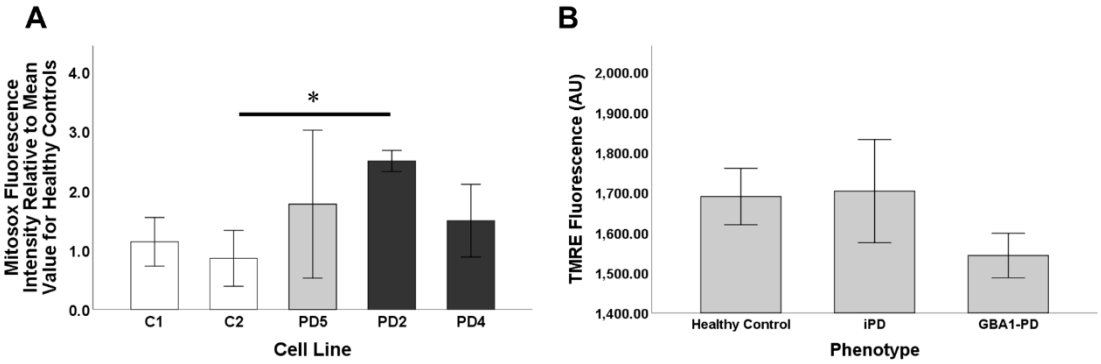

Figure 4.7 – Assessment of mitochondrial health in patient fibroblasts. A) MitoSOX^{TM} red fluorescence intensity in fibroblasts from healthy controls (white bars, n=2), and patients with iPD (light grey bar, n=1) and *GBA1*-PD (dark grey bars, n=2).Bars represent the mean value of triplicates for each line. B) Mitochondrial membrane potential in fibroblasts from healthy controls (n=2), and patients with iPD (n=2) and *GBA1*-PD (n=3). There were no significant differences in mitochondrial superoxide production or mitochondrial membrane potential. Statistical significance determined by one-way ANOVA. Statistically significant difference indicated by asterix.

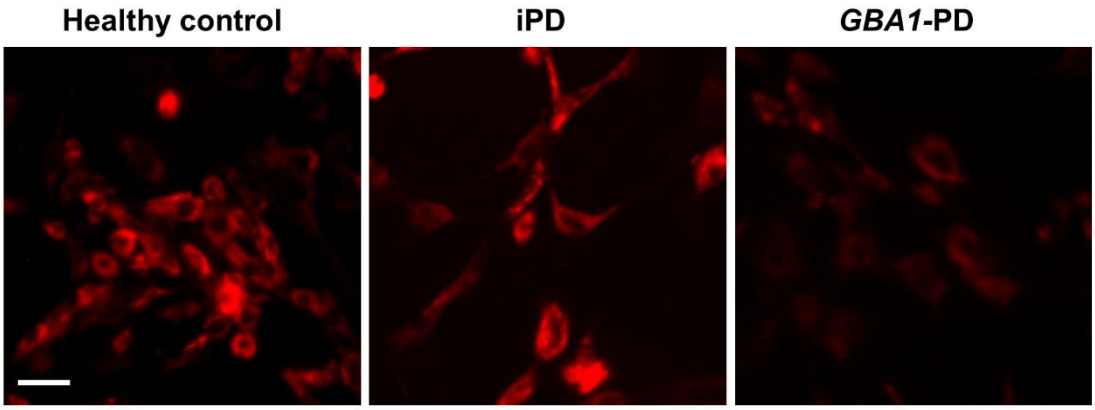

Figure 4.8 – TMRE assay of mitochondrial membrane potential in patient fibroblasts. Scale bar represents 200 µm.

To determine if there were any functional differences in mitochondrial capacity associated with *GBA1* mutations, a luminescence-based ATP production assay was performed. In-keeping with the above observations, ATP production was similar between healthy controls, and patients with iPD or *GBA1*-PD with no significant difference detected (p=0.361) (Figure 4.9). These data suggest that at baseline, there is no major deficit in mitochondrial function, in association with *GBA1* mutation.

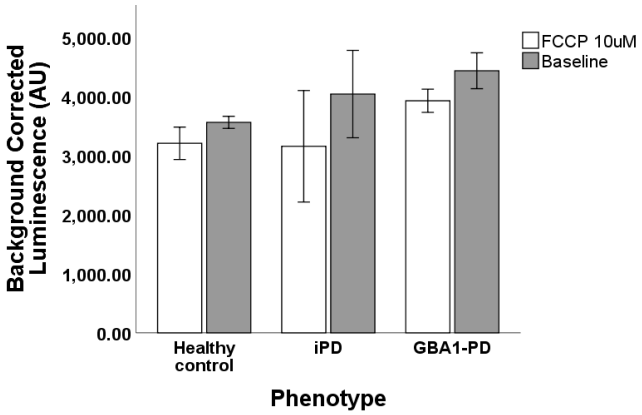

Figure 4.9 – ATP production in patient fibroblasts. ATP production was estimated using a luminescence assay in healthy controls (n=3), and patients with iPD (n=2), *GBA1*-PD (n=3). FCCP 10 µM treated fibroblasts were used as a negative control. There were no significant differences in ATP production between any of the disease groups at baseline (p=0.361).

Mitochondrial parameters were also investigated in iNs derived from healthy controls (n=2), and patients with iPD (n=3) or *GBA1*-PD (n=2). Mitochondrial content was first estimated using MitoTracker™ green dye, with no significant differences between the groups (p=0.177). There were no differences in mitochondrial membrane potential, as judged by TMRE assay (p=0.77), or in the estimate of functional polarised mitochondria (p=0.128), determined as the ratio of TMRE to MitoTracker™ signal. Similarly, there were no significant differences in mitochondrial superoxide production (p=0.766). As expected, treatment with the mitochondrial uncoupler FCCP resulted in a reduction in mitochondrial membrane potential and estimated functional polarised mitochondria, and an increase in superoxide production in all groups.

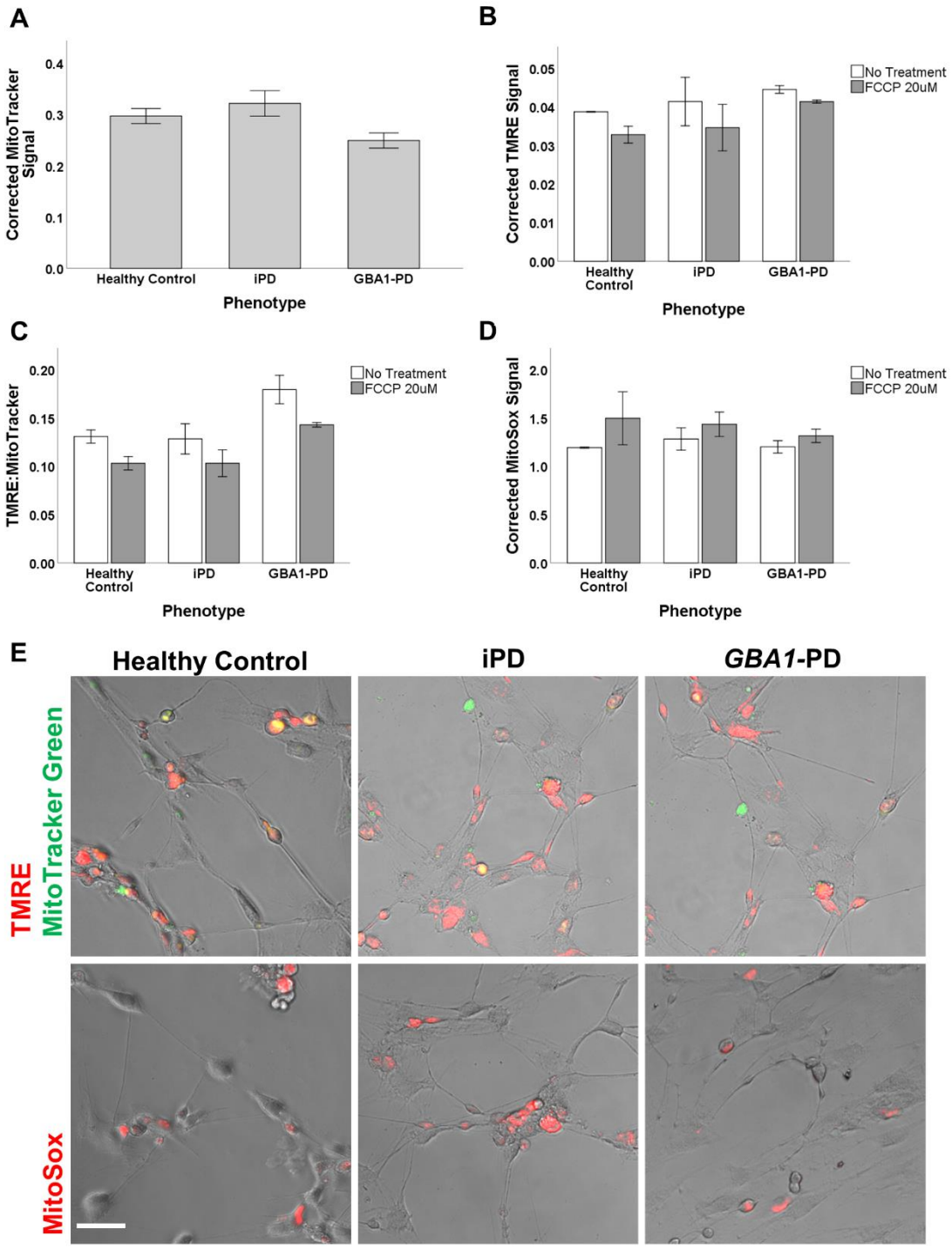

Figure 4.10 – Mitochondrial assays in iNs. There were no significant differences in total mitochondrial content (A), mitochondrial membrane potential (B), estimated total functional polarised mitochondria (C) or mitochondrial superoxide production (D) between healthy controls (n=2), and patients with iPD (n=3) or *GBA1*-PD (n=2). E) Representative images of above. Scale bar represents 200 µm.

4.4.3 Treatment of induced neurons with α-synuclein pre-formed fibrils

In order to use iNs as a novel disease model and in vitro drug-screening tool for PD, PFFs of pathogenic α-synuclein were used to induce PD-relevant pathology. Treatment with PFFs has previously been shown to induce α-synuclein aggregates and neurodegeneration in cultured neurons and animals (Luk et al. 2009, Volpicelli-Daley et al. 2011, Luk et al. 2012a). Initially, iNs from four cell lines (two healthy controls, one patient with iPD and one with *GBA1*-PD) were generated, and treated with a single dose of PFFs (0.3 ng/µl) at day 17 post-transduction. They were cultured for a further 10 days, with ongoing medium changes every two to three days until day 27 post-transduction. All lines demonstrated pFTAA (pentameric formyl theophene acetic acid)-positive aggregates, which were more numerous in the PD cell lines than in the healthy controls. These aggregates were subsequently shown to consist of α-synuclein with immunocytochemistry (Figure 4.11). Immunocytochemistry for β-amyloid (another aggregate-prone protein) was also performed as a negative control, which was not identified in the pFTAA-positive aggregates (Figure 4.12).

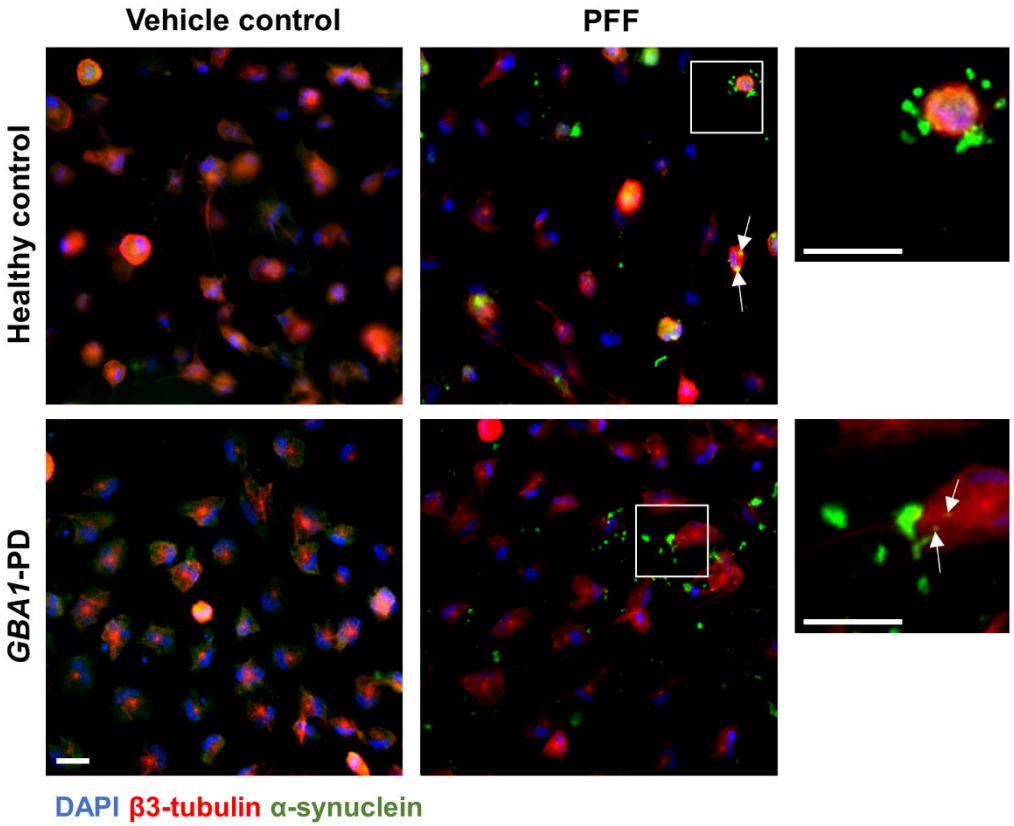

Figure 4.11 – PFF-induced α-synuclein aggregates in patient-derived iNs. The majority of observed aggregates were extracellular, situated adjacent to cells (see magnified boxes). A smaller number of intracellular aggregates could be seen (white arrows). Scale bars represent 50 µm.

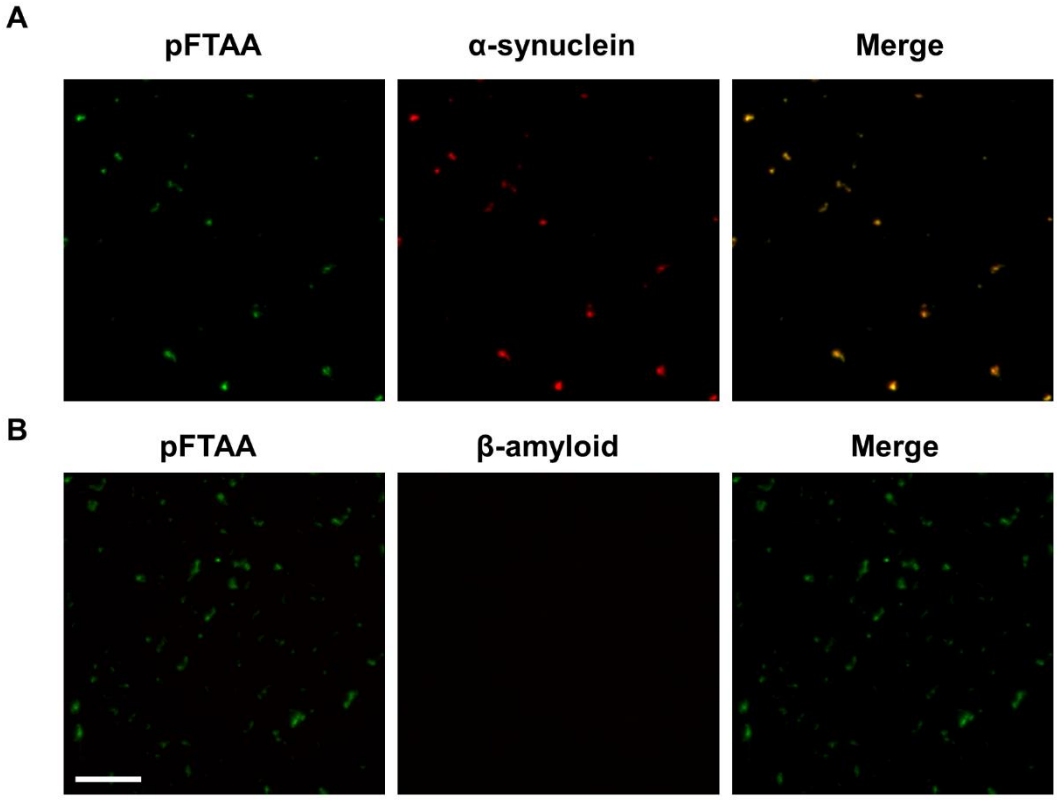

Figure 4.12 – Confocal microscopy images of pFTAA-positive aggregates in iNs. iNs from a *GBA1*-PD cell line were treated with α-synuclein PFFs before staining with pFTAA and immunocytochemistry for α-synuclein and β-amyloid. Aggregates were found to consist of α-synuclein (A) but not to contain β-amyloid (B). Abbreviations: pFTAA = pentameric formyl theophene acetic acid. Scale bar represents 100 µm.

This was subsequently repeated with iNs generated from healthy control lines (n=3), iPD lines (n=2) and *GBA1*-PD lines (n=3), to see if the burden of PFF-induced aggregates differed between the different phenotypes. The healthy controls had a lower number and area of PFF-induced aggregate per iN than all of the other groups, though this did not reach statistical significance, probably due to the low sample size, and the large standard deviation in the PD groups (Figure 4.13). The aggregates were not observed to contain phosphorylated α-synuclein on immunocytochemistry (Supplementary Figure 7.2).

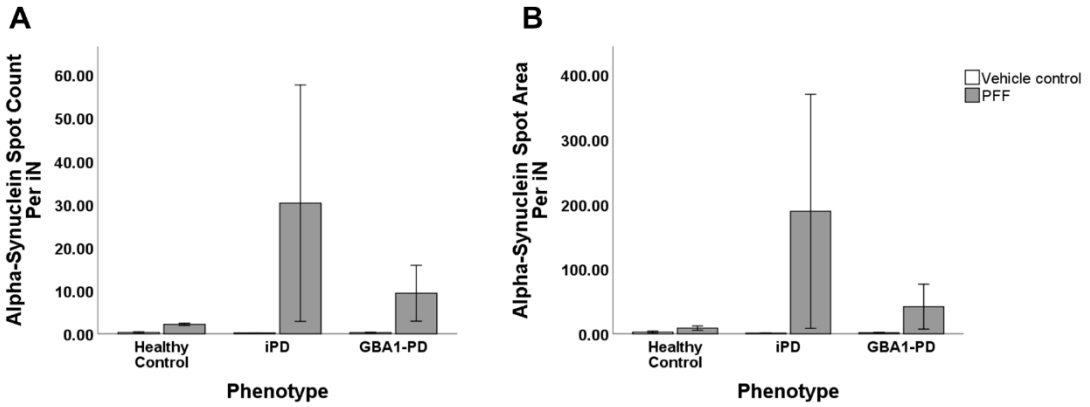

Figure 4.13 – Quantification of PFF-induced aggregates in patient-derived iNs. Number (A) and area (B) of PFF-induced α-synuclein aggregates in iNs derived from healthy controls (n=3), and patients with iPD (n=2) and *GBA1*-PD (n=3). Each cell line was analysed in triplicate and a mean value for each cell line used for statistical analysis. The burden of PFF-induced aggregates was low in healthy controls compared to disease groups. Abbreviations: iN = induced neuron; PFF = pre-formed fibril.

The PFF-induced aggregates were then quantified following exposure to three different doses of PFFs (0.4 ng/µl, 1.9 ng/µl and 2.7 ng/µl) in iNs derived from healthy controls (n=4), iPD patients (n=5), and *GBA1*-PD patients (n=3). In the healthy control, iPD and *GBA1*-PD groups, there were increases in the number of α-synuclein-positive spots at the 0.4 ng/µl PFF dose but this only reached significance for the iPD (p=0.01) and *GBA1*-PD (p=0.024) groups when compared to treatment with vehicle control. There were further increases in the number of α-synuclein-positive aggregates with the two higher PFF doses (Figure 4.14 and Figure 4.15). At the lower PFF dose, the healthy control group had a reduced propensity for aggregate accumulation in comparison to the iPD group (p=0.009) and the *GBA1*-PD group (p=0.002). The total area of aggregates was also greater in the *GBA1*-PD group compared to healthy controls at the highest PFF dose (p=0.05). There were no significant differences in the number of aggregates per cell between the groups at the two higher PFF doses, though at each dose the number of PFF-induced aggregates was lowest in the healthy control group, and highest in the *GBA1*-PD group.

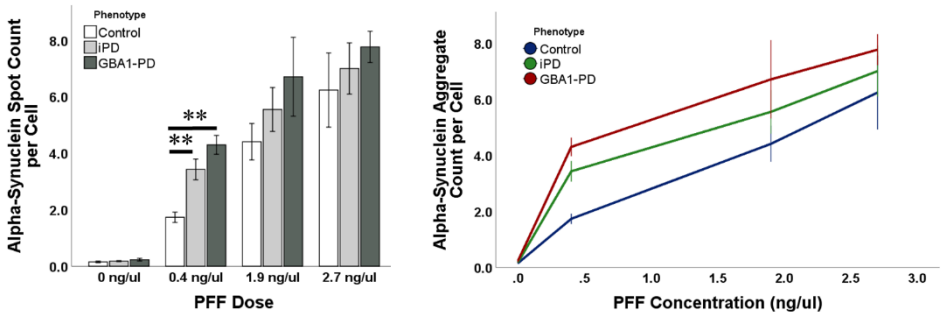

Figure 4.14 – Number of PFF-induced α-synuclein aggregates with different PFF doses. iNs from healthy controls (n=3), and patients with iPD (n=5) and *GBA1*-PD (n=3) were treated with 0.4 ng/µl, 1.9 ng/µl or 2.7 ng/µl of PFFs, or vehicle control. At the lowest dose, the number of aggregates observed was statistically greater in the iPD group (p=0.009) and the *GBA1*-PD group (p=0.002) compared to controls. There were no significant differences between the three groups at the other doses. Statistically significant differences between the phenotypic groups determined by one-way ANOVA with post-hoc Tukey analysis at each PFF dose indicated by asterixes. Abbreviations: PFF = pre-formed fibrils.

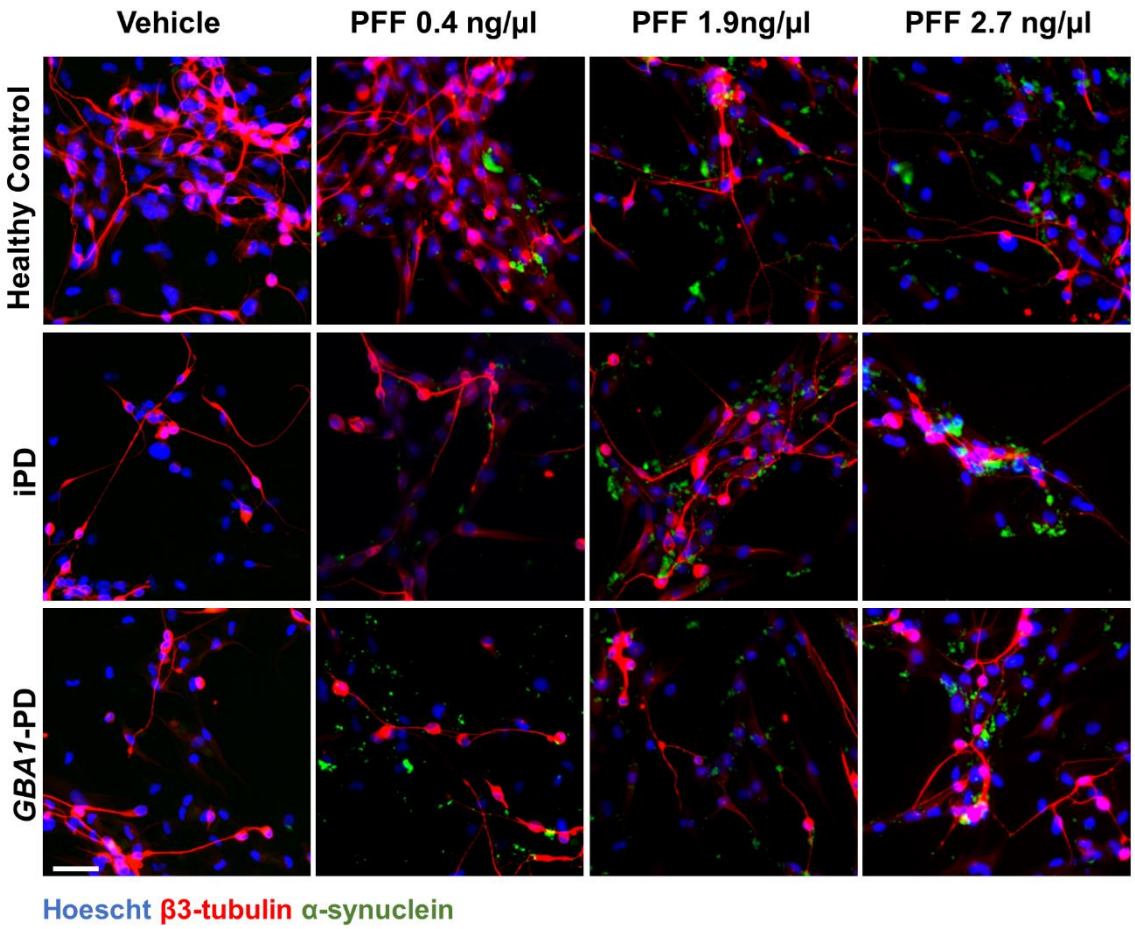

Figure 4.15 – PFF-induced aggregates at different PFF doses. There were dose-dependent increases in the number of PFF-induced aggregates in all disease groups. At the lowest dose, the number of PFF-induced aggregates in healthy controls was low. Scale bar represents 50µm. Abbreviations: PFF = pre-formed fibril.

The majority of the aggregates appeared to be on the perimeter of the cells, and to further determine the location of them, confocal microscopy was performed. This demonstrated that the majority of the aggregates were extracellular, adjacent to cells (Figure 4.16), though a small number of intracellular aggregates were present (Figure 4.11).

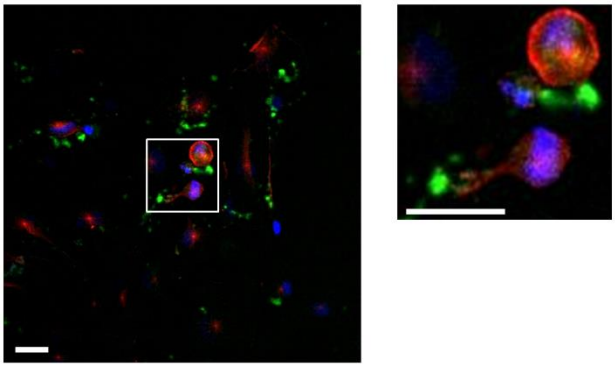

Figure 4.16 – Extracellular PFF-induced aggregates. Confocal microscopy image showing extracellular PFF-induced aggregates in iNs derived from an iPD patient. Scale bars represent 50 µm.

To verify that the pFTAA-positive α-synuclein aggregates were not residual PFFs that had adhered to the culture matrix, PFFs generated from fluorescent-tagged α-synuclein monomers were generated. These were applied to fibroblasts from a healthy control and a *GBA1*-PD cell line. Cells were then fixed and imaged at day one, three, six and eight (Figure 4.17). Fluorescent-tagged PFFs could clearly be observed intracellularly in both cell lines in a proportion of the cells at day one, but their presence declined over the subsequent time-points, being undetectable by day six (Figure 4.18). Fibroblasts from a *GBA1*-PD line were also treated with untagged PFFs, before immunocytochemistry for α-synuclein was performed after 10 days. A small number of α-synuclein-positive spots of small size were observed, though this was significantly fewer than that seen with iNs derived from the same cell line, indicating that the observed aggregates were specific to neuronal cells (Figure 4.19).

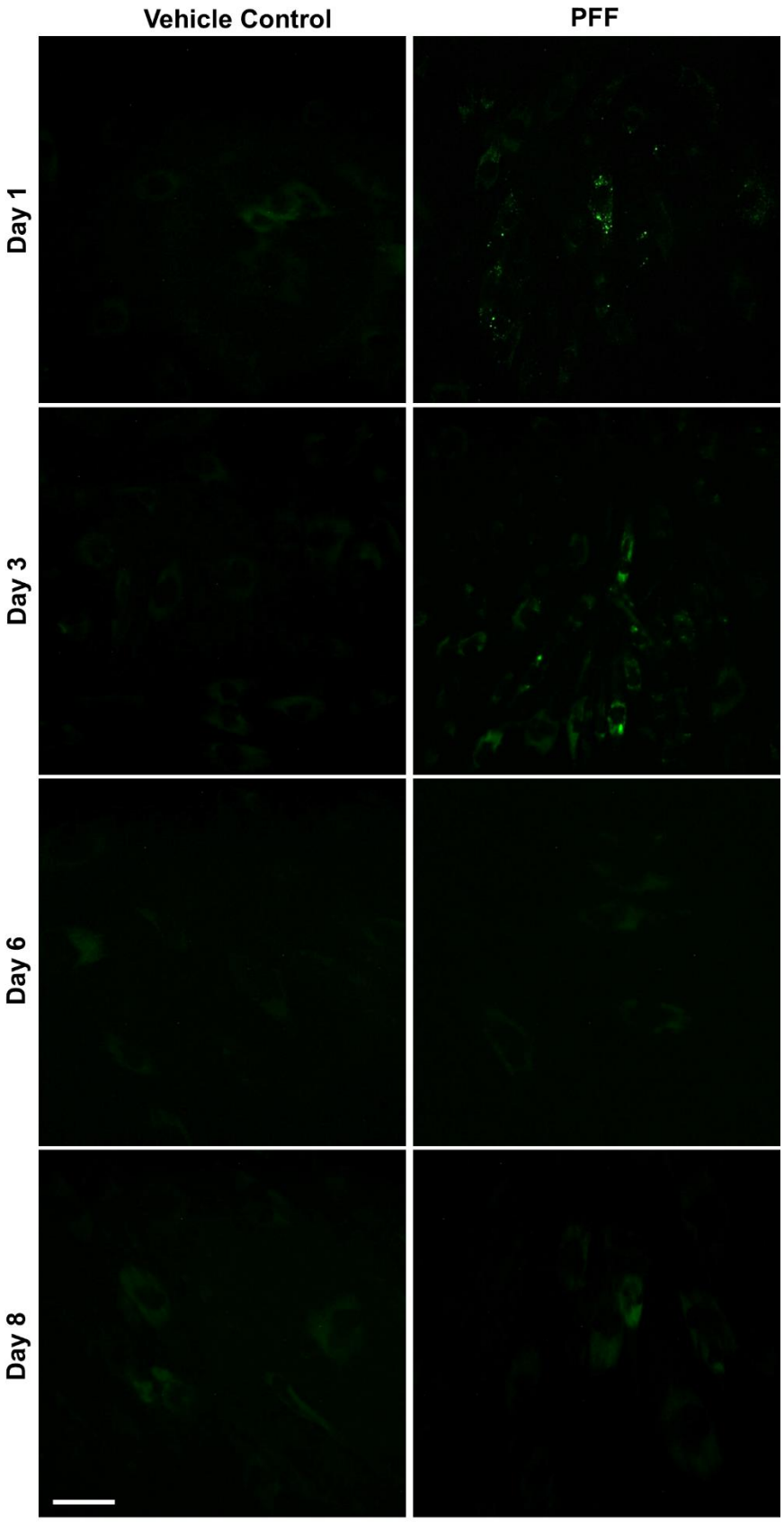

Figure 4.17 – Treatment of patient fibroblasts with fluorophore-tagged PFFs. Fluorescent PFFs could be seen within cells at day one post-treatment, but were undetectable from day six onwards. Scale bar represents 200 µm.

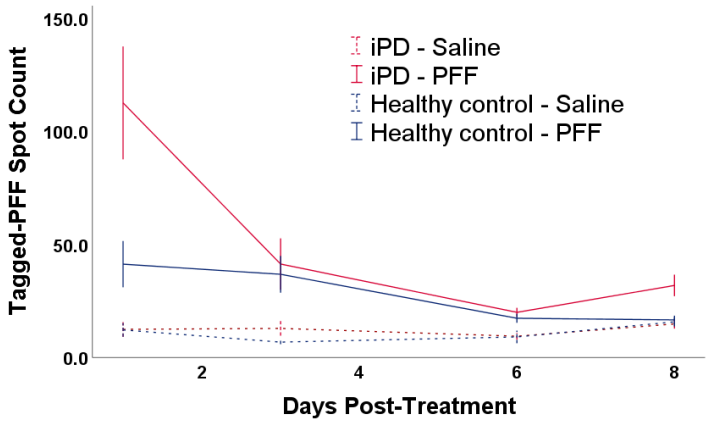

Figure 4.18 – Clearance of fluorophore-tagged PFFs over time. Fibroblasts from a healthy control line and iPD line were treated with fluorophore-tagged PFFs, and fluorescent spot-count determined at 24 hours, three days, six days, and eight days post-treatment. The number of fluorescent puncta decreased to low levels in both lines within six days.

To further demonstrate that PFFs themselves do not persist in the culture vessel, PFFs were added to a six-well plate in the absence of cells. Half-medium changes were performed to mimic the conversion protocol, and after 10 days the wells were washed and stained for α-synuclein – there were no persisting PFFs, confirming that PFFs do not adhere to the culture matrix, and that the observed α-synuclein aggregates in iNs did not consist of residual PFFs (Figure 4.19). Taken together, these observations suggest that the PFFs themselves are cleared by cells within a short time-frame, that they do not adhere to the culture matrix directly, and that the observed PFF-induced aggregates do not occur in fibroblasts, but are specific to the iNs.

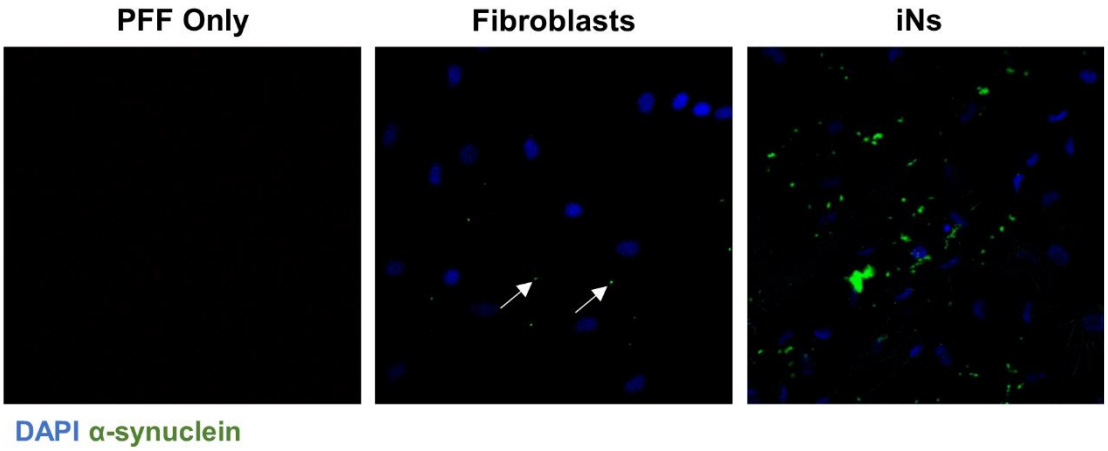

Figure 4.19 – α-synuclein aggregates in fibroblasts and iNs treated with PFFs for 10 days. No aggregates were observed when PFFs were incubated in the absence of cells, and only small numbers were seen in fibroblasts when compared to those seen in iNs from the same *GBA1*-PD cell line.

To confirm that α-synuclein PFFs were able to induce aggregation of α-synuclein expressed within the recipient cell, fibroblasts from an iPD line were transfected with a plasmid encoding GFP-tagged wild-type α-synuclein, and subsequently treated with PFFs or PBS vehicle control. In transfected cells, PFF treatment resulted in the accumulation of GFP and α-synuclein-positive puncta, detected on immunofluorescence (Figure 4.20). The total area of α-synuclein aggregate per cell in the transfected cells treated with PFF was significantly greater than in transfected cells treated with PBS ($p<0.0001$), or untransfected cells treated with PFF ($p<0.0001$) or PBS ($p<0.0001$) (Figure 4.21). A small number of α-synuclein-positive puncta were present in untransfected cells treated with PFFs, thought to represent residual PFFs that were yet to be cleared at this early stage. α-synuclein-positive puncta were only observed in very small numbers in transfected or untransfected cells that were not treated with PFFs.

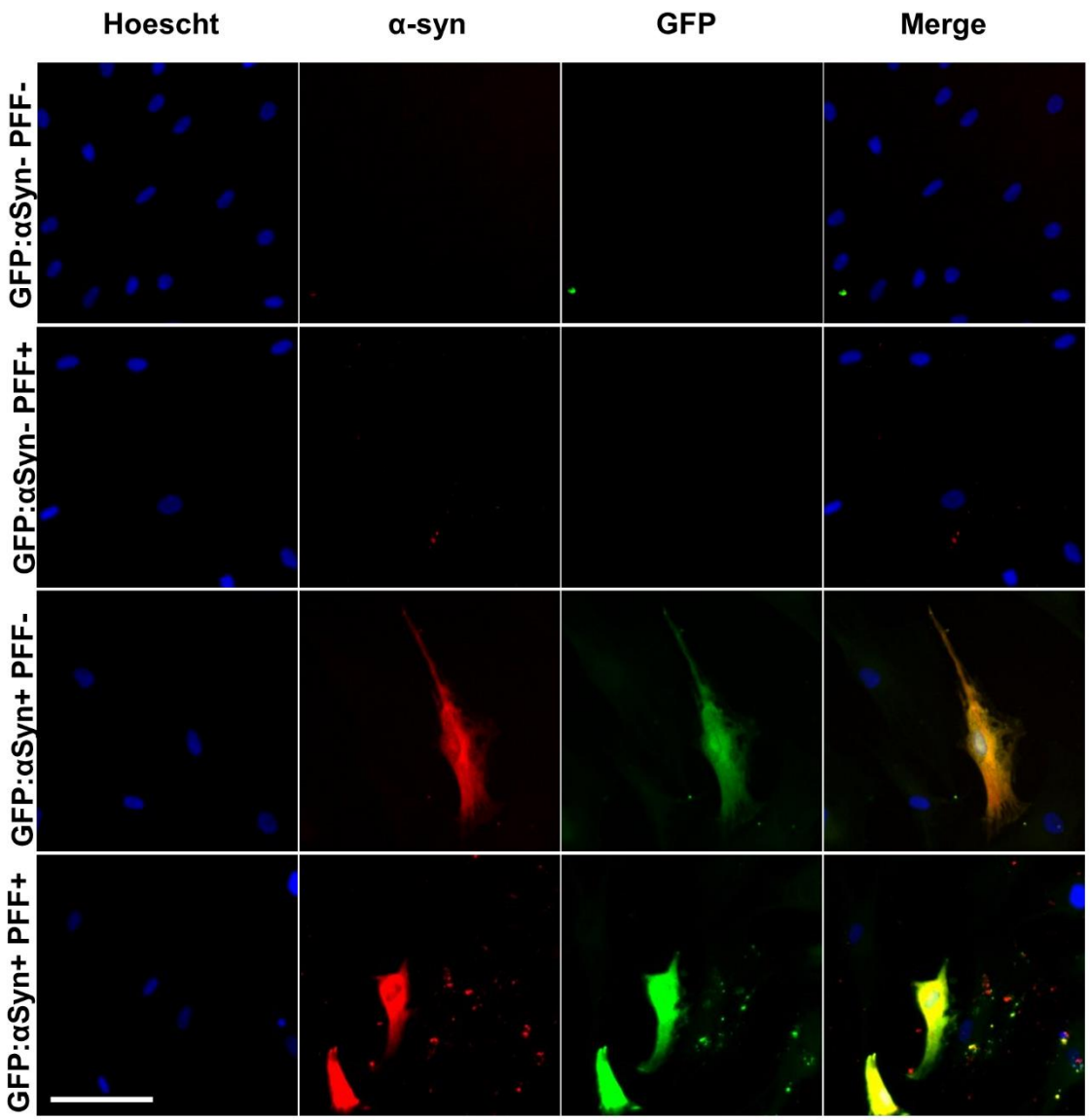

Figure 4.20 – α-synuclein PFF-induced aggregates in fibroblasts expressing GFP-tagged α-synuclein. α-synuclein aggregates were observed in transfected cells treated with PFFs, which were co-localised to GFP signal, indicating that they consisted of α-synuclein from within the cell. These aggregates were not observed in the absence of PFF treatment or in untransfected cells. Abbreviations: αSyn = α-synuclein; GFP = Green fluorescent protein; PFF = Pre-formed fibrils. Scale bar represents 100 μm.

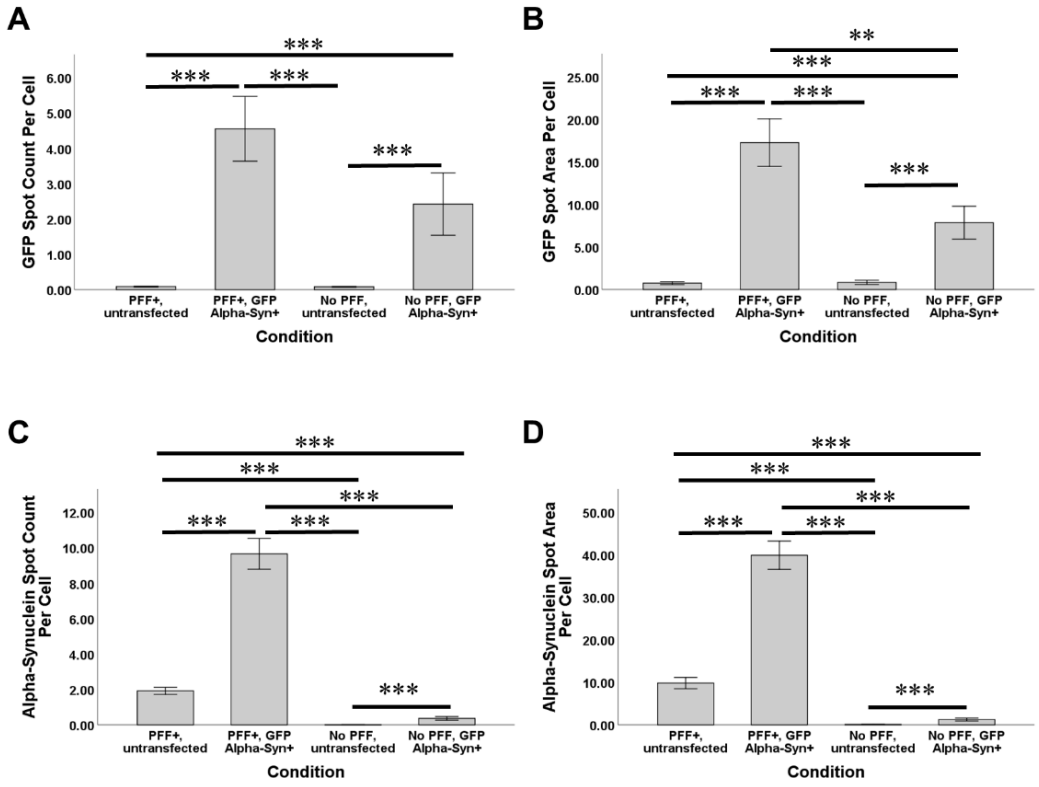

Figure 4.21 – Quantification of PFF-induced α-synuclein aggregates in fibroblasts transfected with GFP-α-synuclein. GFP (A and B) and α-synuclein (C and D) aggregates were numerous in transfected fibroblasts treated with PFFs, but only observed in small numbers in other groups. Statistical significance indicated by asterixes as determined by one-way ANOVA with post-hoc Tukey analysis. Abbreviations: Alpha-syn = α-synuclein; GFP = green fluorescent protein; PFF = pre-formed fibrils.

The dynamic nature of the iN culture system meant that application of PFFs at different time points could alter the degree of α-synuclein aggregation. In the early stages of conversion, endogenous α-synuclein levels are low, theoretically resulting in a reduction in aggregate burden. In contrast, application at too late a stage may preclude culture for sufficient duration for aggregates to form. In order to assess the optimal timeframe for application of PFFs during the conversion, iNs from two iPD lines were generated, with PFFs applied at five different time points (day 3, 5, 10, 17 or 22 post-transduction). Cells were then fixed at day 27 for analysis.

In keeping with the idea that early application of PFFs would limit the development of aggregates, the number of aggregates was low in the wells treated at three and five days,

and was greatest in the wells treated at day 17, which reached statistical significance when compared to treatment at day five (p=0.045). The number was also lower in the wells treated at day 22, suggesting that at least five days of further culture is required for PFF-induced aggregates to accumulate in the greatest numbers. These data suggest that the optimal point of PFF-application in terms of induction of α-synuclein aggregation is between 10 and 17 days post-transduction. Interestingly, the aggregates derived from day 10 PFF administration were largest, suggesting that culture for 17, rather than 10 days post-PFF exposure allows for the aggregates to mature to a greater extent. There were no differences in neuronal purity between the different time points of PFF-administration, suggesting that the changes in aggregate burden were not due to differences in the number of iNs in the well, and that the timing of exposure did not affect differentiation or neuronal death (Figure 4.22 and Figure 4.23).

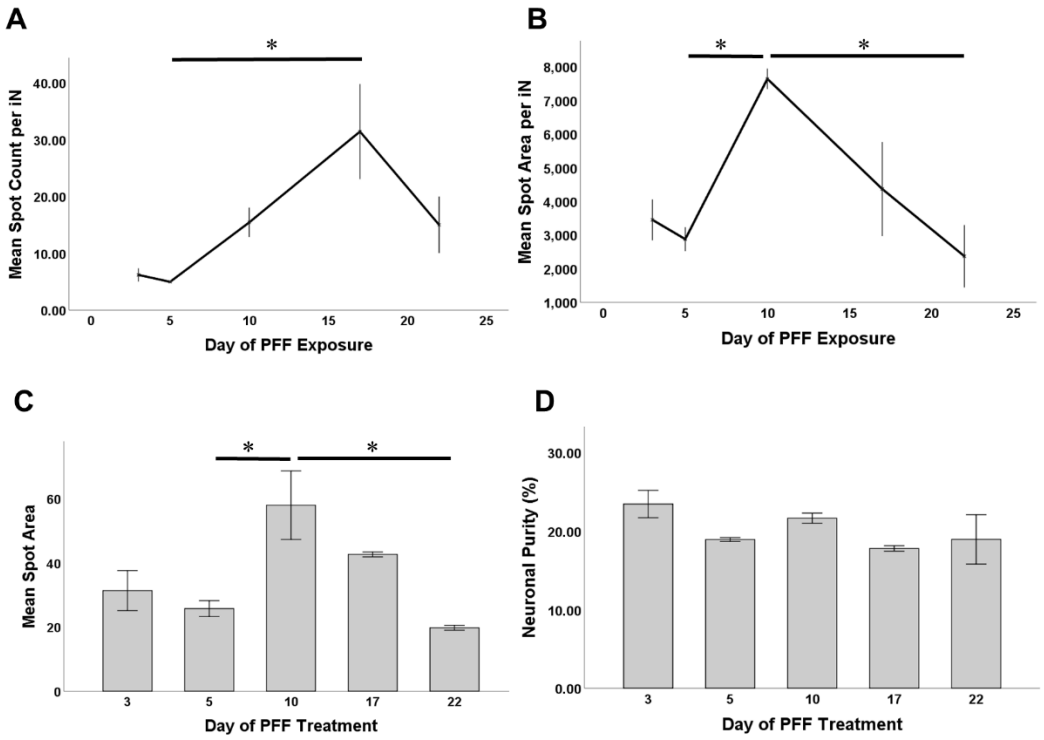

Figure 4.22 – Effect of time of PFF exposure on PFF-induced α-synuclein aggregate development. iNs were generated from two iPD lines, and PFFs applied at day 3, 5, 10, 17 or 22 post-transduction, before α-synuclein aggregate count (A) and area (B) per cell, and aggregate size (C), were quantified with immunocytochemistry. The number and area of PFF-induced aggregates were greatest at day 17 and day 10 respectively. Neuronal purity was calculated based on β3-tubulin expression. Error bars represent standard error

of mean. Statistical significance indicated by asterixes as determined by one-way ANOVA with post-hoc Tukey analysis. Abbreviations: iN = induced neuron; PFF = pre-formed fibrils.

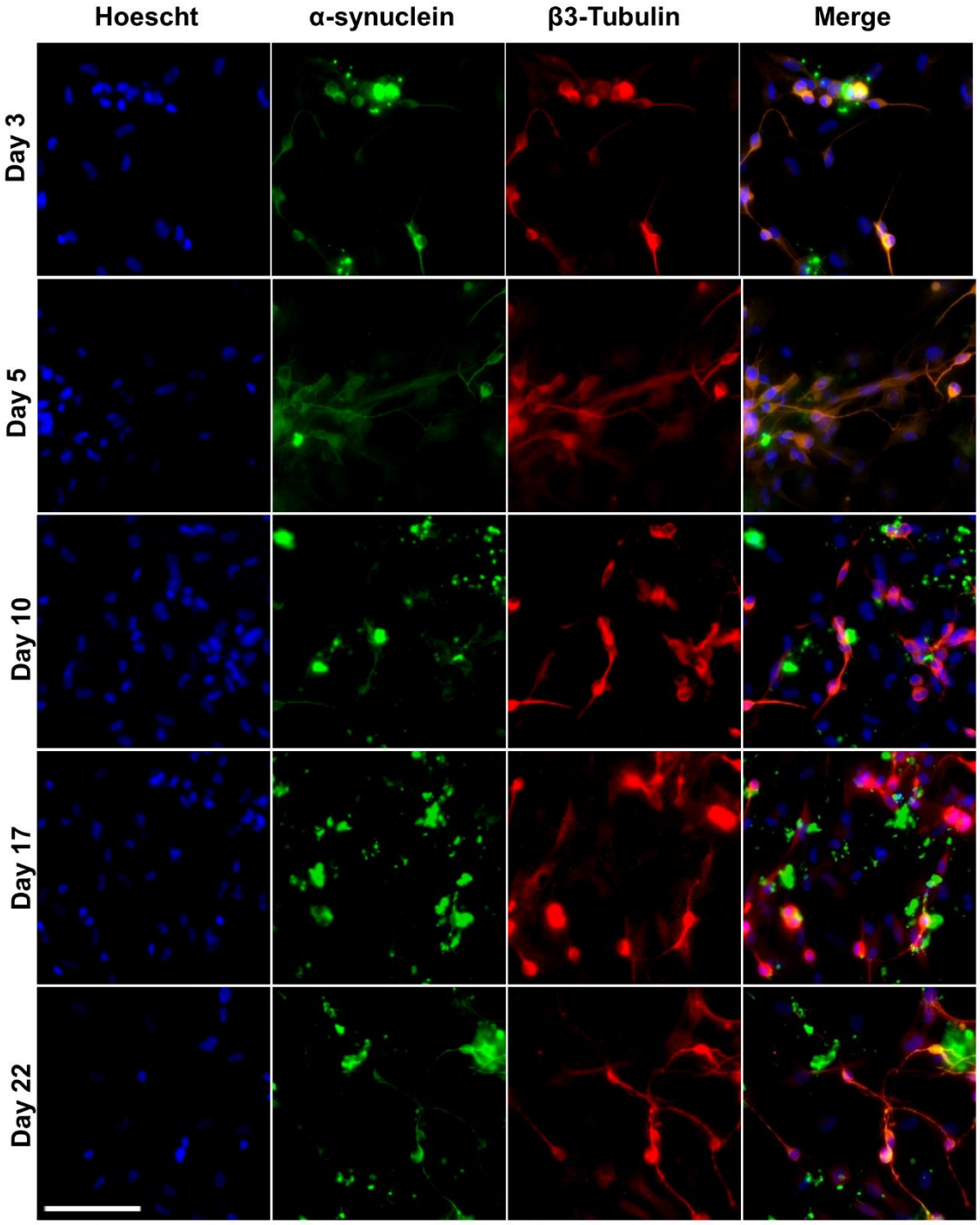

Figure 4.23 – Effect of time of PFF exposure on PFF-induced α-synuclein aggregate development. When PFFs were applied at days 3 and 5 post-transduction few aggregates developed. The number of aggregates was greatest when PFFs were applied at day 17. Images acquired at day 27 post-transduction. Scale bar represents 100 µm.

In order to assess the ability of the PFF-induced aggregates to propagate pathology, iNs were generated from an iPD cell line which consistently developed high numbers of aggregates. Given that the majority of observed aggregates are extracellular, it was assumed that some would be present in the cell culture medium. The cell culture medium from iNs exposed to PFFs for 11 days was transferred to a second plate, containing iNs from the same cell line that were at day 16 post-transduction. These cells were then cultured for a further 11 days, and immunocytochemistry was performed to see if the PFF-induced aggregates could propagate pathology. No aggregates were observed in the recipient plate of the transferred medium, suggesting that the aggregates themselves did not propagate pathology (Figure 4.24). However, it should be noted that the concentration of aggregates in the medium was probably very low, considering the fact that aggregates are not observed in areas of the well in which there are no cells. To investigate whether the aggregates can propagate pathology, it will therefore probably be necessary to purify the aggregates prior to transmission to ensure comparable concentration to the application of PFFs.

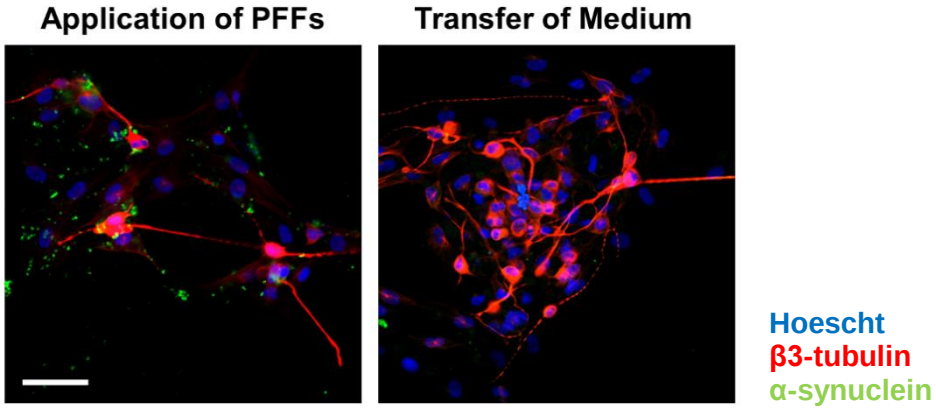

Figure 4.24 – Ability of PFF-induced aggregates to propagate pathology. A) PFF-induced aggregates after PFF exposure in plate one. B) Absence of aggregates after transfer of medium from plate one to plate two. Scale bar represents 100 µm.

4.4.4 Autophagy response to α-synuclein pre-formed fibrils

iNs were generated from iPD and *GBA1*-PD cell lines to assess whether or not PFF treatment induced an autophagy response. PFFs were applied at day 17, and protein was harvested after a further 72 hours for Western blot analysis. Though immunocytochemistry for neuronal markers was not performed, cells had taken on a typical neuronal morphology, with no overt differences between the cell lines (Supplementary Figure 7.5). In all cell lines LC3b-II levels increased following treatment with PFFs, suggesting that they induced an autophagy response, either directly or through the generation of α-synuclein aggregates. The increase in autophagosomes was significant in both the iPD group ($p=0.036$) and the *GBA1*-PD group ($p=0.041$), suggesting that the *GBA1*-PD group retained the ability to mount an autophagy response in this circumstance. P62/SQSTM1 levels were also reduced suggesting that the increase in autophagosome numbers was accompanied by an increase in autophagic flux, though this reduction was lower in the *GBA1-PD* group in which it failed to reach significance ($p=0.101$) suggesting that this response is reduced in this group (Figure 4.25).

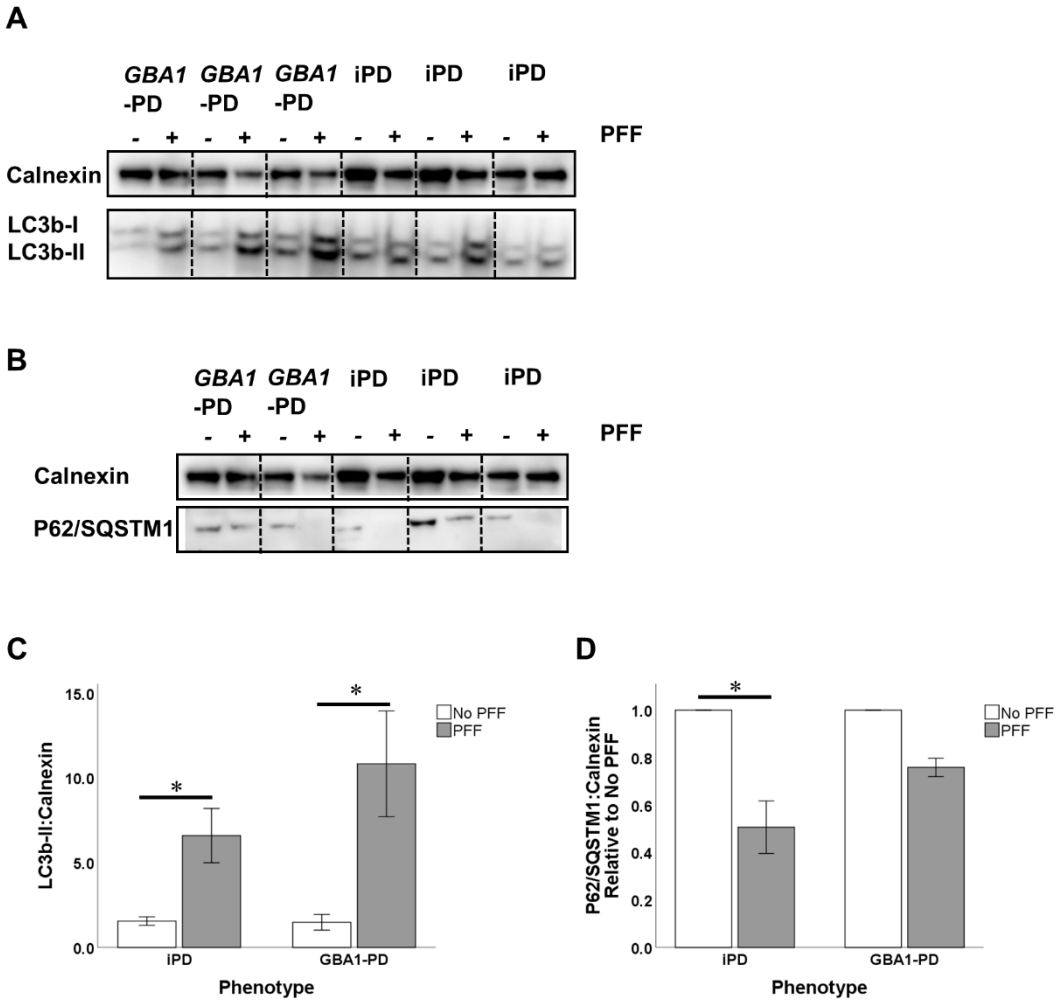

Figure 4.25 – Impact of PFF treatment on autophagy in iNs. A) Western blot for LC3b in iNs from patients with *GBA1*-PD (n=3) and iPD (n=3) with or without PFF treatment. B) Western blot for P62/SQSTM1 in iNs from patients with *GBA1*-PD (n=2) and iPD (n=3) with or without PFF treatment. C) and D) Quantification of above. PFF treatment increased the numbers of autophagosomes in iPD and *GBA1*-PD iNs. P62/SQSTM1 levels were reduced only in iPD iNs but not in *GBA1*-PD iNs. Error bars represent standard error of the mean. Statistical analysis comparing mean values for each group based on independent samples T tests, with significant differences indicated by asterixes. Abbreviations: iNs = induced neurons; PFF = Pre-formed fibrils.

4.4.5 α-synuclein pre-formed fibril-induced mitochondrial pathology

PFF treatment had no effect on neuronal purity (Supplementary Figure 7.6). In order to explore whether treatment with PFFs resulted in mitochondria dysfunction a TMRE assay for mitochondrial membrane potential was performed in iNs derived from *GBA1*-PD and iPD patients that had been exposed to low or high dose PFF for 10 days. Interestingly, the *GBA1*-PD group demonstrated a statistically significant dose-dependent fall in mitochondrial membrane potential as judged by TMRE signal, in response to PFF-exposure. TMRE signal fell by approximately 34.5 % (95 % confidence interval 24.6 % to 106.4 %) with the lower PFF dose (p=0.019), and by 46.2 % (95% confidence interval 31.3 % to 76.4 %) with the higher dose (p=0.005). The mitochondrial membrane potential in the iPD group was reduced with PFF treatment by approximately 12 %, but this was not statistically significant (Figure 4.26).

It was subsequently noted during further trials that in the iPD group, PFFs generally induced a decline in the mitochondrial membrane potential, but that this effect was less than that seen in *GBA1*-PD, such that it did not usually reach statistical significance. To further characterise the effect of PFFs on mitochondrial membrane potential, a retrospective analysis of all trials was performed in which the mean value for relative change in TMRE signal was determined for each cell line. This revealed a significant decline in mitochondrial membrane potential in the *GBA1*-PD group (p=0.015), with a non-significant decline in the iPD group.

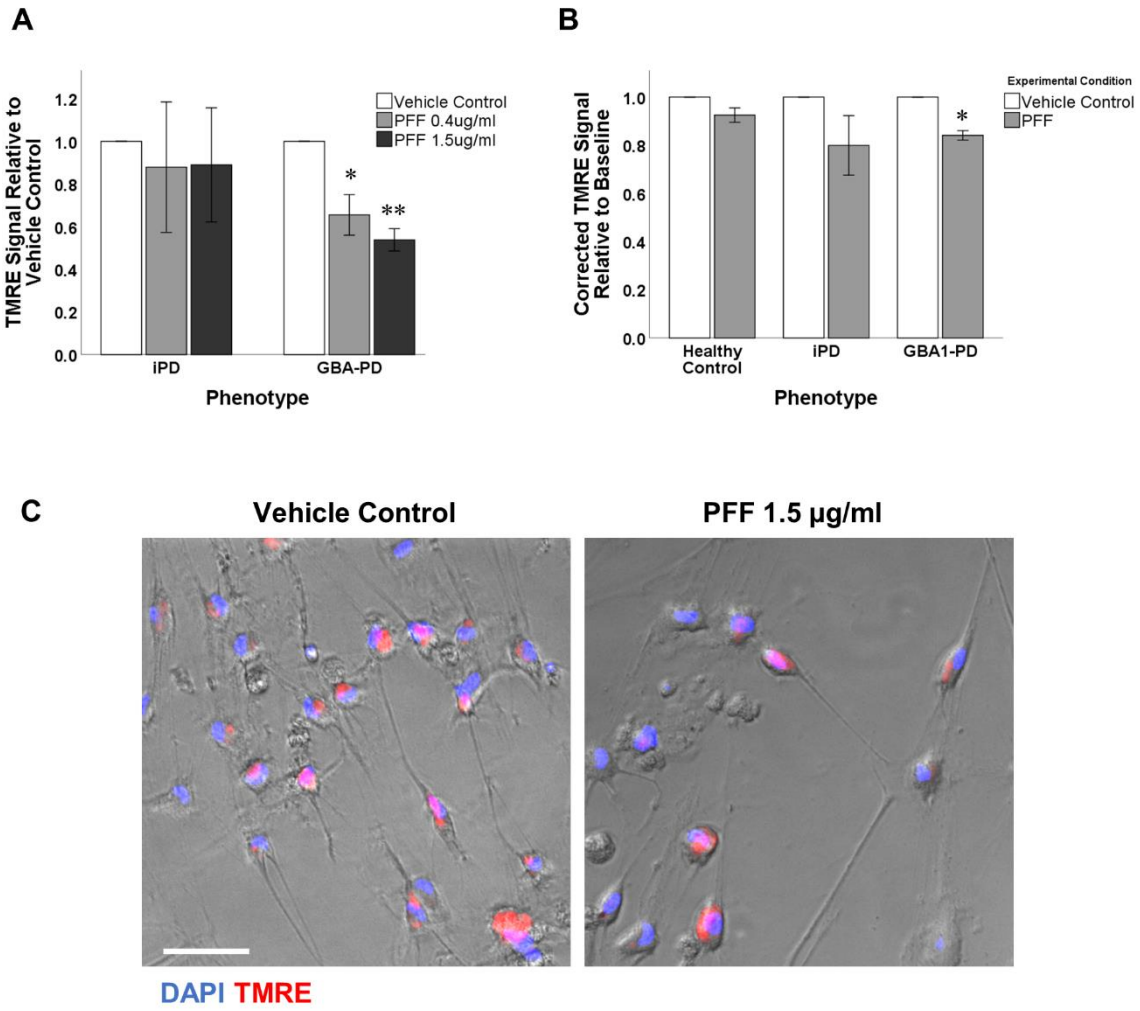

Figure 4.26 – Mitochondrial membrane potential in iNs after treatment with PFFs. A) Treatment with α-synuclein resulted in a dose-dependent reduction in mitochondrial membrane potential in *GBA1*-PD (n=3) but not in the iPD group (n=3). B) A retrospective analysis of all trials of TMRE membrane potential in iNs from healthy controls (n=2), and patients with iPD (n=5) and *GBA1*-PD (n=3) revealed that *GBA1*-PD was the only group to develop a significant reduction in mitochondrial membrane potential. C) Representative images from analysis. Asterixes indicate statistically significant differences from vehicle control condition. Error bars represent standard error of the mean. Scale bar represents 200 µm.

To further evaluate the susceptibility of *GBA1*-PD iNs to α-synuclein PFFs, caspase activity was assessed 10 days post-exposure to PFFs. Whilst there were no differences in caspase activity in the iPD group, the *GBA1*-PD lines demonstrated significantly

increased caspase activity ($p<0.001$ for 0.4 µg/µl PFF dose and $p=0.002$ for 1.5 µg/µl PFF dose), compared to those treated with vehicle control) (Figure 4.27).

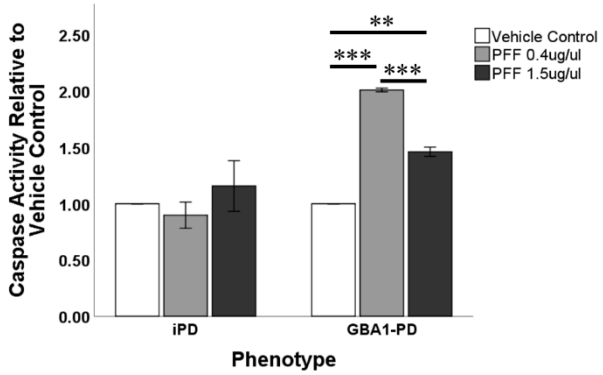

Figure 4.27 – Total caspase activity in iNs after treatment with PFFs. Caspase activity was increased in *GBA1*-PD (n=2) following PFF-exposure, but not in the iPD group. Asterixes indicate statistically significant differences from vehicle control condition as determined by one-way ANOVA with post-hoc Tukey analysis. Error bars represent standard error of the mean. Abbreviations: PFF = pre-formed fibrils.

4.5 Discussion

4.5.1 Lysosome-autophagy system dysfunction in *GBA1* mutation-associated Parkinson's disease

Abnormalities in the lysosome-autophagy system have consistently been observed in models of *GBA1*-PD, though the mechanisms by which autophagy is dysfunctional is not clear. Because macroautophagy is a dynamic process in continuous flux, it is a challenging system to study. Most studies in *GBA1*-PD observe changes in numbers of the constituents of the pathway (i.e. autophagosomes and lysosomes), but are unable to accurately define where the site of dysfunction lies.

In this study, P62/SQSTM1 has been used as a measure of autophagy. LC3b was also studied, but it was not possible to obtain images of sufficient resolution to accurately count puncta in immunocytochemistry analyses. P62/SQSTM1 levels following

starvation were significantly higher in the *GBA1*-PD fibroblasts than in healthy controls and in iPD patients, suggesting that autophagy activity was reduced in this group.

Having found that autophagy activity was reduced in *GBA1*-PD fibroblasts, this was investigated further through inhibition of the late and early parts of the autophagy pathway using bafilomycin A1 and wortmannin respectively. Bafilomycin A1 blocks the fusion between lysosomes and autophagosomes, which, under normal circumstances would be expected to increase the numbers of autophagosomes (due to their reduced clearance), and to reduce the degradative capacity of macroautophagy (through reduced flux) (Klionsky et al. 2016). In the healthy control group bafilomycin treatment did indeed reduce autophagic degradative capacity, as evidenced by a significant increase in P62/SQSTM1 levels. There was a similar rise in the iPD group though this did not reach significance. In contrast, there was only a small change in P62/SQSTM1 levels in *GBA1*-PD with bafilomycin treatment. Taken alone, this could be interpreted to suggest that there is a pre-existing block in the fusion stage of the autophagy pathway, such that introducing an inhibitor of this step causes no additional detriment to the pathway. Alternatively, if there is a problem at the earlier parts of the pathway (i.e. those involved in autophagosome formation), blockade of the fusion stages would have little impact on the degradative capacity of autophagy, because the pathway is already impaired upstream of this.

Although the overall P62/SQSTM1 levels were not significantly altered in *GBA1*-PD, the number of P62/SQSTM1 puncta did rise significantly in this group after bafilomycin treatment, as in both of the other groups. There were no differences in autophagic flux, as determined by the difference between the number of P62/SQSTM1 puncta with bafilomycin treatment or vehicle control between any of the groups. It has been shown that most P62/SQSTM1 puncta represent autophagosomes or late endosomes (Bjørkøy et al. 2005). However, P62/SQSTM1 puncta may also represent sequestosomes – protein collections presumed to be targets for autophagic degradation, which accumulate under conditions in which autophagy is impaired (Klionsky et al. 2016). It would therefore be necessary to perform additional studies, for example visualisation of LC3b, to confirm that the increase in P62/SQSTM1 puncta witnessed with bafilomycin treatment does indeed represent preserved flux in the *GBA*-PD lines. This was attempted, but it was not

possible to visualise LC3b puncta in this project. Whilst the possibility that some P62/SQSTM1 puncta were sequestosomes remains, this data is most in keeping with the site of dysfunction being at the early steps of the autophagosome pathway, with *GBA1*-PD being associated with a failure in the initiation of autophagy.

Furthermore, when *GBA1*-PD lines were treated with the PI3K inhibitor wortmannin, there was a reduction in autophagic flux as evidenced by increased P62/SQSTM1 levels and increased P62/SQSTM1 puncta. In this instance, the puncta could clearly be seen to be relatively large in size, and to resemble sequestosomes. In contrast, there were no changes in these parameters in the other groups, suggesting that the *GBA1*-PD group were particularly susceptible to PI3K inhibition. In the healthy controls and iPD groups there was therefore sufficient reserve in the capacity for autophagy activation through PI3K-dependent or independent pathways, despite wortmannin treatment. In contrast, the *GBA1*-PD group were unable to compensate for this insult, suggesting that they are particularly dependent on the PI3K-mediated pathway for autophagy activation, perhaps due to dysfunction in other PI3K-independent autophagy activation pathways, which are active in the other groups. Alternatively, it may be that there is a pre-existing partial deficit in PI3K-mediated autophagosome formation, such that wortmannin treatment caused complete failure of this process in *GBA1*-PD.

Overall, this data suggests that the major problem with autophagy in *GBA1*-PD is most likely to be in the autophagosome formation stages of autophagy. A previous study using fibroblasts from many of the same cell lines used here was consistent with this idea. In contrast to healthy controls and iPD patients, in *GBA1*-PD patients there was no increase in autophagosome numbers (as determined by LC3b Western blot) after starvation, or with bafilomycin treatment (Collins et al. 2017). Drugs that are able to restore the process of autophagosome formation would therefore be of potential therapeutic interest in the subgroup of PD patients carrying G*BA1* mutations. Lysosome numbers were also increased in *GBA1*-PD cell lines compared to healthy controls and iPD patients. This could occur due to a block in autophagosome-lysosome fusion, but alternatively could reflect a compensatory increase in chaperone-mediated autophagy activity, to compensate for a defect in the macroautophagy pathway.

It must be acknowledged that these experiments were performed in patient fibroblasts, rather than iNs. When P62/SQSTM1 staining was performed in iNs, there were no differences between any of the disease groups at baseline. However, a similar observation was made in the fibroblasts, in which the differences in autophagy function only became apparent when inducing autophagy through starvation, or when inhibiting various stages of the pathway. When LC3b-II levels were quantified after starvation, they were non-significantly lower in iNs derived from *GBA1*-PD lines compared to healthy control and iPD lines, supporting the idea that initiation of autophagy is impaired in *GBA1*-PD. It would however, be useful for these experiments to be repeated in iNs with and without bafilomycin A1 and wortmannin treatment. Although the autophagy machinery behaves differently in different cell types (Menon, Kotlyarov and Gaestel 2011), the structures involved in autophagy are the same in fibroblasts as in neurons, and it is therefore reasonable to assume that the autophagy defect of *GBA1*-PD is present in neuronal cells also, although it is not known how the process of neuronal reprogramming itself affects the lysosome-autophagy pathway. During the reprogramming process, as the cell switches from one cell programme to another, there is likely to be an increase in protein and/or organelle turnover, which may result in altered lysosome-autophagy activity. Investigation of protein-clearance mechanisms in iNs may therefore be misleading, at least up to the point at which fibroblast properties have been fully eradicated, and a mature neuronal phenotype has been reached. Of course, the consequences of a dysfunctional lysosome-autophagy system will differ in relatively short-lived fibroblasts, to those in post-mitotic neurons in which there is the potential for abnormal protein aggregation. iNs were therefore employed to set up a model in which the potential consequences of neuronal autophagy dysfunction on protein aggregation could be investigated, with a view to using this for drug-screening. This model is discussed in section 4.5.3.

4.5.2 Mitochondrial dysfunction in *GBA1* mutation-associated Parkinson's disease

Mitochondrial dysfunction is thought to be important in PD pathogenesis, due to the facts that several of the hereditary forms of PD occur due to mutations in genes involved in mitochondrial health, and that mitochondrial toxins such as MPTP and rotenone can produce PD-like pathology in some models (Testa et al. 2005, Schapira 2008). The

lysosome-autophagy system is important in the turnover and removal of dysfunctional mitochondria, through the specific process of mitophagy (Geisler et al. 2010). *GBA1* mutation-associated autophagy dysfunction could therefore potentially allow for the persistence of abnormal mitochondria that would normally be removed, and mitophagy has indeed been shown to be impaired in the context of *GBA1* mutation (Li et al. 2018).

In this project, three parameters were used as indicators of mitochondrial health – mitochondrial superoxide production, mitochondrial membrane potential, and ATP production (with the latter only assessed in fibroblasts). However, no impairments in the *GBA1*-PD lines were detected in comparison to healthy controls or iPD patients at baseline. However, the sample size here was probably too limited to detect any small biological differences. Previous studies in which mitochondrial abnormalities have been detected in the context of *GBA1* abnormalities have largely involved enzyme suppression, or transgenic rodents or cell lines with severe mutations (Cleeter et al. 2013, Xu et al. 2014, Osellame et al. 2013). In contrast, the cell lines used in this project had mild mutations or variants, which may explain why no deficits in mitochondrial function were detected at baseline.

As is discussed in section 4.5.3, mitochondrial dysfunction was identified specifically in *GBA1*-PD following treatment with α-synuclein PFFs. It is possible that PFF-induced aggregates result in mitochondrial dysfunction through an undefined process, with persistence of these depolarised mitochondria in the *GBA1*-PD group in which autophagy is defective.

4.5.3 Treatment of induced neurons with α-synuclein pre-formed fibrils

iNs offer a novel model for the study of pathology in neurodegenerative diseases. As discussed in chapter 3, there are challenges in working with iNs, including limited long-term survival in culture. During the time-frame that iNs could be kept in culture in this study, no spontaneous formation of α-synuclein aggregates was observed. Other culture systems have required the introduction of a significant insult in order for α-synuclein aggregates to develop, such as overexpression of aggregate-prone mutant α-synuclein, or

inhibition of the ubiquitin-proteasome system (Rideout et al. 2001, El-Agnaf et al. 1998). Any manipulation of the system takes the model further away from the *in vivo* processes involved in pathogenesis in patients, so it is desirable to minimise such insults as much as possible. In this study, treatment with a single dose of α-synuclein PFFs were used to seed pathology in the recipient cell (Figure 4.28). PFFs have been used in other systems to result in aggregation of endogenous α-synuclein (Luk et al. 2009, Volpicelli-Daley et al. 2011). Whilst this acute dose of PFFs is not representative of the pathogenic processes occurring in patients, it allows for the generation of α-synuclein pathology *in vitro*, consisting of native endogenous α-synuclein without manipulation of other intracellular biochemical pathways.

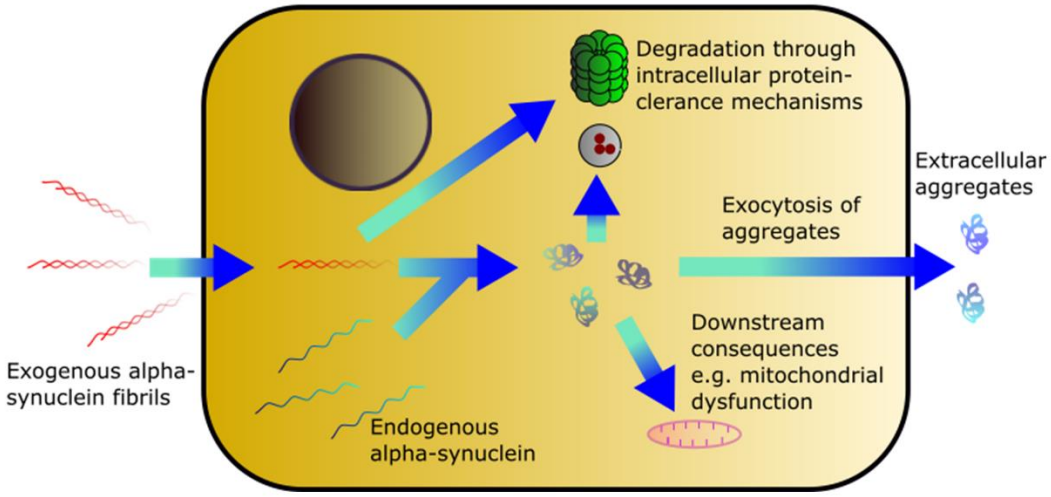

Figure 4.28 – PFF-induced α-synuclein aggregation in iNs. Treatment of iNs with α-synuclein PFFs results in accumulation of extracellular aggregates, with smaller numbers of intracellular aggregates observed. It is presumed that PFFs seed aggregation of endogenous α-synuclein, and that the cell is able to clear the majority of these through exocytosis.

The PFF-induced aggregates observed in this iN model were predominantly found extracellularly, situated adjacent to cells, with small numbers of intracellular aggregates observed. It was first important therefore to exclude the possibility that the observed aggregates in fact represented persisting PFFs. The observations that the aggregates were situated adjacent to cells, and not found in acellular regions within the well suggested that they were arising from the cells. Additionally, PFFs did not adhere to the culture matrix,

and fluorescent-tagged PFFs were cleared within a few days. These findings were in keeping with the hypothesis the α-synuclein content in the PFF-induced aggregates consisted of endogenous α-synuclein arising from the cells. This was supported by that fact that PFFs did not result in aggregates in fibroblasts (in which α-synuclein is not expressed), and confirmed through the transgenic expression of α-synuclein in fibroblasts, following which similar aggregates to those seen in iNs could be induced through PFF treatment.

The nature by which the aggregates form remains unclear. It is possible that PFFs are taken up into the iNs, serving as a seed for aggregation of endogenous α-synuclein. A proportion of these aggregates may then be released by exocytosis, resulting in the accumulation of extracellular aggregates. The release of α-synuclein aggregates in the context of *GBA1* dysfunction has been described in other *in vitro* models (Bae et al. 2014, Papadopoulos et al. 2018). The alternative possibility is that iNs release endogenous α-synuclein into the culture medium, and PFFs lead to formation of the aggregates outside the cell. The latter explanation seems less likely given that:

i. Aggregates are only observed adjacent to cells, and not in empty areas of the well. Whilst α-synuclein concentration in the medium may be greatest in the vicinity of cells, one would expect to see aggregates in all areas of the well if they were formed from extracellular α-synuclein
ii. Some aggregates are observed intracellularly
iii. There are downstream consequences of PFF treatment in intracellular processes (including a reduction in mitochondrial membrane potential and elevation of caspase activity).

The PFF-induced aggregates do not resemble the Lewy bodies seen in patients with PD, but they potentially serve as a surrogate marker for the way in which the patient-derived iNs cope with α-synuclein aggregation. Additionally, the downstream consequences of PFF-induced aggregation can provide information about the vulnerability of a particular cell line to α-synuclein pathology. It has been argued that the progressive nature of PD occurs due to transmission of pathology between cells in a prion-like fashion, and the presence of the PFF-induced extracellular aggregates could relate to the degree to which

pathology would spread between cells in a particular cell line (Bae et al. 2014, Angot et al. 2010). As such, a reduction in the number of external aggregates would be a useful outcome measure when testing putative disease-modifying treatments. This is speculative however, and it should be acknowledged that transfer of medium from PFF-treated cells did not result in propagation of pathology (although it would be desirable to have purified the aggregates before attempting propagation, so that adequate concentrations could be used).

The burden of PFF-induced aggregates was consistently higher in PD lines when compared to healthy controls, occurring in greater numbers and with lower concentrations of PFFs. This could mean that they are inherently more prone to the development of α-synuclein aggregation, but the formation of these PFF-induced structures is dependent on a range of factors which will be discussed here. It is possible that variation in any of these factors could account for differences in the number of PFF-induced aggregates between cell lines.

4.5.3.1 Factors relating to α-synuclein pre-formed fibril administration

The extent of PFF aggregate accumulation in part depends on technical factors. These factors are consistent for all cell lines, so do not account for differences in the burden of aggregates between different groups. It is important to consider however, the timing of administration and duration of culture following administration of PFFs. At the early stages of conversion, only a limited number of cells will have progressed in their reprogramming to the point that α-synuclein is expressed at sufficiently high levels for PFFs to seed pathology. Application of PFFs at an early stage therefore results in only low levels of aggregate formation. Another requirement for the generation of aggregates is allowing sufficient time for endogenous α-synuclein to aggregate. Given that analyses in this system were generally performed between day 25 and 30 due to poor survival at later time points, application of PFFs at too late a stage will limit the time that cells can be cultured following PFF exposure, and therefore limit the formation of these aggregates.

The optimum time point of PFF administration is therefore a balance such that it is late enough for α-synuclein to be expressed at sufficient levels, and early enough to allow culture to continue for a sufficient duration. On testing different time points of administration, day 17 yielded the greatest number of aggregates, whilst administration at day 10 resulted in larger aggregates. Administration at day 22, which only allowed for five days of further culture reduced the number of aggregates that formed in comparison to early time points. Therefore, the optimal time for PFF administration is between day 10 and day 17 in this system.

4.5.3.2 Cell-related factors

The significant variation that is observed in the number of aggregates between different lines could be due to a number of intrinsic factors related to the cell. Firstly, uptake of PFFs into the cell is likely to vary between different cell lines, which would influence the seeding effect, and the number of aggregates that form. Perhaps the most important variable in determining the number of aggregates is the ability of the particular cell line to reprogram, and to induce α-synuclein expression. Cell lines in which reprogramming is more effective will have greater levels of endogenous α-synuclein, and therefore a greater potential for aggregate development. In contrast, cell lines which reprogram poorly will have more limited expression of endogenous α-synuclein, and a lower capacity to generate aggregates. It is also possible that variations in the splicing of α-synuclein or polymorphisms in the *SNCA* gene alter the propensity for aggregate formation between different cell-lines (Beyer 2006).

Additionally, the activity of intracellular protein clearance mechanisms including the ubiquitin-proteasome and lysosome-autophagy systems is important. The rate by which cells clear PFFs, PFF-induced aggregates and any potential intermediate structures will influence the degree to which aggregates are able to accumulate. It is feasible that the trend towards higher PFF-induced aggregate counts in *GBA1*-PD is due to the fact that autophagy is impaired in these lines, but there are clearly several confounders. Even the *GBA1*-PD lines were able to initiate autophagy in response to PFF-treatment as evidenced by an increase in LC3b-II levels, though this response appeared diminished in comparison to the iPD group in which a decline in P62/SQSMT1 levels were also detected. The

relationship between PFF treatment and the lysosome-autophagy system is complex. The observed increase in LC3-II and reduction in P62/SQSTM1 levels imply that PFF treatment leads to activation of macroautophagy. It should be noted that these experiments were performed at an early stage following PFF-exposure, at a point when PFF-induced aggregates are not seen in high numbers. It is therefore likely that the autophagy response observed was against the PFFs themselves, potentially being important in their clearance. It has also been noted that PFF-induced aggregates in cell models impair autophagosome-lysosome-fusion, and that the aggregates are resistant to degradation through autophagy (Tanik et al. 2013, Redmann et al. 2017). There seems therefore to be a picture in which the autophagy system is important in the clearance of exogenous PFFs, but that the proteasome is more important in the clearance of the PFF-induced endogenous α-synuclein aggregates, which themselves impair function of the autophagy system. The apparent increase in vulnerability of *GBA1*-cell lines to PFF treatment could therefore either be due to a reduction in clearance of PFFs, or due to an aggregate-induced insult to an already impaired lysosome-autophagy system.

Given these variables, it is not possible to say what the significance of a high number of aggregates is. Paradoxically, healthy cell lines which may be more likely to reprogram well may have higher levels of endogenous α-synuclein, and may therefore actually manifest a higher number of the aggregates. The relative degree to which each of these influences the accumulation of aggregates is not clear, and this is an area for further characterisation in the future. Having said this, the number of PFF-induced aggregates can be a useful marker for the handling of α-synuclein when comparing different conditions within the same line – for example determining the ability of a drug to reduce the number of aggregates. This system was therefore used for drug-screening, which is discussed in the next chapter.

Technical Factors	Cell-Related Factors
- Concentration of PFFs - Timing of PFF exposure - Duration of culture post-PFF	- Uptake of PFFs - Endogenous α-synuclein levels - α-synuclein splicing pattern - Activity of intracellular protein-clearance mechanisms - Ability to secrete via exocytosis - Vulnerability to α-synuclein-induced dysfunction - Disease-related factors - Health of cells in culture

Table 4.2 – Variables contributing to burden of PFF-induced pathology in iN model.
Abbreviations: PFF = Pre-formed fibrils.

Furthermore, treatment with PFFs resulted in mitochondrial abnormalities in the *GBA1*-PD group, in the form of reduced mitochondrial membrane potential. The effect in iPD was less, with this group developing smaller declines in mitochondrial membrane potential, which generally failed to reach statistical significance. One could speculate that the PFF-induced aggregates (or an unseen intermediate) result in mitochondrial dysfunction, with abnormal mitochondria being cleared in healthy controls and iPD cell lines. With the autophagy, and presumably mitophagy, defect associated with *GBA1*-PD these unhealthy mitochondria may persist in the cell. Furthermore, there was an increase in caspase activity following PFF-treatment in the *GBA1*-PD group, with no change in the iPD group, supporting the fact that the *GBA1*-PD group are more susceptible to PFF-induced pathology than the iPD group. Whilst caspase activity was elevated in *GBA1*-PD after treatment with PFFs, this effect was not dose-dependent, with a smaller increase after exposure to the higher dose. This may be explained by increased prior cell death after exposure to the higher dose, and it would be useful to test this after exposing iNs to multiple intermediate doses of PFFs. iNs seemed to mount an autophagy response following PFF treatment, as evidenced by increased LC3b-II levels. This happened in *GBA1*-PD iNs as well as iPD iNs, suggesting that dysfunction of autophagy initiation does not fully explain the increased susceptibility of *GBA1*-PD iNs to PFF-treatment. It could be speculated that dysfunction of mitophagy specifically (of which there is evidence in *GBA1*-PD (Li et al. 2018)), accounts for the increased vulnerability to PFF-induced pathology in *GBA1*-PD, though this has not been investigated here.

The relationship between PFF-induced aggregates and mitochondrial function would be interesting to characterise further, for example through the determination of other mitochondrial parameters including ATP production and oxygen consumption, following PFF treatment. In particular, it would be interesting to see whether the PFF-induced aggregates themselves were pathological (which could be achieved by purifying these and applying them to the cells), or whether this was due to an alternative mechanism.

4.5.4 Concluding remarks

In this study, abnormalities in the function of the lysosome-autophagy system have been demonstrated in *GBA1*-PD fibroblasts, in keeping with previous evidence. In order to develop a drug-screening model using a relevant cell type, iNs were generated as described in chapter 3. Because no spontaneous α-synuclein aggregates were observed, a single dose of α-synuclein PFFs was used to induce aggregate formation, without interfering with biochemical pathways within the cells. This resulted in the formation of aggregates, and the development of relevant downstream pathology, which was much greater in the *GBA1*-PD group compared to healthy controls and iPD patients. These objective and reproducible outcome measures were used as the basis for drug-screening studies in *GBA1*-PD which are discussed in the next chapter.

5 *IN VITRO* DRUG TESTING FOR *GBA1* VARIANT-ASSOCIATED PARKINSON'S DISEASE

5.1 Abstract

There are currently no disease-modifying treatments for PD, with medical treatment focussing on the control of motor symptoms through restoration of striatal dopamine levels. The failure of promising pre-clinical results to translate to clinical benefit in trials is in part due to limitations of our existing experimental models, which rely on the use of transgenic animals or cell lines, or neurotoxins, which fail to mimic the pathogenic processes occurring in patients. In this study, patient-derived iNs have been used to provide a source of adult human neurons, which retain the age signature and genetic risk profile of the host. Four agents were tested for their ability to reduce pathology in this system. Of these, trehalose significantly reduced the burden of α-synuclein PFF-induced pathology in the *GBA1*-PD group, whilst nortriptyline produced similar results in the iPD group. These drugs are therefore of interest for further testing, and consideration of trialling in patients.

5.2 Introduction to chapter

There are currently no disease-modifying treatments for PD, with pharmaceutical treatment being limited to dopaminergic drugs which improve some of the motor symptoms without altering the course of disease or treating many of the non-motor manifestations. Discovery of novel putative disease-modifying treatments has been hindered by the lack of a truly representative model for PD. Animal models involve a significant insult (often acutely), such as overexpression of mutant *SNCA* or the use of

toxins, to yield a clinical phenotype or relevant pathology, which does not reflect the pathogenic mechanisms seen in patients, so even if an agent is shown to be beneficial in these systems, the ability to translate it to a clinical setting will remain uncertain (Beal 2001). As is discussed in chapter 3, iPS-derived neuronal *in vitro* models essentially represent embryonic neurons, so it is likely that the effect of a drug in these cells will differ to that in the cells affected in PD (aged neurons), so that these models may also have a limited ability to predict clinical utility of a drug (Horvath 2013, Lapasset et al. 2011, Prigione et al. 2011). As well as the development of novel agents, there is much recent interest in the repurposing of existing drugs for their possible use in neurodegenerative diseases, meaning that there are potentially large libraries of compounds that may be considered for trials. Given the expense associated with conducting clinical trials, an effective drug-screening model would be invaluable in prioritising the choice of drugs for entry into the clinical setting. Demonstration of efficacy in a number of model systems including *in vitro* and animal models is likely to be required for progression of a novel agent to clinical trials, but for existing drugs in which safety data is well established, efficacy in a representative *in vitro* system may be sufficient to proceed to clinical testing.

iNs theoretically offer a useful *in vitro* system for drug screening. iNs are patient-derived, so retain the intracellular environment associated with PD risk determined by as yet poorly understood polygenic risk factors, and also retain the effects of age (Mertens et al. 2015, Kim et al. 2018, Huh et al. 2016) . In doing so, the effect of a drug in an iN system, may more closely represent the effect that the drug will have in an aged neuron in a patient. iNs may therefore be more useful in predicting the utility of a drug than existing models are. The use of iNs for drug screening to date has however been limited to only a small number of studies (Liu et al. 2016b). In this project, iNs have been used to screen a number of agents for their ability to reduce pathology in *GBA1*-PD neurons.

5.3 Drug screening models for Parkinson's disease

Translation of promising experimental results to clinical trials in PD has been disappointing, with no disease modifying treatments identified (Stocchi and Olanow

2003, Elizan et al. 1989). This is in part due to the fact that existing disease models fail to truly reflect the pathogenic processes occurring in patients. Here, the main established models for drug screening in PD are discussed.

Transgenic or neurotoxin-based animal models are frequently used to investigate the potential neuroprotective effects of drugs in PD. Ideally, these animal models should possess a relevant phenotype (a slowly progressive motor disorder with non-motor features such as cognitive impairment), neurodegeneration of relevant brain regions, and relevant pathology in the form of α-synuclein inclusions. However, most published models fail to recapitulate at least one of these features, and reproducibility is often a problem. The use of MPTP in non-human primates is perhaps the most representative model for drug screening, in that animals develop the cardinal motor features of PD, in addition to non-motor features including constipation and cognitive impairment, associated with neurodegeneration at relevant sites (Varastet et al. 1994, Forno et al. 1986, Bergman, Wichmann and DeLong 1990, Kowall et al. 2000). However, Lewy body inclusions are not consistently observed, and the neurodegeneration occurs acutely, which is not representative of PD. Furthermore, the way in which a drug behaves and is metabolised in a non-human cell may be significantly different to the way in which it acts in a human cell, which may partly explain why clinical trials have so far been disappointing. The use of transgenic animals in which mutant, aggregation-prone forms of α-synuclein or supraphysiological levels of wild-type α-synuclein are expressed are limited by the fact that these insults fail to provide any insight into the upstream processes that lead to α-synuclein accumulation under physiological circumstances, and that they do not recapitulate the cardinal features of PD (Beal 2001).

While animal models will continue to play an important role in pre-clinical studies of putative treatments for PD, a human model would potentially more faithfully represent the ability of a drug to impact on relevant pathological pathways. Given the emerging interest in the potential for repurposing drugs, it is also important for a model to be scalable, to allow for large numbers of drugs to be easily tested, and prioritised for entry to clinical trials. Overexpression of wild-type or mutant α-synuclein in standard human cell lines, such as neuroblastoma cells, potentially allows for investigation of the effects of test drugs on α-synuclein homeostasis and aggregation (Bar-On et al. 2008). However,

an immortal cell line is inherently different to the post-mitotic neurons in which PD pathology occurs, so the relevance of findings in these models is questionable, when it comes to deciding which drugs are likely to herald a clinical benefit.

In order to more closely recapitulate the environment in which PD pathology occurs in patients, iPSC-derived neurons have also been employed (Cooper et al. 2012). This approach uses cells from PD patients, so retains the currently poorly defined polygenic risk profile associated with the development of PD. Additionally, it allows for the investigation of drugs in human post-mitotic, subtype-specific neurons, potentially providing a more relevant intracellular environment for the study of pathology and drug effects. However, as discussed in chapter 3, the neurons derived from iPSCs are embryonic, and given that embryonic neural cells do not develop PD pathology *in vivo*, these cells may miss important contributors to PD pathogenesis. Indeed, the induction of α-synuclein aggregates has not been possible without introducing additional insults, such as proteasome inhibition (Rideout et al. 2001).

A potential novel alternative system for screening drugs in human neurons is to use iNs. As well as retaining inherent genetic risk factors, iNs also retain the effects of ageing on intracellular processes such as mitochondrial function and protein-clearance mechanisms, so may have a greater value in terms of predicting the behaviour of a drug on protein aggregation and related pathology (Mertens et al. 2015, Kim et al. 2018, Huh et al. 2016). However, to date the use of iNs for drug screening has been limited to only a few studies, which are discussed in chapter 3, and the practicality of using iNs as a drug-screening model for PD has not been clearly established.

5.4 Overview of putative disease-modifying approaches in Parkinson's disease

For a drug to have a disease-modifying effect in PD, it will need to slow or stop the death of affected neurons in the substantia nigra, as well as the other sites of pathology such as the cortex. Given the importance of α-synuclein in PD pathology, most proposed disease-modifying approaches centre on reducing production or aggregation of α-synuclein,

enhancing clearance of α-synuclein, or limiting the consequences of α-synuclein aggregation on intracellular processes and pathways (Figure 5.1) (Brundin et al. 2017). In addition, there are subgroups of PD patients, for example *GBA1*-PD, in which a specific genetic abnormality may be targeted. Here, the existing experimental therapeutic approaches are introduced.

5.4.1 Approaches involving reduction of α-synuclein

The pathogenic potential of α-synuclein may be reduced at several levels:

i. Reduced synthesis of α-synuclein
ii. Reduced aggregation of α-synuclein
iii. Enhanced clearance of α-synuclein through intracellular pathways
iv. Removal of extracellular α-synuclein (Stoker et al. 2018b)

One approach to reducing α-synuclein synthesis is to inhibit transcription of the *SNCA* gene. α-synuclein expression is reduced by the β_2-adrenergic receptor agonist clenbuterol in neuroblastoma cells and rat cortical neurons, and the use of such agonists has been associated with a reduced risk of PD in a large epidemiological study (Mittal et al. 2017). α-synuclein production may also be targeted at the level of translation, through RNA interference technologies, using synthetic RNA molecules to trigger degradation of the *SNCA* mRNA. Lentiviral delivery of a shRNA targeting α-synuclein suppressed α-synuclein expression in neuroblastoma cells and in a rodent model (Sapru et al. 2006), while infusion of a short-interfering RNA (siRNA) reduced α-synuclein levels in mice and non-human primates (Lewis et al. 2008, McCormack et al. 2010). It should be noted that the normal function of α-synuclein is not known, and there are concerns about the potential effects of loss of the physiological function of α-synuclein, with some studies reporting significant neurotoxicity when α-synuclein expression is suppressed (Gorbatyuk et al. 2010, Robertson et al. 2004, Kanaan and Manfredsson 2012).

The clearance of α-synuclein may potentially occur through intracellular or extracellular mechanisms. A number of α-synuclein immunotherapies have entered clinical trials, which are designed to reduce extracellular α-synuclein and hence prevent propagation of pathology – these treatments are not discussed in detail here, given that they are not suitable for trialling in the iN model (Stoker et al. 2018b). Drugs that enhance macroautophagy, chaperone-mediated autophagy or proteasome activity (pathways all known to be involved in α-synuclein clearance (Webb et al. 2003)) would potentially reduce baseline levels of α-synuclein within the cell. In particular, in groups such as *GBA1*-PD in which there is an inherent autophagy deficit, targeting the lysosome-autophagy system may offer the optimal approach to reducing α-synuclein pathology. Indeed, some chaperone molecules which facilitate the transfer of GCase to the lysosome, and hence restore GCase enzyme activity have entered clinical trials (Bendikov-Bar et al. 2013, McNeill et al. 2014, Stoker et al. 2018b).

5.4.2 Other putative disease-modifying approaches

Other experimental treatments in PD have involved delivery of genes or molecules thought to be protective. For example, GDNF and its naturally occurring analogue, neurturin, have been found to enhance survival of dopaminergic neurons in animal models of PD (Eslamboli et al. 2005, Gash et al. 1996, Gasmi et al. 2007, Kordower et al. 2006). However, clinical trials have yielded disappointing results so far (Marks et al. 2010, Whone et al. 2019).

Because mitochondrial dysfunction has been implicated in PD, mitochondrial oxidant stress has also been considered as a target for treatment in PD. Results have however, been inconsistent with no clear benefit demonstrated. Co-enzyme Q_{10} (an antioxidant molecule) was reported to reduce accumulation of disability in a small study (Shults et al. 2002), though this could not be reproduced in other trials (Storch et al. 2007). Similarly, the antioxidants mitoquinone (a compound designed to enhance delivery of ubiquinone (the active element of Co-enzyme Q_{10}) to mitochondria) and tocopherol failed to show any clinical benefit (Snow et al. 2010, Parkinson_Study_Group 1993).

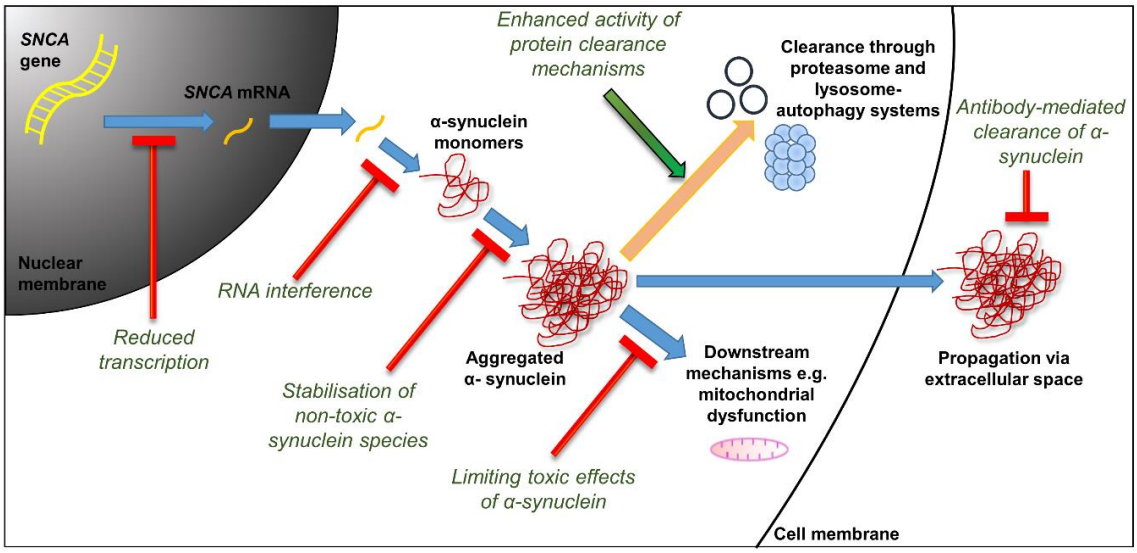

Figure 5.1 – Experimental disease-modifying strategies for PD. Adapted from (Stoker et al. 2018b)

5.4.3 Introduction to drugs investigated in the induced neuron model

It is likely that the PD population consists of subgroups of patients in whom different pathogenic mechanisms predominate. As such, the optimal disease-modifying approach may differ in different groups, and as disease-modifying treatments emerge, precision medicine may mean that patients receive tailored treatment regimes in which the predominant pathogenic mechanisms are targeted. The use of iNs, in which the hosts genetic susceptibility factors are retained, allows for the investigation of, and targeting of the most relevant pathogenic processes in individual patients or specific groups of patients. Here, iNs have been used to screen drugs for their ability to reduce pathology in *GBA1*-PD. Since *GBA1*-PD pathology has been consistently shown to involve lysosome-autophagy dysfunction, drugs potentially augmenting autophagy have been selected. Additionally, because mitochondrial dysfunction was evident in the PFF-model in *GBA1*-PD iNs, drugs with putative effects on mitochondrial health have also been tested in this model.

5.4.3.1 Drugs targeting the lysosome-autophagy system

In this project, trehalose and nortriptyline have been tested in the iN model, both of which have been shown to increase autophagy activity in experimental models. Trehalose is a naturally occurring non-mammalian disaccharide which plays an important role against cellular stresses, such as temperature aberrations, oxidation and dehydration, which has in particular been characterised in yeast (Kandror et al. 2004, Chen and Haddad 2004). Trehalose reduces *in vitro* formation of amyloid from bovine insulin (Arora, Ha and Park 2004) and aggregation of amyloid-β (Liu et al. 2005), prompting interest as a putative therapeutic agent for neurodegenerative disorders associated with protein aggregation. Similarly, trehalose reduced the aggregation of aggregation-prone tau (with the fronto-temporal dementia with Parkinsonism-associated with chromosome 17 (FTDP-17) mutation ΔK280) (Krüger et al. 2012). In these *in vitro* studies it was suggested that trehalose was able to reduce aggregation by stabilisation of hydrophilic groups on the protein, allowing for the normal structure to be maintained (Arora et al. 2004).

In another study of neuroblastoma cells expressing huntingtin with 60 or 150 polyglutamine tracts, trehalose led to a dose-dependent reduction in huntingtin aggregate formation, and increase in cell viability (Tanaka et al. 2004). The authors suggested that the mechanism of action was the binding of trehalose to the expanded polyglutamine repeats, stabilising the partially unfolded protein. Trehalose also reduces the aggregation of poly-A-binding nuclear protein-1 (*PABPN1*) – another protein containing an abnormal trinucleotide repeat (Davies, Sarkar and Rubinsztein 2006).

These studies all provided some evidence that trehalose directly reduces the aggregation of proteins. However, in addition to reducing the formation of aggregates, trehalose has also been shown to increase their clearance through activation of autophagy, and it is possible that it acts through multiple mechanisms (Table 5.1). In Cos-7 cells expressing huntingtin with a 74 polyglutamine repeat, trehalose reduced the burden of huntingtin aggregates – an effect that was abrogated by concomitant treatment with the autophagy inhibitor three-methyladenine (3-MA). The therapeutic role of autophagy was supported by the fact that trehalose could not induce clearance of aggregates in autophagy incompetent murine fibroblasts. Trehalose also increased autophagosome formation as demonstrated by increased LC3b-II levels and puncta in a number of cell types, including primary cortical neurons (Krüger et al. 2012, Sarkar et al. 2007). mTOR activity was not

affected by trehalose treatment, suggesting that trehalose activated autophagy in an mTOR-independent manner (Sarkar et al. 2007). Trehalose has also been shown to increase autophagy *in vivo*, using a PD mouse model, in which decreased P62/SQSTM1 levels were detected after 2.5 months of treatment, along with increased LC3b-II levels indicative of increased autophagosome numbers (Rodríguez-Navarro et al. 2010). Increased LC3b-II levels have also been seen in primary mouse cortical neurons after treatment with trehalose, with this effect increasing with time over 14 days of treatment (Redmann et al. 2017). However, in this latter study in which α-synuclein PFFs were used to induce formation of phosphorylated α-synuclein aggregates in primary cortical neurons trehalose did not alter the number of aggregates that accumulated (Redmann et al. 2017).

Clinical benefits have also been noted with trehalose treatment in animal models of neurodegenerative diseases. Trehalose led to preserved strength in transgenic mice expressing mutant *PABPN1* in a model of oculopharyngeal muscular dystrophy (Davies et al. 2006). It has also been shown to reduce weight loss and improve motor function in the R6/2 model of Huntington's disease, as well as pathology including striatal atrophy and intranuclear protein inclusions (Tanaka et al. 2004). Motor function was also improved, and loss of TH-positive neurons prevented with trehalose in transgenic and neurotoxin rodent models of PD (Rodríguez-Navarro et al. 2010, Sarkar et al. 2014). Striatal dopaminergic neurons and dopamine metabolites were also increased by treatment in this model, suggesting a neuroprotective effect for trehalose.

Study	Protein	Model	Effect of trehalose
Arora et al. 2004	Insulin	*In vitro* purified protein aggregation	Reduced aggregation
Liu et al. 2005	Amyloid-β	*In vitro* purified protein aggregation	Reduced aggregation
Tanaka et al. 2004	Myoglobulin (35 polyQ repeat)	*In vitro* purified protein aggregation	Reduced aggregation
	Huntingtin (60 or 150 polyQ repeats	Neuroblastoma neuro2A cells	Reduced aggregation Increased cell viability
	Huntingtin (expanded polyQ repeat)	R6/2 transgenic mice	Reduced weight loss Reduced striatal atrophy Reduced intranuclear aggregates Improved motor function and survival
Davies et al. 2006	PolyA binding protein nuclear 1 (17 polyA repeat)	Cos7 cells	Reduced proportion of cells containing aggregates
		Transgenic mice	Improved motor performance Reduced intranuclear aggregates
Sarkar et al. 2007	Huntingtin (74 polyQ repeat)	Cos7 cells SK-N-SH cells	Reduced aggregate numbers Reduced cell death
		Inducible PC12 cells	Increased clearance of soluble and insoluble Huntingtin polyQ74 Reduced aggregate numbers
	α-synuclein (A53T and A30P)	Inducible PC12 cells	Increased clearance of mutant α-synuclein
Sarkar et al. 2014	N/A	MPTP-treated mice	Reduced loss of nigral and striatal dopaminergic neurons and terminals Reduced astroglial and microglial activation
Rodríguez-Navarro et al. 2010	Tau	Transgenic mice overexpressing human tau with double knock-out of parkin	Improved motor and cognitive performance Reduced levels of tau Reduced numbers of tau neuritic plaques Reduced astrogliosis Preservation of TH^+ neurons and fibres in midbrain and striatum (benefits only short-term in striatum)
Krüger et al. 2012	Tau	Primary rat cortical neurons	Reduced levels of tau
		Transgenic N2A cells with pro-aggregant tau	Reduced proportion of cells with tau aggregates Reduced cytotoxicity
		In vitro protein aggregation	Reduced aggregation
Redmann et al. 2017	α-synuclein	Primary mouse cortical neurons treated with α-synuclein PFFs	No change in number of aggregates

Table 5.1 – Effects of trehalose in studies of protein aggregation and neurodegenerative disease. Abbreviations: polyA = polyalanine, polyQ = polyglutamine.

Nortriptyline is a tricyclic antidepressant drug used predominantly to treat depression and neuropathic pain. It has been used in clinical practice since the 1960s and is commonly prescribed, meaning that its safety profile is well known. Several studies have shown nortriptyline and the tricyclic antidepressant drug amitriptyline (of which nortriptyline is the active metabolite) to increase autophagy activity. In neuronal and astrocytic cultures, amitriptyline was shown to increase autophagosome levels within 12 hours. The increased LC3b puncta were found to co-localise with acidic vesicles suggesting that the increase was due to activation of autophagy rather than a fusion block. The use of bafilomycin A1 had an additive effect, supporting the fact that amitriptyline was leading to increased autophagosome formation (Zschocke and Rein 2011). LC3b puncta have also been seen to increase in HeLa cells treated with nortriptyline (Rossi et al. 2009). Similar findings have been reported *in vivo*, after injection of amitriptyline into mice, where increases in beclin, and the autophagy-related protein atg12 were observed. However, it should be noted that atg12 is also known to promote apoptosis, and it is possible that activation of apoptotic pathways could account for this. Increased LC3b-II to LC3-I ratio was seen in the prefrontal cortex of mice injected with amitriptyline, suggesting that autophagosome numbers were increased (Gassen et al. 2014).

In another study, a high-throughput assay was developed, in which mycobacterial survival in macrophages was measured and used to test 2000 compounds from a bioactive library (Sundaramurthy et al. 2013). Autophagy is impaired by mycobacteria – an adaptation of the microorganisms that facilitates intracellular survival (Gutierrez et al. 2004). Three agents were found to reduce mycobacterial survival, one of which was nortriptyline. The reduction in mycobacterial survival was brought about by the ability of nortriptyline to overcome the arrest in phagosome maturation induced by mycobacteria. Nortriptyline resulted in increased delivery of mycobacteria into late endocytic compartments, increased autophagosome numbers, and a reduction in the number of surviving mycobacteria, which was reversed by the autophagy inhibitor 3-MA. Combined with the fact that fusion blocking agents (bafilomycin and chloroquine) led to a further increase in autophagosome numbers, this data supports the suggestion that nortriptyline is able to increase autophagy activity. It should be noted that the effective concentrations were higher than that achieved in the serum of patients currently treated with nortriptyline, so more potent preparations may be necessary for nortriptyline to be clinically useful with regard to interaction with autophagy and the treatment of PD.

Finally, it is also possible that nortriptyline could reduce α-synuclein pathology through other mechanisms. In a recent study involving numerous models, nortriptyline was found to reduce aggregation of α-synuclein, rather than increase its clearance. This included a dose-dependent delay in aggregation of recombinant α-synuclein, thought to be due to interaction with monomeric α-synuclein and prevention of the formation of high-molecular weight species. In neuroblastoma cells overexpressing mutant aggregation-prone α-synuclein, nortriptyline at a concentration of 3 μM led to a reduction in inclusions, without reducing overall protein levels. Aggregate numbers were also reduced in the brains of rats injected with α-synuclein PFFs, and neuronal survival was improved in the nigra of rats, and the retina of drosophila expressing mutant α-synuclein (Collier et al. 2017).

5.4.3.2 Drugs targeting mitochondrial function

Two drugs were investigated in the iN model, due to previous studies suggesting that they had beneficial effects on mitochondrial homeostasis – metformin and ghrelin.

Metformin (1,1-dimethylbiguanide hydrochloride) is a drug widely used in the treatment of diabetes mellitus type two. It has been shown to affect a number of intracellular pathways, and has been suggested to have beneficial effects on mitochondrial function, and has thus been considered to be of potential interest in targeting PD pathogenesis.

Clinical data regarding the effect of metformin on PD is very limited. In a retrospective cohort of patients with type two diabetes, it was found that sulphonylurea drugs increased the risk of PD, but concomitant treatment with metformin abrogated this risk, with the authors suggesting that metformin potentially played a protective role against the development of PD (Wahlqvist et al. 2012). In MPTP-treated mice, metformin has been found to have neuroprotective effects and improved motor performance (Lu et al. 2016, Patil et al. 2014). Similar findings have been reported in mice treated with 3,4-methylenedioxymethamphetamine (MDMA), in which metformin prevented loss of nigral and striatal TH-positive neurons and fibres (Porceddu et al. 2016).

Metformin has been found to correct mitochondrial abnormalities in *LRRK2* G2019S transgenic *Drosophila* (Ng et al. 2012), reduce oxidative stress in MPTP-treated mice (Patil et al. 2014), and reduce reactive oxygen species, and correct mitochondrial membrane potential in SH-SY5Y cells treated with MPP^+ (Lu et al. 2016). Additionally, metformin reduces levels of phosphorylated α-synuclein in SH-SY5Y cells overexpressing human α-synuclein, and in primary hippocampal neurons and normal mouse brain (Pérez-Revuelta et al. 2014).

Though the mechanisms through which metformin may act remain unclear, it is known to activate AMPK (Zhou et al. 2001, Lu et al. 2016), which results in changes to a number of intracellular processes with the aim of conserving and generating energy (Hardie 2004, Amato and Man 2011). As has been discussed in section 4.2.1.1 AMPK is also involved in the initiation of autophagy, directly or through inhibition of mTOR, and metformin has been shown to increase autophagy activity in MPTP-treated mice (Lu et al. 2016) and PC12 cells treated with rotenone (Hou et al. 2015). Metformin has also been reported to inhibit mitochondrial complex one, thereby causing a reduction in oxidative phosphorylation (El-Mir et al. 2000). Whilst a reduction in mitochondrial energy production may seem detrimental, it is possible that this action of metformin leads to a reduction in reactive oxygen species and subsequent oxidative stress. To summarise, metformin alters mitochondrial biology in a number of models, and has been reported to have beneficial effects on PD-relevant pathology. However, the mechanisms through which it acts remain poorly defined.

Ghrelin is a growth hormone secretagogue produced predominantly in the gastric mucosal cells, with its main biological function being to increase appetite (Stoyanova 2014). It exists in the plasma in acylated and de-acylated forms, and acts on the growth hormone secretagogue receptor one-a (GHSR1a), which is expressed abundantly in the substantia nigra (Jiang et al. 2008, Moon et al. 2009). The post-prandial ghrelin response has been reported to be altered in PD patients compared to healthy controls, prompting some interest that ghrelin may play a role in PD (Unger et al. 2011).

Several studies have found that ghrelin protects against loss of TH-positive neurons in the substantia nigra, and dopaminergic terminals in the striatum in mice treated with MPTP (Bayliss et al. 2016b, Andrews et al. 2009, Jiang et al. 2008, Moon et al. 2009). Similar results have been seen in a cell model, in which ghrelin prevented MPP^+ induced cell death (Dong et al. 2009). Additionally, ghrelin knock-out mice are more susceptible to MPTP-induced neurodegeneration than their wild-type counterparts (Andrews et al. 2009). Ghrelin treatment has also been associated with improved motor performance in MPTP-treated mice (Bayliss et al. 2016b, Moon et al. 2009).

Several potentially important mechanisms have been identified that may contribute to ghrelin's protective effect. Microglial activation is reduced by ghrelin in MPTP-treated mice (Bayliss et al. 2016a, Moon et al. 2009). Other studies have found ghrelin to reduce levels of the pro-apoptotic protein Bcl-2, and reduce caspase-3 activity indicating reduced levels of apoptosis, following MPTP treatment (Jiang et al. 2008, Dong et al. 2009). An important effect of ghrelin in these neurotoxin models is improvements in mitochondrial function. Mitochondrial numbers and functional capacity have been noted to be improved by ghrelin treatment, including in the substantia nigra of mice, possibly due to increased expression of the transcription factor nuclear respiratory factor 1 (Nrf1) which is known to be important in mitochondrial biogenesis (Andrews et al. 2008, Andrews et al. 2009). In cells treated with MPP^+, ghrelin led to restoration of mitochondrial membrane potential, and reduced reactive oxygen species production (Dong et al. 2009). These effects are dependent on the expression of the mitochondrial uncoupling protein UCP-2, which is known to be important in neuronal survival following MPTP treatment (Andrews et al. 2005, Andrews et al. 2008, Andrews et al. 2009). Similarly to metformin, ghrelin is known to activate AMPK (Andrews et al. 2008, Bayliss et al. 2016b, Andersson et al. 2004), which has been suggested to have an effect upstream of UCP-2 (Andrews et al. 2008).

The protective effects of ghrelin also appear to be dependent on GHSR1a, as they are diminished in transgenic animals deficient of this receptor, and when GHSR1a antagonists are employed (Andrews et al. 2008, Moon et al. 2009, Jiang et al. 2008). Another point of note is that acylated ghrelin is required to convey protection in MPTP-treated mice, with deacylated ghrelin being ineffective (Bayliss et al. 2016a).

Here, four drugs have been tested in the iN model of PFF-induced α-synuclein aggregation. Two of these, trehalose and nortriptyline, were selected for their previously reported ability to enhance autophagy and potentially enhance the clearance of PFFs and induced aggregates. Metformin and ghrelin where also selected for their beneficial effects on mitochondrial function, with the hypothesis that they would reduce the downstream consequences of PFF treatment.

5.5 Materials and methods

5.5.1 Immunocytochemistry

Immunocytochemistry was performed as described in section 4.3.1. Primary antibodies used were anti-P62/SQSTM1 (1:500; abcam 91526), anti-β3 tubulin mouse (1:1000; abcam 78078), anti-β3 tubulin rabbit (1:1000; abcam 18207), and anti-α-synuclein mouse (1:1000; BD biosciences 610787). High-throughput analysis using the Cellomics^{TM} XTI microscope was used to determine mean intensity and spot count data using the spot count and cell health profiling protocols. When assessing the effect of nortriptyline treatment on PFF-induced α-synuclein spot count, images were acquired manually using the Leica DMi8 epifluorescence platform microscope. Five images per condition were acquired, and spot analysis was performed using ImageJ software, with the mean value for the five fields used for statistical analysis.

5.5.2 Western blot analysis

Western blot analysis was performed as described in section 4.3.9

5.5.3 Treatments and Reagents

Trehalose (Sigma T0167) was dissolved directly into fibroblast or neuronal medium to give a working concentration as indicated below. Nortriptyline (Sigma N7261) was dissolved in ultrapure water to give a 10mM stock solution. Metformin hydrochloride (Sigma BP2227) was dissolved in ultrapure water to give a 200 mM stock solution. Recombinant human ghrelin (Tocris 1463) was dissolved in ultrapure water to give a 1 mM stock solution. Stock solutions of nortriptyline, metformin or ghrelin were diluted to the appropriate concentration in cell culture medium. All treatments were passed through a sterile 0.2 µm filter prior to application to cells. Bafilomycin A1 was prepared as described in section 4.3.1.

5.5.4 TMRE assay for mitochondrial membrane potential

TMRE assays were performed as described in section 4.3.4.

5.5.5 Lysotracker™ red DND-99 assay

Fibroblasts from *GBA1*-PD (n=3) and iPD (n=4) patients were passaged and plated at a density of 3000 cells per well in a 96-well plate (Ibidi).Cells were resuspended in medium containing no treatment, trehalose 25 mM or 100 mM, or notrtiptyline 0.5 µM or 2 µM prior to plating. The cells were incubated at $37^{O}C$ for four days. The plate was then washed with HBSS before 25 nM Lysotracker™ DND-99 and DAPI 1 µg/ml in HBSS with Ca^{2+} and Mg^{2+} was added and the cells incubated at $37^{O}C$ for 15 minutes. The cells were then fixed in 4 % paraformaldehyde for 15 minutes, and spot analysis was performed using the Cellomics™ XTI microscope.

5.5.6 Statistical analysis

Statistical analysis was performed as described in section 3.3.10

5.6 Results

5.6.1 Trehalose

5.6.1.1 Effect of trehalose on lysosome-autophagy system

To first investigate whether trehalose was able to increase autophagic activity in patient cells, fibroblasts were plated from healthy controls (n=2), and patients with *GBA1*-PD (n=3), and then treated with low dose (10 mM) and high dose (100 mM) trehalose for four days. In both groups, trehalose increased the P62/SQSTM1 spot count, though this only reached significance in the *GBA1*-PD group ($p=0.006$ for the 100 mM dose compared to vehicle control). The rise in spot count was largest in the healthy control group though this did not reach statistical significance, probably due to the smaller sample size (Figure 5.2). Surprisingly, P62/SQSTM1 intensity was significantly increased with trehalose treatment in both the healthy control ($p=0.026$ and $p=0.001$ for trehalose 10 mM and 100 mM compared to vehicle control respectively) and the *GBA1*-PD group ($p<0.0001$ for both trehalose 10 mM and 100 mM compared to vehicle control).

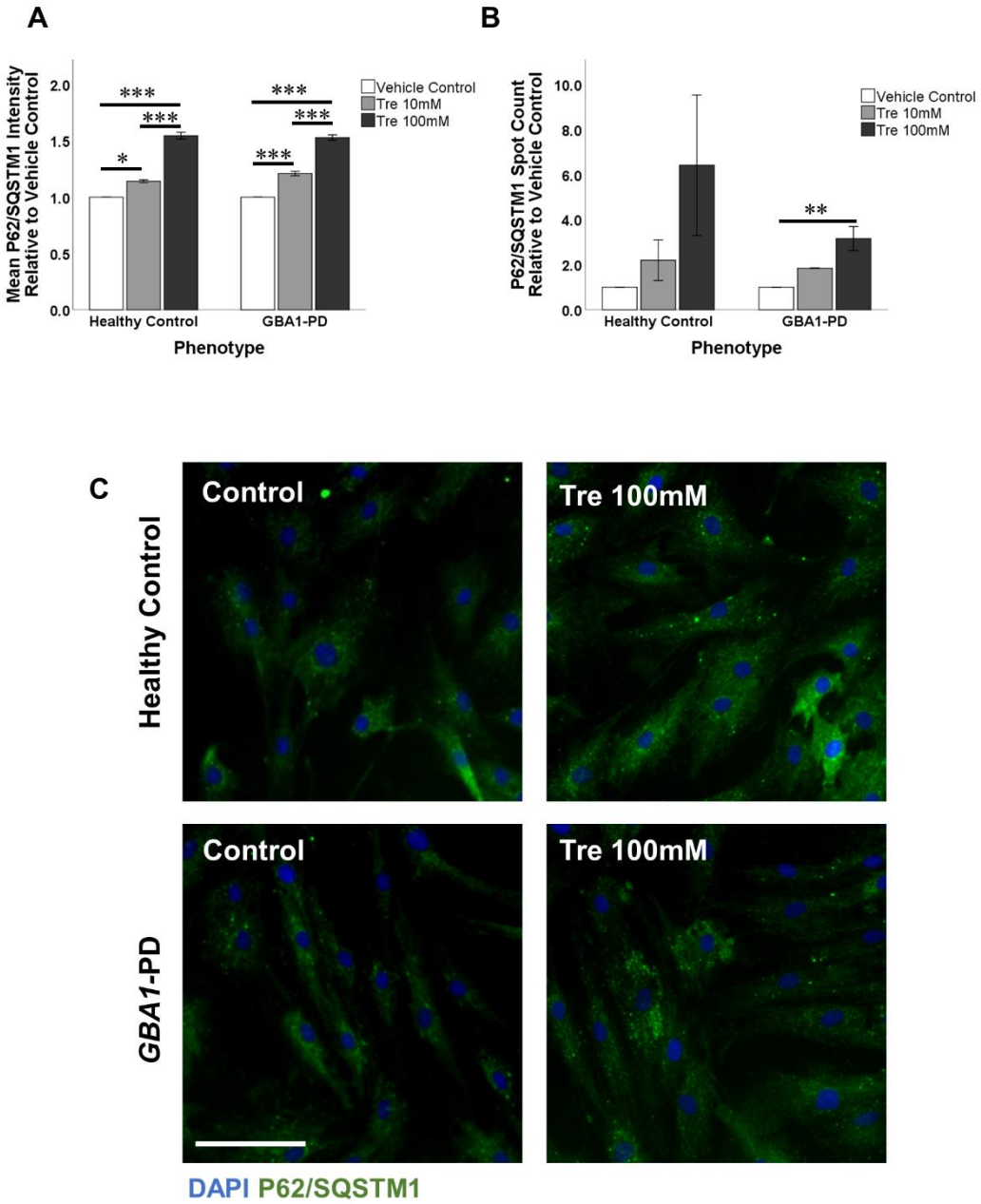

Figure 5.2 – P62/SQSTM1 immunocytochemistry in fibroblasts after treatment with trehalose. Fibroblasts from healthy controls (n=2) and patients with *GBA1*-PD (n=3) were treated with vehicle control, or low or high dose trehalose for four days. P62/SQSTM1 spot count (A) and intensity (B) increased with trehalose treatment. Error bars show standard error of mean. Statistically significant differences indicated by asterixes as determined by one-way ANOVA with post-hoc Tukey analysis. Scale bar represents 50 µm. Abbreviations: Tre = trehalose.

As has been discussed previously, the increase in P62/SQSTM1 spot count could represent an increase in autophagosome numbers, or an increase in sequestosomes due to

a block in autophagy. To investigate this further, fibroblasts were treated with vehicle control, trehalose 50 mM, bafilomycin A1 100 nM or both trehalose and bafilomycin A1. As expected, blockade of autophagy with bafilomycin A1 increased P62/SQSTM1 spot count in both healthy controls and *GBA1*-PD. Trehalose and bafilomycin had an additive effect, with a dramatic increase in the observed spot count, which was statistically significant in the *GBA1*-PD group (p=0.001). This suggests that the rise in P62/SQSTM1 spot count seen with trehalose was not due to a blockage in autophagy, but more likely due to an increase in autophagosome numbers. These changes were not statistically significant in the healthy control group, which is most likely due to the small sample sizes, but a clear trend was seen (Figure 5.3 and Figure 5.4).

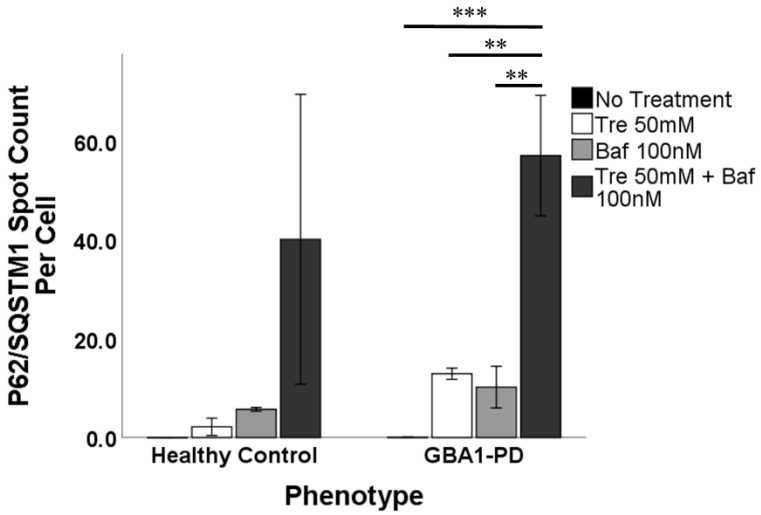

Figure 5.3 – P62/SQSTM1 spot count in fibroblasts after treatment with trehalose and bafilomycin A1. Fibroblasts from healthy controls (n=2) and patients with *GBA1*-PD (n=3) were treated with vehicle control, or trehalose 50 mM with or without bafilomycin A1 100 nM. As seen previously, P62/SQSTM1 spot count and total area per cell increased with trehalose treatment. The presence of bafilomycin A1 increased P62/SQSTM1 spot count further. Error bars show standard error of mean. Statistical significance indicated by asterixes as determined by one-way ANOVA with post-hoc Tukey analysis for each group. Abbreviations: Baf = bafilomycin A1; Tre = trehalose.

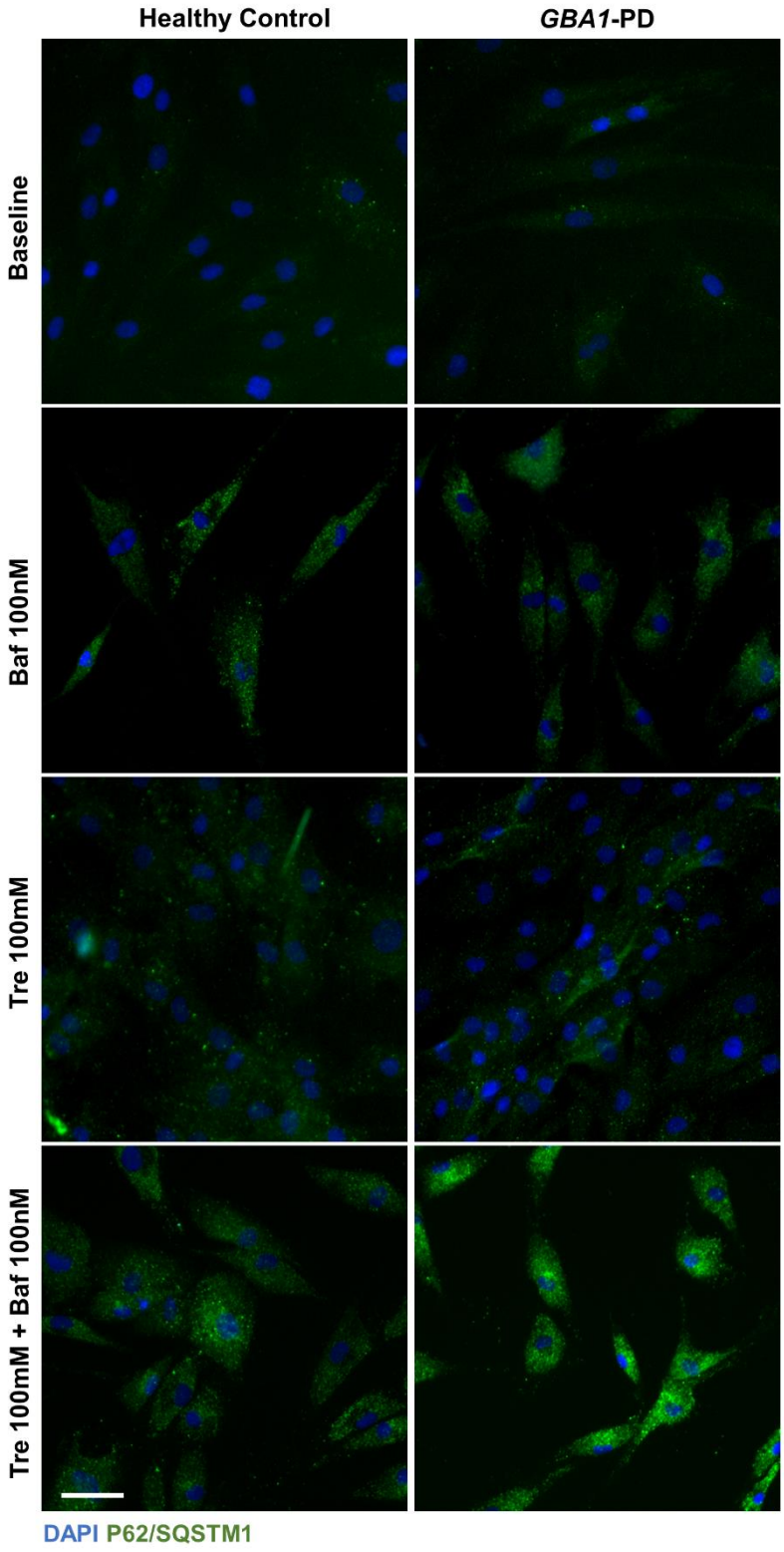

Figure 5.4 – P62/SQSTM1 immunocytochemistry in fibroblasts after treatment with trehalose and/or bafilomycin A1. Bafilomycin A1 and trehalose increased the number of small P62/SQSMT1 puncta. The use of both trehalose and bafilomycin A1 had an additive effect. Scale bar represents 50 µm. Abbreviations: Baf = bafilomycin A1; Tre = trehalose.

The effect of trehalose on P62/SQSTM1 levels was also assessed in iNs from healthy controls, and patients with iPD and *GBA1*-PD after treatment with trehalose 100 mM for 48 hours. The observed changes in P62/SQSTM1 were smaller than those previously seen in the fibroblasts (possibly due to the shorter duration of treatment). The P62/SQSTM1 intensity increased in all groups with trehalose, though this did not reach significance for any group.

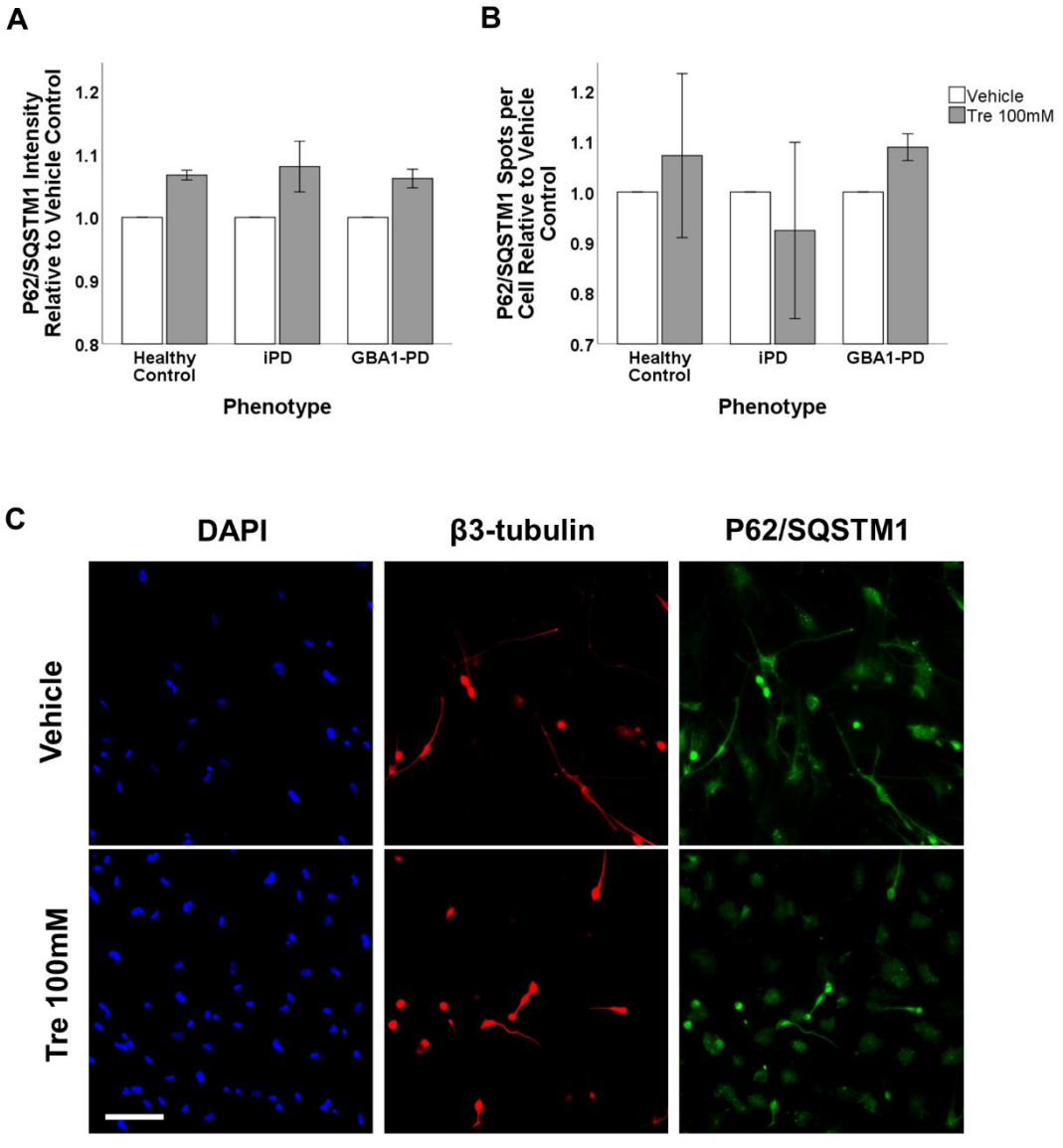

Figure 5.5 – P62/SQSTM1 immunocytochemistry in iNs following treatment with trehalose 100mM. iNs were generated from healthy control (n=2), iPD (n=2) and *GBA1*-PD (n=3) fibroblast lines. At day 27 trehalose 100 mM was added to the medium and the cells were cultured for a further 48 hours before fixation. Trehalose resulted in a non-

significant increase in P62/SQSTM1 intensity all groups. Bars represent mean values for iNs, defined as those cells expressing the neuronal marker β3-tubulin, with error bars representing the standard error of the mean. Scale bar represents 100 μm. Abbreviations: Tre = trehalose.

To confirm the finding of increased autophagosome numbers associated with trehalose treatment, western blotting was performed for the autophagosome marker LC3b, after treatment of fibroblasts with 25 mM or 100 mM trehalose, or vehicle control for four days (Figure 5.6). This was initially performed with a healthy control, as well as two iPD cell lines. There was an increase in LC3b-II (the autophagosome-associated form of LC3b) levels with trehalose 25 mM compared to vehicle control, with a further increase at the higher dose ($p=0.004$) (Figure 5.6). LC3b-I signal was too low to allow one to accurately determine LC3b-II:LC3b-I ratios. The increase in LC3b-II was seen in the healthy control as well as both iPD lines (Supplementary Figure 7.8). Western blot analysis for LC3b-II following trehalose treatment was subsequently performed on three *GBA1*-PD cell lines, which demonstrated a similar increase in LC3b-II:β-actin ratio ($p=0.018$) and LC3b-II:LC3b-I ratio ($p=0.002$) at the higher dose (Figure 5.6 and Supplementary Figure 7.9). Taken together with the finding that trehalose had an additive effect on the number of P62/SQSTM1 puncta with bafilomycin A1, these data suggest that trehlaose does indeed increase the formation of autophagosomes, including in the context of *GBA1*-PD.

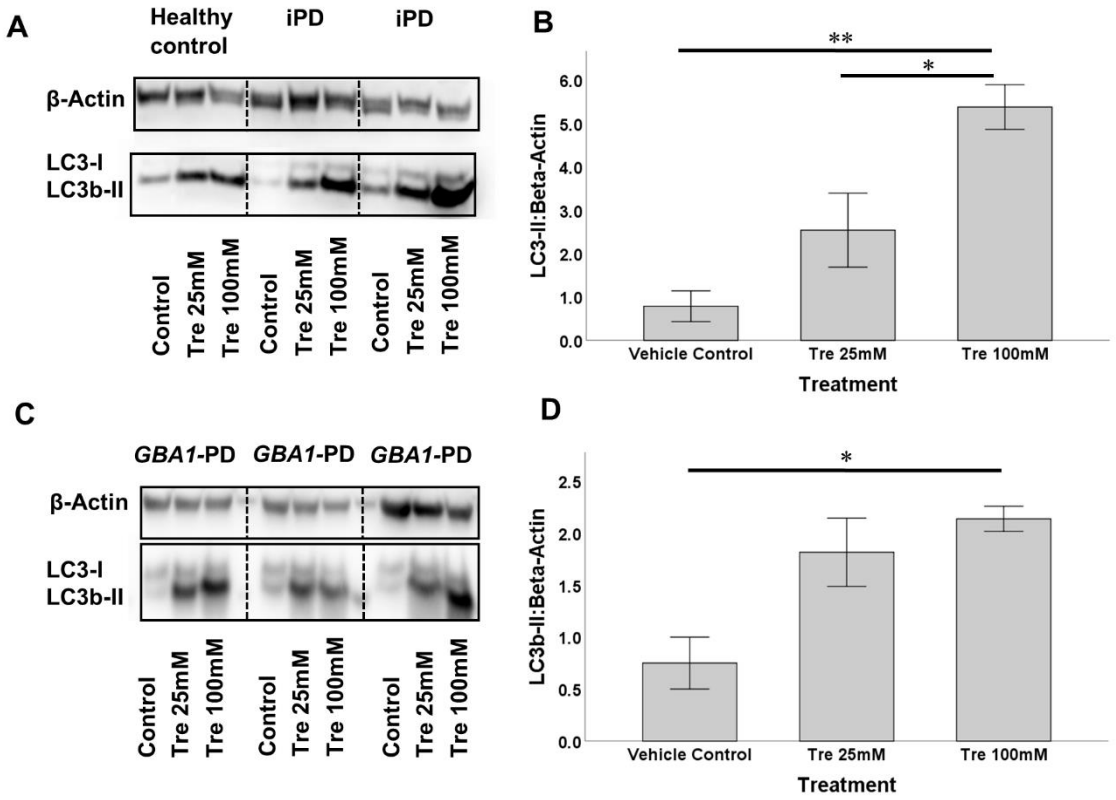

Figure 5.6 - LC3b Western blot following trehalose treatment in fibroblasts. Trehalose led to a dose-dependent increase in autophagosome numbers in fibroblasts from iPD and *GBA1*-PD patients. A) Western blot for LC3b on fibroblast lysate from a healthy control and two iPD cell lines treated with vehicle control, or trehalose 25 mM or 100 mM for four days. Quantification of this is shown in B), with bars representing the mean value for LC3b-II to β-actin ratio of all three lines. C) Western blot for LC3b on fibroblast lysate from three *GBA1*-PD cell lines treated with vehicle control, or trehalose 25 mM or 100 mM for six days. The mean LC3b-II to β-actin from all three lines is shown in D). Error bars represent standard error of the mean. Statistical significance indicated by asterixes as determined by one-way ANOVA with post-hoc Tukey analysis. Abbreviations: Tre = trehalose.

To further explore the impact of trehalose on the lysosome-autophagy system, lysosomal mass was quantified through staining of fibroblasts from patients with iPD (n=4) or *GBA1*-PD (n=3) with Lysotracker^{TM} DND-99 after treatment with vehicle control, or trehalose 25 mM or 100 mM for four days. Trehalose treatment was associated with a dose-dependent significant reduction in Lysotracker^{TM} spot count and area per cell in both

the iPD and *GBA1*-PD groups, which would be consistent with their increased clearance (Figure 5.7).

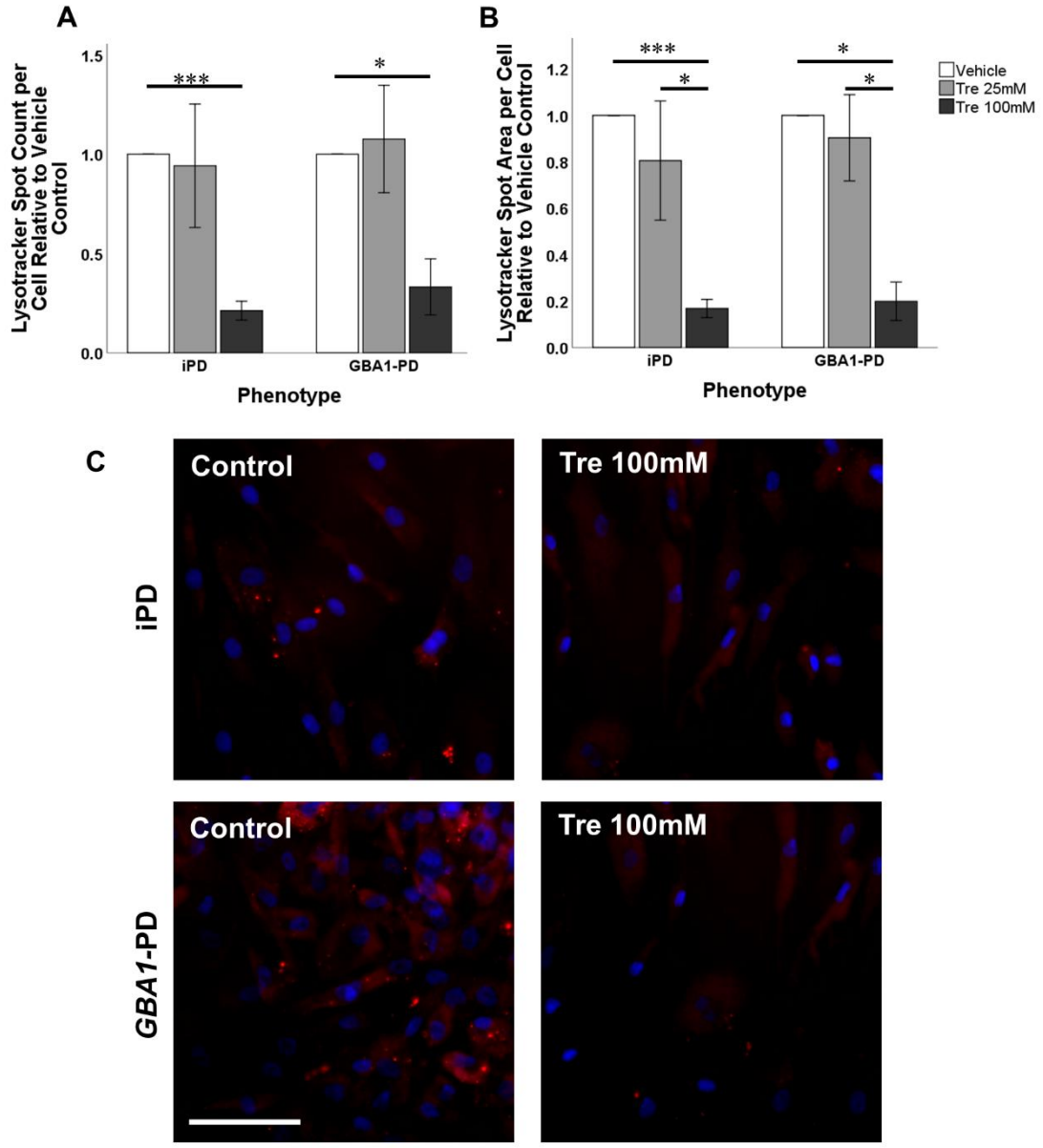

Figure 5.7 – Lysotracker™ DND-99 staining following trehalose treatment in fibroblasts. Trehalose reduced lysosomal mass in iPD and *GBA1*-PD fibroblasts. Lysotracker™ DND-99 spot count (A) and spot area (B) per cell after four days treatment with vehicle control, or trehalose 25 mM or 100 mM. Images for vehicle control and high-dose trehalose are shown in (C). Statistical significance indicated by asterixes as determined by independent-samples T tests. Error bars represent standard error of the mean. Scale bar represents 100 µm. Abbreviations: Tre = trehalose.

5.6.1.2 Ability of trehalose to impact on α-synuclein-induced pathology

As discussed above, trehalose significantly altered the function of the lysosome-autophagy system, with the aforementioned findings being most consistent with an increase in activation of autophagy. This was seen in *GBA1* mutation-carrying lines as well as wild-type *GBA1* lines, suggesting that its action on the autophagy system was not significantly altered by the underlying autophagy defect of *GBA1*-PD. In order to investigate whether these effects of trehalose could potentially benefit neuronal pathology, the impact on PFF-induced pathology in iNs was assessed.

iNs were generated from three *GBA1*-PD lines. At 15 days post-transduction trehalose or vehicle control, was added to the cell culture medium, to give final concentrations of 2.5 mM or 10 mM. Higher doses, such as those used over short durations in the fibroblasts, had a detrimental effect resulting in abnormal cell morphology, with swollen cell bodies, presumably due to osmotic forces, when used for longer periods (Supplementary Figure 7.10). Cells were treated with α-synuclein PFFs on day 17, and analysed at day 27 post-transduction.

Trehalose led to a dose-dependent reduction in PFF-induced α-synuclein aggregates per cell, which was statistically significant when normalised to the PFF only condition ($p=0.001$) (Figure 5.8 and Supplementary Figure 7.7). The total spot area per cell was also lower following trehalose treatment, though this was just short of statistical significance ($p=0.053$). Additionally, trehalose restored the mitochondrial membrane potential level following PFF treatment to that seen at baseline, in a dose-dependent fashion. However, trehalose alone resulted in a non-significant increase in mitochondrial membrane potential in the absence of PFF, so it is not clear whether the restoration of membrane potential following PFF treatment is specific to α-synuclein-induced pathology. Neither PFFs nor trehalose significantly altered neuronal purity (Figure 5.8).

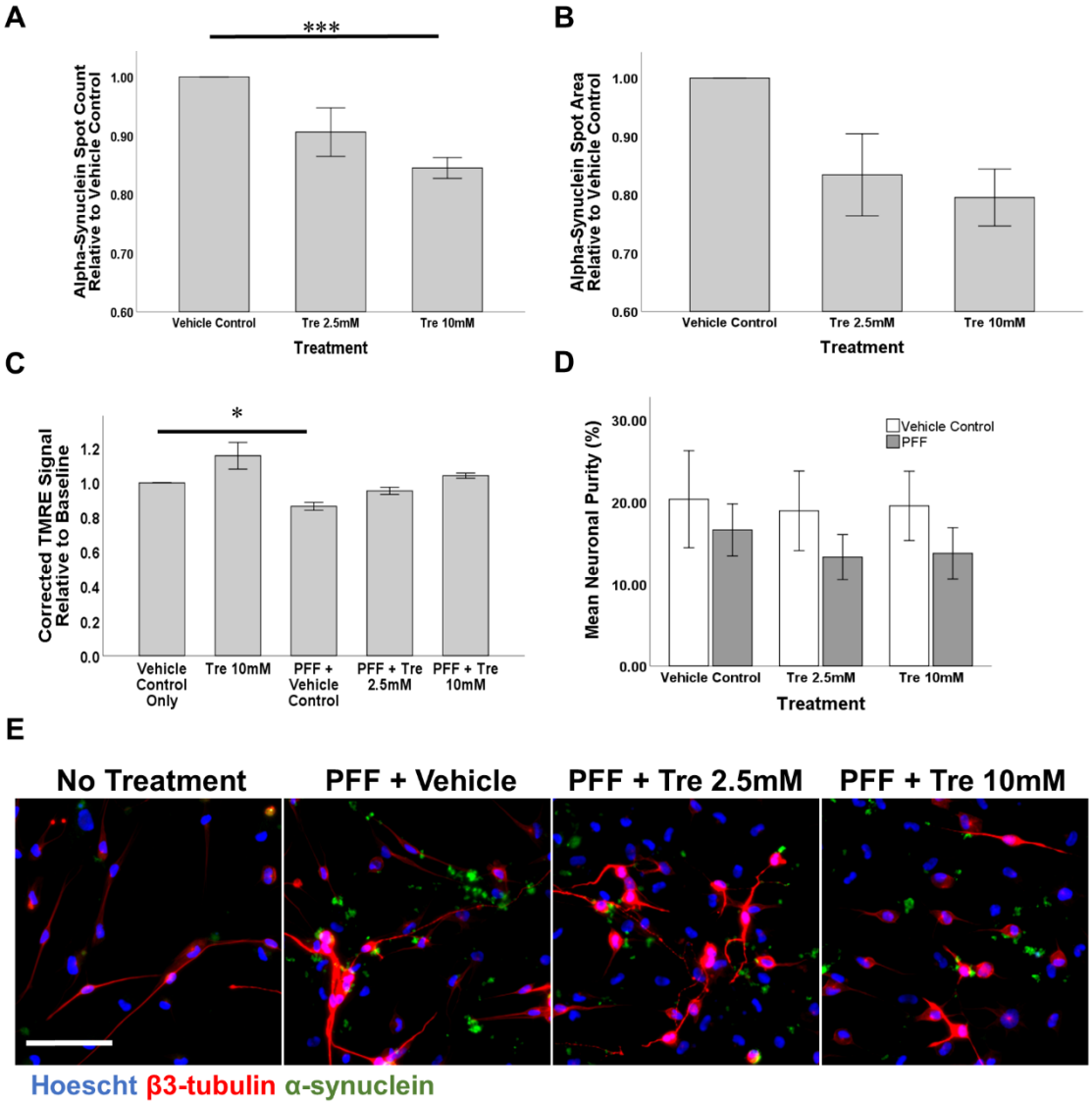

Figure 5.8 – Impact of trehalose on PFF-induced pathology in iNs of *GBA1*-PD patients. Trehalose treatment led to a reduction in the number (A) and total area (B) of PFF-induced α-synuclein aggregates per cell. C) Trehalose led to a restoration of mitochondrial membrane potential following PFF treatment. D) Neither trehalose nor PFFs had a significant impact on neuronal purity. E) Representative images of PFF-induced α-synuclein aggregates. Statistical significance determined by independent samples T tests is indicated by asterixes. Scale bar represents 100 µm. Abbreviations: PFF = pre-formed fibrils; Tre = trehalose.

In order to study whether trehalose could augment the autophagy response to PFFs in iNs, immunocytochemistry for P62/SQSTM1 was performed in iNs from three *GBA1*-PD patients following treatment with PFFs. As seen before, treatment with PFFs led to an increase in autophagy as evidenced by a small reduction in P62/SQSTM1 intensity

(p=0.028). Trehalose treatment led to a greater decline in P62/SQSTM1 intensity after treatment with PFFs suggesting that it was able to augment the autophagy response in this setting, though this only reached significance with the smaller dose (p=0.001). The decline in P62/SQSMT1 intensity brought on by PFF treatment was significantly greater in the trehalose 2.5 mM group compared to vehicle control (p=0.011), suggesting that the autophagy response to PFFs was enhanced by trehalose.

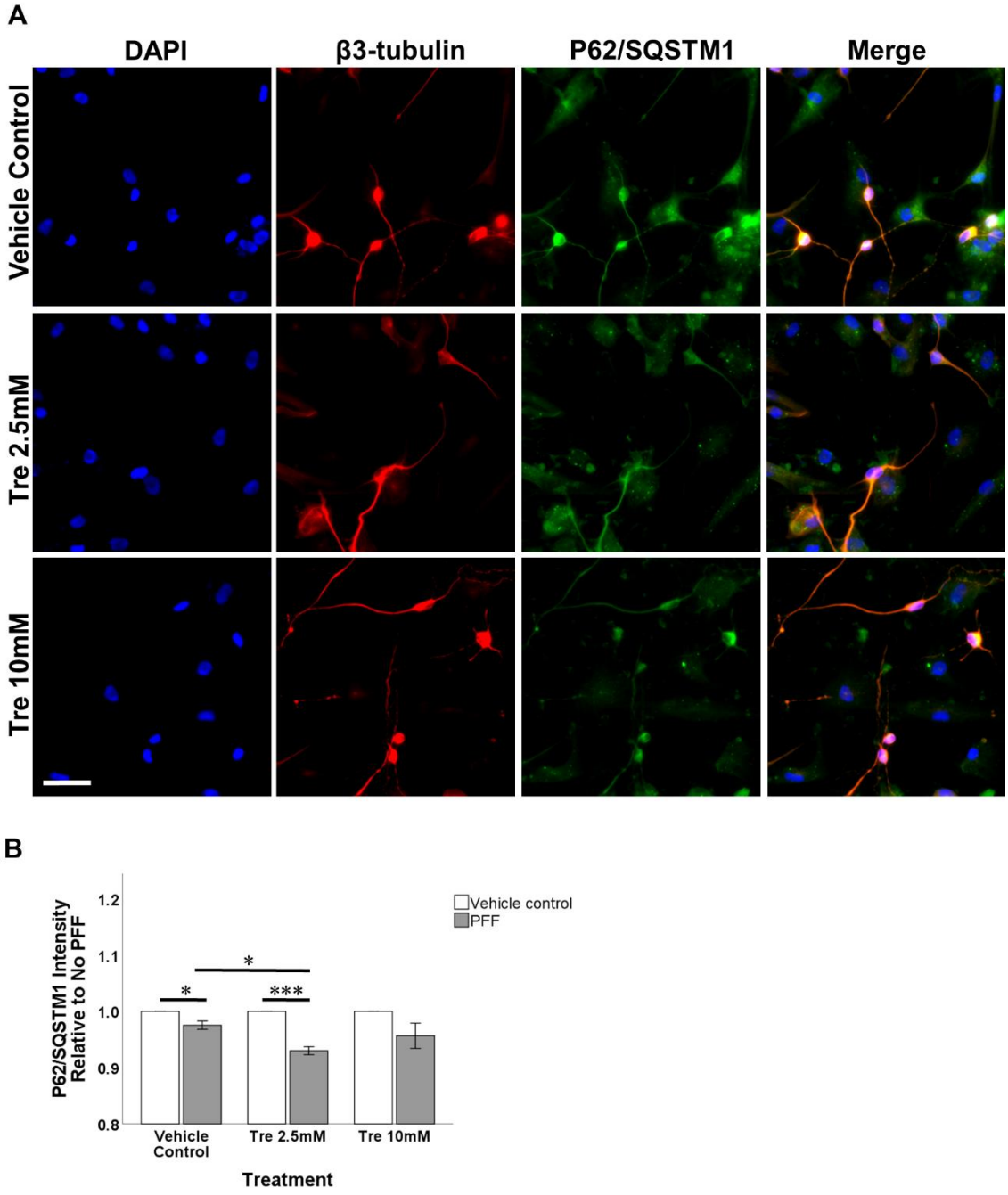

Figure 5.9 – Effect of trehalose on autophagy response to PFFs. iNs were generated from three *GBA1*-PD cell lines. At day 15 post-transduction vehicle control or trehalose 2.5 mM or 10 mM was added to the cells. At day 17, PFFs (0.5 ng/µl) were added, and the cells were cultured for a further seven days, before immunocytochemistry for P62/SQSTM1 was performed. Representative images shown in A) and quantification of P62/SQSTM1 intensity relative to the no PFF condition shown in B). Statistical significance determined by independent samples T tests indicated by asterixes. Scale bar represents 50 µm. Abbreviations: iN = induced neurons; PFF = pre-formed fibrils; Tre = trehalose.

5.6.2 Nortriptyline

5.6.2.1 The effects of nortriptyline on the lysosome-autophagy system

To first assess whether nortriptyline could affect the lysosome autophagy system, fibroblasts from two iPD cell lines were treated with vehicle control, or 2 µM or 5 µM nortriptyline for six days, and autophagosome numbers were quantified with LC3b Western blot (Figure 5.10). Nortriptyline treatment led to a dose dependent increase in LC3b-II, though this did not reach statistical significance, probably due to the low number of cell lines. This was repeated in fibroblasts from *GBA1*-PD cell lines (n=3), in which there was no increase in LC3b-II levels with nortriptyline treatment (Figure 5.10 and Supplementary Figure 7.11). It had been found that prolonged culture of iNs with doses of 5 µM or higher resulted in poor cell survival, so the lower maximum dose of 2 µM was employed for this repeat experiment with *GBA1*-PD lines.

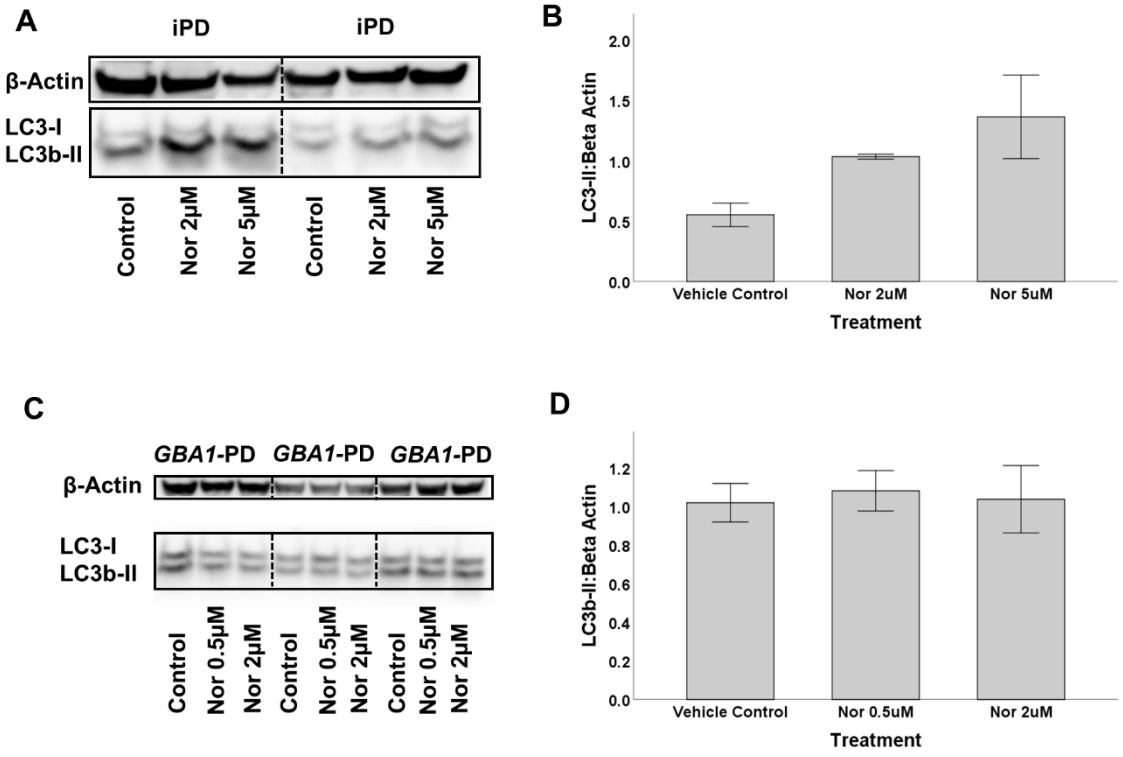

Figure 5.10 LC3b Western blot in iPD and *GBA1*-PD lines after treatment with nortriptyline. Nortriptyline increased autophagosome numbers in iPD, but not *GBA1*-PD fibroblasts. A) Western blot for LC3b on fibroblast lysate from two iPD cell lines

treated with vehicle control, or nortriptyline 2 µM or 5 µM for one week. Quantification of this is shown in B), with bars representing the mean value for LC3b-II to β-actin ratio of both lines. C) Western blot for LC3b on fibroblast lysate from three *GBA1*-PD cell lines treated with vehicle control, or nortriptyline 0.5 µM or 2 µM for one week. The mean LC3b-II to β-actin for these lines is shown in D). Error bars represent standard error of the mean. Abbreviations: Nor = nortriptyline.

The effect of nortriptyline in iNs was then assessed with immunostaining for P62/SQSTM1, after 48 hours treatment. Only cells that expressed β3-tubulin were included in the analysis. Nortriptyline resulted in a reduction in P62/SQSTM1 intensity in all groups to similar extents, suggesting an increase in autophagic flux, which reached significance in the *GBA1*-PD group ($p=0.021$).

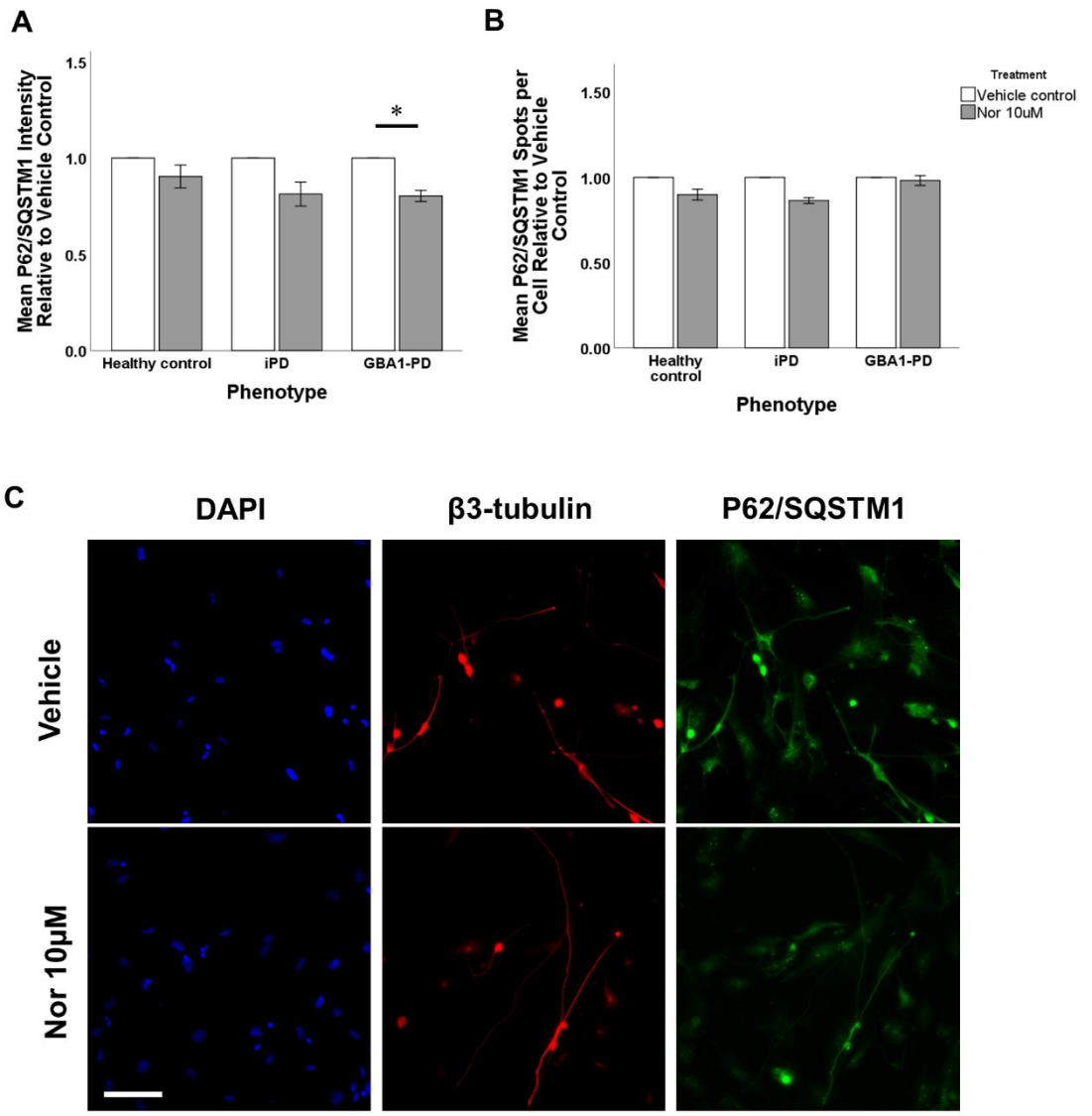

Figure 5.11. P62/SQSTM1 immunocytochemistry in iNs after treatment with nortriptyline. Fibroblasts from healthy control (n=2), iPD (n=2) and *GBA1*-PD (n=3)] individuals were reprogrammed to iNs. At day 27, iNs were treated with nortriptyline 10 µM or vehicle control for 48 hours, before immunocytochemistry for P62/SQSTM1 was performed. A) and B) P62/SQSTM1 levels were non-significantly reduced in iNs from all groups, which reached significance in the *GBA1*-PD group (p=0.021) (Only cells expressing β3-tubulin were included in the analysis). C) Images for *GBA1*-PD cell line at 20X magnification. Scale bar represents 100 µm. Asterix indicates statistical significance as determined by independent samples T tests. Abbreviations: Nor = nortriptyline.

In order to assess whether or not nortriptyline altered the lysosome count, fibroblasts from patients with *GBA1*-PD (n=3) and iPD (n=4) were incubated with nortriptyline 0.5 µM or

2 µM, or vehicle control for four days, before staining with Lysotracker™ DND-99. In the iPD group the lysosome count (p=0.01) and area (p=0.023) were significantly increased with nortriptyline, with further increased with the higher dose (p=0.003 and 0.019 for lysosome count and area respectively). In the *GBA1*-PD group there was a smaller rise in lysosome count and area which only reached significance for the higher dose p<0.0001 and p=0.001 respectively). (Figure 5.12).

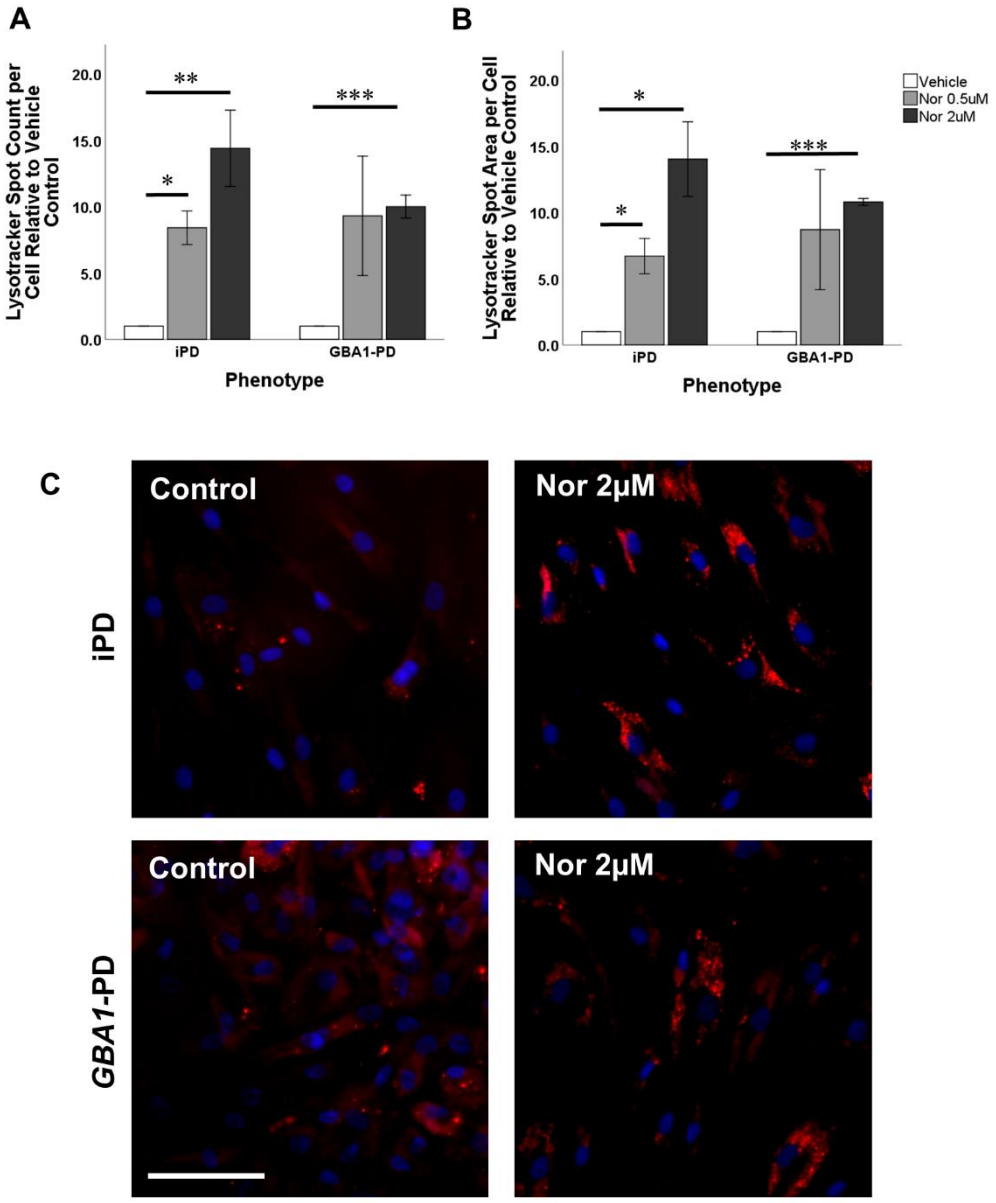

Figure 5.12. Effect of nortriptyline treatment on lysosomal mass in fibroblasts. Fibroblasts from patients with *GBA1*-PD (n=3) and iPD (n=4) were stained with Lysotracker™ DND-99. In both groups there were significant increases in lysosomal count and total lysosomal area. Statistical significance indicated by asterixes as

determined by independent samples T-tests. Scale bar represents 100 µm. Abbreviations: Nor = nortriptyline.

5.6.2.2 Ability of nortriptyline to impact on α-synuclein-induced pathology

Having found that nortriptyline resulted in changes to the lysosome-autophagy system, it was then tested in the PFF model, to see whether it could impact on α-synuclein pathology. Initially, iNs from *GBA1*-PD cell lines were treated with nortriptyline 0.5 µM or 2.5 µM from day 15 post-transduction, with addition of PFFs at day 17. As with previous experiments, half medium changes were then carried out until day 27 before analysis. In the *GBA1*-PD lines, nortriptyline had no effect on the number of PFF-induced α-synuclein aggregates. Neither nortriptyline treatment, nor PFF treatment had any significant effect on neuronal purity. The effect of nortriptyline on mitochondrial membrane potential was also assessed after PFF exposure, using a TMRE assay. Nortriptyline alone did not significantly alter mitochondrial membrane potential in the *GBA1*-PD iNs. The decline in mitochondrial membrane potential with PFFs was less than that previously seen, such that it did not reach significance. It was therefore not possible to comment on whether the nortriptyline protected against the PFF-induced decline in mitochondrial membrane potential. Nevertheless, nortriptyline did not seem to offer any significant benefit in the *GBA1*-PD iNs in terms of reducing PFF-induced pathology.

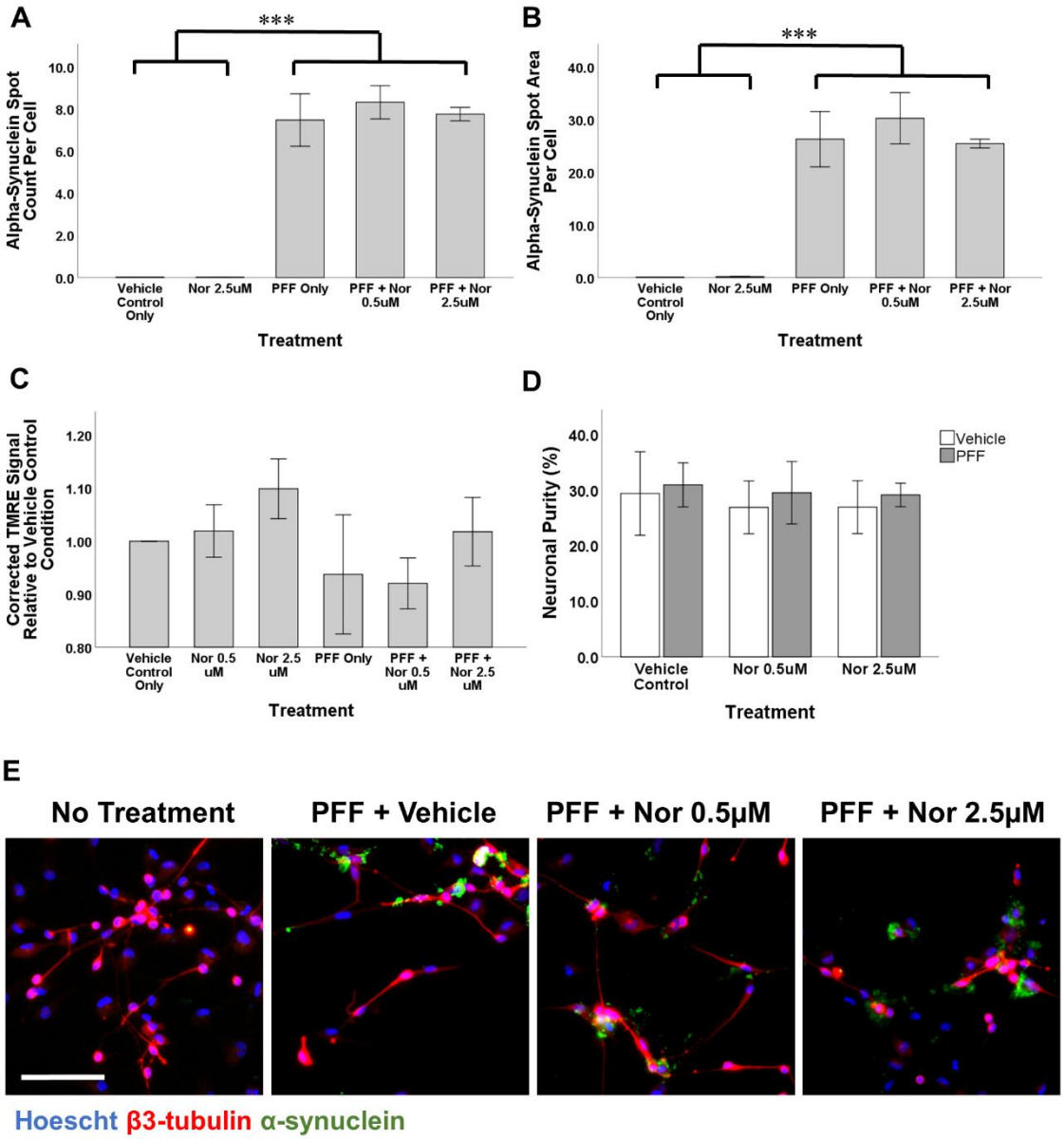

Figure 5.13 – Effect of nortriptyline on PFF-induced α-synuclein aggregates in *GBA1*-PD. Nortriptyline treatment did not reduce the burden of α-synuclein aggregates in *GBA1*-PD iNs (n=3). There were no significant differences in mitochondrial membrane potential with nortriptyline treatment. Asterixes indicate statistical significance as determined by one-way ANOVA with post-hoc Tukey analysis. Scale bar represents 100 μm. Abbreviations: PFF = pre-formed fibrils; Nor = nortriptyline.

Because nortriptyline seemed to have a more significant effect on autophagy in the iPD lines in comparison to the *GBA1*-PD lines, the effect of nortriptyline on PFF-induced pathology was also assessed in iPD iNs (n=5). Two healthy control lines were also

included. As had previously been observed, the number of PFF-induced α-synuclein aggregates was low in the healthy controls, and nortriptyline did not significantly alter the number of these. In contrast, in the iPD group, nortriptyline led to a dose-dependent reduction in the number of α-synuclein spots ($p=0.048$ and $p=0.021$ for the low and high dose respectively). The effect on TMRE signal was then assessed. Nortriptyline treatment alone did not alter the mitochondrial membrane potential in either group. PFFs resulted in a reduction in mitochondrial membrane potential in the iPD group ($p=0.003$), which was partially corrected with nortriptyline treatment. In the healthy control group PFF treatment did not alter the mitochondrial membrane potential.

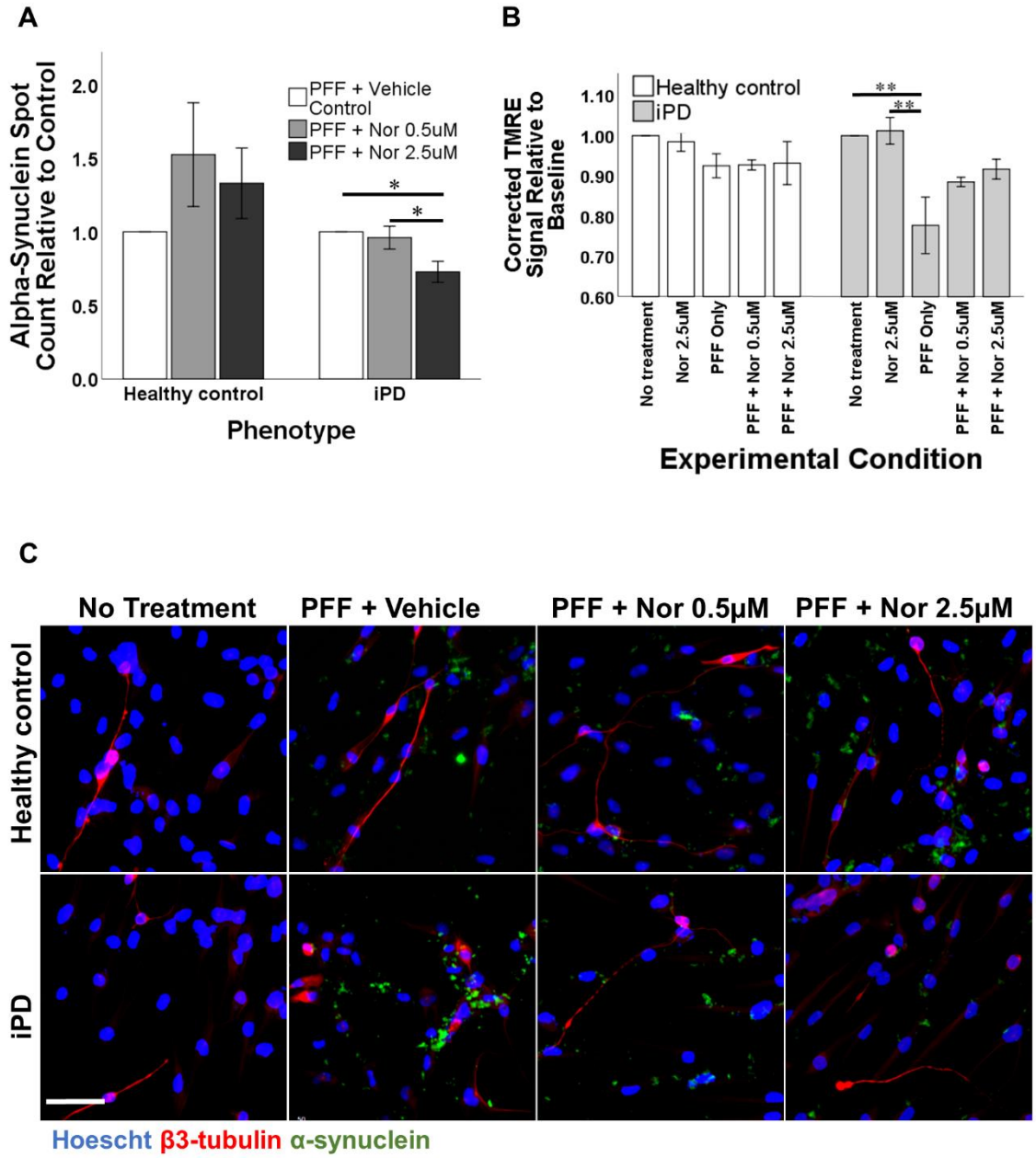

Figure 5.14. Effect of nortriptyline in iNs from healthy control and iPD individuals. A) and C) Nortriptyline reduced PFF-induced aggregates in iPD but not in healthy controls (n=2). B). Nortriptyline led to a restoration in mitochondrial membrane potential after PFF treatment in iNs from iPD lines (n=5). Asterixes represent statistically significant differences determined by one-way ANOVA with post-hoc Tukey analysis. Scale bar represents 100 µm. Abbreviations: Nor = nortriptyline; PFF = pre-formed fibrils.

5.6.3 Other Drugs

Metformin and ghrelin were also tested in the iN model given that they have been suggested to have beneficial effects on mitochondrial function. iNs were generated from three *GBA1*-PD lines, which were treated with 1 mM or 4 mM metformin, or 1 µm or 5 µm ghrelin from day 15. As before, PFFs were added at day 17 post-transduction, and analyses performed after a further 10 days. Neither metformin nor ghrelin had a significant effect on neuronal purity or the number or area of PFF-induced α-synuclein aggregates, when compared to the PFF only condition. Metformin was associated with a dose-dependent increase in mitochondrial membrane potential ($p=0.003$ and $p=0.001$ for the low and high dose respectively). It also corrected the decline in mitochondrial membrane potential induced by PFFs to baseline levels. Ghrelin had no effect on mitochondrial membrane potential alone or following PFF-exposure (Figure 5.15 and Figure 5.16).

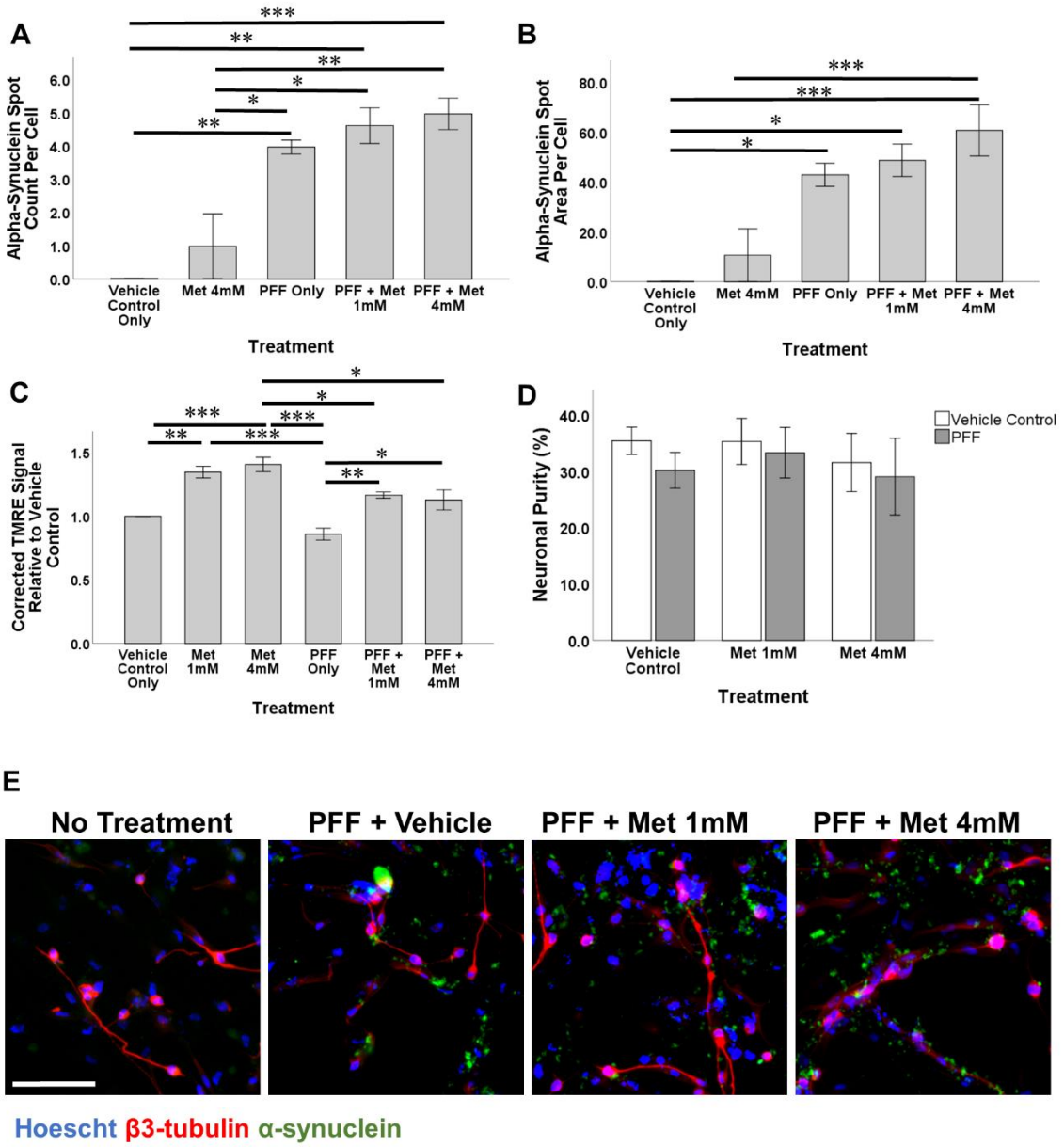

Figure 5.15 – Impact of metformin on PFF-induced pathology in iNs of *GBA1*-PD patients. The number (A) and total area (B) of PFF-induced α-synuclein aggregates per cell was not significantly altered by metformin treatment. C) Metformin increased mitochondrial membrane potential alone, and following PFF treatment. D) Neither metformin nor PFFs had a significant impact on neuronal purity. E) Representative images of PFF-induced α-synuclein aggregates. Asterixes indicate statistically significant differences as determined by one-way ANOVA with post-hoc Tukey analysis. Scale bar represents 100 µm. Abbreviations: Met = metformin; PFF = pre-formed fibrils.

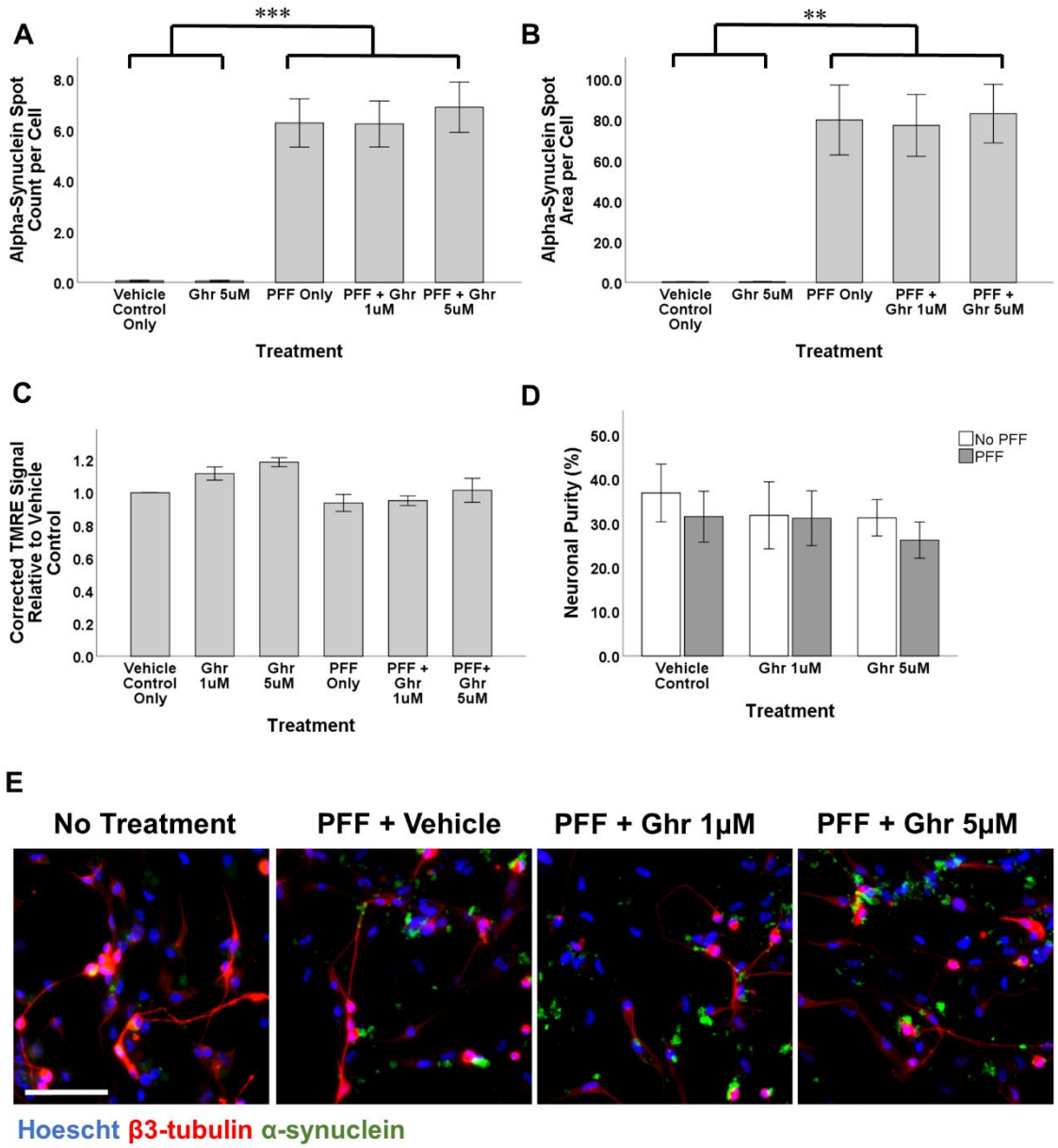

Figure 5.16– Impact of ghrelin on PFF-induced pathology in iNs of *GBA1*-PD patients. The number (A) and total area (B) of PFF-induced α-synuclein aggregates per cell was not significantly altered by ghrelin treatment. C) Ghrelin did not significantly alter mitochondrial membrane potential alone, or following PFF exposure. D) Neither ghrelin nor PFFs had a significant impact on neuronal purity. E) Representative images of PFF-induced α-synuclein aggregates. Asterixes indicate statistically significant differences as determined by one-way ANOVA with post-hoc Tukey analysis. Scale bar represents 100 µm. Abbreviations: Ghr = ghrelin; PFF = pre-formed fibrils.

5.7 Discussion

Here, the abilities of putative disease-modifying treatments to reduce α-synuclein-induced pathology in *GBA1*-PD have been tested in a novel iN model. This focus of this study was predominantly on two drugs purported to enhance activity in the lysosome-autophagy system (trehalose and nortriptyline), which will be discussed in turn.

5.7.1 Trehalose

Trehalose has previously been shown to reduce the burden of protein aggregates and improve clinical features in models of a number of neurodegenerative disorders (Davies et al. 2006, Sarkar et al. 2007, Rodríguez-Navarro et al. 2010). The mechanism by which trehalose achieves this is not clear, and may be multi-modal. Some studies have suggested that trehalose binds to and stabilises mutant proteins, preventing aggregation (Tanaka et al. 2004, Davies et al. 2006). Others have demonstrated that trehalose affects the activity of the lysosome-autophagy system, and it has been suggested to activate autophagy in an mTOR-independent manner (Sarkar et al. 2007, Rodríguez-Navarro et al. 2010, Redmann et al. 2017). It was therefore selected for investigation as a potential treatment for *GBA1*-PD in which the autophagy system is dysfunctional.

Trehalose clearly had an effect on the lysosome-autophagy system, which was similar in *GBA1*-PD to that in iPD. An increase in LC3b-II levels demonstrates that trehalose increased autophagosome numbers, either through increased activation of autophagy, or a fusion block. Taking into account the previous literature, the former is more likely, and this is supported by the fact that trehalose had an additive effect on the number of P62/SQSMT1 puncta induced by bafilomycin A1 treatment. Trehalose also led to a reduction in lysosome numbers, whereas one would expect an increase in lysosome count in the context of a fusion block in the autophagy pathway. The reduction in lysosome numbers would be consistent with their increased clearance due to increased flux through the lysosome-autophagy system. In order to more fully classify the mechanism by which trehalose altered autophagosome numbers it would be useful to perform LC3b-II and P62/SQSMT1 Western blot analysis in the context of autophagy inducing conditions (e.g.

starvation) and with blockers of the fusion stage. The mean intensity of P62/SQSTM1 in fibroblasts and iNs increased with trehalose (though the effect was much lower, and not significant in the latter). Increased P62/SQSTM1 levels normally indicate a reduction in autophagy flux, which conflicts with the prior literature and the other findings here. It should be acknowledged that immunocytochemistry is only semi-quantitative, and the increase in mean intensity may not represent an increase in P62/SQSTM1 levels. The apparent increase in P62/SQSTM1 intensity may have been a limitation of the analysis protocol, and it is possible that in conditions in which high numbers of brightly fluorescent puncta are present (such as with bafilomycin or trehalose treatment), that the mean intensity is raised. Furthermore, there are some circumstances in which increased P62/SQSTM1 levels have been associated with increases in autophagy activity (Colosetti et al. 2009, Toepfer et al. 2011).

Inhibition of PI3K selectively led to impairment in autophagy activity in *GBA1*-PD as discussed in chapter 4. Trehalose is known to activate autophagy in an mTOR-independent manner (Sarkar et al. 2007), and it would be interesting to determine if it is activating autophagy through PI3K-dependent pathways, thus overcoming the autophagy dysfunction of *GBA1*-PD.

Importantly, trehalose led to a significant reduction in the burden of PFF-induced α-synuclein aggregates, and was also able to prevent the PFF-induced reduction in mitochondrial membrane potential. Though the mechanisms behind this have not been investigated, PFF treatment induced an autophagy response, which was augmented by trehalose in the *GBA1*-PD group (section 4.4.4), and it is therefore plausible that trehalose was able to reduce the number of PFF-induced aggregates through an induction of autophagy. The restoration of mitochondrial membrane potential could be explained through clearance of depolarised mitochondria via a restored mitophagy pathway, or through a reduction in aggregate-induced mitochondrial dysfunction. Although investigation of these mechanisms would be important, the fact that trehalose is able to reduce this α-synuclein-related pathology, even in the context of *GBA1* abnormalities makes this an interesting agent for further therapeutic testing.

5.7.2 Nortriptyline

In this study, the ability of nortriptyline to alter the function of the lysosome-autophagy system was first assessed in fibroblasts and iNs from PD patients, before being tested in the PFF-iN model, to see if it was able to reduce α-synuclein pathology.

Nortriptyline was found to increase autophagosome numbers in iPD cell lines, but not in *GBA1*-PD cell lines. As discussed above, the increase in autophagosome numbers could be explained by increased activation of macroautophagy, or by a blockade in the fusion steps of the pathway. The subsequent observation that nortriptyline resulted in increased autophagic flux, as demonstrated by reduced P62/SQSTM1 levels in iNs, suggests that increased activation of autophagy is the more likely explanation. In order to confirm this suspicion, it would be necessary to perform this experiment with the addition of blockers of the lysosome-autophagosome fusion stage, such as bafilomycin A1.

Additionally, nortriptyline led to an increase in lysosome numbers in the iPD lines, and to a lesser extent in the *GBA1*-PD group. It is not possible to comment on whether the increase in lysosomes is due to their increased biosynthesis or reduced clearance, but it raises the possibility that nortriptyline may have multiple actions on the lysosome-autophagy system.

In fibroblasts, nortriptyline had a much lesser effect on autophagy parameters in *GBA1*-PD than in iPD, suggesting that it is acting via a mechanism that is not able to fully overcome the autophagy deficit of *GBA1*-PD, and that it is probably acting upstream of the site of dysfunction in *GBA1*-PD. However, when tested in iNs rather than fibroblasts, nortriptyline did significantly increase autophagy activity, which may be a reflection of the fact that autophagy activity is different in different cell types, and consequently the effect of drugs on this system differs between cell types. Having said this, nortriptyline did not offer any significant benefit in reducing PFF-induced pathology in the *GBA1*-PD iNs. In contrast, in the iPD group in which nortriptyline clearly increased autophagy activity, treatment resulted in a reduction in PFF-induced α-synuclein aggregates, and restoration of mitochondrial membrane potential following PFF-treatment. Taken

together, this data suggests that nortriptyline may have a beneficial effect in iPD through action on the lysosome-autophagy pathway, but that this effect is probably reduced in *GBA1*-PD.

5.7.3 Other Drugs Tested

Metformin and ghrelin were tested in the iN system given that they have previously been suggested to have beneficial effects on mitochondrial health, with the aim of targeting the presumed downstream pathology in the PFF model. Unsurprisingly, neither treatment significantly altered the burden of PFF-induced aggregates. In fact, there was a non-significant trend towards an increase in these structures with metformin. As is discussed in section 4.5.3, this apparent increase could be due to a number of potential factors, such as increased expression of α-synuclein or a detrimental effect on protein-clearance systems.

Treatment with metformin did however result in an increase in the mitochondrial membrane potential, suggesting that it did have a beneficial effect on mitochondria in the iNs. Whilst metformin did seem to restore the mitochondrial membrane potential to baseline levels following PFF treatment, it had the same effect in the absence of PFFs. It is not known therefore whether or not metformin is altering the relationship between PFF-induced aggregates and mitochondrial health, and it would be useful to perform a cell viability or caspase activity assay, to determine whether or not this effect was truly beneficial. Ghrelin did not significantly affect mitochondrial membrane potential.

5.7.4 Induced Neurons for drug testing in Parkinson's disease

As has been mentioned, the use of iNs for drug screening studies has been very limited to date, and this study is possibly the largest in which iNs have been used for this purpose. Of the four drugs tested here, trehalose treatment yielded some promising results in the context of *GBA1*-PD, in which it reduced the number of PFF-induced α-synuclein

aggregates and also corrected the decline in mitochondrial membrane potential, with similar results occurring with nortriptyline treatment in the iPD group.

One particular aspect of this model was that the pathological insult was relatively minor – a single dose of α-synuclein PFFs. Of course, this acute dose of PFFs is not reflective of the chronic degenerative process of PD, but the purpose of this is to induce the development of endogenous α-synuclein pathology, more closely representing the presumed pathogenic process in patients. However, the fact that this insult was minor posed limitations, in that the pathology that developed in the iNs was relatively mild, and that the significance of the (predominantly extracellular) α-synuclein aggregates was of uncertain significance (discussed in section 4.5.3). As has been discussed, the decline in mitochondrial membrane potential following PFF treatment was a consistent finding in the *GBA1*-PD cell lines. However, the biological effect of this was relatively small, and therefore often did not reach statistical significance for individual experiments, sometimes precluding any firm conclusions about the effects of a drug on this pathology. Future exploration of this model will require work with a greater number of cell lines so that findings regarding the effects of drugs on pathology are more robust. Additionally, other than the development of the PFF-induced aggregates, there were little pathological findings in the iPD group, making this model of more limited use in studying the effects of drugs in this population. Having said this, when a greater number of cell lines were employed (Figure 5.3) when testing the effects of nortriptyline in iPD, the decline in mitochondrial membrane potential was statistically apparent.

Going forward, the utility of this model would be significantly enhanced by using a greater number of cell lines, both in the iPD and *GBA1*-PD group. It would also be useful to search for and test additional outcome measures, such as PFF-induced impairments in ATP production or oxygen consumption, or increases in mitochondrial superoxide formation for example. Additionally, PFF-treatment resulted in an increase in caspase activity in the *GBA1* group (Figure 4.27), and it would be useful to test whether or not trehalose (or other drugs) prevented this. In addition, a greater degree of pathology would be desirable for future studies, which would best be achieved through increased culture time, so studies in which the culture conditions are optimised may facilitate this. Alternatively, pathology could be exaggerated by knocking-in mutant forms of, or

overexpressing wild-type α-synuclein, but these approaches would take the model further away from the pathogenic processes occurring in patients, thus negating one of the advantages of this model.

6 DISCUSSION

6.1 Clinical significance of *GBA1* variants in Parkinson's disease

The aim of the first study in this project was to better characterise the natural history of *GBA1*-PD, using a study population of incident PD patients. Though the sample size was a limiting factor, the long follow-up time meant that most participants were followed-up from the time of diagnosis, to the time to development of dementia, postural instability and death – three critical milestones in the evolution of PD. This meant that is was possible to establish a clear picture of the clinical course of *GBA1*-PD, and contrast it to that in PD patients without *GBA1* variants.

This study replicated the findings of most previous studies, in that it demonstrated an increased risk of motor progression and dementia in association with *GBA1* variants. In contrast to most other studies, the long follow-up period in this analysis allowed for the impact of *GBA1* variants on mortality to be determined. It was found that carrying a pathogenic mutation or polymorphism increased the risk of death, which occurred approximately a year earlier in comparison to non-carriers – an effect that was independent of the development of dementia.

The other main conclusion from this study, is that *GBA1* polymorphisms (in addition to GD-causing pathogenic mutations) such as the E326K variant, adversely affect the course of PD. This finding is important for two reasons in particular. Firstly, this approximately doubles the proportion of PD patients in which *GBA1* abnormalities potentially play a pathogenic role, such that around 10 % of PD patients will carry a relevant *GBA1*-variant. As such, as targeted disease-modifying therapies becomes available, and as regenerative therapies begin to enter clinical trials, testing for *GBA1* variants may have important

implications for practice. Secondly, the fact that these polymorphisms do not predispose to GD implies that their pathogenic consequences are unique to *GBA1*-PD (and potentially other α-synucleinopathies such as DLB). Experimental therapies that augment GCase activity are likely therefore to be of limited use in this population, and the focus should be on restoring correct folding of GCase or targeting the dysfunctional intracellular pathways associated with *GBA1* variants.

6.2 A novel model for drug testing in *GBA1* variant-associated Parkinson's disease

The second arm of this project was the establishment of a novel model using iNs that could be used for drug-screening studies. iNs were chosen because of the fact that they retain the age signature of the host, meaning that they uniquely offer a source of aged, adult human neurons – a relevant cell-type when studying neurodegenerative diseases. Despite having first been described almost a decade ago, the application of iNs to answer questions about disease processes has been limited to a small number of studies, and to answer questions about putative treatments has been confined to an even smaller number of studies. The focus of this study was on developing a model in which iN technology could be applied to answer clinically relevant questions.

The baseline pathology in the iNs was limited, and in order to manifest α-synuclein-related pathology, a single dose of pathogenic α-synuclein PFFs was necessary. Though this represented an artificial insult, the PFFs were cleared quickly, and subsequent pathology therefore came from endogenous processes. Treatment with PFFs yielded some reproducible outcome measures, such as the accumulation of α-synuclein aggregates and reduction in mitochondrial membrane potential which were used for drug testing studies here, as well as other outcome measures such as elevated caspase activity, which could be used for future projects. Effects such as the decline in mitochondrial membrane potential tended to be of low magnitude, and future studies should employ a greater number of cell lines to ensure that they are adequately powered to determine differences. As is discussed in detail in chapter 4, the significance of the PFF-induced, predominantly extra-cellular aggregates is not known, but they were considered to serve as a surrogate

marker for α-synuclein accumulation. Further characterisation of this system will be useful in future studies.

Though a number of challenges with the use of iNs remain, such as variability in reprogramming potential between cell lines, limited culture longevity, and impurities in cell populations as unconverted or partially converted cells persist, this study demonstrates that iNs can potentially be applied, and play an important role, in disease-modelling studies.

6.3 Putative disease-modifying treatments

A series of experiments were performed as part of this study in which the lysosome-autophagy system and mitochondrial health were assessed, to explore whether *GBA1*-variants were associated with dysfunction in these systems. Though the exact nature of dysfunction was not studied in depth, it was clear that there were differences in the lysosome-autophagy system in *GBA1*-PD compared to iPD and healthy controls. These studies, along with the existing literature, were useful in providing some rationale for the initial selection of drugs to test in the iN model. Trehalose and nortriptyline were therefore chosen, for their previously reported ability to augment autophagy activity in a number of models. Because mitochondrial dysfunction had been identified in the iN model following PFF treatment, metformin and ghrelin were also tested in this system.

When testing the two drugs targeting autophagy, both yielded interesting results. Only trehalose was found to enhance autophagy in *GBA1*-PD, with no changes in LC3b-II levels associated with nortriptyline treatment. Trehalose, but not nortriptyline, was associated with a reduction in PFF-induced pathology in the iN system in *GBA1*-PD. In contrast, nortriptyline reduced pathology in the iPD group. Both of these drugs readily cross the blood-brain-barrier, and safety data for nortriptyline which is already widely used for other conditions is well established. Trehalose is not currently used in a clinical setting, but early clinical trials have begun to confirm its safety (clinicaltrials.gov identifier NCT02725957). Both drugs therefore could potentially be prioritised for entry into clinical trials, if they continue to show promise in experimental models.

6.4 Further Work

Going forward with this work, a number of other studies would be useful. With regard to the iN system, the most important aim will be to increase the longevity of the cell culture, to potentially allow for the development of relevant intracellular pathology. Of course, limitations in the survival of cells in the culture system may relate to underlying disease-related factors, but a systematic assessment of the different culture matrices to determine the optimal culture conditions would be useful.

In this study, the use of α-synuclein PFFs in iNs provided a number of outcome measures that could be used for drug screening. It would however, be useful to characterise the PFF pathology further. One of the outcome measures used for drug testing in this project was a reduction in mitochondrial membrane potential after PFF treatment. It is important to assess other mitochondrial parameters including ATP production and oxygen consumption following PFF exposure, to further quantify the effect on mitochondrial function. Caspase activity was also increased following PFF exposure in this study, and it would be useful to perform a cell death assay to explore this further. PFF-induced changes in any of these parameters could be used for further drug testing.

The nature of the PFF-induced aggregates, and the intracellular α-synuclein pathology has not been established. It would therefore be interesting to perform immunoprecipitation assays to determine the effect of PFFs on the accumulation of pathogenic α-synuclein species. Immunocytochemistry failed to detect any serine-129 phosphorylated α-synuclein, but it is possible that the levels of phosphorylated α-synuclein were below the detection limit for this assay. Immunoprecipitation would allow for a greater sensitivity in detecting phosphorylated and high molecular weight α-synuclein species. If such α-synuclein pathology is detected on immunoprecipitation, these would provide further useful outcome measures for drug screening.

Preliminary results suggested that trehalose and nortriptyline reduced PFF-induced α-synuclein pathology in different groups. Whilst both drugs altered autophagy parameters, the mechanisms by which they do this have not been established, and it is not clear whether or not the reduction in PFF-induced pathology is due to an effect on the lysosome-autophagy system. It would therefore be useful to visualise autophagosomes and lysosomes following treatment with these drugs to explore whether or not they are affecting autophagosome formation or the fusion stage of the pathway. It would also be useful to see whether or not autophagy inhibitors such as 3-MA diminish the effects of trehalose and nortriptyline in the PFF model.

6.5 Concluding remarks

GBA1-PD continues to be a PD subpopulation of considerable interest. *GBA1*-variants are common in PD, occurring in approximately 10 % of patients, and it is increasingly clear that they adversely affect clinical course. Targeting this population therefore could have a significant impact on the overall burden of PD-related morbidity and mortality. Furthermore, in this group of patients there are specific pathogenic processes, and experimental therapies should target these. iNs offer a means of rapidly generating aged adult neurons, which can be used for disease-modelling and drug screening. As with all models, there are disadvantages to the use of iNs, but they potentially offer a useful *in vitro* system for the study of neurological disease, and future studies should focus on the applicability of these cells for this purpose.

7 SUPPLEMENTARY MATERIAL

Plasmid	Size (kb)	Restriction Endonuclease	Splice Site	Fragment Sizes
3410	10279	BsrGI	2251	8466
		ScaI	438	1813
RSV/Rev	4174	BamHI	928	1752
		ScaI	2680	2422
MDL	8895	AseI	183	7962
			8145	933
Md2g	5824	AseI	183	4891
			5074	933

Supplementary Table 7.1 – Restriction endonucleases used for agarose gel plasmid verification.

Gene	Primer / Probe	Sequence
Albumin	Forward primer	5'-TGAAACATACGTTCCCAAAGAGTTT-3'
	Reverse primer	5'-CTCTCCTTCTCAGAAAGTGTGCATAT-3'
	Probe	5'Fam-TGCTGAAACATTCACCTTCCATGCAGA-Tamra-3'
WPRE	Forward primer	GGCACTGACAATTCCGTGGT
	Reverse primer	AGGGACGTAGCAGAAGGACG
	Probe	5'Fam-ACGTCCTTTCCATGGCTGCTCGC -Tamra-3'

Supplementary Table 7.2 – Primer and probe sequences for qPCR lentivirus titration.

Target	Species	Supplier	Catalogue Number	Dilution
Tau	Mouse	Thermo Fisher	MN1000	1:500
Map2	Rabbit	EMD Millipore	AB5622	1:500
α-synuclein-42	Mouse	BD Biosciences	610787	1:1000
Neurofilament-200	Mouse	Sigma	N0142	1:1000
MAP2	Chicken	Abcam	Ab5392	1:100
LC3B	Rabbit	Sigma	L7543	1:500
P62/SQSTM1	Mouse	Genetex	GTX629890	1:500
P62/SQSTM1	Rabbit	Abcam	Ab91526	1:500
β3-tubulin	Mouse	Abcam	Ab78078	1:1000
β3-tubulin	Rabbit	Abcam	Ab18207	1:1000
NCAM	Mouse	Abcam	Ab9018	1:1000
GFP	Rabbit	Abcam	Ab6556	1:2000
Phospho-α-Synuclein (Ser129) Antibody, clone 81A	Mouse	Millipore	MABN826	1:1000
Calnexin	Rabbit	Enzo Life Sciences	ADI-SPA-860-D	1:1000

Supplementary Table 7.3 – Primary antibodies used in immunocytochemistry and Western blot analyses.

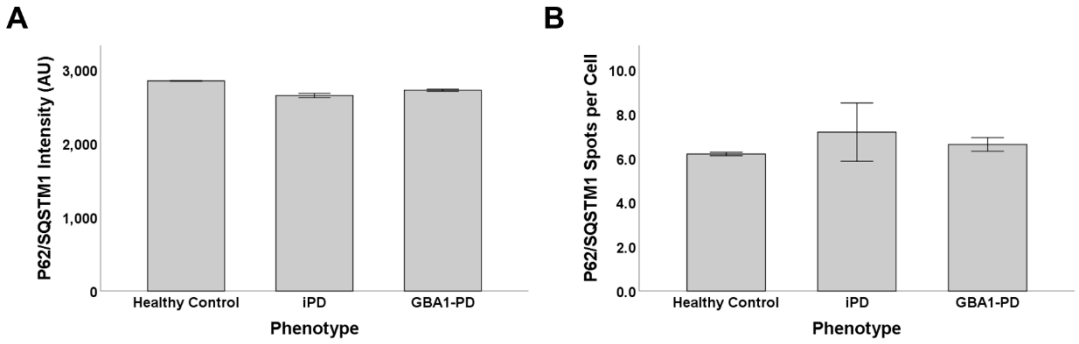

Supplementary Figure 7.1 – P62/SQSTM1 immunocytochemistry in iNs under baseline conditions. iNs from healthy controls (n=2) and patients with iPD (n=2) and *GBA1*-PD (n=3) were fixed at day 29 post-transduction and immunocytochemistry for P62/SQSMT1 was performed. There were no significant differences in P62/SQSTM1 intensity or P62/SQSTM1 spot count as determined by one-way ANOVA and post-hoc Tukey analysis. Error bars represent standard error of the mean.

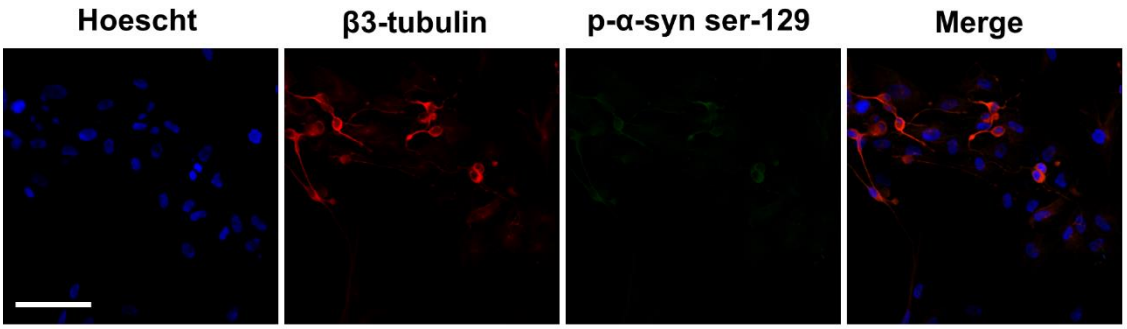

Supplementary Figure 7.2 – Immunocytochemistry for phosphorylated serine 129 α-synuclein. iNs from a *GBA1*-PD line were generated. PFFs were applied at day 17 and the cells were fixed nine days later. Confocal microscopy images were obtained at 20x magnification. No phosphorylated α-synuclein was detected. Scale bar represents 200 µm. Abbreviations: p-α-syn ser-129 = phosphorylated serine 129 α-synuclein.

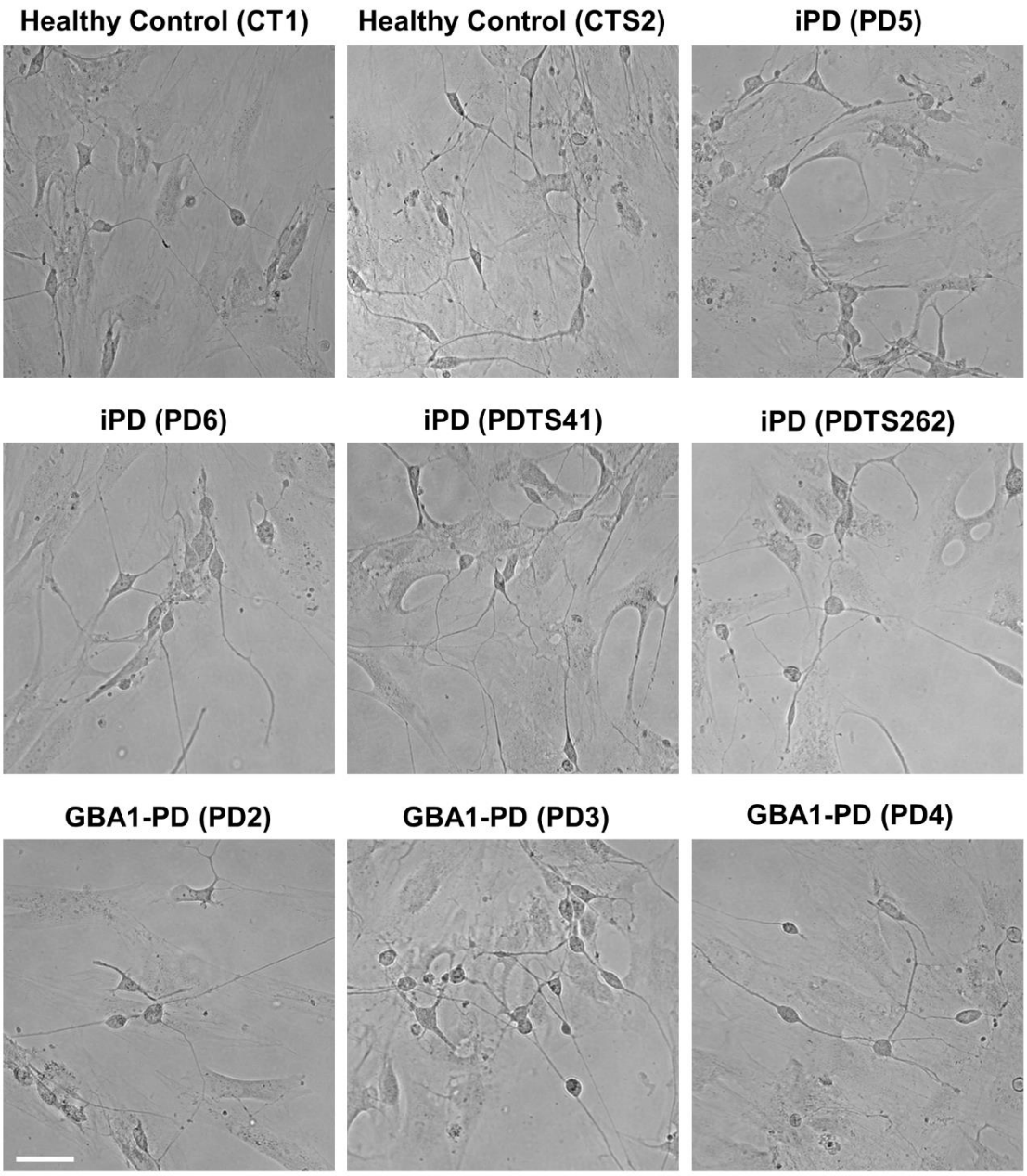

Supplementary Figure 7.3 – Brightfield images of starved iNs prior to lysing for protein harvest for LC3b and P62/SQSTM1 Western blots. Scale bar represents 200 µm.

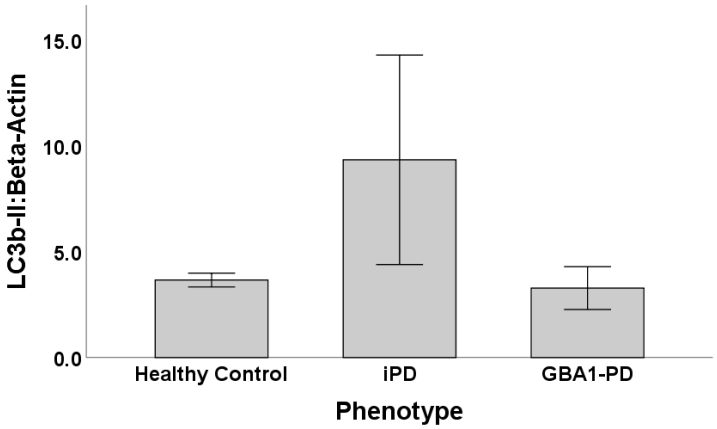

Supplementary Figure 7.4 – LC3b quantification in iNs under baseline conditions. iNs were generated from healthy controls (n=2), and patients with iPD (n=4) and *GBA1*-PD (n=3). At day 22 post-transduction protein was harvested in 5 M urea lysis buffer for Western blot analysis. Graph shows quantification of LC3b-II levels showing no differences across groups. Error bars represent standard error of the mean.

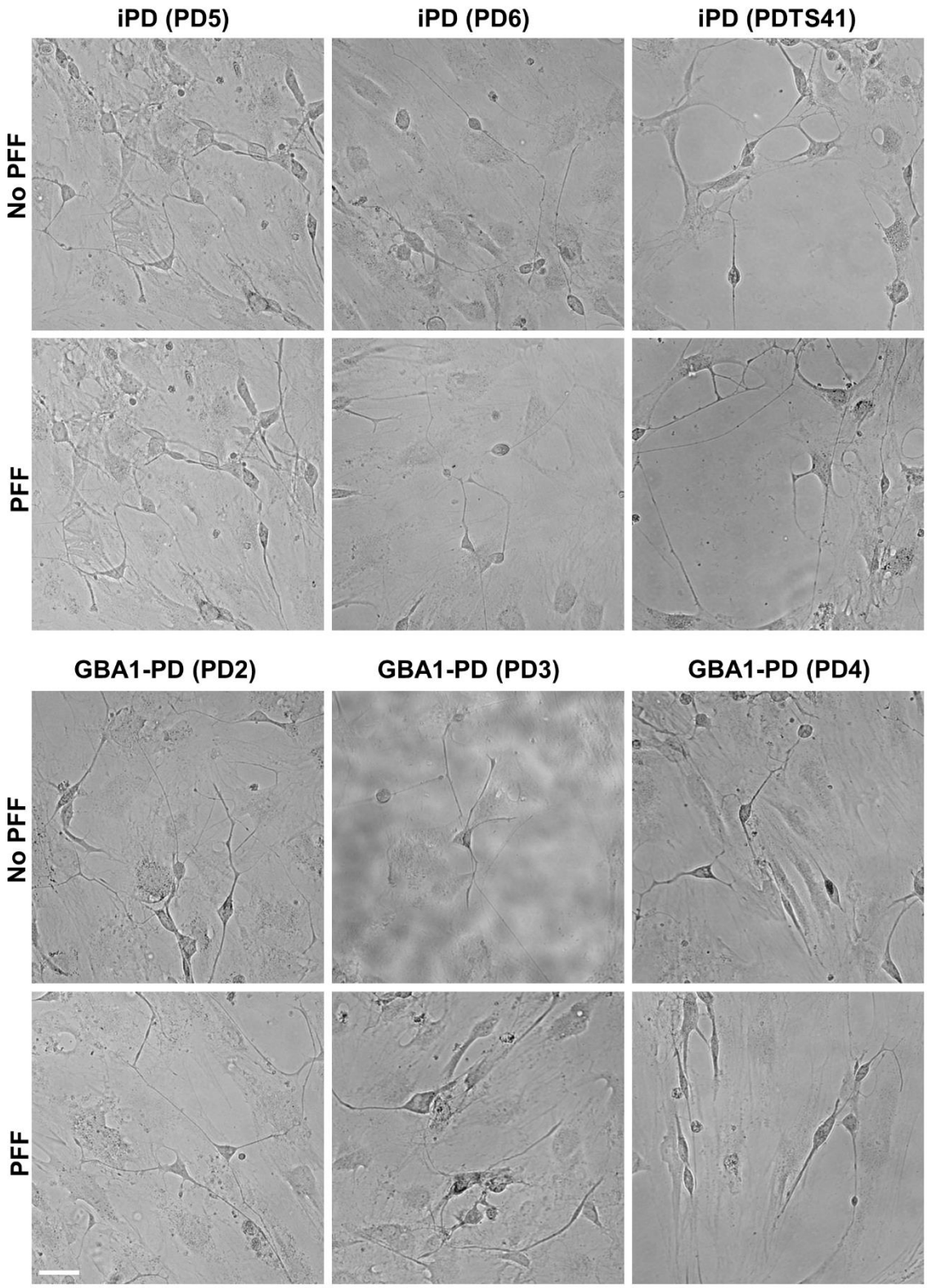

Supplementary Figure 7.5 – Brightfield images of iNs treated with PFFs or vehicle control prior to lysing for protein harvest for LC3b and P62/SQSTM1 Western blots. Scale bar represents 200 µm.

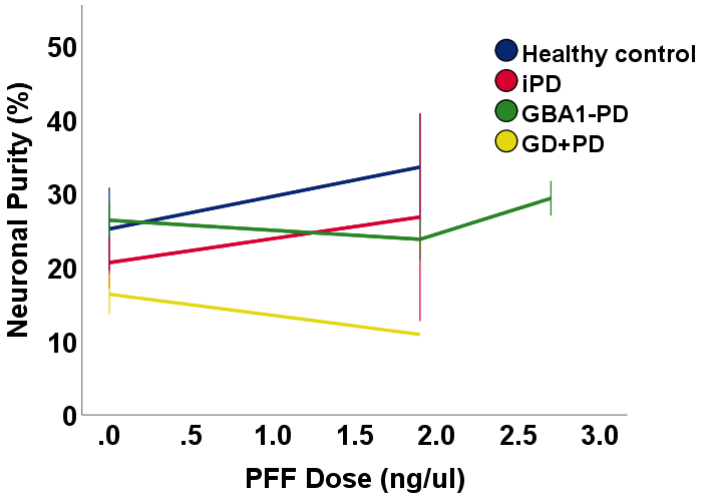

Supplementary Figure 7.6 – Effect of PFF-treatment on neuronal purity. Post-hoc analysis of 12 conversions involving 14 cell lines. PFF treatment did not alter neuronal purity. Abbreviations: PFF = pre-formed fibrils.

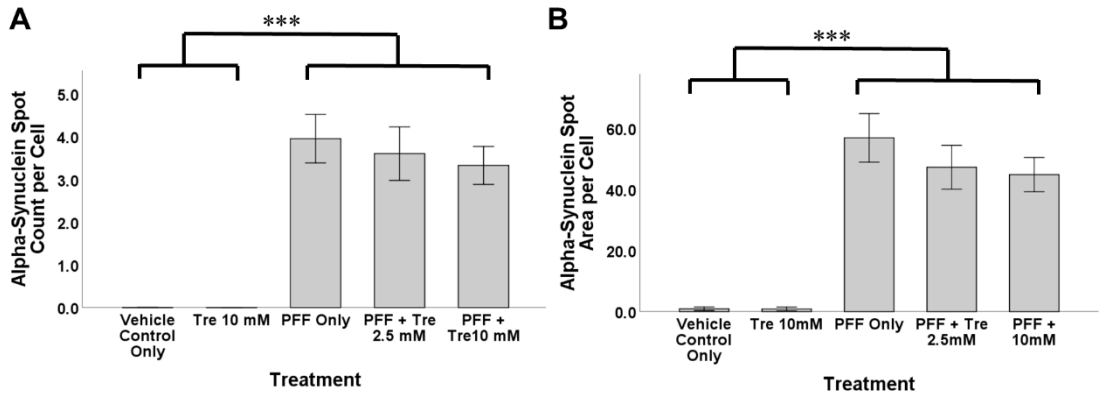

Supplementary Figure 7.7 – Effect of trehalose on PFF-induced α-synuclein aggregate count and area. Trehalose led to a dose-dependent trend in the numbers and area of PFF-induced aggregates per cell. Statistical significance indicated by asterixes as determined by one-way ANOVA with post-hoc Tukey analysis. Abbreviations: PFF = pre-formed fibrils. Tre = trehalose.

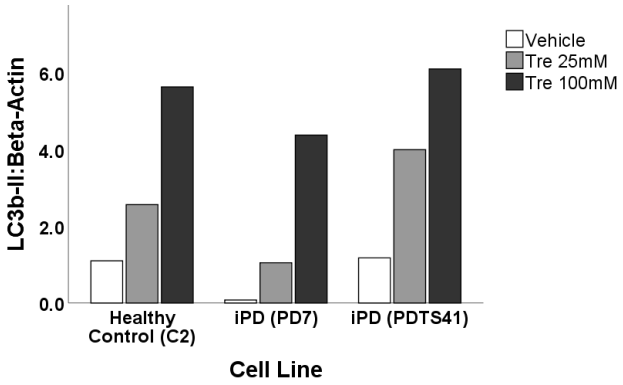

Supplementary Figure 7.8 – LC3b-II levels in individual cell lines after treatment with trehalose. Trehalose increased autophagosome numbers in all three cell lines. Abbreviations: Tre = trehalose.

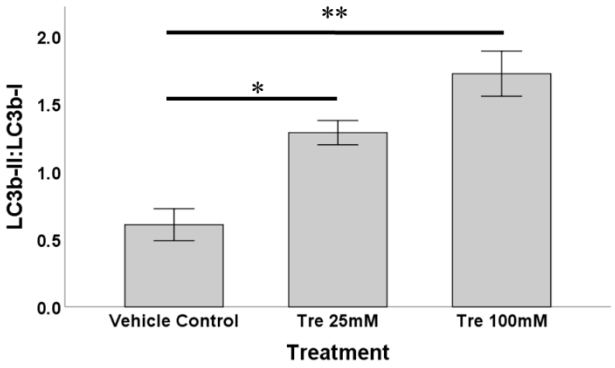

Supplementary Figure 7.9 – Western blot analysis of LC3b-II:LC3b-I ratio in *GBA1*-PD cell lines after trehalose treatment. Trehalose led to a dose-dependent increase in autophagosome numbers in *GBA1*-PD fibroblasts. Statistical significance indicated by asterixes as determined by one-way ANOVA with post-hoc Tukey analysis. Abbreviations: Tre = trehalose.

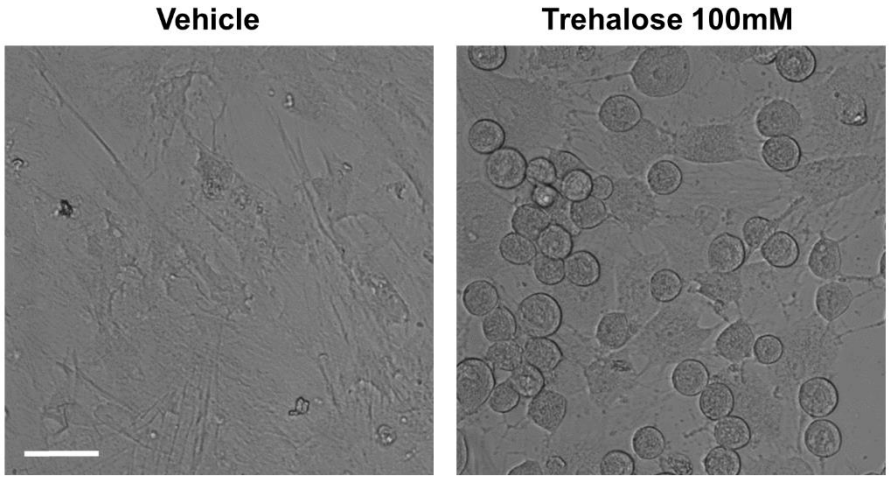

Supplementary Figure 7.10 – Morphology of iNs after treatment with high-dose trehalose. iNs from an iPD line were generated and at day three post-transduction, trehalose 100mM was added. Images obtained at day 10 post-transduction demonstrated abnormal cell morphology associated with high-dose trehalose treatment. Scale bar represents 200 µm.

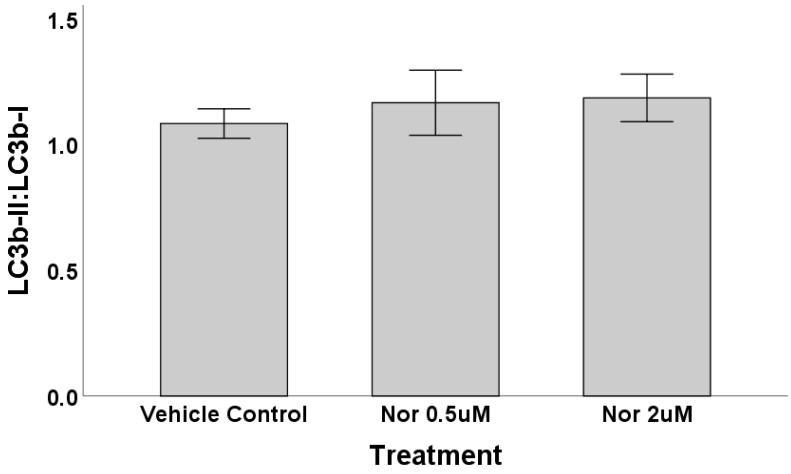

Supplementary Figure 7.11 – Western blot analysis of LC3b-II:LC3b-I ratio in *GBA1*-PD cell lines after nortriptyline treatment. Nortriptyline did not alter LC3b-II:LC3b-I ratio in fibroblasts from *GBA1*-PD iNs. Abbreviations: Nor = nortriptyline.

8 REFERENCES

Agarwal, S., Y. H. Loh, E. M. McLoughlin, J. Huang, I. H. Park, J. D. Miller, H. Huo, M. Okuka, R. M. Dos Reis, S. Loewer, H. H. Ng, D. L. Keefe, F. D. Goldman, A. J. Klingelhutz, L. Liu & G. Q. Daley (2010) Telomere elongation in induced pluripotent stem cells from dyskeratosis congenita patients. *Nature,* 464**,** 292-6.

Akiyama, H. & P. L. McGeer (1989) Microglial response to 6-hydroxydopamine-induced substantia nigra lesions. *Brain Res,* 489**,** 247-53.

Alcalay, R. N., O. A. Levy, C. C. Waters, S. Fahn, B. Ford, S. H. Kuo, P. Mazzoni, M. W. Pauciulo, W. C. Nichols, Z. Gan-Or, G. A. Rouleau, W. K. Chung, P. Wolf, P. Oliva, J. Keutzer, K. Marder & X. Zhang (2015) Glucocerebrosidase activity in Parkinson's disease with and without GBA mutations. *Brain,* 138**,** 2648-58.

Alvarez-Erviti, L., Y. Seow, A. H. Schapira, C. Gardiner, I. L. Sargent, M. J. Wood & J. M. Cooper (2011) Lysosomal dysfunction increases exosome-mediated alpha-synuclein release and transmission. *Neurobiol Dis,* 42**,** 360-7.

Amato, S. & H. Y. Man (2011) Bioenergy sensing in the brain: the role of AMP-activated protein kinase in neuronal metabolism, development and neurological diseases. *Cell Cycle,* 10**,** 3452-60.

Ambasudhan, R., M. Talantova, R. Coleman, X. Yuan, S. Zhu, S. A. Lipton & S. Ding (2011) Direct reprogramming of adult human fibroblasts to functional neurons under defined conditions. *Cell Stem Cell,* 9**,** 113-8.

Andersson, U., K. Filipsson, C. R. Abbott, A. Woods, K. Smith, S. R. Bloom, D. Carling & C. J. Small (2004) AMP-activated protein kinase plays a role in the control of food intake. *J Biol Chem,* 279**,** 12005-8.

Andrews, Z. B., D. Erion, R. Beiler, Z. W. Liu, A. Abizaid, J. Zigman, J. D. Elsworth, J. M. Savitt, R. DiMarchi, M. Tschoep, R. H. Roth, X. B. Gao & T. L. Horvath (2009) Ghrelin promotes and protects nigrostriatal dopamine function via a UCP2-dependent mitochondrial mechanism. *J Neurosci,* 29**,** 14057-65.

Andrews, Z. B., B. Horvath, C. J. Barnstable, J. Elsworth, J. Elseworth, L. Yang, M. F. Beal, R. H. Roth, R. T. Matthews & T. L. Horvath (2005) Uncoupling protein-2 is critical for nigral dopamine cell survival in a mouse model of Parkinson's disease. *J Neurosci,* 25**,** 184-91.

Andrews, Z. B., Z. W. Liu, N. Walllingford, D. M. Erion, E. Borok, J. M. Friedman, M. H. Tschöp, M. Shanabrough, G. Cline, G. I. Shulman, A. Coppola, X. B. Gao, T. L. Horvath & S. Diano (2008) UCP2 mediates ghrelin's action on NPY/AgRP neurons by lowering free radicals. *Nature,* 454**,** 846-51.

Angot, E., J. A. Steiner, C. Hansen, J. Y. Li & P. Brundin (2010) Are synucleinopathies prion-like disorders? *Lancet Neurol,* 9**,** 1128-38.

Arora, A., C. Ha & C. B. Park (2004) Inhibition of insulin amyloid formation by small stress molecules. *FEBS Lett,* 564**,** 121-5.

Bae, E. J., N. Y. Yang, C. Lee, H. J. Lee, S. Kim, S. P. Sardi & S. J. Lee (2015) Loss of glucocerebrosidase 1 activity causes lysosomal dysfunction and α-synuclein aggregation. *Exp Mol Med,* 47**,** e153.

Bae, E. J., N. Y. Yang, M. Song, C. S. Lee, J. S. Lee, B. C. Jung, H. J. Lee, S. Kim, E. Masliah, S. P. Sardi & S. J. Lee (2014) Glucocerebrosidase depletion enhances cell-to-cell transmission of α-synuclein. *Nat Commun,* 5**,** 4755.

Baker, M., I. Litvan, H. Houlden, J. Adamson, D. Dickson, J. Perez-Tur, J. Hardy, T. Lynch, E. Bigio & M. Hutton (1999) Association of an extended haplotype in the tau gene with progressive supranuclear palsy. *Hum Mol Genet,* 8**,** 711-5.

Ballas, N., C. Grunseich, D. D. Lu, J. C. Speh & G. Mandel (2005) REST and its corepressors mediate plasticity of neuronal gene chromatin throughout neurogenesis. *Cell,* 121**,** 645-57.

Bar-On, P., L. Crews, A. O. Koob, H. Mizuno, A. Adame, B. Spencer & E. Masliah (2008) Statins reduce neuronal alpha-synuclein aggregation in in vitro models of Parkinson's disease. *J Neurochem,* 105**,** 1656-67.

Barker, R. A., M. Parmar, L. Studer & J. Takahashi (2017) Human Trials of Stem Cell-Derived Dopamine Neurons for Parkinson's Disease: Dawn of a New Era. *Cell Stem Cell,* 21**,** 569-573.

Bayliss, J. A., M. Lemus, V. V. Santos, M. Deo, J. D. Elsworth & Z. B. Andrews (2016a) Acylated but not des-acyl ghrelin is neuroprotective in an MPTP mouse model of Parkinson's disease. *J Neurochem,* 137**,** 460-71.

Bayliss, J. A., M. B. Lemus, R. Stark, V. V. Santos, A. Thompson, D. J. Rees, S. Galic, J. D. Elsworth, B. E. Kemp, J. S. Davies & Z. B. Andrews (2016b) Ghrelin-AMPK Signaling Mediates the Neuroprotective Effects of Calorie Restriction in Parkinson's Disease. *J Neurosci,* 36**,** 3049-63.

Beal, M. F. (2001) Experimental models of Parkinson's disease. *Nat Rev Neurosci,* 2**,** 325-34.

Beavan, M., A. McNeill, C. Proukakis, D. A. Hughes, A. Mehta & A. H. Schapira (2015) Evolution of prodromal clinical markers of Parkinson disease in a GBA mutation-positive cohort. *JAMA Neurol,* 72**,** 201-8.

Bell, J. T., P. C. Tsai, T. P. Yang, R. Pidsley, J. Nisbet, D. Glass, M. Mangino, G. Zhai, F. Zhang, A. Valdes, S. Y. Shin, E. L. Dempster, R. M. Murray, E. Grundberg, A. K. Hedman, A. Nica, K. S. Small, E. T. Dermitzakis, M. I. McCarthy, J. Mill, T. D. Spector, P. Deloukas & M. Consortium (2012) Epigenome-wide scans identify differentially methylated regions for age and age-related phenotypes in a healthy ageing population. *PLoS Genet,* 8**,** e1002629.

Bendikov-Bar, I., G. Maor, M. Filocamo & M. Horowitz (2013) Ambroxol as a pharmacological chaperone for mutant glucocerebrosidase. *Blood Cells Mol Dis,* 50**,** 141-5.

Berchtold, N. C., D. H. Cribbs, P. D. Coleman, J. Rogers, E. Head, R. Kim, T. Beach, C. Miller, J. Troncoso, J. Q. Trojanowski, H. R. Zielke & C. W. Cotman (2008) Gene expression changes in the course of normal brain aging are sexually dimorphic. *Proc Natl Acad Sci U S A,* 105**,** 15605-10.

Berge-Seidl, V., L. Pihlstrøm, J. Maple-Grødem, L. Forsgren, J. Linder, J. P. Larsen, O. B. Tysnes & M. Toft (2017) The GBA variant E326K is associated with

Parkinson's disease and explains a genome-wide association signal. *Neurosci Lett,* 658**,** 48-52.

Bergman, H., T. Wichmann & M. R. DeLong (1990) Reversal of experimental parkinsonism by lesions of the subthalamic nucleus. *Science,* 249**,** 1436-8.

Betarbet, R., T. B. Sherer, G. MacKenzie, M. Garcia-Osuna, A. V. Panov & J. T. Greenamyre (2000) Chronic systemic pesticide exposure reproduces features of Parkinson's disease. *Nat Neurosci,* 3**,** 1301-6.

Beutler, E. (1992) Gaucher disease: new molecular approaches to diagnosis and treatment. *Science,* 256**,** 794-9.

Beyer, K. (2006) Alpha-synuclein structure, posttranslational modification and alternative splicing as aggregation enhancers. *Acta Neuropathol,* 112**,** 237-51.

Biddy, B. A., W. Kong, K. Kamimoto, C. Guo, S. E. Waye, T. Sun & S. A. Morris (2018) Single-cell mapping of lineage and identity in direct reprogramming. *Nature,* 564**,** 219-224.

Bien, B. A., G. L. Wojcik, N. Zubair, C. R. Gignoux, A. R. Martin, J. M. Kocarnik, L. W. Martin, S. Buyske, J. Haessler, R. W. Walker, I. Cheng, M. Graff, L. Xia, N. Franceschini, T. Matise, R. James, L. Hindorff, L. Le Marchand, K. E. North, C. A. Haiman, U. Peters, R. J. Loos, C. L. Kooperberg, C. D. Bustamante, E. E. Kenny, C. S Carlson; PAGE Study. (2016) Strategies for Enriching Variant Coverage in Candidate Disease Loci on a Multiethnic Genotyping Array. *Plos One,* 11(12).

Bjørkøy, G., T. Lamark, A. Brech, H. Outzen, M. Perander, A. Overvatn, H. Stenmark & T. Johansen (2005) p62/SQSTM1 forms protein aggregates degraded by autophagy and has a protective effect on huntingtin-induced cell death. *J Cell Biol,* 171**,** 603-14.

Blanchard, J. W., K. T. Eade, A. Szűcs, V. Lo Sardo, R. K. Tsunemoto, D. Williams, P. P. Sanna & K. K. Baldwin (2015) Selective conversion of fibroblasts into peripheral sensory neurons. *Nat Neurosci,* 18**,** 25-35.

Bollati, V., J. Schwartz, R. Wright, A. Litonjua, L. Tarantini, H. Suh, D. Sparrow, P. Vokonas & A. Baccarelli (2009) Decline in genomic DNA methylation through aging in a cohort of elderly subjects. *Mech Ageing Dev,* 130**,** 234-9.

Bonifati, V., P. Rizzu, M. J. van Baren, O. Schaap, G. J. Breedveld, E. Krieger, M. C. Dekker, F. Squitieri, P. Ibanez, M. Joosse, J. W. van Dongen, N. Vanacore, J. C. van Swieten, A. Brice, G. Meco, C. M. van Duijn, B. A. Oostra & P. Heutink (2003) Mutations in the DJ-1 gene associated with autosomal recessive early-onset parkinsonism. *Science,* 299**,** 256-9.

Braak, H., K. Del Tredici, U. Rüb, R. A. de Vos, E. N. Jansen Steur & E. Braak (2003) Staging of brain pathology related to sporadic Parkinson's disease. *Neurobiol Aging,* 24**,** 197-211.

Bras, J., C. Paisan-Ruiz, R. Guerreiro, M. H. Ribeiro, A. Morgadinho, C. Januario, E. Sidransky, C. Oliveira & A. Singleton (2009) Complete screening for glucocerebrosidase mutations in Parkinson disease patients from Portugal. *Neurobiol Aging,* 30**,** 1515-7.

Brockmann, K., K. Srulijes, S. Pflederer, A. K. Hauser, C. Schulte, W. Maetzler, T. Gasser & D. Berg (2015) GBA-associated Parkinson's disease: reduced survival

and more rapid progression in a prospective longitudinal study. *Mov Disord,* 30**,** 407-11.

Brodsky, J. L. & A. A. McCracken (1999) ER protein quality control and proteasome-mediated protein degradation. *Semin Cell Dev Biol,* 10**,** 507-13.

Brundin, P., K. D. Dave & J. H. Kordower (2017) Therapeutic approaches to target alpha-synuclein pathology. *Exp Neurol,* 298**,** 225-235.

Burbulla, L. F., P. Song, J. R. Mazzulli, E. Zampese, Y. C. Wong, S. Jeon, D. P. Santos, J. Blanz, C. D. Obermaier, C. Strojny, J. N. Savas, E. Kiskinis, X. Zhuang, R. Krüger, D. J. Surmeier & D. Krainc (2017) Dopamine oxidation mediates mitochondrial and lysosomal dysfunction in Parkinson's disease. *Science,* 357**,** 1255-1261.

Burchell V. S., D. E. Nelson, A. Sanchez-Martinex, M. Delgado-Camprubi, R. M. Ivatt, J. H Pogson, S. J. Randall, S. Wray, P. A. Lewis, H. Houlden, A. Y. Abramov, J. Hardy, N. W. Wood, A. J. Whitworth, H. Laman & H. Plun-Favreau (2013) The Parkinson's disease-linked proteins Fbxo7 and Parkin interact to mediate mitophagy. *Nat Neurosci,* 16, 1257-65.

Burré, J., M. Sharma & T. C. Südhof (2014) α-Synuclein assembles into higher-order multimers upon membrane binding to promote SNARE complex formation. *Proc Natl Acad Sci U S A,* 111**,** E4274-83.

Caiazzo, M., M. T. Dell'Anno, E. Dvoretskova, D. Lazarevic, S. Taverna, D. Leo, T. D. Sotnikova, A. Menegon, P. Roncaglia, G. Colciago, G. Russo, P. Carninci, G. Pezzoli, R. R. Gainetdinov, S. Gustincich, A. Dityatev & V. Broccoli (2011) Direct generation of functional dopaminergic neurons from mouse and human fibroblasts. *Nature,* 476**,** 224-7.

Chen, Q. & G. G. Haddad (2004) Role of trehalose phosphate synthase and trehalose during hypoxia: from flies to mammals. *J Exp Biol,* 207**,** 3125-9.

Chen, R., Y. Zou, D. Mao, D. Sun, G. Gao, J. Shi, X. Liu, C. Zhu, M. Yang, W. Ye, Q. Hao, R. Li & L. Yu (2014) The general amino acid control pathway regulates mTOR and autophagy during serum/glutamine starvation. *J Cell Biol,* 206**,** 173-82.

Chen, Y. & G. W. Dorn (2013) PINK1-phosphorylated mitofusin 2 is a Parkin receptor for culling damaged mitochondria. *Science,* 340**,** 471-5.

Chiang, H. L., S. R. Terlecky, C. P. Plant & J. F. Dice (1989) A role for a 70-kilodalton heat shock protein in lysosomal degradation of intracellular proteins. *Science,* 246**,** 382-5.

Chiueh, C. C., G. Krishna, P. Tulsi, T. Obata, K. Lang, S. J. Huang & D. L. Murphy (1992) Intracranial microdialysis of salicylic acid to detect hydroxyl radical generation through dopamine autooxidation in the caudate nucleus: effects of MPP+. *Free Radic Biol Med,* 13**,** 581-3.

Chong, J. A., J. Tapia-Ramírez, S. Kim, J. J. Toledo-Aral, Y. Zheng, M. C. Boutros, Y. M. Altshuller, M. A. Frohman, S. D. Kraner & G. Mandel (1995) REST: a mammalian silencer protein that restricts sodium channel gene expression to neurons. *Cell,* 80**,** 949-57.

Christensen, B. C., E. A. Houseman, C. J. Marsit, S. Zheng, M. R. Wrensch, J. L. Wiemels, H. H. Nelson, M. R. Karagas, J. F. Padbury, R. Bueno, D. J. Sugarbaker, R. F. Yeh, J. K. Wiencke & K. T. Kelsey (2009) Aging and environmental

exposures alter tissue-specific DNA methylation dependent upon CpG island context. *PLoS Genet,* 5**,** e1000602.

Cilia, R., S. Tunesi, G. Marotta, E. Cereda, C. Siri, S. Tesei, A. L. Zecchinelli, M. Canesi, C. B. Mariani, N. Meucci, G. Sacilotto, M. Zini, M. Barichella, C. Magnani, S. Duga, R. Asselta, G. Soldà, A. Seresini, M. Seia, G. Pezzoli & S. Goldwurm (2016) Survival and dementia in GBA-associated Parkinson's disease: The mutation matters. *Ann Neurol,* 80**,** 662-673.

Clark, L. N., B. M. Ross, Y. Wang, H. Mejia-Santana, J. Harris, E. D. Louis, L. J. Cote, H. Andrews, S. Fahn, C. Waters, B. Ford, S. Frucht, R. Ottman & K. Marder (2007) Mutations in the glucocerebrosidase gene are associated with early-onset Parkinson disease. *Neurology,* 69**,** 1270-7.

Cleeter, M. W., K. Y. Chau, C. Gluck, A. Mehta, D. A. Hughes, M. Duchen, N. W. Wood, J. Hardy, J. Mark Cooper & A. H. Schapira (2013) Glucocerebrosidase inhibition causes mitochondrial dysfunction and free radical damage. *Neurochem Int,* 62**,** 1-7.

Collier, T. J., K. R. Srivastava, C. Justman, T. Grammatopoulous, B. Hutter-Paier, M. Prokesch, D. Havas, J. C. Rochet, F. Liu, K. Jock, P. de Oliveira, G. L. Stirtz, U. Dettmer, C. E. Sortwell, M. B. Feany, P. Lansbury, L. Lapidus & K. L. Paumier (2017) Nortriptyline inhibits aggregation and neurotoxicity of alpha-synuclein by enhancing reconfiguration of the monomeric form. *Neurobiol Dis,* 106**,** 191-204.

Collins, L. M., J. Drouin-Ouellet, W. L. Kuan, T. Cox & R. A. Barker (2017) Dermal fibroblasts from patients with Parkinson's disease have normal GCase activity and autophagy compared to patients with PD and GBA mutations. *F1000Res,* 6**,** 1751.

Colosetti, P., A. Puissant, G. Robert, F. Luciano, A. Jacquel, P. Gounon, J. P. Cassuto & P. Auberger (2009) Autophagy is an important event for megakaryocytic differentiation of the chronic myelogenous leukemia K562 cell line. *Autophagy,* 5**,** 1092-8.

Conaco, C., S. Otto, J. J. Han & G. Mandel (2006) Reciprocal actions of REST and a microRNA promote neuronal identity. *Proc Natl Acad Sci U S A,* 103**,** 2422-7.

Cooper, O., H. Seo, S. Andrabi, C. Guardia-Laguarta, J. Graziotto, M. Sundberg, J. R. McLean, L. Carrillo-Reid, Z. Xie, T. Osborn, G. Hargus, M. Deleidi, T. Lawson, H. Bogetofte, E. Perez-Torres, L. Clark, C. Moskowitz, J. Mazzulli, L. Chen, L. Volpicelli-Daley, N. Romero, H. Jiang, R. J. Uitti, Z. Huang, G. Opala, L. A. Scarffe, V. L. Dawson, C. Klein, J. Feng, O. A. Ross, J. Q. Trojanowski, V. M. Lee, K. Marder, D. J. Surmeier, Z. K. Wszolek, S. Przedborski, D. Krainc, T. M. Dawson & O. Isacson (2012) Pharmacological rescue of mitochondrial deficits in iPSC-derived neural cells from patients with familial Parkinson's disease. *Sci Transl Med,* 4**,** 141ra90.

Cuervo, A. M., L. Stefanis, R. Fredenburg, P. T. Lansbury & D. Sulzer (2004) Impaired degradation of mutant alpha-synuclein by chaperone-mediated autophagy. *Science,* 305**,** 1292-5.

Cuervo, A. M. & E. Wong (2014) Chaperone-mediated autophagy: roles in disease and aging. *Cell Res,* 24**,** 92-104.

Cullen, V., S. P. Sardi, J. Ng, Y. H. Xu, Y. Sun, J. J. Tomlinson, P. Kolodziej, I. Kahn, P. Saftig, J. Woulfe, J. C. Rochet, M. A. Glicksman, S. H. Cheng, G. A. Grabowski, L. S. Shihabuddin & M. G. Schlossmacher (2011) Acid β-glucosidase

mutants linked to Gaucher disease, Parkinson disease, and Lewy body dementia alter α-synuclein processing. *Ann Neurol,* 69**,** 940-53.

Cárdenas, C., R. A. Miller, I. Smith, T. Bui, J. Molgó, M. Müller, H. Vais, K. H. Cheung, J. Yang, I. Parker, C. B. Thompson, M. J. Birnbaum, K. R. Hallows & J. K. Foskett (2010) Essential regulation of cell bioenergetics by constitutive InsP3 receptor Ca2+ transfer to mitochondria. *Cell,* 142**,** 270-83.

Damier, P., E. C. Hirsch, P. Zhang, Y. Agid & F. Javoy-Agid (1993) Glutathione peroxidase, glial cells and Parkinson's disease. *Neuroscience,* 52**,** 1-6.

Danzer, K. M., L. R. Kranich, W. P. Ruf, O. Cagsal-Getkin, A. R. Winslow, L. Zhu, C. R. Vanderburg & P. J. McLean (2012) Exosomal cell-to-cell transmission of alpha synuclein oligomers. *Mol Neurodegener,* 7**,** 42.

Davies, J. E., S. Sarkar & D. C. Rubinsztein (2006) Trehalose reduces aggregate formation and delays pathology in a transgenic mouse model of oculopharyngeal muscular dystrophy. *Hum Mol Genet,* 15**,** 23-31.

Davis, A. A., K. M. Andruska, B. A. Benitez, B. A. Racette, J. S. Perlmutter & C. Cruchaga (2016a) Variants in GBA, SNCA, and MAPT influence Parkinson disease risk, age at onset, and progression. *Neurobiol Aging,* 37**,** 209.e1-209.e7.

Davis, M. Y., C. O. Johnson, J. B. Leverenz, D. Weintraub, J. Q. Trojanowski, A. Chen-Plotkin, V. M. Van Deerlin, J. F. Quinn, K. A. Chung, A. L. Peterson-Hiller, L. S. Rosenthal, T. M. Dawson, M. S. Albert, J. G. Goldman, G. T. Stebbins, B. Bernard, Z. K. Wszolek, O. A. Ross, D. W. Dickson, D. Eidelberg, P. J. Mattis, M. Niethammer, D. Yearout, S. C. Hu, B. A. Cholerton, M. Smith, I. F. Mata, T. J. Montine, K. L. Edwards & C. P. Zabetian (2016b) Association of GBA Mutations and the E326K Polymorphism With Motor and Cognitive Progression in Parkinson Disease. *JAMA Neurol,* 73**,** 1217-1224.

de la Mata, M., D. Cotán, M. Oropesa-Ávila, J. Garrido-Maraver, M. D. Cordero, M. Villanueva Paz, A. Delgado Pavón, E. Alcocer-Gómez, I. de Lavera, P. Ybot-González, A. Paula Zaderenko, C. Ortiz Mellet, J. M. García Fernández & J. A. Sánchez-Alcázar (2015) Pharmacological Chaperones and Coenzyme Q10 Treatment Improves Mutant β-Glucocerebrosidase Activity and Mitochondrial Function in Neuronopathic Forms of Gaucher Disease. *Sci Rep,* 5**,** 10903.

Devi, L., V. Raghavendran, B. M. Prabhu, N. G. Avadhani & H. K. Anandatheerthavarada (2008) Mitochondrial import and accumulation of alpha-synuclein impair complex I in human dopaminergic neuronal cultures and Parkinson disease brain. *J Biol Chem,* 283**,** 9089-100.

Di Fonzo A., M. C. Dekker, P. Montagna, A. Baruzzi, E. H. Yonova, L. Correia Guedes, A. Szczerbinska, T. Zhao, L. O. Dubbel-Hulsman, C. H. Wouters, E. de Graaff, W. J. Oyen, E. J. Simons, G. J. Breedveld, B. A. Oostra, M. W. Horstink & V. Bonifati (2009) FBXO7 mutations cause autosomal recessive, early-onset parkinsonian-pyramidal syndrome. *Neurology,* 72**,** 240-5.

Dickson, D. W. (2012) Parkinson's disease and parkinsonism: neuropathology. *Cold Spring Harb Perspect Med,* 2.

Dong, J., N. Song, J. Xie & H. Jiang (2009) Ghrelin antagonized 1-methyl-4-phenylpyridinium (MPP(+))-induced apoptosis in MES23.5 cells. *J Mol Neurosci,* 37**,** 182-9.

Dooley, H. C., M. Razi, H. E. Polson, S. E. Girardin, M. I. Wilson & S. A. Tooze (2014) WIPI2 links LC3 conjugation with PI3P, autophagosome formation, and pathogen clearance by recruiting Atg12-5-16L1. *Mol Cell,* 55**,** 238-52.

Drouin-Ouellet, J., S. Lau, P. L. Brattås, D. Rylander Ottosson, K. Pircs, D. A. Grassi, L. M. Collins, R. Vuono, A. Andersson Sjöland, G. Westergren-Thorsson, C. Graff, L. Minthon, H. Toresson, R. A. Barker, J. Jakobsson & M. Parmar (2017) REST suppression mediates neural conversion of adult human fibroblasts via microRNA-dependent and -independent pathways. *EMBO Mol Med,* 9**,** 1117-1131.

Duran, R., N. E. Mencacci, A. V. Angeli, M. Shoai, E. Deas, H. Houlden, A. Mehta, D. Hughes, T. M. Cox, P. Deegan, A. H. Schapira, A. J. Lees, P. Limousin, P. R. Jarman, K. P. Bhatia, N. W. Wood, J. Hardy & T. Foltynie (2013) The glucocerobrosidase E326K variant predisposes to Parkinson's disease, but does not cause Gaucher's disease. *Mov Disord,* 28**,** 232-236.

Dvir, H., M. Harel, A. A. McCarthy, L. Toker, I. Silman, A. H. Futerman & J. L. Sussman (2003) X-ray structure of human acid-beta-glucosidase, the defective enzyme in Gaucher disease. *EMBO Rep,* 4**,** 704-9.

El-Agnaf, O. M., R. Jakes, M. D. Curran, D. Middleton, R. Ingenito, E. Bianchi, A. Pessi, D. Neill & A. Wallace (1998) Aggregates from mutant and wild-type alpha-synuclein proteins and NAC peptide induce apoptotic cell death in human neuroblastoma cells by formation of beta-sheet and amyloid-like filaments. *FEBS Lett,* 440**,** 71-5.

El-Mir, M. Y., V. Nogueira, E. Fontaine, N. Avéret, M. Rigoulet & X. Leverve (2000) Dimethylbiguanide inhibits cell respiration via an indirect effect targeted on the respiratory chain complex I. *J Biol Chem,* 275**,** 223-8.

Elizan, T. S., M. D. Yahr, D. A. Moros, M. R. Mendoza, S. Pang & C. A. Bodian (1989) Selegiline as an adjunct to conventional levodopa therapy in Parkinson's disease. Experience with this type B monoamine oxidase inhibitor in 200 patients. *Arch Neurol,* 46**,** 1280-3.

Eslamboli, A., B. Georgievska, R. M. Ridley, H. F. Baker, N. Muzyczka, C. Burger, R. J. Mandel, L. Annett & D. Kirik (2005) Continuous low-level glial cell line-derived neurotrophic factor delivery using recombinant adeno-associated viral vectors provides neuroprotection and induces behavioral recovery in a primate model of Parkinson's disease. *J Neurosci,* 25**,** 769-77.

Evans, J. R., S. L. Mason, C. H. Williams-Gray, T. Foltynie, C. Brayne, T. W. Robbins & R. A. Barker (2011) The natural history of treated Parkinson's disease in an incident, community based cohort. *J Neurol Neurosurg Psychiatry,* 82**,** 1112-8.

Farrer, L. A., L. A. Cupples, J. L. Haines, B. Hyman, W. A. Kukull, R. Mayeux, R. H. Myers, M. A. Pericak-Vance, N. Risch & C. M. van Duijn (1997) Effects of age, sex, and ethnicity on the association between apolipoprotein E genotype and Alzheimer disease. A meta-analysis. APOE and Alzheimer Disease Meta Analysis Consortium. *JAMA,* 278**,** 1349-56.

Fernandes, H. J., E. M. Hartfield, H. C. Christian, E. Emmanoulidou, Y. Zheng, H. Booth, H. Bogetofte, C. Lang, B. J. Ryan, S. P. Sardi, J. Badger, J. Vowles, S. Evetts, G. K. Tofaris, K. Vekrellis, K. Talbot, M. T. Hu, W. James, S. A. Cowley & R. Wade-Martins (2016) ER Stress and Autophagic Perturbations Lead to Elevated

Extracellular α-Synuclein in GBA-N370S Parkinson's iPSC-Derived Dopamine Neurons. *Stem Cell Reports,* 6**,** 342-56.

Ferreira, M. & J. Massano (2017) An updated review of Parkinson's disease genetics and clinicopathological correlations. *Acta Neurol Scand,* 135**,** 273-284.

Fishbein, I., Y. M. Kuo, B. I. Giasson & R. L. Nussbaum (2014) Augmentation of phenotype in a transgenic Parkinson mouse heterozygous for a Gaucher mutation. *Brain,* 137**,** 3235-47.

Foltynie, T., T. E. Goldberg, S. G. Lewis, A. D. Blackwell, B. S. Kolachana, D. R. Weinberger, T. W. Robbins & R. A. Barker (2004) Planning ability in Parkinson's disease is influenced by the COMT val158met polymorphism. *Mov Disord,* 19**,** 885-91.

Forno, L. S., J. W. Langston, L. E. DeLanney, I. Irwin & G. A. Ricaurte (1986) Locus ceruleus lesions and eosinophilic inclusions in MPTP-treated monkeys. *Ann Neurol,* 20**,** 449-55.

Fraga, M. F. & M. Esteller (2007) Epigenetics and aging: the targets and the marks. *Trends Genet,* 23**,** 413-8.

Fraser, H. B., P. Khaitovich, J. B. Plotkin, S. Pääbo & M. B. Eisen (2005) Aging and gene expression in the primate brain. *PLoS Biol,* 3**,** e274.

Furuya, N., J. Yu, M. Byfield, S. Pattingre & B. Levine (2005) The evolutionarily conserved domain of Beclin 1 is required for Vps34 binding, autophagy and tumor suppressor function. *Autophagy,* 1**,** 46-52.

Furuya, T., H. Hayakawa, M. Yamada, K. Yoshimi, S. Hisahara, M. Miura, Y. Mizuno & H. Mochizuki (2004) Caspase-11 mediates inflammatory dopaminergic cell death in the 1-methyl-4-phenyl-1,2,3,6-tetrahydropyridine mouse model of Parkinson's disease. *J Neurosci,* 24**,** 1865-72.

Gan-Or, Z., P. A. Dion & G. A. Rouleau (2015) Genetic perspective on the role of the autophagy-lysosome pathway in Parkinson disease. *Autophagy,* 11**,** 1443-57.

Gan-Or, Z., N. Giladi, U. Rozovski, C. Shifrin, S. Rosner, T. Gurevich, A. Bar-Shira & A. Orr-Urtreger (2008) Genotype-phenotype correlations between GBA mutations and Parkinson disease risk and onset. *Neurology,* 70**,** 2277-83.

Gash, D. M., Z. Zhang, A. Ovadia, W. A. Cass, A. Yi, L. Simmerman, D. Russell, D. Martin, P. A. Lapchak, F. Collins, B. J. Hoffer & G. A. Gerhardt (1996) Functional recovery in parkinsonian monkeys treated with GDNF. *Nature,* 380**,** 252-5.

Gasmi, M., E. P. Brandon, C. D. Herzog, A. Wilson, K. M. Bishop, E. K. Hofer, J. J. Cunningham, M. A. Printz, J. H. Kordower & R. T. Bartus (2007) AAV2-mediated delivery of human neurturin to the rat nigrostriatal system: long-term efficacy and tolerability of CERE-120 for Parkinson's disease. *Neurobiol Dis,* 27**,** 67-76.

Gassen, N. C., J. Hartmann, J. Zschocke, J. Stepan, K. Hafner, A. Zellner, T. Kirmeier, L. Kollmannsberger, K. V. Wagner, N. Dedic, G. Balsevich, J. M. Deussing, S. Kloiber, S. Lucae, F. Holsboer, M. Eder, M. Uhr, M. Ising, M. V. Schmidt & T. Rein (2014) Association of FKBP51 with priming of autophagy pathways and mediation of antidepressant treatment response: evidence in cells, mice, and humans. *PLoS Med,* 11**,** e1001755.

Ge, H., L. Tan, P. Wu, Y. Yin, X. Liu, H. Meng, G. Cui, N. Wu, J. Lin, R. Hu & H. Feng (2015) Poly-L-ornithine promotes preferred differentiation of neural stem/progenitor cells via ERK signalling pathway. *Sci Rep,* 5**,** 15535.

Gegg, M. E, J. M. Cooper, K. Y. Chau, M. Rojo, A. H. Schapira & J. W. Taanman (2010) Mitofusin 1 and mitofusin 2 are ubiquitinated in a PINK1/parkin-dependent manner upon induction of mitophagy. *Hum Mol Genet,* 19**,** 4861-70.

Gegg, M. E., D. Burke, S. J. Heales, J. M. Cooper, J. Hardy, N. W. Wood & A. H. Schapira (2012) Glucocerebrosidase deficiency in substantia nigra of parkinson disease brains. *Ann Neurol,* 72**,** 455-63.

Gegg, M. E., L. Sweet, B. H. Wang, L. S. Shihabuddin, S. P. Sardi & A. H. Schapira (2015) No evidence for substrate accumulation in Parkinson brains with GBA mutations. *Mov Disord,* 8**,** 1085-9.

Geisler, S., K. M. Holmström, D. Skujat, F. C. Fiesel, O. C. Rothfuss, P. J. Kahle & W. Springer (2010) PINK1/Parkin-mediated mitophagy is dependent on VDAC1 and p62/SQSTM1. *Nat Cell Biol,* 12**,** 119-31.

Giasson, B. I., J. E. Duda, S. M. Quinn, B. Zhang, J. Q. Trojanowski & V. M. Lee (2002) Neuronal alpha-synucleinopathy with severe movement disorder in mice expressing A53T human alpha-synuclein. *Neuron,* 34**,** 521-33.

Glass, D., A. Viñuela, M. N. Davies, A. Ramasamy, L. Parts, D. Knowles, A. A. Brown, A. K. Hedman, K. S. Small, A. Buil, E. Grundberg, A. C. Nica, P. Di Meglio, F. O. Nestle, M. Ryten, R. Durbin, M. I. McCarthy, P. Deloukas, E. T. Dermitzakis, M. E. Weale, V. Bataille, T. D. Spector, U. B. E. consortium & M. consortium (2013) Gene expression changes with age in skin, adipose tissue, blood and brain. *Genome Biol,* 14**,** R75.

Goker-Alpan, O., B. I. Giasson, M. J. Eblan, J. Nguyen, H. I. Hurtig, V. M. Lee, J. Q. Trojanowski & E. Sidransky (2006) Glucocerebrosidase mutations are an important risk factor for Lewy body disorders. *Neurology,* 67**,** 908-10.

Goker-Alpan, O., G. Lopez, J. Vithayathil, J. Davis, M. Hallett & E. Sidransky (2008) The spectrum of parkinsonian manifestations associated with glucocerebrosidase mutations. *Arch Neurol,* 65**,** 1353-7.

Goker-Alpan, O., R. Schiffmann, M. E. LaMarca, R. L. Nussbaum, A. McInerney-Leo & E. Sidransky (2004) Parkinsonism among Gaucher disease carriers. *J Med Genet,* 41**,** 937-40.

Goker-Alpan, O., B. K. Stubblefield, B. I. Giasson & E. Sidransky (2010) Glucocerebrosidase is present in α-synuclein inclusions in Lewy body disorders. *Acta Neuropathol,* 120**,** 641-9.

Gorbatyuk, O. S., S. Li, K. Nash, M. Gorbatyuk, A. S. Lewin, L. F. Sullivan, R. J. Mandel, W. Chen, C. Meyers, F. P. Manfredsson & N. Muzyczka (2010) In vivo RNAi-mediated alpha-synuclein silencing induces nigrostriatal degeneration. *Mol Ther,* 18**,** 1450-7.

Gore A., Z. Li, H. L. Fung, J. E. Young, S. Agarwal, J. Antosiewicz-Bourget, I. Canto, A. Giorgetti, M. A. Israel, E. Kiskinis, J. H. Lee, Y. H. Loh, P. D. Manos, N. Monteserrat, A. D. Panopoulos, S. Ruiz, M. L Wilbert, J. Yu, E. F. Kirkness, J. C. Izpisua Belmonte, D. J. Rossi, J. A. Thomson, K. Eggan, G. Q. Daley, L. S. Goldstein & K. Zhang (2011) Somatic coding mutations in human induced pluripotent stem cells. *Nature,* 471**,** 63-7.

Goris, A., C. H. Williams-Gray, G. R. Clark, T. Foltynie, S. J. Lewis, J. Brown, M. Ban, M. G. Spillantini, A. Compston, D. J. Burn, P. F. Chinnery, R. A. Barker & S. J. Sawcer (2007) Tau and alpha-synuclein in susceptibility to, and dementia in, Parkinson's disease. *Ann Neurol,* 62**,** 145-53.

Grabowski, G. A. (2008) Phenotype, diagnosis, and treatment of Gaucher's disease. *Lancet,* 372**,** 1263-71.

Gray, D. A., M. Tsirigotis & J. Woulfe (2003) Ubiquitin, proteasomes, and the aging brain. *Sci Aging Knowledge Environ,* 2003**,** RE6.

Greenland, J. C., C. H. Williams-Gray & R. A. Barker (2019) The clinical heterogeneity of Parkinson's disease and its therapeutic implications. *Eur J Neurosci,* 49**,** 328-338.

Grskovic, M., A. Javaherian, B. Strulovici, & G. Q. Daley (2011) Induced pluripotent stem cells--opportunities for disease modelling and drug discovery. *Nat Rev Drug Discov,* 10**,** 915-29.

Guo, S., X. Zi, V. P. Schulz, J. Cheng, M. Zhong, S. H. Koochaki, C. M. Megyola, X. Pan, K. Heydari, S. M. Weissman, P. G. Gallagher, D. S. Krause, R. Fan & J. Lu (2014) Nonstochastic reprogramming from a privileged somatic cell state. *Cell,* 156**,** 649-62.

Gutierrez, M. G., S. S. Master, S. B. Singh, G. A. Taylor, M. I. Colombo & V. Deretic (2004) Autophagy is a defense mechanism inhibiting BCG and Mycobacterium tuberculosis survival in infected macrophages. *Cell,* 119**,** 753-66.

Halperin, A., D. Elstein & A. Zimran (2006) Increased incidence of Parkinson disease among relatives of patients with Gaucher disease. *Blood Cells Mol Dis,* 36**,** 426-8.

Hardie, D. G. (2004) The AMP-activated protein kinase pathway--new players upstream and downstream. *J Cell Sci,* 117**,** 5479-87.

Hardie, D. G., F. A. Ross & S. A. Hawley (2012) AMPK: a nutrient and energy sensor that maintains energy homeostasis. *Nat Rev Mol Cell Biol,* 13**,** 251-62.

Hartfield, E. M., M. Yamasaki-Mann, H. J. Ribeiro Fernandes, J. Vowles, W. S. James, S. A. Cowley & R. Wade-Martins (2014) Physiological characterisation of human iPS-derived dopaminergic neurons. *PLos One,* 9, e87388.

Hasegawa, T., M. Matsuzaki, A. Takeda, A. Kikuchi, H. Akita, G. Perry, M. A. Smith & Y. Itoyama (2004) Accelerated alpha-synuclein aggregation after differentiation of SH-SY5Y neuroblastoma cells. *Brain Res,* 1013**,** 51-9.

HD_iPSC_Consortium (2012) Induced pluripotent stem cells from patients with Huntington's disease show CAG-repeat-expansion-associated phenotypes. *Cell Stem Cell,* 11**,** 264-78.

Hebron, M. L., I. Lonskaya & C. E. Moussa (2013) Nilotinib reverses loss of dopamine neurons and improves motor behavior via autophagic degradation of α-synuclein in Parkinson's disease models. *Hum Mol Genet,* 22**,** 3315-28.

Hennekam R. C. (2006) Hutchinson-Gilford progeria syndrome: review of the phenotype. *J Med Genet A,* 140**,** 2603-24.

Hernán MA, Takkouche B, Caamaño-Isorna F, Gestal-Otero JJ (2002) A meta-analysis of coffee drinking, cigarette smoking, and the risk of Parkinson's disease. *Ann Neurol,* Sep;52(3):276-84.

Hirsch, E. C. & S. Hunot (2009) Neuroinflammation in Parkinson's disease: a target for neuroprotection? *Lancet Neurol,* 8**,** 382-97.

Horowitz, M., S. Wilder, Z. Horowitz, O. Reiner, T. Gelbart & E. Beutler (1989) The human glucocerebrosidase gene and pseudogene: structure and evolution. *Genomics,* 4**,** 87-96.

Horvath, S. (2013) DNA methylation age of human tissues and cell types. *Genome Biol,* 14**,** R115.

Horvath, S., Y. Zhang, P. Langfelder, R. S. Kahn, M. P. Boks, K. van Eijk, L. H. van den Berg & R. A. Ophoff (2012) Aging effects on DNA methylation modules in human brain and blood tissue. *Genome Biol,* 13**,** R97.

Hosokawa, N., T. Hara, T. Kaizuka, C. Kishi, A. Takamura, Y. Miura, S. Iemura, T. Natsume, K. Takehana, N. Yamada, J. L. Guan, N. Oshiro & N. Mizushima (2009) Nutrient-dependent mTORC1 association with the ULK1-Atg13-FIP200 complex required for autophagy. *Mol Biol Cell,* 20**,** 1981-91.

Hou, Y. S., J. J. Guan, H. D. Xu, F. Wu, R. Sheng & Z. H. Qin (2015) Sestrin2 Protects Dopaminergic Cells against Rotenone Toxicity through AMPK-Dependent Autophagy Activation. *Mol Cell Biol,* 35**,** 2740-51.

Hruska, K. S., M. E. LaMarca, C. R. Scott & E. Sidransky (2008) Gaucher disease: mutation and polymorphism spectrum in the glucocerebrosidase gene (GBA). *Hum Mutat,* 29**,** 567-83.

Hsu, L. J., Y. Sagara, A. Arroyo, E. Rockenstein, A. Sisk, M. Mallory, J. Wong, T. Takenouchi, M. Hashimoto & E. Masliah (2000) alpha-synuclein promotes mitochondrial deficit and oxidative stress. *Am J Pathol,* 157**,** 401-10.

Hu, W., B. Qiu, W. Guan, Q. Wang, M. Wang, W. Li, L. Gao, L. Shen, Y. Huang, G. Xie, H. Zhao, Y. Jin, B. Tang, Y. Yu, J. Zhao & G. Pei (2015) Direct Conversion of Normal and Alzheimer's Disease Human Fibroblasts into Neuronal Cells by Small Molecules. *Cell Stem Cell,* 17**,** 204-12.

Huh, C. J., B. Zhang, M. B. Victor, S. Dahiya, L. F. Batista, S. Horvath & A. S. Yoo (2016) Maintenance of age in human neurons generated by microRNA-based neuronal conversion of fibroblasts. *Elife,* 5.

Hussein S. M., N. N. Batada, S. Vuoristo, R. W. Ching, R. Autio, E. Närvä, S. Ng, M. Sourour, R. Hämäläinen, C. Olsson, K. Lundin, M. Mikkola, R. Trokovic, M. Peitz, O. Brüstle, D. P. Bazett-Jones, K. Alitalo, R. Lahesmaa, A. Nagy & T. Otonkoski (2011) Copy number variation and selection during reprogramming to pluripotency. *Nature,* 471, 58-62

Høyer-Hansen, M. & M. Jäättelä (2007) Connecting endoplasmic reticulum stress to autophagy by unfolded protein response and calcium. *Cell Death Differ,* 14**,** 1576-82.

Imamura, K., N. Hishikawa, M. Sawada, T. Nagatsu, M. Yoshida & Y. Hashizume (2003) Distribution of major histocompatibility complex class II-positive microglia and cytokine profile of Parkinson's disease brains. *Acta Neuropathol,* 106**,** 518-26.

Ishii, T., T. Yanagawa, K. Yuki, T. Kawane, H. Yoshida & S. Bannai (1997) Low micromolar levels of hydrogen peroxide and proteasome inhibitors induce the 60-kDa A170 stress protein in murine peritoneal macrophages. *Biochem Biophys Res Commun,* 232**,** 33-7.

Jenner, P. (2003) Dopamine agonists, receptor selectivity and dyskinesia induction in Parkinson's disease. *Curr Opin Neurol,* 16 Suppl 1**,** S3-7.

Jeon, I., N. Lee, J. Y. Li, I. H. Park, K. S. Park, J. Moon, S. H. Shim, C. Choi, D. J. Chang, J. Kwon, S. H. Oh, D. A. Shin, H. S. Kim, J. T. Do, D. R. Lee, M. Kim, K. S. Kang, G. Q. Daley, P. Brundin & J. Song (2012) Neuronal properties, in vivo effects, and pathology of a Huntington's disease patient-derived induced pluripotent stem cells. *Stem Cells,* 30**,** 2054-62.

Jesús, S., I. Huertas, I. Bernal-Bernal, M. Bonilla-Toribio, M. T. Cáceres-Redondo, L. Vargas-González, M. Gómez-Llamas, F. Carrillo, E. Calderón, M. Carballo, P. Gómez-Garre & P. Mir (2016) GBA Variants Influence Motor and Non-Motor Features of Parkinson's Disease. *PLoS One,* 11**,** e0167749.

Jiang, H., L. J. Li, J. Wang & J. X. Xie (2008) Ghrelin antagonizes MPTP-induced neurotoxicity to the dopaminergic neurons in mouse substantia nigra. *Exp Neurol,* 212**,** 532-7.

Johnson, D. S., A. Mortazavi, R. M. Myers & B. Wold (2007) Genome-wide mapping of in vivo protein-DNA interactions. *Science,* 316**,** 1497-502.

Joselin, A. P., S. J. Hewitt, S. M. Callaghan, R. H. Kim, Y. H. Chung, T. W. Mak, J. Shen, R. S. Slack & D. S. Park (2012) ROS-dependent regulation of Parkin and DJ-1 localization during oxidative stress in neurons. *Hum Mol Genet,* 21**,** 4888-903.

Jović, M., M. J. Kean, Z. Szentpetery, G. Polevoy, A. C. Gingras, J. A. Brill & T. Balla (2012) Two phosphatidylinositol 4-kinases control lysosomal delivery of the Gaucher disease enzyme, β-glucocerebrosidase. *Mol Biol Cell,* 23**,** 1533-45.

Jovičić, A., J. Mertens, S. Boeynaems, E. Bogaert, N. Chai, S. B. Yamada, J. W. Paul, S. Sun, J. R. Herdy, G. Bieri, N. J. Kramer, F. H. Gage, L. Van Den Bosch, W. Robberecht & A. D. Gitler (2015) Modifiers of C9orf72 dipeptide repeat toxicity connect nucleocytoplasmic transport defects to FTD/ALS. *Nat Neurosci,* 18**,** 1226-9.

Kalia, L. V., S. K. Kalia, P. J. McLean, A. M. Lozano & A. E. Lang (2013a) α-Synuclein oligomers and clinical implications for Parkinson disease. *Ann Neurol,* 73**,** 155-69.

Kalia, L. V. & A. E. Lang (2015) Parkinson's disease. *Lancet,* 386**,** 896-912.

Kalia, L. V., A. E. Lang, L. N. Hazrati, S. Fujioka, Z. K. Wszolek, D. W. Dickson, O. A. Ross, V. M. Van Deerlin, J. Q. Trojanowski, H. I. Hurtig, R. N. Alcalay, K. S. Marder, L. N. Clark, C. Gaig, E. Tolosa, J. Ruiz-Martínez, J. F. Marti-Masso, I. Ferrer, A. López de Munain, S. M. Goldman, B. Schüle, J. W. Langston, J. O. Aasly, M. T. Giordana, V. Bonifati, A. Puschmann, M. Canesi, G. Pezzoli, A. Maues De Paula, K. Hasegawa, C. Duyckaerts, A. Brice, A. J. Stoessl & C. Marras (2015) Clinical correlations with Lewy body pathology in LRRK2-related Parkinson disease. *JAMA Neurol,* 72**,** 100-5.

Kalia, S. K., T. Sankar & A. M. Lozano (2013b) Deep brain stimulation for Parkinson's disease and other movement disorders. *Curr Opin Neurol,* 26**,** 374-80.

Kamp, F., N. Exner, A. K. Lutz, N. Wender, J. Hegermann, B. Brunner, B. Nuscher, T. Bartels, A. Giese, K. Beyer, S. Eimer, K. F. Winklhofer & C. Haass (2010) Inhibition of mitochondrial fusion by α-synuclein is rescued by PINK1, Parkin and DJ-1. *EMBO J,* 29**,** 3571-89.

Kanaan, N. M. & F. P. Manfredsson (2012) Loss of functional alpha-synuclein: a toxic event in Parkinson's disease? *J Parkinsons Dis,* 2**,** 249-67.

Kandror, O., N. Bretschneider, E. Kreydin, D. Cavalieri & A. L. Goldberg (2004) Yeast adapt to near-freezing temperatures by STRE/Msn2,4-dependent induction of trehalose synthesis and certain molecular chaperones. *Mol Cell,* 13**,** 771-81.

Khoo, T. K., A. J. Yarnall, G. W. Duncan, S. Coleman, J. T. O'Brien, D. J. Brooks, R. A. Barker & D. J. Burn (2013) The spectrum of nonmotor symptoms in early Parkinson disease. *Neurology,* 80**,** 276-81.

Kieburtz, K. & B. Ravina (2007) Why hasn't neuroprotection worked in Parkinson's disease? *Nat Clin Pract Neurol,* 3**,** 240-1.

Kikuchi, T., A. Morizane, D. Doi, H. Magotani, H. Onoe, T. Hayashi, H. Mizuma, S. Takara, R. Takahashi, H. Inoue, S. Morita, M. Yamamoto, K. Okita, M. Nakagawa, M. Parmar & J. Takahashi (2017) Human iPS cell-derived dopaminergic neurons function in a primate Parkinson's disease model. *Nature,* 548**,** 592-596.

Kim, Y., X. Zheng, Z. Ansari, M. C. Bunnell, J. R. Herdy, L. Traxler, H. Lee, A. C. M. Paquola, C. Blithikioti, M. Ku, J. C. M. Schlachetzki, J. Winkler, F. Edenhofer, C. K. Glass, A. A. Paucar, B. N. Jaeger, S. Pham, L. Boyer, B. C. Campbell, T. Hunter, J. Mertens & F. H. Gage (2018) Mitochondrial Aging Defects Emerge in Directly Reprogrammed Human Neurons due to Their Metabolic Profile. *Cell Rep,* 23**,** 2550-2558.

Kitada, T., S. Asakawa, N. Hattori, H. Matsumine, Y. Yamamura, S. Minoshima, M. Yokochi, Y. Mizuno & N. Shimizu (1998) Mutations in the parkin gene cause autosomal recessive juvenile parkinsonism. *Nature,* 392**,** 605-8.

Klein, C. & A. Westenberger (2012) Genetics of Parkinson's disease. *Cold Spring Harb Perspect Med,* 2**,** a008888.

Klionsky, D. J., K. Abdelmohsen, A. Abe, M. J. Abedin, H. Abeliovich, A. Acevedo Arozena, H. Adachi, C. M. Adams, P. D. Adams, K. Adeli, P. J. Adhihetty, S. G. Adler, G. Agam, R. Agarwal, M. K. Aghi, M. Agnello, P. Agostinis, P. V. Aguilar, J. Aguirre-Ghiso, E. M. Airoldi, S. Ait-Si-Ali, T. Akematsu, E. T. Akporiaye, M. Al-Rubeai, G. M. Albaiceta, C. Albanese, D. Albani, M. L. Albert, J. Aldudo, H. Algül, M. Alirezaei, I. Alloza, A. Almasan, M. Almonte-Beceril, E. S. Alnemri, C. Alonso, N. Altan-Bonnet, D. C. Altieri, S. Alvarez, L. Alvarez-Erviti, S. Alves, G. Amadoro, A. Amano, C. Amantini, S. Ambrosio, I. Amelio, A. O. Amer, M. Amessou, A. Amon, Z. An, F. A. Anania, S. U. Andersen, U. P. Andley, C. K. Andreadi, N. Andrieu-Abadie, A. Anel, D. K. Ann, S. Anoopkumar-Dukie, M. Antonioli, H. Aoki, N. Apostolova, S. Aquila, K. Aquilano, K. Araki, E. Arama, A. Aranda, J. Araya, A. Arcaro, E. Arias, H. Arimoto, A. R. Ariosa, J. L. Armstrong, T. Arnould, I. Arsov, K. Asanuma, V. Askanas, E. Asselin, R. Atarashi, S. S. Atherton, J. D. Atkin, L. D. Attardi, P. Auberger, G. Auburger, L. Aurelian, R. Autelli, L. Avagliano, M. L. Avantaggiati, L. Avrahami, S. Awale, N. Azad, T. Bachetti, J. M. Backer, D. H. Bae, J. S. Bae, O. N. Bae, S. H. Bae, E. H. Baehrecke, S. H. Baek, S. Baghdiguian, A. Bagniewska-Zadworna, et al. (2016) Guidelines for the use and interpretation of assays for monitoring autophagy (3rd edition). *Autophagy,* 12**,** 1-222.

Kopito, R. R. (1997) ER quality control: the cytoplasmic connection. *Cell,* 88**,** 427-30.

Kordower, J. H., Y. Chu, R. A. Hauser, T. B. Freeman & C. W. Olanow (2008) Lewy body-like pathology in long-term embryonic nigral transplants in Parkinson's disease. *Nat Med,* 14**,** 504-6.

Kordower, J. H., C. D. Herzog, B. Dass, R. A. Bakay, J. Stansell, M. Gasmi & R. T. Bartus (2006) Delivery of neurturin by AAV2 (CERE-120)-mediated gene transfer provides structural and functional neuroprotection and neurorestoration in MPTP-treated monkeys. *Ann Neurol,* 60**,** 706-15.

Kowall, N. W., P. Hantraye, E. Brouillet, M. F. Beal, A. C. McKee & R. J. Ferrante (2000) MPTP induces alpha-synuclein aggregation in the substantia nigra of baboons. *Neuroreport,* 11**,** 211-3.

Krüger, U., Y. Wang, S. Kumar & E. M. Mandelkow (2012) Autophagic degradation of tau in primary neurons and its enhancement by trehalose. *Neurobiol Aging,* 33**,** 2291-305.

Kumar, K. R., A. Ramirez, A. Göbel, N. Kresojević, M. Svetel, K. Lohmann, C. M Sue, A. Rolfs, J. R. Mazzulli, R. N. Alcalay, D. Krainc, C. Klein, V. Kostic & A. Grünewald (2013) Glucocerebrosidase mutations in a Serbian Parkinson's disease population. *Eur J Neurol,* 20**,** 402-5.

Kuusisto, E., T. Suuronen & A. Salminen (2001) Ubiquitin-binding protein p62 expression is induced during apoptosis and proteasomal inhibition in neuronal cells. *Biochem Biophys Res Commun,* 280**,** 223-8.

Lachman, H. M., D. F. Papolos, T. Saito, Y. M. Yu, C. L. Szumlanski & R. M. Weinshilboum (1996) Human catechol-O-methyltransferase pharmacogenetics: description of a functional polymorphism and its potential application to neuropsychiatric disorders. *Pharmacogenetics,* 6**,** 243-50.

Ladewig, J., J. Mertens, J. Kesavan, J. Doerr, D. Poppe, F. Glaue, S. Herms, P. Wernet, G. Kögler, F. J. Müller, P. Koch & O. Brüstle (2012) Small molecules enable highly efficient neuronal conversion of human fibroblasts. *Nat Methods,* 9**,** 575-8.

Langston, J. W., P. Ballard, J. W. Tetrud & I. Irwin (1983) Chronic Parkinsonism in humans due to a product of meperidine-analog synthesis. *Science,* 219**,** 979-80.

Langston, J. W. & P. A. Ballard (1983) Parkinson's disease in a chemist working with 1-methyl-4-phenyl-1,2,5,6-tetrahydropyridine. *N Engl J Med,* 309**,** 310.

Lapasset, L., O. Milhavet, A. Prieur, E. Besnard, A. Babled, N. Aït-Hamou, J. Leschik, F. Pellestor, J. M. Ramirez, J. De Vos, S. Lehmann & J. M. Lemaitre (2011) Rejuvenating senescent and centenarian human cells by reprogramming through the pluripotent state. *Genes Dev,* 25**,** 2248-53.

Lee, S. W., Y. M. Oh, Y. L. Lu, W. K. Kim & A. S. Yoo (2018) MicroRNAs Overcome Cell Fate Barrier by Reducing EZH2-Controlled REST Stability during Neuronal Conversion of Human Adult Fibroblasts. *Dev Cell,* 46**,** 73-84.e7.

Leroy, E., R. Boyer, G. Auburger, B. Leube, G. Ulm, E. Mezey, G. Harta, M. J. Brownstein, S. Jonnalagada, T. Chernova, A. Dehejia, C. Lavedan, T. Gasser, P. J. Steinbach, K. D. Wilkinson & M. H. Polymeropoulos (1998) The ubiquitin pathway in Parkinson's disease. *Nature,* 395**,** 451-2.

Lesage, S., M. Anheim, C. Condroyer, P. Pollak, F. Durif, C. Dupuits, F. Viallet, E. Lohmann, J. C. Corvol, A. Honoré, S. Rivaud, M. Vidailhet, A. Dürr, A. Brice & F. P. s. D. G. S. Group (2011) Large-scale screening of the Gaucher's disease-

related glucocerebrosidase gene in Europeans with Parkinson's disease. *Hum Mol Genet,* 20**,** 202-10.

Lesage, S. & A. Brice (2009) Parkinson's disease: from monogenic forms to genetic susceptibility factors. *Hum Mol Genet,* 18**,** R48-59.

Lessard, J., J. I. Wu, J. A. Ranish, M. Wan, M. M. Winslow, B. T. Staahl, H. Wu, R. Aebersold, I. A. Graef & G. R. Crabtree (2007) An essential switch in subunit composition of a chromatin remodeling complex during neural development. *Neuron,* 55**,** 201-15.

Lewis, J., H. Melrose, D. Bumcrot, A. Hope, C. Zehr, S. Lincoln, A. Braithwaite, Z. He, S. Ogholikhan, K. Hinkle, C. Kent, I. Toudjarska, K. Charisse, R. Braich, R. K. Pandey, M. Heckman, D. M. Maraganore, J. Crook & M. J. Farrer (2008) In vivo silencing of alpha-synuclein using naked siRNA. *Mol Neurodegener,* 3**,** 19.

Li, H., A. Ham, T. C. Ma, S. H. Kuo, E. Kanter, D. Kim, H. S. Ko, Y. Quan, S. P. Sardi, A. Li, O. Arancio, U. J. Kang, D. Sulzer & G. Tang (2018) Mitochondrial dysfunction and mitophagy defect triggered by heterozygous GBA mutations. *Autophagy***,** 1-18.

Li, W., E. Englund, H. Widner, B. Mattsson, D. van Westen, J. Lätt, S. Rehncrona, P. Brundin, A. Björklund, O. Lindvall & J. Y. Li (2016) Extensive graft-derived dopaminergic innervation is maintained 24 years after transplantation in the degenerating parkinsonian brain. *Proc Natl Acad Sci U S A,* 113**,** 6544-9.

Lill, C. M., J. T. Roehr, M. B. McQueen, F. K. Kavvoura, S. Bagade, B. M. Schjeide, L. M. Schjeide, E. Meissner, U. Zauft, N. C. Allen, T. Liu, M. Schilling, K. J. Anderson, G. Beecham, D. Berg, J. M. Biernacka, A. Brice, A. L. DeStefano, C. B. Do, N. Eriksson, S. A. Factor, M. J. Farrer, T. Foroud, T. Gasser, T. Hamza, J. A. Hardy, P. Heutink, E. M. Hill-Burns, C. Klein, J. C. Latourelle, D. M. Maraganore, E. R. Martin, M. Martinez, R. H. Myers, M. A. Nalls, N. Pankratz, H. Payami, W. Satake, W. K. Scott, M. Sharma, A. B. Singleton, K. Stefansson, T. Toda, J. Y. Tung, J. Vance, N. W. Wood, C. P. Zabetian, P. Young, R. E. Tanzi, M. J. Khoury, F. Zipp, H. Lehrach, J. P. Ioannidis, L. Bertram, a. G. E. o. P. s. D. Consortium, I. P. s. D. G. Consortium, P. s. D. G. Consortium & W. T. C. C. C. 2) (2012) Comprehensive research synopsis and systematic meta-analyses in Parkinson's disease genetics: The PDGene database. *PLoS Genet,* 8**,** e1002548.

Lim, L. P., N. C. Lau, P. Garrett-Engele, A. Grimson, J. M. Schelter, J. Castle, D. P. Bartel, P. S. Linsley & J. M. Johnson (2005) Microarray analysis shows that some microRNAs downregulate large numbers of target mRNAs. *Nature,* 433**,** 769-73.

Liu, G., B. Boot, J. J. Locascio, I. E. Jansen, S. Winder-Rhodes, S. Eberly, A. Elbaz, A. Brice, B. Ravina, J. J. van Hilten, F. Cormier-Dequaire, J. C. Corvol, R. A. Barker, P. Heutink, J. Marinus, C. H. Williams-Gray, C. R. Scherzer & f. t. G. o. P. D. P. I. Consortium (2016a) Neuropathic Gaucher's mutations accelerate cognitive decline in Parkinson's. *Ann Neurol*.

Liu, M. L., T. Zang & C. L. Zhang (2016b) Direct Lineage Reprogramming Reveals Disease-Specific Phenotypes of Motor Neurons from Human ALS Patients. *Cell Rep,* 14**,** 115-28.

Liu, M. L., T. Zang, Y. Zou, J. C. Chang, J. R. Gibson, K. M. Huber & C. L. Zhang (2013) Small molecules enable neurogenin 2 to efficiently convert human fibroblasts into cholinergic neurons. *Nat Commun,* 4**,** 2183.

Liu, R., H. Barkhordarian, S. Emadi, C. B. Park & M. R. Sierks (2005) Trehalose differentially inhibits aggregation and neurotoxicity of beta-amyloid 40 and 42. *Neurobiol Dis,* 20**,** 74-81.

Lo, L. C., J. E. Johnson, C. W. Wuenschell, T. Saito & D. J. Anderson (1991) Mammalian achaete-scute homolog 1 is transiently expressed by spatially restricted subsets of early neuroepithelial and neural crest cells. *Genes Dev,* 5**,** 1524-37.

Lu, M., C. Su, C. Qiao, Y. Bian, J. Ding & G. Hu (2016) Metformin Prevents Dopaminergic Neuron Death in MPTP/P-Induced Mouse Model of Parkinson's Disease via Autophagy and Mitochondrial ROS Clearance. *Int J Neuropsychopharmacol,* 19.

Lu, T., Y. Pan, S. Y. Kao, C. Li, I. Kohane, J. Chan & B. A. Yankner (2004) Gene regulation and DNA damage in the ageing human brain. *Nature,* 429**,** 883-91.

Ludwig, T., R. Le Borgne & B. Hoflack (1995) Roles for mannose-6-phosphate receptors in lysosomal enzyme sorting, IGF-II binding and clathrin-coat assembly. *Trends Cell Biol,* 5**,** 202-6.

Luk, K. C., V. Kehm, J. Carroll, B. Zhang, P. O'Brien, J. Q. Trojanowski & V. M. Lee (2012a) Pathological α-synuclein transmission initiates Parkinson-like neurodegeneration in nontransgenic mice. *Science,* 338**,** 949-53.

Luk, K. C., V. M. Kehm, B. Zhang, P. O'Brien, J. Q. Trojanowski & V. M. Lee (2012b) Intracerebral inoculation of pathological α-synuclein initiates a rapidly progressive neurodegenerative α-synucleinopathy in mice. *J Exp Med,* 209**,** 975-86.

Luk, K. C., C. Song, P. O'Brien, A. Stieber, J. R. Branch, K. R. Brunden, J. Q. Trojanowski & V. M. Lee (2009) Exogenous alpha-synuclein fibrils seed the formation of Lewy body-like intracellular inclusions in cultured cells. *Proc Natl Acad Sci U S A,* 106**,** 20051-6.

Lunde, K. A., J. Chung, I. Dalen, K. F. Pedersen, J. Linder, M. E. Domellöf, E. Elgh, A. D. Macleod, C. Tzoulis, J. P. Larsen, O. B. Tysnes, L. Forsgren, C. E. Counsell, G. Alves & J. Maple-Grødem (2018) Association of glucocerebrosidase polymorphisms and mutations with dementia in incident Parkinson's disease. *Alzheimers Dement,* 14**,** 1293-1301.

Lwin, A., E. Orvisky, O. Goker-Alpan, M. E. LaMarca & E. Sidransky (2004) Glucocerebrosidase mutations in subjects with parkinsonism. *Mol Genet Metab,* 81**,** 70-3.

Lyons, K. E., J. P. Hubble, A. I. Tröster, R. Pahwa & W. C. Koller (1998) Gender differences in Parkinson's disease. *Clin Neuropharmacol,* 21**,** 118-21.

Maherali, N., R. Sridharan, W. Xie, J. Utikal, S. Eminli, K. Arnold, M. Stadtfeld, R. Yachechko, J. Tchieu, R. Jaenisch, K. Plath & K. Hochedlinger (2007) Directly reprogrammed fibroblasts show global epigenetic remodeling and widespread tissue contribution. *Cell Stem Cell,* 1**,** 55-70.

Mall, M., M. S. Kareta, S. Chanda, H. Ahlenius, N. Perotti, B. Zhou, S. D. Grieder, X. Ge, S. Drake, C. Euong Ang, B. M. Walker, T. Vierbuchen, D. R. Fuentes, P. Brennecke, K. R. Nitta, A. Jolma, L. M. Steinmetz, J. Taipale, T. C. Südhof & M. Wernig (2017) Myt1l safeguards neuronal identity by actively repressing many non-neuronal fates. *Nature,* 544**,** 245-249.

Mallett, V., J. P. Ross, R. N. Alcalay, A. Ambalavanan, E. Sidransky, P. A. Dion, G. A. Rouleau & Z. Gan-Or (2016) GBA p.T369M substitution in Parkinson disease: Polymorphism or association? A meta-analysis. *Neurol Genet,* 2**,** e104.

Manning-Boğ, A. B., B. Schüle & J. W. Langston (2009) Alpha-synuclein-glucocerebrosidase interactions in pharmacological Gaucher models: a biological link between Gaucher disease and parkinsonism. *Neurotoxicology,* 30**,** 1127-32.

Marion, R. M., K. Strati, H. Li, A. Tejera, S. Schoeftner, S. Ortega, M. Serrano & M. A. Blasco (2009) Telomeres acquire embryonic stem cell characteristics in induced pluripotent stem cells. *Cell Stem Cell,* 4**,** 141-54.

Marks, W. J., R. T. Bartus, J. Siffert, C. S. Davis, A. Lozano, N. Boulis, J. Vitek, M. Stacy, D. Turner, L. Verhagen, R. Bakay, R. Watts, B. Guthrie, J. Jankovic, R. Simpson, M. Tagliati, R. Alterman, M. Stern, G. Baltuch, P. A. Starr, P. S. Larson, J. L. Ostrem, J. Nutt, K. Kieburtz, J. H. Kordower & C. W. Olanow (2010) Gene delivery of AAV2-neurturin for Parkinson's disease: a double-blind, randomised, controlled trial. *Lancet Neurol,* 9**,** 1164-1172.

Marro, S., Z. P. Pang, N. Yang, M. C. Tsai, K. Qu, H. Y. Chang, T. C. Südhof & M. Wernig (2011) Direct lineage conversion of terminally differentiated hepatocytes to functional neurons. *Cell Stem Cell,* 9**,** 374-82.

Martin, L. J., Y. Pan, A. C. Price, W. Sterling, N. G. Copeland, N. A. Jenkins, D. L. Price & M. K. Lee (2006) Parkinson's disease alpha-synuclein transgenic mice develop neuronal mitochondrial degeneration and cell death. *J Neurosci,* 26**,** 41-50.

Masliah, E., E. Rockenstein, I. Veinbergs, M. Mallory, M. Hashimoto, A. Takeda, Y. Sagara, A. Sisk & L. Mucke (2000) Dopaminergic loss and inclusion body formation in alpha-synuclein mice: implications for neurodegenerative disorders. *Science,* 287**,** 1265-9.

Masserdotti, G., S. Gillotin, B. Sutor, D. Drechsel, M. Irmler, H. F. Jørgensen, S. Sass, F. J. Theis, J. Beckers, B. Berninger, F. Guillemot & M. Götz (2015) Transcriptional Mechanisms of Proneural Factors and REST in Regulating Neuronal Reprogramming of Astrocytes. *Cell Stem Cell,* 17**,** 74-88.

Mata, I. F., J. B. Leverenz, D. Weintraub, J. Q. Trojanowski, A. Chen-Plotkin, V. M. Van Deerlin, B. Ritz, R. Rausch, S. A. Factor, C. Wood-Siverio, J. F. Quinn, K. A. Chung, A. L. Peterson-Hiller, J. G. Goldman, G. T. Stebbins, B. Bernard, A. J. Espay, F. J. Revilla, J. Devoto, L. S. Rosenthal, T. M. Dawson, M. S. Albert, D. Tsuang, H. Huston, D. Yearout, S. C. Hu, B. A. Cholerton, T. J. Montine, K. L. Edwards & C. P. Zabetian (2016) GBA Variants are associated with a distinct pattern of cognitive deficits in Parkinson's disease. *Mov Disord,* 31**,** 95-102.

Mata, I. F., A. Samii, S. H. Schneer, J. W. Roberts, A. Griffith, B. C. Leis, G. D. Schellenberg, E. Sidransky, T. D. Bird, J. B. Leverenz, D. Tsuang & C. P. Zabetian (2008) Glucocerebrosidase gene mutations: a risk factor for Lewy body disorders. *Arch Neurol,* 65**,** 379-82.

Mazzulli, J. R., Y. H. Xu, Y. Sun, A. L. Knight, P. J. McLean, G. A. Caldwell, E. Sidransky, G. A. Grabowski & D. Krainc (2011) Gaucher disease glucocerebrosidase and α-synuclein form a bidirectional pathogenic loop in synucleinopathies. *Cell,* 146**,** 37-52.

Mazzulli, J. R., F. Zunke, T. Tsunemi, N. J. Toker, S. Jeon, L. F. Burbulla, S. Patnaik, E. Sidransky, J. J. Marugan, C. M. Sue & D. Krainc (2016) Activation of β-

Glucocerebrosidase Reduces Pathological α-Synuclein and Restores Lysosomal Function in Parkinson's Patient Midbrain Neurons. *J Neurosci,* 36**,** 7693-706.

McCormack, A. L., S. K. Mak, J. M. Henderson, D. Bumcrot, M. J. Farrer & D. A. Di Monte (2010) Alpha-synuclein suppression by targeted small interfering RNA in the primate substantia nigra. *PLoS One,* 5**,** e12122.

McCormack, A. L., M. Thiruchelvam, A. B. Manning-Bog, C. Thiffault, J. W. Langston, D. A. Cory-Slechta & D. A. Di Monte (2002) Environmental risk factors and Parkinson's disease: selective degeneration of nigral dopaminergic neurons caused by the herbicide paraquat. *Neurobiol Dis,* 10**,** 119-27.

McGeer, P. L., S. Itagaki, B. E. Boyes & E. G. McGeer (1988) Reactive microglia are positive for HLA-DR in the substantia nigra of Parkinson's and Alzheimer's disease brains. *Neurology,* 38**,** 1285-91.

McGeer, P. L., C. Schwab, A. Parent & D. Doudet (2003) Presence of reactive microglia in monkey substantia nigra years after 1-methyl-4-phenyl-1,2,3,6-tetrahydropyridine administration. *Ann Neurol,* 54**,** 599-604.

McNeill, A., J. Magalhaes, C. Shen, K. Y. Chau, D. Hughes, A. Mehta, T. Foltynie, J. M. Cooper, A. Y. Abramov, M. Gegg & A. H. Schapira (2014) Ambroxol improves lysosomal biochemistry in glucocerebrosidase mutation-linked Parkinson disease cells. *Brain,* 137**,** 1481-95.

Menon, M. B., A. Kotlyarov & M. Gaestel (2011) SB202190-induced cell type-specific vacuole formation and defective autophagy do not depend on p38 MAP kinase inhibition. *PLoS One,* 6**,** e23054.

Mertens, J., A. C. Paquola, M. Ku, E. Hatch, L. Böhnke, S. Ladjevardi, S. McGrath, B. Campbell, H. Lee, J. R. Herdy, J. T. Gonçalves, T. Toda, Y. Kim, J. Winkler, J. Yao, M. W. Hetzer & F. H. Gage (2015) Directly Reprogrammed Human Neurons Retain Aging-Associated Transcriptomic Signatures and Reveal Age-Related Nucleocytoplasmic Defects. *Cell Stem Cell,* 17**,** 705-18.

Migdalska-Richards, A. & A. H. Schapira (2016) The relationship between glucocerebrosidase mutations and Parkinson disease. *J Neurochem*.

Miller, J. D., Y. M. Ganat, S. Kishinevsky, R. L. Bowman, B. Liu, E. Y. Tu, P. K. Mandal, E. Vera, J. W. Shim, S. Kriks, T. Taldone, N. Fusaki, M. J. Tomishima, D. Krainc, T. A. Milner, D. J. Rossi & L. Studer (2013) Human iPSC-based modeling of late-onset disease via progerin-induced aging. *Cell Stem Cell,* 13**,** 691-705.

Mittal, S., K. Bjørnevik, D. S. Im, A. Flierl, X. Dong, J. J. Locascio, K. M. Abo, E. Long, M. Jin, B. Xu, Y. K. Xiang, J. C. Rochet, A. Engeland, P. Rizzu, P. Heutink, T. Bartels, D. J. Selkoe, B. J. Caldarone, M. A. Glicksman, V. Khurana, B. Schüle, D. S. Park, T. Riise & C. R. Scherzer (2017) β2-Adrenoreceptor is a regulator of the α-synuclein gene driving risk of Parkinson's disease. *Science,* 357**,** 891-898.

Moon, M., H. G. Kim, L. Hwang, J. H. Seo, S. Kim, S. Hwang, D. Lee, H. Chung, M. S. Oh, K. T. Lee & S. Park (2009) Neuroprotective effect of ghrelin in the 1-methyl-4-phenyl-1,2,3,6-tetrahydropyridine mouse model of Parkinson's disease by blocking microglial activation. *Neurotox Res,* 15**,** 332-47.

Murphy, K. E., A. M. Gysbers, S. K. Abbott, N. Tayebi, W. S. Kim, E. Sidransky, A. Cooper, B. Garner & G. M. Halliday (2014) Reduced glucocerebrosidase is associated with increased α-synuclein in sporadic Parkinson's disease. *Brain,* 137**,** 834-48.

Nagaoka, U., K. Kim, N. R. Jana, H. Doi, M. Maruyama, K. Mitsui, F. Oyama & N. Nukina (2004) Increased expression of p62 in expanded polyglutamine-expressing cells and its association with polyglutamine inclusions. *J Neurochem,* 91**,** 57-68.

Nalls, M. A., R. Duran, G. Lopez, M. Kurzawa-Akanbi, I. G. McKeith, P. F. Chinnery, C. M. Morris, J. Theuns, D. Crosiers, P. Cras, S. Engelborghs, P. P. De Deyn, C. Van Broeckhoven, D. M. Mann, J. Snowden, S. Pickering-Brown, N. Halliwell, Y. Davidson, L. Gibbons, J. Harris, U. M. Sheerin, J. Bras, J. Hardy, L. Clark, K. Marder, L. S. Honig, D. Berg, W. Maetzler, K. Brockmann, T. Gasser, F. Novellino, A. Quattrone, G. Annesi, E. V. De Marco, E. Rogaeva, M. Masellis, S. E. Black, J. M. Bilbao, T. Foroud, B. Ghetti, W. C. Nichols, N. Pankratz, G. Halliday, S. Lesage, S. Klebe, A. Durr, C. Duyckaerts, A. Brice, B. I. Giasson, J. Q. Trojanowski, H. I. Hurtig, N. Tayebi, C. Landazabal, M. A. Knight, M. Keller, A. B. Singleton, T. G. Wolfsberg & E. Sidransky (2013) A multicenter study of glucocerebrosidase mutations in dementia with Lewy bodies. *JAMA Neurol,* 70**,** 727-35.

Nalls, M. A., N. Pankratz, C. M. Lill, C. B. Do, D. G. Hernandez, M. Saad, A. L. DeStefano, E. Kara, J. Bras, M. Sharma, C. Schulte, M. F. Keller, S. Arepalli, C. Letson, C. Edsall, H. Stefansson, X. Liu, H. Pliner, J. H. Lee, R. Cheng, M. A. Ikram, J. P. Ioannidis, G. M. Hadjigeorgiou, J. C. Bis, M. Martinez, J. S. Perlmutter, A. Goate, K. Marder, B. Fiske, M. Sutherland, G. Xiromerisiou, R. H. Myers, L. N. Clark, K. Stefansson, J. A. Hardy, P. Heutink, H. Chen, N. W. Wood, H. Houlden, H. Payami, A. Brice, W. K. Scott, T. Gasser, L. Bertram, N. Eriksson, T. Foroud, A. B. Singleton, I. P. s. D. G. C. (IPDGC), P. s. S. G. P. P. s. R. T. O. G. I. (PROGENI), 23andMe, GenePD, N. R. C. (NGRC), H. I. o. H. G. (HIHG), A. J. D. Investigator, C. f. H. a. A. R. i. G. E. (CHARGE), N. A. B. E. C. (NABEC), U. K. B. E. C. (UKBEC), G. P. s. D. Consortium & A. G. A. Group (2014) Large-scale meta-analysis of genome-wide association data identifies six new risk loci for Parkinson's disease. *Nat Genet,* 46**,** 989-93.

Nalls, M. A., V. Plagnol, D. G. Hernandez, M. Sharma, U. M. Sheerin, M. Saad, J. Simón-Sánchez, C. Schulte, S. Lesage, S. Sveinbjörnsdóttir, K. Stefánsson, M. Martinez, J. Hardy, P. Heutink, A. Brice, T. Gasser, A. B. Singleton, N. W. Wood & I. P. D. G. Consortium (2011) Imputation of sequence variants for identification of genetic risks for Parkinson's disease: a meta-analysis of genome-wide association studies. *Lancet,* 377**,** 641-9.

Narendra D. P., A. Tanaka, D. F. Suen & R. J. Youle. (2008) Parkin is recruited selectively to impaired mitochondria and promotes their autophagy. *J Cell Biol,* 183**,** 795-803.

Narendra D. P., S. M. Jin, A. Tanaka, D. F. Suen, C. A. Gautier, J. Shen, M. R. Cookson & R. J. Youle. (2010) PINK1 is selectively stabilized on impaired mitochondria to activate Parkin. *PLoS Biol,* 8, e1000298.

Nekrasov, E. D., V. A. Vigont, S. A. Klyushnikov, O. S. Lebedeva, E. M. Vassina, A. N. Bogomazova, I. V. Chestkov, T. A. Semashko, E. Kiseleva, L. A. Suldina, P. A. Bobrovsky, O. A. Zimina, M. A. Ryazantseva, A. Y. Skopin, S. N. Illarioshkin, E. V. Kaznacheyeva, M. A. Lagarkova & S. L. Kiselev (2016) Manifestation of Huntington's disease pathology in human induced pluripotent stem cell-derived neurons. *Mol Neurodegener,* 11**,** 27.

Neudorfer, O., N. Giladi, D. Elstein, A. Abrahamov, T. Turezkite, E. Aghai, A. Reches, B. Bembi & A. Zimran (1996) Occurrence of Parkinson's syndrome in type I Gaucher disease. *QJM,* 89**,** 691-4.

Neumann, J., J. Bras, E. Deas, S. S. O'Sullivan, L. Parkkinen, R. H. Lachmann, A. Li, J. Holton, R. Guerreiro, R. Paudel, B. Segarane, A. Singleton, A. Lees, J. Hardy, H. Houlden, T. Revesz & N. W. Wood (2009) Glucocerebrosidase mutations in clinical and pathologically proven Parkinson's disease. *Brain,* 132**,** 1783-94.

Ng, C. H., M. S. Guan, C. Koh, X. Ouyang, F. Yu, E. K. Tan, S. P. O'Neill, X. Zhang, J. Chung & K. L. Lim (2012) AMP kinase activation mitigates dopaminergic dysfunction and mitochondrial abnormalities in Drosophila models of Parkinson's disease. *J Neurosci,* 32**,** 14311-7.

Nichols, W. C., N. Pankratz, D. K. Marek, M. W. Pauciulo, V. E. Elsaesser, C. A. Halter, A. Rudolph, J. Wojcieszek, R. F. Pfeiffer, T. Foroud & P. S. G.-P. Investigators (2009) Mutations in GBA are associated with familial Parkinson disease susceptibility and age at onset. *Neurology,* 72**,** 310-6.

Noda, T. & Y. Ohsumi (1998) Tor, a phosphatidylinositol kinase homologue, controls autophagy in yeast. *J Biol Chem,* 273**,** 3963-6.

Noyce, A. J., J. P. Bestwick, L. Silveira-Moriyama, C. H. Hawkes, G. Giovannoni, A. J. Lees & A. Schrag (2012) Meta-analysis of early nonmotor features and risk factors for Parkinson disease. *Ann Neurol,* 72**,** 893-901.

O'Brien, J. S. & Y. Kishimoto (1991) Saposin proteins: structure, function, and role in human lysosomal storage disorders. *FASEB J,* 5**,** 301-8.

Oeda, T., A. Umemura, Y. Mori, S. Tomita, M. Kohsaka, K. Park, K. Inoue, H. Fujimura, H. Hasegawa, H. Sugiyama & H. Sawada (2015) Impact of glucocerebrosidase mutations on motor and nonmotor complications in Parkinson's disease. *Neurobiol Aging,* 36**,** 3306-3313.

Olave, I., W. Wang, Y. Xue, A. Kuo & G. R. Crabtree (2002) Identification of a polymorphic, neuron-specific chromatin remodeling complex. *Genes Dev,* 16**,** 2509-17.

Osellame, L. D., A. A. Rahim, I. P. Hargreaves, M. E. Gegg, A. Richard-Londt, S. Brandner, S. N. Waddington, A. H. Schapira & M. R. Duchen (2013) Mitochondria and quality control defects in a mouse model of Gaucher disease--links to Parkinson's disease. *Cell Metab,* 17**,** 941-53.

Pagan, F., M. Hebron, E. H. Valadez, Y. Torres-Yaghi, X. Huang, R. R. Mills, B. M. Wilmarth, H. Howard, C. Dunn, A. Carlson, A. Lawler, S. L. Rogers, R. A. Falconer, J. Ahn, Z. Li & C. Moussa (2016) Nilotinib Effects in Parkinson's disease and Dementia with Lewy bodies. *J Parkinsons Dis,* 6**,** 503-17.

Palfi, S., J. M. Gurruchaga, G. S. Ralph, H. Lepetit, S. Lavisse, P. C. Buttery, C. Watts, J. Miskin, M. Kelleher, S. Deeley, H. Iwamuro, J. P. Lefaucheur, C. Thiriez, G. Fenelon, C. Lucas, P. Brugières, I. Gabriel, K. Abhay, X. Drouot, N. Tani, A. Kas, B. Ghaleb, P. Le Corvoisier, P. Dolphin, D. P. Breen, S. Mason, N. V. Guzman, N. D. Mazarakis, P. A. Radcliffe, R. Harrop, S. M. Kingsman, O. Rascol, S. Naylor, R. A. Barker, P. Hantraye, P. Remy, P. Cesaro & K. A. Mitrophanous (2014) Long-term safety and tolerability of ProSavin, a lentiviral vector-based gene therapy for Parkinson's disease: a dose escalation, open-label, phase 1/2 trial. *Lancet,* 383**,** 1138-46.

Pang, Z. P., N. Yang, T. Vierbuchen, A. Ostermeier, D. R. Fuentes, T. Q. Yang, A. Citri, V. Sebastiano, S. Marro, T. C. Südhof & M. Wernig (2011) Induction of human neuronal cells by defined transcription factors. *Nature,* 476**,** 220-3.

Pankiv, S., T. H. Clausen, T. Lamark, A. Brech, J. A. Bruun, H. Outzen, A. Øvervatn, G. Bjørkøy & T. Johansen (2007) p62/SQSTM1 binds directly to Atg8/LC3 to facilitate degradation of ubiquitinated protein aggregates by autophagy. *J Biol Chem,* 282**,** 24131-45.

Papadopoulos, V. E., G. Nikolopoulou, I. Antoniadou, A. Karachaliou, G. Arianoglou, E. Emmanouilidou, S. P. Sardi, L. Stefanis & K. Vekrellis (2018) Modulation of β-glucocerebrosidase increases α-synuclein secretion and exosome release in mouse models of Parkinson's disease. *Hum Mol Genet,* 27**,** 1696-1710.

Parihar, M. S., A. Parihar, M. Fujita, M. Hashimoto & P. Ghafourifar (2009) Alpha-synuclein overexpression and aggregation exacerbates impairment of mitochondrial functions by augmenting oxidative stress in human neuroblastoma cells. *Int J Biochem Cell Biol,* 41**,** 2015-24.

Park, J. K., N. Tayebi, B. K. Stubblefield, M. E. LaMarca, J. J. MacKenzie, D. L. Stone & E. Sidransky (2002) The E326K mutation and Gaucher disease: mutation or polymorphism? *Clin Genet,* 61**,** 32-4.

Parker, W. D., S. J. Boyson & J. K. Parks (1989) Abnormalities of the electron transport chain in idiopathic Parkinson's disease. *Ann Neurol,* 26**,** 719-23.

Parkinson_Study_Group (1993) Effects of tocopherol and deprenyl on the progression of disability in early Parkinson's disease. *N Engl J Med,* 328**,** 176-83.

Patil, S. P., P. D. Jain, P. J. Ghumatkar, R. Tambe & S. Sathaye (2014) Neuroprotective effect of metformin in MPTP-induced Parkinson's disease in mice. *Neuroscience,* 277**,** 747-54.

Patterson, M., D. N. Chan, I. Ha, D. Case, Y. Cui, B. Van Handel, H. K. Mikkola & W. E. Lowry (2012) Defining the nature of human pluripotent stem cell progeny. *Cell Res,* 22**,** 178-93.

Pfisterer, U., A. Kirkeby, O. Torper, J. Wood, J. Nelander, A. Dufour, A. Björklund, O. Lindvall, J. Jakobsson & M. Parmar (2011a) Direct conversion of human fibroblasts to dopaminergic neurons. *Proc Natl Acad Sci U S A,* 108**,** 10343-8.

Pfisterer, U., J. Wood, K. Nihlberg, O. Hallgren, L. Bjermer, G. Westergren-Thorsson, O. Lindvall & M. Parmar (2011b) Efficient induction of functional neurons from adult human fibroblasts. *Cell Cycle,* 10**,** 3311-6.

Polito, L., A. Greco & D. Seripa (2016) Genetic Profile, Environmental Exposure, and Their Interaction in Parkinson's Disease. *Parkinsons Dis,* 2016**,** 6465793.

Polymeropoulos, M. H., C. Lavedan, E. Leroy, S. E. Ide, A. Dehejia, A. Dutra, B. Pike, H. Root, J. Rubenstein, R. Boyer, E. S. Stenroos, S. Chandrasekharappa, A. Athanassiadou, T. Papapetropoulos, W. G. Johnson, A. M. Lazzarini, R. C. Duvoisin, G. Di Iorio, L. I. Golbe & R. L. Nussbaum (1997) Mutation in the alpha-synuclein gene identified in families with Parkinson's disease. *Science,* 276**,** 2045-7.

Porceddu, P. F., I. O. Ishola, L. Contu & M. Morelli (2016) Metformin Prevented Dopaminergic Neurotoxicity Induced by 3,4-Methylenedioxymethamphetamine Administration. *Neurotox Res,* 30**,** 101-9.

Prigione, A., A. M. Hossini, B. Lichtner, A. Serin, B. Fauler, M. Megges, R. Lurz, H. Lehrach, E. Makrantonaki, C. C. Zouboulis & J. Adjaye (2011) Mitochondrial-associated cell death mechanisms are reset to an embryonic-like state in aged donor-derived iPS cells harboring chromosomal aberrations. *PLoS One,* 6**,** e27352.

Pringsheim, T., N. Jette, A. Frolkis & T. D. Steeves (2014) The prevalence of Parkinson's disease: a systematic review and meta-analysis. *Mov Disord,* 29**,** 1583-90.

Pérez-Revuelta, B. I., M. M. Hettich, A. Ciociaro, C. Rotermund, P. J. Kahle, S. Krauss & D. A. Di Monte (2014) Metformin lowers Ser-129 phosphorylated α-synuclein levels via mTOR-dependent protein phosphatase 2A activation. *Cell Death Dis,* 5**,** e1209.

Rais, Y., A. Zviran, S. Geula, O. Gafni, E. Chomsky, S. Viukov, A. A. Mansour, I. Caspi, V. Krupalnik, M. Zerbib, I. Maza, N. Mor, D. Baran, L. Weinberger, D. A. Jaitin, D. Lara-Astiaso, R. Blecher-Gonen, Z. Shipony, Z. Mukamel, T. Hagai, S. Gilad, D. Amann-Zalcenstein, A. Tanay, I. Amit, N. Novershtern & J. H. Hanna (2013) Deterministic direct reprogramming of somatic cells to pluripotency. *Nature,* 502**,** 65-70.

Ramirez, A., A. Heimbach, J. Gründemann, B. Stiller, D. Hampshire, L. P. Cid, I. Goebel, A. F. Mubaidin, A. L. Wriekat, J. Roeper, A. Al-Din, A. M. Hillmer, M. Karsak, B. Liss, C. G. Woods, M. I. Behrens & C. Kubisch (2006) Hereditary parkinsonism with dementia is caused by mutations in ATP13A2, encoding a lysosomal type 5 P-type ATPase. *Nat Genet,* 38**,** 1184-91.

Ramsay, R. R., M. J. Krueger, S. K. Youngster, M. R. Gluck, J. E. Casida & T. P. Singer (1991) Interaction of 1-methyl-4-phenylpyridinium ion (MPP+) and its analogs with the rotenone/piericidin binding site of NADH dehydrogenase. *J Neurochem,* 56**,** 1184-90.

Rao, X., X. Huang, Z. Zhou & X. Lin (2013) An improvement of the 2ˆ(-delta delta CT) method for quantitative real-time polymerase chain reaction data analysis. *Biostat Bioinforma Biomath,* 3**,** 71-85.

Recasens, A., B. Dehay, J. Bové, I. Carballo-Carbajal, S. Dovero, A. Pérez-Villalba, P. O. Fernagut, J. Blesa, A. Parent, C. Perier, I. Fariñas, J. A. Obeso, E. Bezard & M. Vila (2014) Lewy body extracts from Parkinson disease brains trigger α-synuclein pathology and neurodegeneration in mice and monkeys. *Ann Neurol,* 75**,** 351-62.

Reczek, D., M. Schwake, J. Schröder, H. Hughes, J. Blanz, X. Jin, W. Brondyk, S. Van Patten, T. Edmunds & P. Saftig (2007) LIMP-2 is a receptor for lysosomal mannose-6-phosphate-independent targeting of beta-glucocerebrosidase. *Cell,* 131**,** 770-83.

Redmann, M., W. Y. Wani, L. Volpicelli-Daley, V. Darley-Usmar & J. Zhang (2017) Trehalose does not improve neuronal survival on exposure to alpha-synuclein pre-formed fibrils. *Redox Biol,* 11**,** 429-437.

Richner, M., M. B. Victor, Y. Liu, D. Abernathy & A. S. Yoo (2015) MicroRNA-based conversion of human fibroblasts into striatal medium spiny neurons. *Nat Protoc,* 10**,** 1543-55.

Rideout, H. J., K. E. Larsen, D. Sulzer & L. Stefanis (2001) Proteasomal inhibition leads to formation of ubiquitin/alpha-synuclein-immunoreactive inclusions in PC12 cells. *J Neurochem,* 78**,** 899-908.

Ritz, B., P. C. Lee, C. F. Lassen & O. A. Arah (2014) Parkinson disease and smoking revisited: ease of quitting is an early sign of the disease. *Neurology,* 83**,** 1396-402.

Robertson, D. C., O. Schmidt, N. Ninkina, P. A. Jones, J. Sharkey & V. L. Buchman (2004) Developmental loss and resistance to MPTP toxicity of dopaminergic neurones in substantia nigra pars compacta of gamma-synuclein, alpha-synuclein and double alpha/gamma-synuclein null mutant mice. *J Neurochem,* 89**,** 1126-36.

Rocha, E. M., G. A. Smith, E. Park, H. Cao, E. Brown, P. Hallett & O. Isacson (2015a) Progressive decline of glucocerebrosidase in aging and Parkinson's disease. *Ann Clin Transl Neurol,* 2**,** 433-8.

Rocha, E. M., G. A. Smith, E. Park, H. Cao, A. R. Graham, E. Brown, J. R. McLean, M. A. Hayes, J. Beagan, S. C. Izen, E. Perez-Torres, P. J. Hallett & O. Isacson (2015b) Sustained Systemic Glucocerebrosidase Inhibition Induces Brain α-Synuclein Aggregation, Microglia and Complement C1q Activation in Mice. *Antioxid Redox Signal,* 23**,** 550-64.

Rodríguez-Navarro, J. A., L. Rodríguez, M. J. Casarejos, R. M. Solano, A. Gómez, J. Perucho, A. M. Cuervo, J. García de Yébenes & M. A. Mena (2010) Trehalose ameliorates dopaminergic and tau pathology in parkin deleted/tau overexpressing mice through autophagy activation. *Neurobiol Dis,* 39**,** 423-38.

Rodríguez-Rodero, S., J. L. Fernández-Morera, A. F. Fernandez, E. Menéndez-Torre & M. F. Fraga (2010) Epigenetic regulation of aging. *Discov Med,* 10**,** 225-33.

Ron, I. & M. Horowitz (2005) ER retention and degradation as the molecular basis underlying Gaucher disease heterogeneity. *Hum Mol Genet,* 14**,** 2387-98.

Rosenbloom, B., M. Balwani, J. M. Bronstein, E. Kolodny, S. Sathe, A. R. Gwosdow, J. S. Taylor, J. A. Cole, A. Zimran & N. J. Weinreb (2011) The incidence of Parkinsonism in patients with type 1 Gaucher disease: data from the ICGG Gaucher Registry. *Blood Cells Mol Dis,* 46**,** 95-102.

Rossi, M., E. R. Munarriz, S. Bartesaghi, M. Milanese, D. Dinsdale, M. A. Guerra-Martin, E. T. Bampton, P. Glynn, G. Bonanno, R. A. Knight, P. Nicotera & G. Melino (2009) Desmethylclomipramine induces the accumulation of autophagy markers by blocking autophagic flux. *J Cell Sci,* 122**,** 3330-9.

Rubinsztein, D. C., C. F. Bento & V. Deretic (2015) Therapeutic targeting of autophagy in neurodegenerative and infectious diseases. *J Exp Med,* 212**,** 979-90.

Ruetz, T., U. Pfisterer, B. Di Stefano, J. Ashmore, M. Beniazza, T. V. Tian, D. F. Kaemena, L. Tosti, W. Tan, J. R. Manning, E. Chantzoura, D. R. Ottosson, S. Collombet, A. Johnsson, E. Cohen, K. Yusa, S. Linnarsson, T. Graf, M. Parmar & K. Kaji (2017) Constitutively Active SMAD2/3 Are Broad-Scope Potentiators of Transcription-Factor-Mediated Cellular Reprogramming. *Cell Stem Cell,* 21**,** 791-805.e9.

Ruskey, J. A., L. Greenbaum, L. Roncière, A. Alam, D. Spiegelman, C. Liong, O. A. Levy, C. Waters, S. Fahn, K. S. Marder, W. Chung, G. Yahalom, S. Israeli-Korn, V. Livneh, T. Fay-Karmon, R. N. Alcalay, S. Hassin-Baer & Z. Gan-Or (2019) Increased yield of full GBA sequencing in Ashkenazi Jews with Parkinson's disease. *Eur J Med Genet,* 62**,** 65-69.

Ryan B. J., S. Hoek, E. A. Fon & R. Wade-Martins (2015) Mitochondrial dysfunction and mitophagy in Parkinson's: from familial to sporadic disease. *Trends Biochem Sci,* 40, 200-10.

Saiki M, Baker A, Williams-Gray, Foltynie T, Goodman RS, Taylor CJ, Compston DA, Barker RA, Sawcer SJ, Goris A (2010) Association of the human leucocyte antigen region with susceptibility to Parkinson's disease. *J Neurol Neurosurg Psychiatry,* Aug;81(8):890-1.

Sanchez-Martinez, A., M. Beavan, M. E. Gegg, K. Y. Chau, A. J. Whitworth & A. H. Schapira (2016) Parkinson disease-linked GBA mutation effects reversed by molecular chaperones in human cell and fly models. *Sci Rep,* 6**,** 31380.

Sapru, M. K., J. W. Yates, S. Hogan, L. Jiang, J. Halter & M. C. Bohn (2006) Silencing of human alpha-synuclein in vitro and in rat brain using lentiviral-mediated RNAi. *Exp Neurol,* 198**,** 382-90.

Sardi, S. P., J. Clarke, C. Viel, M. Chan, T. J. Tamsett, C. M. Treleaven, J. Bu, L. Sweet, M. A. Passini, J. C. Dodge, W. H. Yu, R. L. Sidman, S. H. Cheng & L. S. Shihabuddin (2013) Augmenting CNS glucocerebrosidase activity as a therapeutic strategy for parkinsonism and other Gaucher-related synucleinopathies. *Proc Natl Acad Sci U S A,* 110**,** 3537-42.

Sarkar, S., S. Chigurupati, J. Raymick, D. Mann, J. F. Bowyer, T. Schmitt, R. D. Beger, J. P. Hanig, L. C. Schmued & M. G. Paule (2014) Neuroprotective effect of the chemical chaperone, trehalose in a chronic MPTP-induced Parkinson's disease mouse model. *Neurotoxicology,* 44**,** 250-62.

Sarkar, S., J. E. Davies, Z. Huang, A. Tunnacliffe & D. C. Rubinsztein (2007) Trehalose, a novel mTOR-independent autophagy enhancer, accelerates the clearance of mutant huntingtin and alpha-synuclein. *J Biol Chem,* 282**,** 5641-52.

Sánchez-Danés A., Y. Richaud Patin, I. Carballo-Carbajal, S. Jiménez-Delgado, C. Caig, S. Mora, C. Guglielmo, M. Ezquerra, B. Patel, A. Giralt, J. M. Canals, M. Memo, J. Alberch, J. López-Barneo M. Vila, A. M. Cuervo, E. Tolosa, A. Consiglio & A. Raya (2012) Disease-specific phenotypes in dopamine neurons from human iPS-based models of genetic and sporadic Parkinson's disease. *EMBO Mol Med,* 4**,** 380-95.

Schapira, A. H. (2008) Mitochondria in the aetiology and pathogenesis of Parkinson's disease. *Lancet Neurol,* 7**,** 97-109.

Schapira, A. H., J. M. Cooper, D. Dexter, P. Jenner, J. B. Clark & C. D. Marsden (1989) Mitochondrial complex I deficiency in Parkinson's disease. *Lancet,* 1**,** 1269.

Schöndorf, D. C., M. Aureli, F. E. McAllister, C. J. Hindley, F. Mayer, B. Schmid, S. P. Sardi, M. Valsecchi, S. Hoffmann, L. K. Schwarz, U. Hedrich, D. Berg, L. S. Shihabuddin, J. Hu, J. Pruszak, S. P. Gygi, S. Sonnino, T. Gasser & M. Deleidi (2014) iPSC-derived neurons from GBA1-associated Parkinson's disease patients show autophagic defects and impaired calcium homeostasis. *Nat Commun,* 5**,** 4028.

Selikhova, M., D. R. Williams, P. A. Kempster, J. L. Holton, T. Revesz & A. J. Lees (2009) A clinico-pathological study of subtypes in Parkinson's disease. *Brain,* 132**,** 2947-57.

Setó-Salvia, N., J. Pagonabarraga, H. Houlden, B. Pascual-Sedano, O. Dols-Icardo, A. Tucci, C. Paisán-Ruiz, A. Campolongo, S. Antón-Aguirre, I. Martín, L. Muñoz, E. Bufill, L. Vilageliu, D. Grinberg, M. Cozar, R. Blesa, A. Lleó, J. Hardy, J. Kulisevsky & J. Clarimón (2012) Glucocerebrosidase mutations confer a greater risk of dementia during Parkinson's disease course. *Mov Disord,* 27**,** 393-9.

Shults, C. W., D. Oakes, K. Kieburtz, M. F. Beal, R. Haas, S. Plumb, J. L. Juncos, J. Nutt, I. Shoulson, J. Carter, K. Kompoliti, J. S. Perlmutter, S. Reich, M. Stern, R. L. Watts, R. Kurlan, E. Molho, M. Harrison, M. Lew & P. S. Group (2002) Effects of coenzyme Q10 in early Parkinson disease: evidence of slowing of the functional decline. *Arch Neurol,* 59**,** 1541-50.

Sidransky, E. (2005) Gaucher disease and parkinsonism. *Mol Genet Metab,* 84**,** 302-4.

Sidransky, E., M. A. Nalls, J. O. Aasly, J. Aharon-Peretz, G. Annesi, E. R. Barbosa, A. Bar-Shira, D. Berg, J. Bras, A. Brice, C. M. Chen, L. N. Clark, C. Condroyer, E. V. De Marco, A. Dürr, M. J. Eblan, S. Fahn, M. J. Farrer, H. C. Fung, Z. Gan-Or, T. Gasser, R. Gershoni-Baruch, N. Giladi, A. Griffith, T. Gurevich, C. Januario, P. Kropp, A. E. Lang, G. J. Lee-Chen, S. Lesage, K. Marder, I. F. Mata, A. Mirelman, J. Mitsui, I. Mizuta, G. Nicoletti, C. Oliveira, R. Ottman, A. Orr-Urtreger, L. V. Pereira, A. Quattrone, E. Rogaeva, A. Rolfs, H. Rosenbaum, R. Rozenberg, A. Samii, T. Samaddar, C. Schulte, M. Sharma, A. Singleton, M. Spitz, E. K. Tan, N. Tayebi, T. Toda, A. R. Troiano, S. Tsuji, M. Wittstock, T. G. Wolfsberg, Y. R. Wu, C. P. Zabetian, Y. Zhao & S. G. Ziegler (2009) Multicenter analysis of glucocerebrosidase mutations in Parkinson's disease. *N Engl J Med,* 361**,** 1651-61.

Siegert, S., J. Seo, E. J. Kwon, A. Rudenko, S. Cho, W. Wang, Z. Flood, A. J. Martorell, M. Ericsson, A. E. Mungenast & L. H. Tsai (2015) The schizophrenia risk gene product miR-137 alters presynaptic plasticity. *Nat Neurosci,* 18**,** 1008-16.

Silveira, C. R. A., J. MacKinley, K. Coleman, Z. Li, E. Finger, R. Bartha, S. A. Morrow, J. Wells, M. Borrie, R. G. Tirona, C. A. Rupar, G. Zou, R. A. Hegele, D. Mahuran, P. MacDonald, M. E. Jenkins, M. Jog & S. H. Pasternak (2019) Ambroxol as a novel disease-modifying treatment for Parkinson's disease dementia: protocol for a single-centre, randomized, double-blind, placebo-controlled trial. *BMC Neurol,* 19**,** 20.

Sitia, R. & I. Braakman (2003) Quality control in the endoplasmic reticulum protein factory. *Nature,* 426**,** 891-4.

Snow, B. J., F. L. Rolfe, M. M. Lockhart, C. M. Frampton, J. D. O'Sullivan, V. Fung, R. A. Smith, M. P. Murphy, K. M. Taylor & P. S. Group (2010) A double-blind, placebo-controlled study to assess the mitochondria-targeted antioxidant MitoQ as a disease-modifying therapy in Parkinson's disease. *Mov Disord,* 25**,** 1670-4.

Son, E. Y., J. K. Ichida, B. J. Wainger, J. S. Toma, V. F. Rafuse, C. J. Woolf & K. Eggan (2011) Conversion of mouse and human fibroblasts into functional spinal motor neurons. *Cell Stem Cell,* 9**,** 205-18.

Sorge, J. A., C. West, W. Kuhl, L. Treger & E. Beutler (1987) The human glucocerebrosidase gene has two functional ATG initiator codons. *Am J Hum Genet,* 41**,** 1016-24.

Spillantini, M. G., R. A. Crowther, R. Jakes, N. J. Cairns, P. L. Lantos & M. Goedert (1998a) Filamentous alpha-synuclein inclusions link multiple system atrophy with Parkinson's disease and dementia with Lewy bodies. *Neurosci Lett,* 251**,** 205-8.

Spillantini, M. G., R. A. Crowther, R. Jakes, M. Hasegawa & M. Goedert (1998b) alpha-Synuclein in filamentous inclusions of Lewy bodies from Parkinson's disease and dementia with lewy bodies. *Proc Natl Acad Sci U S A,* 95**,** 6469-73.

Spillantini, M. G. & M. Goedert (2013) Tau pathology and neurodegeneration. *Lancet Neurol,* 12**,** 609-22.

Spillantini, M. G., M. L. Schmidt, V. M. Lee, J. Q. Trojanowski, R. Jakes & M. Goedert (1997) Alpha-synuclein in Lewy bodies. *Nature,* 388**,** 839-40.

Stefansson H., A. Helgason, G. Thorleifsson, V. Steinthorsdottir, G. Masson, J. Barnard, A. Baker, A Jonasdottir, A. Ingason, V. G. Gudnadottir, N. Desnica, A. Hicks, A. Gylfason, D. F. Gudbjartsson, G. M. Jonsdorrir, J. Sainz, K. Agnarsson, B. Birgisdottir, S. Ghosh, A. Olafsdottir, J. B. Cazier, K. Kristjansson, M. L. Frigge, T. E. Thorgeirsson, J. R. Gulcher, A. Kong, & Stefansson K. (2005) A common inversion under selection in Europeans. Nat Genet, 37, 129-37.

Stocchi, F. & C. W. Olanow (2003) Neuroprotection in Parkinson's disease: clinical trials. *Ann Neurol,* 53 Suppl 3**,** S87-97; discussion S97-9.

Stone D. L., N. Tayebi, E. Orvisky, B. Stubblefield, V. Madike & E. Sidransky (2000) Glucocerebrosidase gene mutations in patients with type 2 Gaucher disease. *Hum Mutat,* 15, 181-8

Stoker, T. B., K.M. Torsney & R.A. Barker (2018a). Pathological Mechanisms and Clinical Aspects of GBA1 Mutation-Associated Parkinson's Disease. ed. K. M. Torsney. Parkinson's Disease:Pathogenesis and Clinical Aspects [Internet]. Codon Publications.

Stoker, T. B., K. M. Torsney & R. A. Barker (2018b) Emerging Treatment Approaches for Parkinson's Disease. *Front Neurosci,* 12**,** 693.

Storch, A., W. H. Jost, P. Vieregge, J. Spiegel, W. Greulich, J. Durner, T. Müller, A. Kupsch, H. Henningsen, W. H. Oertel, G. Fuchs, W. Kuhn, P. Niklowitz, R. Koch, B. Herting, H. Reichmann & G. C. Q. S. Group (2007) Randomized, double-blind, placebo-controlled trial on symptomatic effects of coenzyme Q(10) in Parkinson disease. *Arch Neurol,* 64**,** 938-44.

Stoyanova, I. I. (2014) Ghrelin: a link between ageing, metabolism and neurodegenerative disorders. *Neurobiol Dis,* 72 Pt A**,** 72-83.

Suhr, S. T., E. A. Chang, J. Tjong, N. Alcasid, G. A. Perkins, M. D. Goissis, M. H. Ellisman, G. I. Perez & J. B. Cibelli (2010) Mitochondrial rejuvenation after induced pluripotency. *PLoS One,* 5**,** e14095.

Sun, R., S. Yang, B. Zheng, J. Liu & X. Ma (2019) Apolipoprotein E Polymorphisms and Parkinson Disease With or Without Dementia: A Meta-Analysis Including 6453 Participants. *J Geriatr Psychiatry Neurol,* 32**,** 3-15.

Sundaramurthy, V., R. Barsacchi, N. Samusik, G. Marsico, J. Gilleron, I. Kalaidzidis, F. Meyenhofer, M. Bickle, Y. Kalaidzidis & M. Zerial (2013) Integration of chemical and RNAi multiparametric profiles identifies triggers of intracellular mycobacterial killing. *Cell Host Microbe,* 13**,** 129-42.

Suzuki, T., M. Shimoda, K. Ito, S. Hanai, H. Aizawa, T. Kato, K. Kawasaki, T. Yamaguchi, H. D. Ryoo, N. Goto-Inoue, M. Setou, S. Tsuji & N. Ishida (2013) Expression of human Gaucher disease gene GBA generates neurodevelopmental defects and ER stress in Drosophila eye. *PLoS One,* 8**,** e69147.

Swan, M., N. Doan, R. A. Ortega, M. Barrett, W. Nichols, L. Ozelius, J. Soto-Valencia, S. Boschung, A. Deik, H. Sarva, J. Cabassa, B. Johannes, D. Raymond, K. Marder, N. Giladi, J. Miravite, W. Severt, R. Sachdev, V. Shanker, S. Bressman

& R. Saunders-Pullman (2016) Neuropsychiatric characteristics of GBA-associated Parkinson disease. *J Neurol Sci,* 370**,** 63-69.

Tanaka, M., Y. Machida, S. Niu, T. Ikeda, N. R. Jana, H. Doi, M. Kurosawa, M. Nekooki & N. Nukina (2004) Trehalose alleviates polyglutamine-mediated pathology in a mouse model of Huntington disease. *Nat Med,* 10**,** 148-54.

Tang, Y., M. L. Liu, T. Zang & C. L. Zhang (2017) Direct Reprogramming Rather than iPSC-Based Reprogramming Maintains Aging Hallmarks in Human Motor Neurons. *Front Mol Neurosci,* 10**,** 359.

Tanik, S. A., C. E. Schultheiss, L. A. Volpicelli-Daley, K. R. Brunden & V. M. Lee (2013) Lewy body-like α-synuclein aggregates resist degradation and impair macroautophagy. *J Biol Chem,* 288**,** 15194-210.

Tansey, M. G. & M. S. Goldberg (2010) Neuroinflammation in Parkinson's disease: its role in neuronal death and implications for therapeutic intervention. *Neurobiol Dis,* 37**,** 510-8.

Tayebi, N., J. Walker, B. Stubblefield, E. Orvisky, M. E. LaMarca, K. Wong, H. Rosenbaum, R. Schiffmann, B. Bembi & E. Sidransky (2003) Gaucher disease with parkinsonian manifestations: does glucocerebrosidase deficiency contribute to a vulnerability to parkinsonism? *Mol Genet Metab,* 79**,** 104-9.

Testa, C. M., T. B. Sherer & J. T. Greenamyre (2005) Rotenone induces oxidative stress and dopaminergic neuron damage in organotypic substantia nigra cultures. *Brain Res Mol Brain Res,* 134**,** 109-18.

Thomas, K. J., M. K. McCoy, J. Blackinton, A. Beilina, M. van der Brug, A. Sandebring, D. Miller, D. Maric, A. Cedazo-Minguez & M. R. Cookson (2011) DJ-1 acts in parallel to the PINK1/parkin pathway to control mitochondrial function and autophagy. *Hum Mol Genet,* 20**,** 40-50.

Toepfer, N., C. Childress, A. Parikh, D. Rukstalis & W. Yang (2011) Atorvastatin induces autophagy in prostate cancer PC3 cells through activation of LC3 transcription. *Cancer Biol Ther,* 12**,** 691-9.

Tofaris, G. K., R. Layfield & M. G. Spillantini (2001) alpha-synuclein metabolism and aggregation is linked to ubiquitin-independent degradation by the proteasome. *FEBS Lett,* 509**,** 22-6.

Unger, M. M., J. C. Möller, K. Mankel, K. M. Eggert, K. Bohne, M. Bodden, K. Stiasny-Kolster, P. H. Kann, G. Mayer, J. J. Tebbe & W. H. Oertel (2011) Postprandial ghrelin response is reduced in patients with Parkinson's disease and idiopathic REM sleep behaviour disorder: a peripheral biomarker for early Parkinson's disease? *J Neurol,* 258**,** 982-90.

Valente, E. M., P. M. Abou-Sleiman, V. Caputo, M. M. Muqit, K. Harvey, S. Gispert, Z. Ali, D. Del Turco, A. R. Bentivoglio, D. G. Healy, A. Albanese, R. Nussbaum, R. González-Maldonado, T. Deller, S. Salvi, P. Cortelli, W. P. Gilks, D. S. Latchman, R. J. Harvey, B. Dallapiccola, G. Auburger & N. W. Wood (2004) Hereditary early-onset Parkinson's disease caused by mutations in PINK1. *Science,* 304**,** 1158-60.

Varastet, M., D. Riche, M. Maziere & P. Hantraye (1994) Chronic MPTP treatment reproduces in baboons the differential vulnerability of mesencephalic dopaminergic neurons observed in Parkinson's disease. *Neuroscience,* 63**,** 47-56.

Verstraeten A, Theuns J, Van Broeckhoven C. Progress in unraveling the genetic etiology of Parkinson's disease in a genomic era. Trends Genet. 2015 Mar;31(3):140-9.

Victor, M. B., M. Richner, T. O. Hermanstyne, J. L. Ransdell, C. Sobieski, P. Y. Deng, V. A. Klyachko, J. M. Nerbonne & A. S. Yoo (2014) Generation of human striatal neurons by microRNA-dependent direct conversion of fibroblasts. *Neuron,* 84**,** 311-23.

Victor, M. B., M. Richner, H. E. Olsen, S. W. Lee, A. M. Monteys, C. Ma, C. J. Huh, B. Zhang, B. L. Davidson, X. W. Yang & A. S. Yoo (2018) Striatal neurons directly converted from Huntington's disease patient fibroblasts recapitulate age-associated disease phenotypes. *Nat Neurosci,* 21**,** 341-352.

Vierbuchen, T., A. Ostermeier, Z. P. Pang, Y. Kokubu, T. C. Südhof & M. Wernig (2010) Direct conversion of fibroblasts to functional neurons by defined factors. *Nature,* 463**,** 1035-41.

Villanueva-Paz, M., S. Povea-Cabello, I. Villalón-García, J. M. Suárez-Rivero, M. Álvarez-Córdoba, M. de la Mata, M. Talaverón-Rey, S. Jackson & J. A. Sánchez-Alcázar (2019) Pathophysiological characterization of MERRF patient-specific induced neurons generated by direct reprogramming. *Biochim Biophys Acta Mol Cell Res,* 1866**,** 861-881.

Vogiatzi, T., M. Xilouri, K. Vekrellis & L. Stefanis (2008) Wild type alpha-synuclein is degraded by chaperone-mediated autophagy and macroautophagy in neuronal cells. *J Biol Chem,* 283**,** 23542-56.

Volpicelli-Daley, L. A., K. C. Luk, T. P. Patel, S. A. Tanik, D. M. Riddle, A. Stieber, D. F. Meaney, J. Q. Trojanowski & V. M. Lee (2011) Exogenous α-synuclein fibrils induce Lewy body pathology leading to synaptic dysfunction and neuron death. *Neuron,* 72**,** 57-71.

Wahlqvist, M. L., M. S. Lee, C. C. Hsu, S. Y. Chuang, J. T. Lee & H. N. Tsai (2012) Metformin-inclusive sulfonylurea therapy reduces the risk of Parkinson's disease occurring with Type 2 diabetes in a Taiwanese population cohort. *Parkinsonism Relat Disord,* 18**,** 753-8.

Wainger, B. J., E. D. Buttermore, J. T. Oliveira, C. Mellin, S. Lee, W. A. Saber, A. J. Wang, J. K. Ichida, I. M. Chiu, L. Barrett, E. A. Huebner, C. Bilgin, N. Tsujimoto, C. Brenneis, K. Kapur, L. L. Rubin, K. Eggan & C. J. Woolf (2015) Modeling pain in vitro using nociceptor neurons reprogrammed from fibroblasts. *Nat Neurosci,* 18**,** 17-24.

Walker, F. O. (2007) Huntington's disease. *Lancet,* 369**,** 218-28.

Wang, X., T. G. Petrie, Y. Liu, J. Liu, H. Fujioka & X. Zhu (2012) Parkinson's disease-associated DJ-1 mutations impair mitochondrial dynamics and cause mitochondrial dysfunction. *J Neurochem,* 121**,** 830-9.

Wapinski, O. L., T. Vierbuchen, K. Qu, Q. Y. Lee, S. Chanda, D. R. Fuentes, P. G. Giresi, Y. H. Ng, S. Marro, N. F. Neff, D. Drechsel, B. Martynoga, D. S. Castro, A. E. Webb, T. C. Südhof, A. Brunet, F. Guillemot, H. Y. Chang & M. Wernig (2013) Hierarchical mechanisms for direct reprogramming of fibroblasts to neurons. *Cell,* 155**,** 621-35.

Webb, J. L., B. Ravikumar, J. Atkins, J. N. Skepper & D. C. Rubinsztein (2003) Alpha-Synuclein is degraded by both autophagy and the proteasome. *J Biol Chem,* 278**,** 25009-13.

Whone, A., M. Luz, M. Boca, M. Woolley, L. Mooney, S. Dharia, J. Broadfoot, D. Cronin, C. Schroers, N. U. Barua, L. Longpre, C. L. Barclay, C. Boiko, G. A. Johnson, H. C. Fibiger, R. Harrison, O. Lewis, G. Pritchard, M. Howell, C. Irving, D. Johnson, S. Kinch, C. Marshall, A. D. Lawrence, S. Blinder, V. Sossi, A. J. Stoessl, P. Skinner, E. Mohr & S. S. Gill (2019) Randomized trial of intermittent intraputamenal glial cell line-derived neurotrophic factor in Parkinson's disease. *Brain,* 142**,** 512-525.

Williams-Gray, C. H., A. Hampshire, R. A. Barker & A. M. Owen (2008) Attentional control in Parkinson's disease is dependent on COMT val 158 met genotype. *Brain,* 131**,** 397-408.

Williams-Gray, C. H., A. Goris, M. Saiki, T. Foltynie, D. A. Compston, S. J. Sawer & R. A. Barker & (2009) Apolipoprotein E genotype as a risk factor for susceptibility to and dementia in Parkinson's disease. *J Neurol***,** 256, 493-8.

Williams-Gray, C. H., S. L. Mason, J. R. Evans, T. Foltynie, C. Brayne, T. W. Robbins & R. A. Barker (2013) The CamPaIGN study of Parkinson's disease: 10-year outlook in an incident population-based cohort. *J Neurol Neurosurg Psychiatry,* 84**,** 1258-64.

Winder-Rhodes, S. E., J. R. Evans, M. Ban, S. L. Mason, C. H. Williams-Gray, T. Foltynie, R. Duran, N. E. Mencacci, S. J. Sawcer & R. A. Barker (2013) Glucocerebrosidase mutations influence the natural history of Parkinson's disease in a community-based incident cohort. *Brain,* 136**,** 392-9.

Wu, J. I., J. Lessard & G. R. Crabtree (2009) Understanding the words of chromatin regulation. *Cell,* 136**,** 200-6.

Xu, J., S. Y. Kao, F. J. Lee, W. Song, L. W. Jin & B. A. Yankner (2002) Dopamine-dependent neurotoxicity of alpha-synuclein: a mechanism for selective neurodegeneration in Parkinson disease. *Nat Med,* 8**,** 600-6.

Xu, Y. H., Y. Sun, H. Ran, B. Quinn, D. Witte & G. A. Grabowski (2011) Accumulation and distribution of α-synuclein and ubiquitin in the CNS of Gaucher disease mouse models. *Mol Genet Metab,* 102**,** 436-47.

Xu, Y. H., K. Xu, Y. Sun, B. Liou, B. Quinn, R. H. Li, L. Xue, W. Zhang, K. D. Setchell, D. Witte & G. A. Grabowski (2014) Multiple pathogenic proteins implicated in neuronopathic Gaucher disease mice. *Hum Mol Genet,* 23**,** 3943-57.

Xue, Y., K. Ouyang, J. Huang, Y. Zhou, H. Ouyang, H. Li, G. Wang, Q. Wu, C. Wei, Y. Bi, L. Jiang, Z. Cai, H. Sun, K. Zhang, Y. Zhang, J. Chen & X. D. Fu (2013) Direct conversion of fibroblasts to neurons by reprogramming PTB-regulated microRNA circuits. *Cell,* 152**,** 82-96.

Yang, Y., J. Jiao, R. Gao, R. Le, X. Kou, Y. Zhao, H. Wang, S. Gao & Y. Wang (2015) Enhanced Rejuvenation in Induced Pluripotent Stem Cell-Derived Neurons Compared with Directly Converted Neurons from an Aged Mouse. *Stem Cells Dev,* 24**,** 2767-77.

Yap, T. L., J. M. Gruschus, A. Velayati, W. Westbroek, E. Goldin, N. Moaven, E. Sidransky & J. C. Lee (2011) Alpha-synuclein interacts with Glucocerebrosidase providing a molecular link between Parkinson and Gaucher diseases. *J Biol Chem,* 286**,** 28080-8.

Yap, T. L., A. Velayati, E. Sidransky & J. C. Lee (2013) Membrane-bound α-synuclein interacts with glucocerebrosidase and inhibits enzyme activity. *Mol Genet Metab,* 108**,** 56-64.

Yoo, A. S., B. T. Staahl, L. Chen & G. R. Crabtree (2009) MicroRNA-mediated switching of chromatin-remodelling complexes in neural development. *Nature,* 460**,** 642-6.

Yoo, A. S., A. X. Sun, L. Li, A. Shcheglovitov, T. Portmann, Y. Li, C. Lee-Messer, R. E. Dolmetsch, R. W. Tsien & G. R. Crabtree (2011) MicroRNA-mediated conversion of human fibroblasts to neurons. *Nature,* 476**,** 228-31.

Yoshida, H. (2007) ER stress and diseases. *FEBS J,* 274**,** 630-58.

Zhang, Q. J., J. J. Li, X. Lin, Y. Q. Lu, X. X. Guo, E. L. Dong, M. Zhao, J. He, N. Wang & W. J. Chen (2017) Modeling the phenotype of spinal muscular atrophy by the direct conversion of human fibroblasts to motor neurons. *Oncotarget,* 8**,** 10945-10953.

Zheng, S., E. E. Gray, G. Chawla, B. T. Porse, T. J. O'Dell & D. L. Black (2012) PSD-95 is post-transcriptionally repressed during early neural development by PTBP1 and PTBP2. *Nat Neurosci,* 15**,** 381-8, S1.

Zhou, G., R. Myers, Y. Li, Y. Chen, X. Shen, J. Fenyk-Melody, M. Wu, J. Ventre, T. Doebber, N. Fujii, N. Musi, M. F. Hirshman, L. J. Goodyear & D. E. Moller (2001) Role of AMP-activated protein kinase in mechanism of metformin action. *J Clin Invest,* 108**,** 1167-74.

Zimprich, A., A. Benet-Pagès, W. Struhal, E. Graf, S. H. Eck, M. N. Offman, D. Haubenberger, S. Spielberger, E. C. Schulte, P. Lichtner, S. C. Rossle, N. Klopp, E. Wolf, K. Seppi, W. Pirker, S. Presslauer, B. Mollenhauer, R. Katzenschlager, T. Foki, C. Hotzy, E. Reinthaler, A. Harutyunyan, R. Kralovics, A. Peters, F. Zimprich, T. Brücke, W. Poewe, E. Auff, C. Trenkwalder, B. Rost, G. Ransmayr, J. Winkelmann, T. Meitinger & T. M. Strom (2011) A mutation in VPS35, encoding a subunit of the retromer complex, causes late-onset Parkinson disease. *Am J Hum Genet,* 89**,** 168-75.

Ziviani E., R. N. Tao & A. J. Whitworth (2010) Drosophila parkin requires PINK1 for mitochondrial translocation and ubiquitinates mitofusin. *Proc Natl Acad Sci U S A,* 107, 5018-23.

Zschocke, J. & T. Rein (2011) Antidepressants encounter autophagy in neural cells. *Autophagy,* 7**,** 1247-8.

Zunke, F., A. C. Moise, N. R. Belur, E. Gelyana, I. Stojkovska, H. Dzaferbegovic, N. J. Toker, S. Jeon, K. Fredriksen & J. R. Mazzulli (2017) Reversible Conformational Conversion of α-Synuclein into Toxic Assemblies by Glucosylceramide. *Neuron*.